Medizinische Hochschule Hannover

Klinik für Frauenheilkunde und Geburtshilfe

Mechanisms of cellular interaction and role of mesenchymal stroma/stem cells during tumorigenesis

INAUGURALDISSERTATION

zur Erlangung des Grades einer Doktorin der Naturwissenschaften

- Doctor rerum naturalium -

(Dr. rer. nat.)

vorgelegt von

Catharina Melzer

aus Emden

Hannover 2018

Angenommen durch den Senat: 04.03.2019

Präsident:	Prof. Dr. med. Michael P. Manns
Wissenschaftliche Betreuung:	Prof. Dr. rer. nat. Ralf Hass
Wissenschaftliche Zweitbetreuung:	Prof. Dr. rer. nat. Detlef Neumann

1. Referent:	Prof. Dr. rer. nat. Ralf Hass
2. Referent:	Prof. Dr. rer. nat. Detlef Neumann
3. Referent:	Prof. Dr. rer. nat. Florian Kühnel

Tag der mündlichen Prüfung: 04.03.2019

Prüfungsausschuss

Vorsitz:	Prof.‘in Dr. rer. nat. Christine Falk
1. Prüfer:	Prof. Dr. rer. nat. Ralf Hass
2. Prüfer:	Prof. Dr. rer. nat. Detlef Neumann
3. Prüfer:	Prof. Dr. rer. nat. Florian Kühnel

Danksagung

An dieser Stelle möchte ich mich bei all denjenigen bedanken, die mich in den vergangenen Jahren unterstützt haben und damit maßgeblich zum Gelingen dieser Arbeit beigetragen haben.

Ich möchte mich zu allererst bei Herrn Prof. Ralf Hass für die Bereitstellung des spannenden Themas, die Übernahme der Erstbetreuung und die viele Unterstützung auf wissenschaftlicher Ebene bedanken. Die Möglichkeit in seiner Arbeitsgruppe zu promovieren hat entscheidend zu meiner wissenschaftlichen und persönlichen Entwicklung beigetragen.

Herrn Prof. Detlef Neumann danke ich für die Übernahme der Zweitbetreuung und die produktiven Diskussionen während der Projektpräsentationen. Zudem danke ich ihm und Dr. Bastian Schirmer für die Hilfestellung bei der Durchführung und Auswertung von real-time PCRs.

Ganz herzlich möchte ich mich bei dem gesamten Laborteam der Frauenklinik bedanken. Insbesondere danke ich Juliane von der Ohe und Jutta Beu für die alltägliche Unterstützung, besonders zu Beginn meiner Promotion, für die vielen Ratschläge auf wissenschaftlicher und persönlicher Ebene sowie für die angenehme Arbeitsatmosphäre. Ein besonderer Dank gilt Dr. Anna Otte für die Einarbeitung in der Anfangsphase. Dr. Bianca Schröder-Heurich, Peter Schürmann und Britta Wieland danke ich zudem für die entspannten Mittagspausen, die eine tolle Abwechslung zum Laboralltag darstellten. Vielen Dank auch an Dr. Katharina Neuhäuser und Dr. Natalia Bogdanova für das freundliche Arbeitsklima.

Weiterhin möchte ich mich bei einigen Freunden bedanken, die das Studium und die Zeit während der Promotion bereichert haben. Danke an David Weigt, Malena Albers, Alexander Bollenbach, Till Stephan und Josefine Hartung.

Mein größtes Dankeschön gilt meinen Eltern, meinem Bruder und meinem Freund Flo. Ihr habt mich stets bei meinen Vorhaben unterstützt, hattet immer ein offenes Ohr für mich und habt immer hinter mir gestanden. Ohne eure Hilfe wäre diese Arbeit nicht möglich gewesen. Vielen Dank für euer Vertrauen und dafür, dass ihr immer für mich da wart.

Contents

Zusammenfassung ..... **I**

Summary / Abstract ..... **IV**

1. Introduction **1**

1.1 Breast cancer 1

1.1.1 Normal and benign breast epithelial cell lines 3

1.1.2 Malignant breast epithelial cell lines 4

1.2 Ovarian cancer 5

1.3 Mesenchymal stroma/ stem-like cells (MSC) 6

1.3.1 Existence, isolation, expansion and differentiation of MSC 6

1.3.2 Homing capacity, tissue repair and immunologic properties of MSC 10

1.3.3 Therapeutic potential of MSC 11

1.4 MSC and the role in cancer 12

1.4.1 Indirect interactions of MSC with cancer cells 12

1.4.2 Direct interactions of MSC with cancer cells 13

1.5 Cell fusion 15

1.5.1 Fusion-associated proteins and lipids 17

1.5.2 Fusion stimulating soluble factors and pro-fusogenic conditions 18

1.6 Aim of doctoral thesis 20

2. Publications **21**

2.1 In vitro fusion of normal and neoplastic breast epithelial cells with human mesenchymal stroma/stem cells partially involves tumor necrosis factor receptor signaling 22

2.2 Enhanced metastatic capacity of breast cancer cells after interaction and hybrid formation with mesenchymal stroma/stem cells (MSC) 47

2.3 MSC stimulate ovarian tumor growth during intercellular communication but reduce tumorigenicity after fusion with ovarian cancer cells 67

2.4 In vivo cell fusion between mesenchymal stroma/stem-like cells and breast cancer cells 79

3. Summary and discussion of results 93

3.1 MSC fuse with breast (and ovarian) cancer cells in vitro and in vivo 93

3.2 MSC promote ovarian tumor growth in vivo 95

3.3 MSC-cancer cell fusion represents a rare event 96

3.4 MSC-cancer cell fusion gives rise to more aggressive, but also to non-tumorigenic hybrid cells 97

3.5 TNF-α increases neoplastic MCF10A-MSC cell fusion 101

4. Outlook 103

5. References 104

6. List of abbreviations 129

7. Appendix 133

7.1 Curriculum vitae 133

7.2 Publication list 134

7.3 Conference contributions 136

7.4 Erklärung 137

Zusammenfassung

Catharina Melzer

Mechanisms of cellular interaction and role of mesenchymal stroma/stem cells during tumorigenesis

Die heutige Brustkrebsforschung befasst sich nicht mehr ausschließlich mit dem Verhalten von isolierten Tumorzellen. Vielmehr hat sich gezeigt, dass die Tumormikroumgebung einen wesentlichen Einfluss auf das Tumorverhalten hat und zunehmend in der Tumorforschung berücksichtigt wird. Neben Immunzellen, Endothelzellen und unterschiedlichen löslichen Faktoren stellen u.a. mesenchymale Stroma-/Stammzellen (MSC) einen weiteren wichtigen Zelltyp in der Tumormikroumgebung dar. Dabei wurden MSC eine zweideutige Rolle in der Tumorentstehung und Progression zugeordnet. Dieser Zelltyp ist in der Lage, sowohl direkte als auch indirekte Interaktionen mit Krebszellen einzugehen, die das Tumorverhalten beeinflussen. Indirekte Interaktionen umfassen die Freisetzung und Aufnahme von löslichen Faktoren wie Zytokinen, Chemokinen und Wachstumsfaktoren sowie den zellulären Austausch über Exosomen und Mikrovesikel. So konnte gezeigt werden, dass in Gegenwart von MSC das Tumorwachstum bspw. von Ovarialkarzinomzellen im Vergleich zu alleinigen Ovarialkrebszellen erhöht wird, was auf eine tumorfördernde Rolle der MSC durch indirekte Interaktionen hindeutet. Zusätzlich konnte durch MSC eine erhöhte Chemoresistenz in Tumorexplantkulturen beobachtet werden. Im Vergleich zu indirekten Interaktionen erfolgt die direkte Kommunikation über Nanotubes, Gap Junctions, Trogozytose und die Zellfusion.

Besonders die molekularen Mechanismen, die der Krebszellfusion zugrunde liegen, sowie die Rolle der daraus entstehenden Hybridzellen wurden in dieser Arbeit erforscht.

Um mögliche Fusionsereignisse zu untersuchen, wurden MSC, die aus der Nabelschnur gewonnen wurden, und Brust- (und Ovarial-) krebszelllinien verschiedenartig fluoreszenz-markiert mit einem lentiviralen Vektor, der entweder das eGFP Gen oder das mCherry Gen in sich trägt. Über zeitabhängige Fluoreszenzvideomikroskopie konnte der Fusionsprozess zwischen MSC und normalen humanen Brustepithelzellen (HMEC) sowie neoplastischen Brustepithelzellen (MCF10A) beobachtet und eingefangen werden. Die Detektion von Fusionen erfolgte über die Co-Kultur von GFP-markierten MSC zusammen mit mCherry-markierten normalen oder neoplastischen Brustepithelzellen, wobei die resultierenden Hybridzellen eine Doppelfluoreszenz für GFP und mCherry zeigten. Das eigentliche Fusionsereignis lief innerhalb von weniger als 5 Minuten ab.

Daraufhin wurde die Bildung von Hybridzellen nach Fusion von MSC mit verschiedenen Brustkrebszellen quantifiziert und erzielte Ergebnisse im Bereich von 0,1 bis über 2 Prozent. Interessanterweise zeigten Co-Kulturen von immortalen benignen MCF10A Brustepithelzellen mit MSC den höchsten Prozentsatz an fusionierten doppeltfluoreszenz-markierten Zellen. Im Vergleich zu Autofusionsereignissen (Fusion gleicher Zelltypen untereinander) waren Heterofusionen mindestens um das 10-fache erhöht. Basierend auf diesen in vitro Daten wurde das Auftreten von MSC-Brustkrebszellfusionen in NODscid Mäusen in vivo untersucht. Tatsächlich konnte die Bildung von Hybridzellen in vivo detektiert werden, wenn auch nur zu einem geringen Prozentsatz.

Für eine umfassende Analyse der Effekte von Hybridzellen auf die Tumorentwicklung wurden Fusionszellen von unterschiedlichen Co-Kulturen klonal isoliert und charakterisiert. Die verschiedenen Hybridklone wurden entsprechend ihrer Herkunft benannt:

1) MDA-hyb1, -hyb2, -hyb3, -hyb4 (aus Fusion von MSC mit der metastasierenden humanen Brustkrebszelllinie MDA-MB-231)

2) MCF10A-hyb1, -hyb2 (aus Fusion von MSC mit der immortalen humanen Brustepithelzelllinie MCF10A)

3) SK-hyb1, -hyb2 (aus Fusion von MSC mit der metastasierenden humanen Ovarialkarzinomzelllinie SK-OV-3)

Den verschiedenen Hybridzelllinien wurden heterogene Effekte zugeschrieben. Während die betrachteten Hybride aneuploid hinsichtlich ihres Chromosomensatzes waren und meist eine Doppelfluoreszenz von GFP und Cherry aufwiesen, zeigten sich in der Proliferationskapazität und in der Fähigkeit primäres Tumorwachstum auszulösen deutliche Unterschiede. Hybridzellen der parentalen MCF10A und SK-OV-3 kennzeichneten sich durch reduziertes Proliferationspotential aus. Zudem konnte in vivo kein Tumorwachstum detektiert werden. Mit einem teilweise seneszenten Phänotyp ließen diese Daten vermuten, dass die MCF10A- und SK-Hybride einen eher MSC-ähnlichen Phänotyp mit MSC-ähnlichen Charakteristika haben. Im Gegensatz dazu proliferierten die MDA-Hybride ähnlich stark wie die parentalen MDA-MB-231, wobei die MDA-hyb1 und -hyb2 sogar eine deutlich erhöhte Proliferationskapazität besaßen. Dieses konnte in vivo bestätigt werden mit einem deutlich schnelleren Tumorwachstum der MDA-hyb1 und -hyb2 sowie schnellerer Metastasenbildung im Vergleich zu den parentalen Brustkrebszellen. Somit kann geschlussfolgert werden, dass

eine Zellfusion zwischen MSC und Tumorzellen zu Hybridzellen führt, die sowohl maligner sein können als auch nicht-tumorigene Eigenschaften tragen können.

Zusätzlich zur Charakterisierung der Hybridzellen wurden molekulare Mechanismen, die der Zellfusion zugrunde liegen, erforscht, wobei TNF-α als potenzieller Kandidat identifiziert wurde, der die MSC/MCF10A Zellfusion erhöht, dagegen offensichtlich bei der MSC/MDA-MB-231 Hybridbildung keine besondere Rolle spielt. Dieser selektive fusionsfördernde Effekt von TNF-α wurde über die beiden TNF Rezeptoren TNFR1 und TNFR2 vermittelt. Weitere Signalketten liefen über TRADD und involvierten eventuell apoptotische und / oder NF-κB-abhängige Signalwege. Eine Aktivierung über JNK1/MAPK8 spielte dagegen eine untergeordnete Rolle.

Summary / Abstract

Catharina Melzer

Mechanisms of cellular interaction and role of mesenchymal stroma/stem cells during tumorigenesis

Breast cancer research examines not only tumor cells as isolated units but also the tumor microenvironment which exhibits a tremendous impact on tumor development and is therefore considered in cancer cell studies. Apart from immune cells, endothelial cells and various extracellular mediators, mesenchymal stroma/stem cells (MSC) represent a major player in the tumor microenvironment. Thereby, MSC have been attributed a dual role in cancer development and progression. This cell population is capable to directly and indirectly interact with cancer cells altering tumor behavior. Indirect interactions include the secretion and uptake of soluble factors like cytokines, chemokines and growth factors as well as the exchange of exosomes and microvesicles. In this context, MSC stimulated and increased primary ovarian tumor growth in contrast to ovarian cancer cells alone supporting a tumor promoting role of MSC. Additionally, tumor explant cultures exhibited a higher chemoresistance as compared to the normal ovarian carcinoma cells. In addition to indirect interactions, direct communication between MSC and cancer cells involves nanotube signaling, gap junctions, trogocytosis and cell fusion.

Particularly the underlying molecular mechanisms of cancer cell fusion and the role of the emerging hybrid cells were investigated in this thesis.

To study potential fusion events, umbilical cord-derived MSC and breast (and ovarian) cancer cell lines were separately fluorescence-labeled with a lentiviral vector carrying either the eGFP gene or the mCherry gene.

Time lapse fluorescence video microscopy documented the fusion process between MSC and normal human mammary epithelial cells (HMEC) as well as neoplastic breast epithelial cells (MCF10A). The actual fusion event proceeded within less than 5 minutes.

Consequently, the formation of hybrid cells due to fusion of MSC with various breast cancer cell lines was quantified ranging between 0.1 and more than 2%. Of interest, co-cultures of benign MCF10A with MSC revealed the highest percentage of dual fluorescent hybrid cells. Compared to autofusion events, heterofusions were at least 10-fold elevated. Based on these in vitro data, the occurrence of MSC-breast cancer cell fusion was investigated in vivo with

NODscid mice. Indeed, hybrid cell formation was detected in vivo albeit to a very low percentage.

For a comprehensive analysis of the effects of hybrid cells on tumorigenesis, fusion products from distinct co-cultures were isolated and characterized. Thus, these various hybrid clones were named according to their origin leading to

1) MDA-hyb1, -hyb2, -hyb3, -hyb4 (fusion of MSC with the metastasizing human MDA-MB-231 breast cancer cell line)

2) MCF10A-hyb1, -hyb2 (fusion of MSC with the neoplastic human MCF10A breast epithelial cell line)

3) SK-hyb1, -hyb2 (fusion of MSC with the human SK-OV-3 ovarian cancer cell line)

Within these hybrid cell lines, diverse effects have been observed. Whereas examined hybrid cells were commonly aneuploid and mostly dual fluorescent for GFP and cherry, the proliferative capacity and the ability to induce primary tumor growth in vivo appeared heterogenous. Hybrid cells from parental MCF10A and SK-OV-3 exhibited reduced proliferative potential and no detectable tumor growth in vivo concomitant with a partially senescent phenotype suggesting rather MSC-like phenotype and characteristics. On the contrary, MDA-hybrids displayed different proliferative capacities in comparison to MDA-MB-231. Whereas in vivo tumor development was significantly reduced with MDA-hyb3, this was markedly enhanced with MDA-hyb1 and -hyb2 cells accompanied by a rapid metastatic spread to various organs when compared to parental MDA-MB-231. Taken together, cell fusion between MSC and cancer cells can generate hybrid cells with altered malignancy contributing to enhanced overall tumor heterogeneity.

In addition to the characterization of hybrid cells, molecular mechanisms underlying cell fusion were investigated identifying TNF-α as potential candidate that elevates MSC/MCF10A but not /MDA-MB-231 cell fusion. These pro-fusogenic effects of TNF-α were mediated by the TNF receptors 1 and 2. Further downstream signaling was relayed via TRADD and potentially involves apoptotic and / or NF-κB signaling with little if any contribution of the JNK1/MAPK8 activation.

1. Introduction

1.1 Breast cancer

In 2018, the number of new cancer cases is estimated at over 18 million accompanied by 9.6 million cancer deaths. Breast cancer accounts for the most common cancer in women with over 2 million new cases of breast cancer worldwide. Whereas Belgium and Luxembourg show the highest rate of breast cancer in women with 113.2 and 109.3 age-standardized rate per 100,000, Germany occupies the 20th place followed by the US and Canada (place 22 and 23) [1]. These data reflect the fact that although Europe covers only 9% of the global population, 25% of the global cancer incidence appears in Europeans. Thereby, female breast cancer displays the most frequent diagnosed cancer type together with colorectal, lung and prostate cancer representing half of the overall cancer incidence in Europe. Of interest, from 1.93 million deaths in Europe that resulted from cancer, the number of breast cancer deaths reveals 138,000 [2].

Main risk factors besides female gender, genetic predispositions and aging comprise the country of birth, the physical condition including obesity, high breast density or menstrual/reproductive history, and the overall lifestyle including diet, alcohol consumption, physical activity and smoking. Moreover, the exposure to ionizing radiation and both endogenous and exogenous hormones represent further causes for breast cancer [3, 4]. Thereof, family history and inherited factors depict one of the most well-established breast cancer risk factors amounting to 10%. In the 1990s, BRCA1 (Breast Cancer 1) was identified as first cancer susceptibility gene followed by BRCA2 and further genes such as TP53 (Tumor Protein) or CHEK2 (checkpoint kinase 2). Mutations in these genes are associated with high to intermediate risk to develop breast cancer [5-8]. Apart from family history, the country and environment of birth, respectively, might have an impact on breast cancer risk. Whereas the incidence rate is higher in developed countries, mortality is higher in less developed areas [9]. For instance, incidence rate of breast cancer is much higher in Europe as compared to the Asian or African population [1, 10]. Aging still represents one major risk factor. Fewer than 5% of women are diagnosed before the age of 40 years in the US. This rate constantly increases to the age of over 70 years [11]. Besides aging, early menarche and late menopause have been associated with higher breast cancer risk. Explanations suggest the longer exposure of endogenous cycling ovarian hormones increasing the risk of developing breast cancer [12]. Moreover, pregnancy in general is suggested to reduce the risk. Especially multiple pregnancies and young age at first childbirth have been correlated with lower breast

cancer risk [13-15]. However, women with pregnancy older than 30 years have been reported with higher risk in contrast to nulliparous women [16, 17]. Longer exposure of hormones such as estrogen is additionally associated with obesity as risk factor [18, 19]. Nevertheless, clinical data vary within countries, ethnical groups and premenopausal versus postmenopausal women. In addition to endogenous hormones, exogenous hormones like hormonal contraceptives and hormone replacement therapy represent further factors impacting the development of breast cancer [15, 20, 21].

As diverse as risk factors are, breast cancer is categorized into several molecular subtypes mainly depending on hormone receptor (HR) status and therefore differing in prognosis and therapy. The four main subtypes together with HR status and frequently applied therapies are listed in table 1. In general, the expression of three different hormone receptors, namely the estrogen receptor (ER), progesterone receptor (PR) and human epidermal growth factor receptor 2 (HER2), determines suitable therapy and clinical outcome [22].

Table 1: Subtypes of breast cancer (modified from [22]).

subtypes	hormone receptor status	therapy
luminal A-like	ER +, PR + HER2 – Ki-67 low	hormone-based therapy
luminal B-like	ER + HER2 + or – PR low or Ki-67 high	hormone-based therapy, accompanied by chemotherapy if Ki-67 high
HER2 positive (non-luminal)	HER2 + ER –, PR –	anti-HER2 antibodies like trastuzumab
triple negative / basal-like	ER –, PR – HER2 –	chemotherapy

Besides the molecular categorization, pathological subtypes of breast cancer mainly comprise ductal carcinoma (80%), lobular carcinoma (15%) and to lower incidence other rare pathologic variants such as inflammatory medular and tubular carcinoma or male breast cancer. Moreover, both major types exist as invasive and non-invasive tumors impacting therapy and prognosis [23, 24].

1.1.1 Normal and benign breast epithelial cell lines

Nowadays, there exists a plethora of different cell lines and primary cell cultures enabling breast cancer research by imitating the diverse stages of tumor development using in vitro models.

For this doctoral thesis, experiments were performed with 5 different breast cell lines including HMEC (normal human mammary epithelial cells), MCF10A, MCF7, MDA-MB-231 and HBCEC (human breast cancer epithelial cells).

Thereby, HMEC can be regarded as potential starting point of breast cancer since it is a normal human mammary epithelial cell culture generally isolated during mammoplasty or mastectomy [25]. These primary cells exhibit a finite life span after about 50 cell doublings in vitro [26]. Several mechanisms of HMEC are known to prevent infinite growth. Activated by stress and mediated by the retinoblastoma (Rb) tumor suppressor protein, increase of cyclin-dependent kinase inhibitor $p16^{INK4a}$ causes a first senescence barrier, termed stasis [27]. Nevertheless, some so-called post-selected HMEC can escape senescence through loss of p16 and continue proliferation. However, critical length of telomeres due to lack of telomerase activity leads to accumulation of chromosomal abnormalities and DNA damage resulting in agonescence, a second senescence barrier [27]. Agonescent cells, negative for p16, remain viable accompanied by a senescent phenotype such as senescence-associated β-galactosidase (SA-β-Gal) activity and expression of functional p53. Indeed, if p53 is abrogated, HMEC encounter crisis, a massive cell death [28]. Interestingly, reactivation of hTERT (human telomerase reverse transcriptase) can result in malignant transformation of post-selected senescent HMEC [29] suggesting a potential explanation for breast cancer development since telomerase is present in 90 % of all human cancers to enable infinite cell growth [30].

MCF10 stands for Michigan Cancer Foundation and was isolated from a 36-year-old parous premenopausal woman with extensive fibrocystic disease during mastectomy. This cell line exhibits features of normal breast epithelium such as lack of the capacity to invade adjacent tissue and to metastasize or controlled anchorage-dependent growth in culture by hormones and growth factors as well as three-dimensional growth in collagen. In vitro, this cell line senesces and is characterized as diploid cells with a finite life span. However, two immortal cell lines spontaneously arose from these mortal cells. MCF10F represent free floating cells directly derived from the mortal MCF10 and firstly cryopreserved after culturing of MCF10 in low calcium serum free medium for 840 days. Conversely, MCF10A display an adherent immortal sub cell line and were initiated from MCF10F. Whereas MCF10 cells are normal

diploid, the karyotype of MCF10F and MCF10A is near diploid with minimal rearrangements containing 46 and 48 chromosomes, respectively [31]. Furthermore, MCF10A lack expression of the hormone receptors [32]. Besides MCF10A and MCF10F, further subtypes have been non-spontaneously generated and applied for breast cancer research such as MCF10AT (premalignant) or MCF10CA1 (fully malignant) [33].

Considering that especially the nonmalignant, benign MCF10A can be transformed to a malignant stage and that otherwise these cells exhibit normal breast epithelium characteristics, this cell line represents a valuable cell model to investigate breast cancer development. Morphology of MCF10A and of normal human mammary epithelial cells is illustrated in figure 1 strengthening the presence of epithelial characteristics.

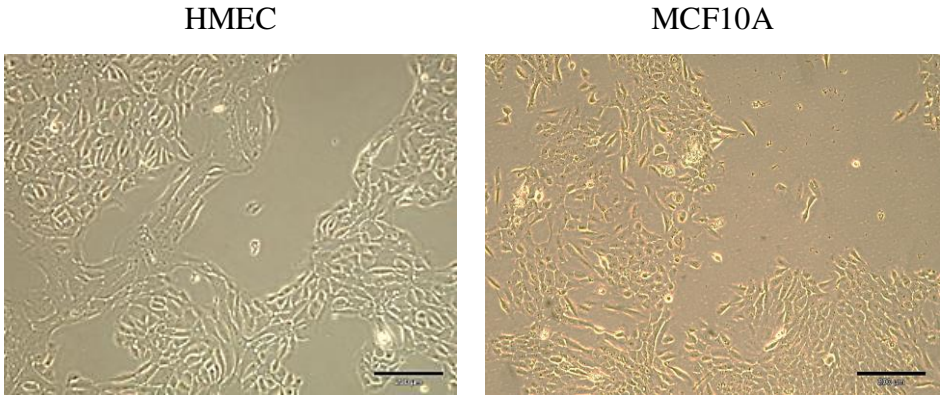


Figure 1: Morphology of HMEC_P9 (left) and MCF10A_P124 (right). Scale bars represent 200µm.

1.1.2 Malignant breast epithelial cell lines

The malignant breast cancer cell line MCF7 was isolated from a pleural effusion of a 69-year-old woman with metastatic breast cancer. Before primary culture of MCF7, the woman had suffered from two mastectomies, one of her right breast (benign tumor) and one radical mastectomy of her left breast (malignant adenocarcinoma) [34]. As a consequence of ER and PR presence and the absence of HER2, MCF7 belong to the molecular subtype of luminal A-like tumors [32, 35]. The karyotype of MCF7 is hypertriploid to hypotetraploid with a modal number of 76 to 88 chromosomes [36]. Moreover, this cell line fails to metastasize in vivo and hence, is characterized as a non-invasive phenotype [37, 38].

Conversely, the basal-like triple negative MDA-MB-231 breast cancer cell line displays high invasive and migration potential [39, 40]. This malignant cell line was isolated from pleural effusions of a 51-year-old patient after mastectomy and chemotherapy and harbors a near triploid karyotype [41, 42].

Morphologies of MCF7 in comparison to MDA-MB-231 are represented in figure 2.

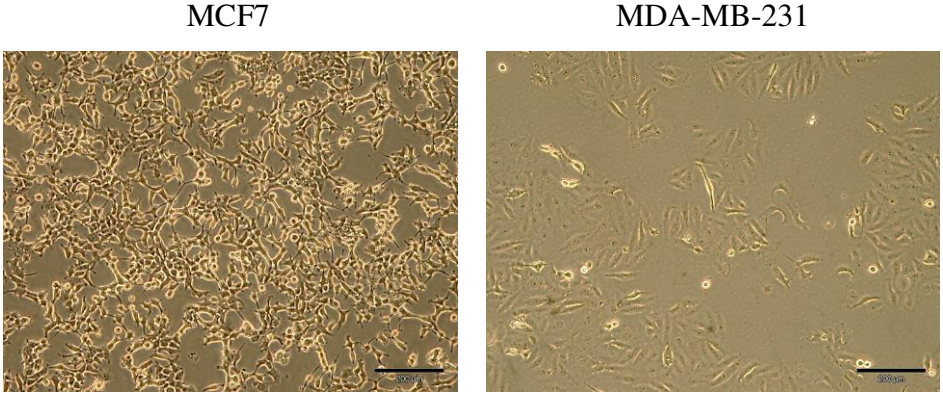


Figure 2: Morphology of MCF7 (left) and MDA-MB-231 (right) breast cancer cell lines. Scale bars represent 200µm.

Besides these two immortal cancerous cell lines, HBCEC (human breast cancer epithelial cells) represent primary cell populations derived from long-term cultured tumor tissues of individual breast cancer patients [43]. These cells have been demonstrated to express cell adhesion molecules or mediators such as CD24 and CD44. Moreover, during long-term culture of HBCEC little, if any SA-β-Gal-positive cells could be detected in certain cultures accompanied by telomerase activity indicating unlimited proliferation potential of these patient-specific primary cells [43]. Of interest, chemotherapeutic effects differed among HBCEC from different patients suggesting an individualized response and strengthening the need of primary breast cancer cultures to study tumorigenesis.

1.2 Ovarian cancer

Ovarian cancer belongs to the twentieth most commonly diagnosed cancer with about 295,000 new cases worldwide in 2018. The number of deaths is estimated to around 185,000 [1]. Annually, between 6,900 and 7,500 women develop ovarian cancer in Germany [44]. The risk to develop ovarian cancer constantly increases with age. Further risk factors are similar to

breast cancer risk factors. Thus, they include obesity, hormonal factors like nulliparity, infertility or hormone replacement therapy and genetic predispositions such as mutations in BRCA1 and BRCA2 [44].

Benign and malignant ovarian tumors are classified due to their origin whereby the most frequent ovarian cancers develop from epithelial cells of the ovary (90%). In addition, ovarian cancer can rise from stromal cells and germ cells (both around 5%) [45]. Each category in turn implies a number of subtypes. For instance, stromal cell tumors include thecomas, fibromas, granulosa or Sertoli-Leydig cell tumors. However, ovarian carcinomas represent the largest group with histological subtypes such as low-grade and high-grade serous carcinoma, mucinous, endometrioid, clear cell, transitional cell, squamous cell, mixed epithelial cell and undifferentiated tumors [45, 46]. One prominent example of ovarian carcinoma cell lines is represented by SK-OV-3 which was used in this thesis [47]. Apart from the common three subtypes, there exist some very rare types of ovarian cancer including the small cell ovarian carcinoma of the hypercalcemic type (SCCOHT) or small cell ovarian carcinoma pulmonary type (SCOCPT) [48, 49].

1.3 Mesenchymal stroma/ stem-like cells (MSC)

Human mesenchymal stroma/stem-like cells (MSC) are multipotent self-renewing cell populations which can be derived from various human organs and tissues and preferentially reside in perivascular niches.

1.3.1 Existence, isolation, expansion and differentiation of MSC

In the 1960s, Alexander Friedenstein firstly described the existence of a different cell population in the bone marrow while culturing hematopoietic stem cells marking the beginning of MSC's history [50, 51]. This heterogeneous cell population was identified as plastic adherent with a fibroblast-like morphology. More importantly, these cells were able to form colonies (colony-forming unit fibroblasts, CFU-F) indicating the existence of precursor cells in the bone marrow [52]. Since then, a variety of studies investigated the occurrence, the isolation, the properties and functions as well as the therapeutic potential of MSC. Fibroblast-like morphology of MSC is exemplary illustrated in figure 3.

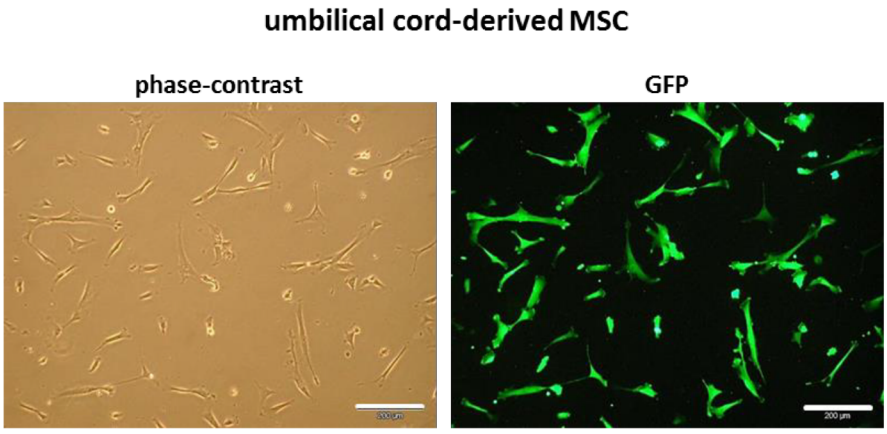


Figure 3: Microcopy image of umbilical cord-derived MSC. After isolation of mesenchymal stroma/stem-like cells from umbilical cord tissue, this cell population was stably transduced with a lentiviral vector carrying the eGFP gene and morphology was documented by fluorescence microcopy. Scale bars represent 200µm.

Today, MSC can be subgrouped into adult MSC and neonatal-tissue or birth-associated tissue-derived MSC [53]. Whereas MSC isolated from for example the bone marrow [54], lung [55], heart [56], adipose tissue [57] or the peripheral blood [58] are designated as adult MSC, neonatal or birth-associated tissues including the placenta [59], Wharton´s jelly [60], the whole umbilical cord [61] or the cord blood [62] delineate a different source of MSC (Figure 4). Even though MSC were first of all isolated from bone marrow (BM-MSC) representing the best characterized, most frequently investigated MSC and are therefore often referred as the gold standard [51, 54], juvenile MSC have crucial advantages compared to adult MSC. Besides the fact that the neonatal tissues arise through nativity anyway and that isolation and usage does not need surgical intervention and does not evoke ethical concerns, these neonatal tissue-derived MSC demonstrated a higher life span and an increased proliferative capacity [63, 64]. As a consequence, in vitro cultivation time is varying within MSC populations. For instance, bone marrow (BM) and adipose-tissue MSC (AT-MSC) could be cultivated up to passage number 7 and 8, respectively with no decrease in doubling time [65], while umbilical cord MSC (UC-MSC) demonstrated senescence after passage number 10 [66-68] or later [69]. Of interest, in a different study AT-MSC have been expanded to passage number 20. Although these cells demonstrated a significant increase in doubling time, surface marker expression was nevertheless slightly altered [70].

Apart from the miscellaneous occurrence and proliferation potential, isolation protocols of MSC are equally diverse. Isolation of BM-MSC starts with surgical intervention via bone

marrow aspiration followed by density gradient centrifugation and cultivation of isolated cells. In general, isolation protocols commonly take advantage of MSC's ability to adhere to plastic in contrast to other cell types such as hematopoietic stem cells within the bone marrow [71]. AT-MSC are typically isolated by other invasive procedures including lipoplasty, liposuction or lipectomy. Thereafter, lipoaspirate is digested by enzymes such as collagenase and subsequent centrifugation steps ending up in cultivation and washing of non-adherent cells the next day [72]. However, rapid isolation without enzyme digestion leads to similar efficiency of MSC isolation [73]. Isolation of birth associated tissue-derived MSC such as UC-MSC involves resembling steps. Nevertheless, distinct isolation protocols for UC-MSC are applied. Although isolation procedure often begins with elimination of umbilical vessels followed by slicing of the tissue into smaller pieces and enzymatic digestions (e.g. hyaluronidase, collagenase and trypsin), other protocols only cut the umbilical cord into small chops without removal of vessels and / or without enzyme digestion. Afterwards, explant cultures of treated UC are started [74-77]. Interestingly, occurrence of MSC within the various niches such as bone marrow, adipose tissue or umbilical cord differs extremely. Moreover, yield of MSC alternates from organs and tissues, but also between donors within one tissue [76, 78-80]. Therefore, it is inevitable to perform research with MSC from multiple donors to exclude donor-specific effects.

Since characteristics and properties of MSC are very diverse due to heterogeneous origin, isolation and expansion, in 2006, the Mesenchymal and Tissue Stem Cell Committee of the International Society for Cellular Therapy (ISCT) defined three criteria to be fulfilled for human MSC [81]. These minimal guidelines encompass that MSC as multipotent cells have to exhibit the property to differentiate at least along the mesodermal lineage which means differentiation into adipocytes, osteoblasts and chondroblasts in vitro under specific culture conditions. Moreover, certain surface marker should be present on MSC covering CD105 (endoglin), CD90 (Thy 1) and CD73 (ecto-5´-nucleotidase) (expression $\geq$ 95%). By contrast, the Committee also defined some surface marker being absent on MSC such as CD34 (hematopoietic stem cell marker), CD45 (lymphocytic), CD79α or CD19 (B-lymphocyte antigen), CD14 (monocytic) or CD11b (integrin) and HLA-DR (human leukocyte antigen) (expression $\leq$ 2%). As a third criterion, MSC must adhere to plastic under standard culture conditions [81] (Figure 4).

Although the criteria of the ISCT still represent the basis for MSC identification and are frequently considered nowadays, there has been discussed both a plethora of additional surface markers and differentiation into non-mesodermal lineages.

Apart from the MSC core marker (CD73, CD90 and CD105), one prominent marker which has been deeply investigated and is often referred as further MSC identifier is CD44. The receptor for hyaluronic acid has been detected in e.g. BM-MSC, AT-MSC, peripheral blood-derived MSC and UC-MSC [58, 74, 82-84]. Moreover, CD29 represents another widely accepted MSC marker coding for integrin β-1 [58, 85, 86].

Besides differentiation along the mesodermal lineage, MSC have been demonstrated to successfully transdifferentiate into cell types of the ectoderm and endoderm (Figure 4). Differentiation along the endodermal lineage resulted in cardiomyocytes, hepatocytes and pancreatic cells among others [87-89]. Neuronal phenotypes have been demonstrated as well indicating differentiation of MSC along the ectodermal lineage [90-92]. Nevertheless, there are enormous contrasts in the differentiation potential of MSC depending on the source of origin.

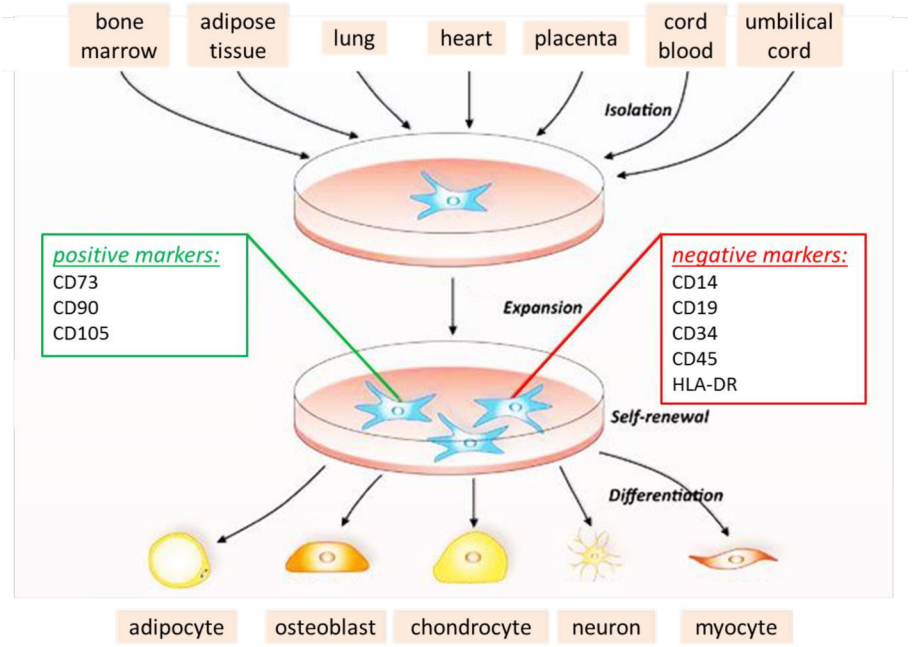


Figure 4: Lifecycle of human MSC in vitro. Isolation from different organs and tissues followed by expansion and enrichment of fibroblast-like cells leads to generation of human MSC with self-renewal capacity and expression of certain surface molecules. Under certain conditions, MSC differentiate along different pathways exhibiting adipocytic, osteoblastic and chondrocytic phenotypes (modified from [93]).

1.3.2 Homing capacity, tissue repair and immunologic properties of MSC

Properties and functions of human MSC are as multifaceted as their occurrence, isolation and differentiation capacity. These involve self-renewal ability, regulation of stem cell homeostasis in the bone marrow, migration and homing capacity to sites of inflammation and injury concomitant with wound healing and tissue repair, and support of angiogenesis [94]. Especially their immunoregulatory capabilities including immunosuppression and immunoprivilege are of interest and render these cells as promising tool for clinical applications [95].

To accomplish their function and exert their potential, MSC are able to migrate and home towards sites of inflammation and injury. Recruitment involves leaving their niches where they reside followed by crossing of the endothelial cell layer mediated by selectin-associated and cell adhesion molecule-mediated (P-selectin and VCAM-1) attachment and dissemination at the sites of injury [96]. Although large mechanistic parts are not fully understood, MSC's homing process was suggested to resemble in part the leukocyte adhesion cascade which is used as role model to study MSC homing [96, 97]. Indeed, chemokine-chemokine receptor axes such as CXCL12-CXCR4 or CCL5-CCR5 are involved in MSC's targeted migration and homing capacity [98-100]. Once approached at sites of inflammation, MSC are involved in regeneration including wound healing, tissue repair and angiogenesis [101, 102]. For instance, MSC are involved cardiovascular repair [103, 104] or bone [105], cartilage [106] and skin repair occurring through replacement of lost cells by differentiation of MSC into various skin cell types [107].

In a plethora of studies MSC have been shown to modulate, mostly suppress, functions of a variety of immune cells such as B- and T-lymphocytes or natural killer (NK) cells [108-111]. Although mechanisms permitting/facilitating MSC to modulate immune cell functions are not fully understood, secretion of soluble factors and cell-cell-contacts have been deeply investigated [112-114]. Prior to MSC's-mediated immunomodulation, appropriate activation of MSC and close proximity to immune cells is required. MSC either constantly or upon activation secrete plenty of soluble factors including cytokines, chemokines and growth factors some of which have been identified to contribute to immune regulation [94]. In particular, IFN-γ together with other pro-inflammatory cytokines IL-1α, IL-1β or TNF-α has been reported to induce MSC's immunosuppression by production of chemokines driving immune cell chemotaxis towards MSC [115]. Moreover, MSC-mediated inhibition of T-lymphocyte activation and proliferation has been associated with indoleamine-2,3-

dioxygenase (IDO) which is inducible by IFN-γ [116], nitric oxide (NO)/ inducible NO synthase (iNOS) [117], prostaglandin E2 (PGE2) [118] and IL10 [119]. In addition to T-cell proliferation inhibition, MSC disrupt B-lymphocyte proliferation and antibody production [120-123]. However, some studies demonstrated supportive effects of MSC on B-cells through e.g. PGE2 [124, 125]. Macrophages, NK cells and dendritic cells (DC) represent further immune cell types being modulated in their functions by MSC. Macrophage properties which are mainly affected by MSC encompass migration and polarization. Whereas production and secretion of MSC-derived chemokines such as CCL2 and CCL7 contribute to macrophage recruitment [126, 127], PGE2 released by MSC increases macrophage conversion of M1 to alternatively activated M2 phenotype [128]. Other soluble factors secreted by MSC have been identified to suppress DC maturation. For instance, IL6 or HGF, but also PGE2, mediate suppressive effects of MSC [129, 130]. Immunomodulation of NK cells finally impacts their proliferation, cytokine production and cytotoxicity via both cell-contact dependent interactions and secreted factors [131, 132].

Apart from immunoregulation, MSC are featured with an immunoprivileged status. That means mesenchymal stem cells are protected from the immune system. Since expression of MHCI is low and MHCII is lacking, MSC do not evoke substantial alloreactivity [133-135]. However, recent animal studies discuss certain immunogenic capacities of MSC indicating rejection of MSC after transfusion or transplantation, respectively [136-138].

1.3.3 Therapeutic potential of MSC

With all these versatile functions, MSC represent a promising candidate for a large number of clinical applications including regenerative medicine, tissue engineering and autoimmune diseases. Indeed, clinical trials applying MSC as tool are ongoing [139]. The increasing demand of MSC in clinical applications is represented by the number of more than 700 listed clinical trials [www.clinicaltrials.gov]. Especially for the treatment of acute and chronic graft-versus-host disease (GvHD) MSC are often applied as therapeutic cell agent [109]. This disease emerges after allogeneic hematopoietic cell transplantation whereby host T cells recognize the recipient organism as foreign. Most commonly skin, gastrointestinal tract and liver are affected leading to skin rash or diarrhea for instance [140]. According to their immunomodulatory properties, infusion of MSC of GvHD patients resulted in reduction up to complete resolution [141, 142].

1.4 MSC and the role in cancer

Regarding tumors as invasive tissues causing an inflammatory milieu, it is not surprising to find MSC in the tumor microenvironment as these cells are attracted by and migrate towards inflammation sites. Besides immune cells, endothelial cells and a burst of soluble factors, MSC contribute to tumor behavior and tumorigenesis [94, 143]. Although literature reports about tumor-promoting and tumor-inhibitory effects of MSC, further research is needed to better estimate the impact on tumor progression, especially with respect to clinical issues. Breast cancer-promoting effects have been widely observed resulting in enhancement of cancer cell proliferation, migration, metastasis formation and chemoresistance. Nevertheless, MSC may facilitate cancer growth inhibition and reduction of metastasis to the same extent. These interferences arise from both indirect interactions and direct interactions of MSC with cancer cells [143].

1.4.1 Indirect interactions of MSC with cancer cells

Indirect interactions of MSC with cancer cells have been intensively studied over the last decades. Although specific mechanisms still need to be elucidated, different types of interaction are generally grouped into secretion and exchange of soluble factors involving cytokines, chemokines, growth factors, hormones and metabolites, and on the other hand, secretion and uptake of extracellular vesicles including microvesicles and exosomes mutually altering behavior of both MSC and cancer cells (Figure 5).

Indirectly mediated effects involve MSC-released chemokines and cytokines such as CXCL1 and CXCL5, CCL5, IL6 or e.g. CXCL12/SDF-1 acting on CXCR4 receptors of cancer cells facilitating tumor growth [144-147]. Human breast cancer cells were able to stimulate the secretion of CCL5 by MSC which in turn stimulated MDA-MB-231 in a paracrine manner leading to enhanced motility, invasion and the promotion of breast cancer metastasis [145]. By contrast, systemically administered MSC were able to migrate towards breast tumor sites in vivo and supported primary tumor growth inhibition and a decrease of metastasis formation via secretion of IFN-β by MSC [148].

Extracellular vesicles additionally contribute to mutual crosstalk. Whereas exosomes are small homogenous 40 to 100nm particles of endocytic origin, heterogenous 50 to 1,000nm microvesicles are directly shed from the plasma membrane [149]. The content of exosomes and microvesicles differs extremely, however, it usually covers proteins, lipids and RNAs like microRNAs and mRNAs [150]. Both MSC and cancer cells can secrete extracellular vesicles

with mutual influence mainly promoting but also inhibiting tumorigenesis. Mouse bone marrow MSC-derived exosomes down-regulated vascular endothelial growth factor (VEGF) in breast cancer cells ending up in inhibition of angiogenesis in vitro and in vivo [151]. By contrast, MSC-derived exosomes facilitated the acquisition of stem cell characteristics in breast and ovarian cancer cells [152], augmented cancer cell migration [153] and supported tumor growth in vivo [154]. Vice versa, cancer cell-derived extracellular vesicles display the ability to reprogram MSC to tumor-supporting or tumor-inhibiting cancer-associated MSC [150]. Treatment of MSC with breast cancer cell-derived microparticles accelerated the expression of tumor-promoting factors like VEGF or CCL5 by differentiating MSC into tumor-associated myofibroblasts [155].

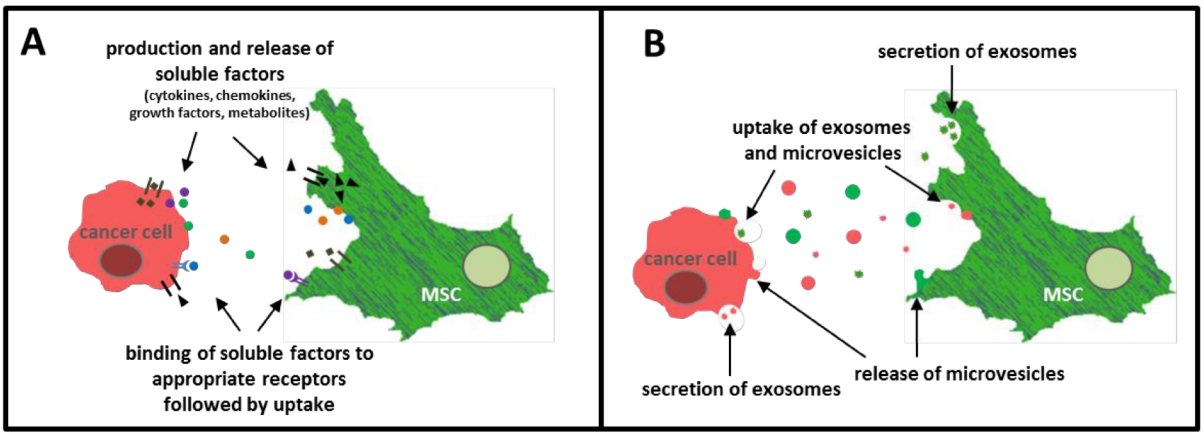


Figure 5: Indirect interplay between MSC and cancer cells involves **(A)** the production and release of soluble factors like cytokines, chemokines, growth factors and metabolites followed by binding and uptake of these factors and **(B)** the secretion and uptake of exosomes as well as the release and uptake of microvesicles (modified from [143]).

1.4.2 Direct interactions of MSC with cancer cells

Direct interactions require MSC and cancer cells in close proximity. Of interest, direct crosstalk encompasses receptor-ligand interactions, nanotube signaling, exchange of whole membrane patches termed trogocytosis, and the strongest and most intimate communication resulting in cell fusion and the formation of MSC-cancer hybrid cells (Figure 6). Similar to indirect interactions, direct MSC-cancer interplay promotes and inhibits tumor development. Nanotube signaling with the transfer of mitochondria from BM-MSC to MDA-MB-231 breast cancer cells altered metabolic activity and increased proliferative and invasive potential of the

latter [156]. By contrast, proliferative capacity of malignant cell lines of hematopoietic origin was extremely diminished in the presence of MSC whereas MSC-conditioned medium only partially reduced cancer cell proliferation [157]. Nevertheless, a different study ascribed opposite observations to MSC enhancing breast cancer cell proliferation and tumor growth in vivo [158]. Notwithstanding that trogocytosis was firstly described as interaction type among immune cells [159], capturing of stromal membrane patches by ovarian cancer cells induced chemoresistance [160].

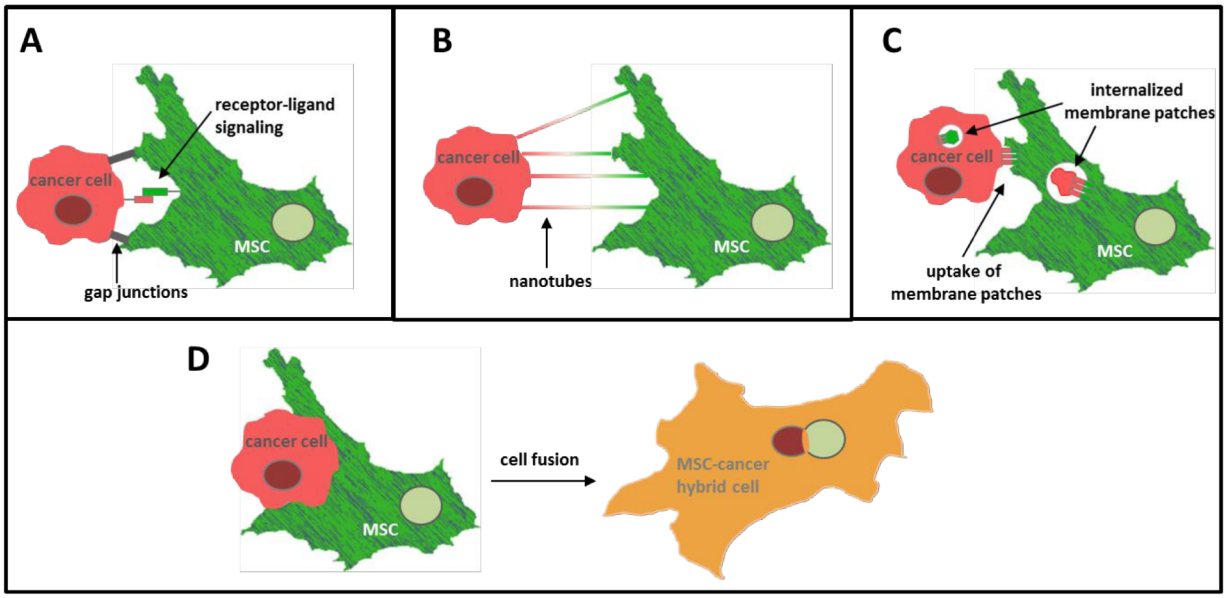


Figure 6: Direct cell-to-cell communications between cancer cells and MSC involve **(A)** receptor-ligand signaling and gap junctions, **(B)** nanotube signaling, **(C)** trogocytosis and **(D)** cell fusion (modified from [143]).

Even though all direct interaction types alter phenotype and function of interacting partners bidirectionally and multidirectionally, respectively, cell fusion represents the type of interaction with the highest potential to obtain extremely diversified cell populations since it may involve a mixture of two or multiple genotypes. Indeed, cell fusion between MSC and cancer cells has been observed with several tumor entities including breast, ovarian, lung and gastric cancer [158, 161-164].

1.5 Cell fusion

Cellular fusion plays a fundamental role in lots of physiological processes. Starting from the fusion during fertilization between egg and sperm as well as the fusion of trophoblasts to syncytiotrophoblasts in the placenta during embryogenesis and ending up in fusion formation among macrophages to generate giant cells or the fusion of muscle cells to form multinucleated muscle fibers it demonstrates the frequent occurrence and importance of cell fusion during development [165-170]. However, cell fusion has been reported under pathophysiological conditions such as cancer impacting tumorigenesis [171-173].

In the 1960s, it has been firstly demonstrated that somatic cells can be stimulated to fuse in vitro. Ehrlich ascites tumor cells formed polynuclear giant cells caused by addition of hemagglutinating virus of Japan (HVJ; also known as Sendai virus) [174-176]. In parallel, hybrid formation of mouse cells among same cell types, between different cell strains or even different species (mouse and rat cells) had been observed and documented by e.g. karyotyping resulting in polyploid cells with characteristics of both parental cell populations [177-180].

Commonly, cell fusion gives rise to different types of hybrid cells depending on the origin of fusion partners and the nuclear constitution of the forming hybrid cell. Syncytia emerge from cells of the same cell type (autofusion) harboring multiple nuclei, but at least two. For instance, syncytiotrophoblasts or multi-nucleated myotubes represent syncytia. Conversely, cell fusion between cells of different origin (heterofusion) leads to heterokaryons, however, featuring multiple nuclei ($\geq$2) as well. Of interest, synkaryons are formed after fusion between cells of the same or a different lineage possessing a single nucleus. Thereby, heterokaryons can be regarded as an intermediate cell fusion product followed by nuclear fusion with subsequent rearrangement of chromosomes accompanied by either partial chromosomal loss or the loss of one intact nucleus [181]. Especially the last hybrid type is of increasing interest since chromosomal rearrangements might lead to a complete new cell type with altered genotype and phenotype.

In particular, cancer cell fusion has been deeply investigated due to chromosomal instability, new cellular behaviors and the possibility that hybrid products contribute to tumor heterogeneity and impact tumorigenesis by increased proliferation potential or elevated metastatic capacities accompanied with elevated chemoresistance. Certainly, fusion among cancer cells needs to be distinguished from cell fusion between cancer cells and adjacent, in

the tumor microenvironment residing, non-cancerous cells like immune cells, endothelial cells as well as MSC.

For instance, bone-tropic and lung-tropic MDA-MB-231 breast cancer cells were spontaneously fused bearing hybrid cells with dual metastasis tropism to both organs. Besides the acquisition of gene signatures from both parental cell types, these hybrids were chromosomal and phenotypic stable [182].

Spontaneous cell fusion between MCF7 breast cancer cells and macrophages generated hybrid cells with elevated survival and less DNA-damage after irradiation in contrast to maternal MCF7 cells indicating hybrid formation as a mechanism to acquire radioresistance concomitant with potential tumor relapse [183]. In a different study, hybridization between tumor-associated macrophages and MCF7 or MDA-MB-231 breast cancer cells revealed acquisition of traits from both parental populations, decreased proliferative potential, but increased migration and invasive capacities in contrast to the maternal cancer cell lines [184].

Breast cancer-endothelial cell fusion has been monitored in co-culture in vitro and in vivo after injection and dissemination of breast cancer cells in mice. Interestingly, the resulting hybrids displayed properties of both maternal cells whereby acquisition of endothelial traits may facilitate penetration of the endothelial barrier to enhance metastasis [185]. Moreover, endothelial characteristics have been acquired after glioblastoma-endothelial cell fusion and oral cancer-endothelial hybrid cells have been associated with elevated drug resistance and enhanced survival potential [186, 187].

Cell fusion between breast cancer cells and mesenchymal stem cells has been demonstrated with two different cell lines, MDA-MB-231 and MA11 [158, 161]. Hybrids exhibited a mixed gene expression with the capacity to form tumors in vivo. In addition, MSC-breast cancer hybrids were able to form more lung metastasis than the parental MDA-MB-231 [161]. Furthermore, hybrid cells generated by fusion of MSC with different breast cancer cell lines including MCF10A, T47D, MCF7 and MDA-MB-231 were documented by bimolecular fluorescence complementation and acquired enhanced motility from MSC in contrast to less motile parental breast cancer cells [188].

Although several fusion-associated genes and soluble factors have been identified in recent years, molecular mechanisms underlying fusion formation between cancer cells and non-cancer cells, especially with MSC, are poorly understood. In general, membrane fusions encompass a multistep cascade and are thought to require fusogenic receptors which enable

membrane contact of two close interacting cell partner and induce fusion followed by effectors which accomplish membrane reorganization to facilitate fusion pore formation [189, 190].

1.5.1 Fusion-associated proteins and lipids

To better understand the molecular mechanisms underlying cell-cell fusion, deeper insights into vesicle/organelle fusion as well as cell-virus fusion are helpful.

During the study of vesicle/organelle fusion, osmotic and ionic gradients have been shown to be required for membrane fusion processes including exocytosis, endocytosis and vacuole fusion [191, 192]. A decrease of the osmolyte concentration in the cytoplasm elevated vacuole autofusion while an increase of osmolyte concentration inhibited fusion events revealing that osmotic shifts impact fusion [191]. Moreover, the $Na^+(K^+)/H^+$ exchanger ubiquitous to all cells and regulating compartmental osmolytes, volume and pH [193] has been demonstrated to be important for the fusion of multivesicular bodies with vacuoles, the last step of the endocytic pathway [194]. Deletion of the exchanger disturbed the fusogenicity of the multivesicular bodies. By contrast, heterofusion of sodium/proton transporter-negative vacuoles with wildtype multivesicular bodies was similar to heterofusion between wildtype organelles [194].

During the study of cell-virus fusion, a plethora of viral proteins has been identified as fusogens. In particular, two prominent fusogenic proteins, namely syncytin-1 and syncytin-2, have been deeply investigated in cell fusion. Acquired during evolution as envelope gene from a retrovirus by a mammalian host, both proteins are involved in the fusion process of placental trophoblasts to syncytiotrophoblasts. Whereas syncytin-1 is encoded by the envelope gene of human endogenous retrovirus (HERV-W), syncytin-2 is encoded by the HERV-FRD retroviral gene [195]. Both proteins exert their fusogenic potential together with their appropriate receptors. The human sodium-dependent neutral amino acid transporters type 1 and 2 (ASCT-1 and ASCT-2) can serve as receptors for syncytin-1 [196]. Alternatively, the major facilitator superfamily domain containing protein-2A (MFSD-2A) represents a multi-spanning membrane protein and functions as receptor for syncytin-2 [197]. In addition to the involvement of trophoblast fusion, syncytin-1 and syncytin-2 have been identified as regulators for cancer-cancer and cancer-endothelial cell fusion. Down-regulation of syncytin-1 inhibited fusion of MCF7 and MDA-MB-231 breast cancer cells with

endothelial cells [198]. Likewise, activation of syncytin-2 and MFSD-2A expression in MCF7 breast cancer cells facilitated MCF7 cell fusion [199].

Further proteins stimulating fusion of cells are represented by OC- (osteoclast-stimulatory transmembrane protein) and DC- (dendritic cell-specific transmembrane protein) stamp promoting the fusion of mononuclear osteoclast precursors or macrophages to multinucleated osteoclasts and giant cells, respectively [169, 200]. By contrast, the fusion of sperm and egg is mediated by sperm-localized IZUMO1 in cooperation with egg-derived tetraspanin CD9 which might cooperate with additional proteins like integrins and glycosylphosphatidylinositol (GPI)-anchored proteins [201]. Of interest, members of the ADAM (a disintegrin and metalloproteinase domain) family have been correlated to both physiological cell fusion processes, sperm-egg-fusion and multinucleation of osteoclast precursors and macrophages [202].

Nevertheless, it seems more likely that an orchestrated network of proteins, lipids and soluble factors mediates the fusion of two adjacent cells generating hybrid cells. Indeed, there is increasing evidence that adhesion proteins together with lipid rafts and rearrangement of the actin cytoskeleton are prerequisite for cellular fusion processes [189, 190, 203, 204]. For instance, despite the presence of cell-cell adhesion disruption of lipid rafts (areas on plasma membrane abundant of sphingolipids and cholesterol) by sequestering cholesterol inhibited the fusion of osteoclasts [205].

Overall, the initial steps of cell-cell fusion can be summarized into two parts. Firstly, fusing cell partners require the expression of transmembrane fusogenic proteins and secondly, a fully functional actin cytoskeleton is necessary for an active driving force generating membrane protrusions such as lamellipodia and filopodia for the promotion of cell fusion [190].

1.5.2 Fusion stimulating soluble factors and pro-fusogenic conditions

In addition to membrane-bound proteins, lipids, and actin cytoskeleton rearrangements, soluble factors, particularly cytokines, impact cell fusion by exertion of pro-fusogenic functions. Mainly described in the formation of osteoclasts or giant cells are cytokines like e.g. IFN-γ, IL-3, IL-4, IL-6 or TNF-α which have been discussed to stimulate cell fusion [206-209].

Certain microenvironmental conditions might impact the cell fusion rate including hypoxia, low pH and apoptosis. Hybrid cell formation between MSC and various breast cancer cell lines such as MDA-MB-231 and MCF10A could be increased during hypoxic conditions (2% O_2, 5% CO_2, and 93% N_2) in contrast to normoxic conditions with 21% of oxygen. Moreover, apoptosis-enhanced cell fusion by treatment with a caspase inhibitor lowered cell fusion whereas incubation with apoptotic cells increased the cell fusion rate [188]. Especially, viral mediated cell-to-cell fusion has been demonstrated to depend on pH. The majority of studies reports an increase in fusion under acidic / low pH conditions [210, 211].

Even though these various factors and specific conditions have been described to enhance cell fusion, an explanation about the detailed mechanism how cell fusion is regulated is still missing.

1.6 Aim of doctoral thesis

The observations that direct and indirect crosstalk between MSC and cancer cells, in particular breast cancer cells, leads to bidirectional alterations in phenotype and function is more than accepted although the outcome of these interactions, whether they contribute to tumorigenesis or they inhibit tumor growth, is still controversially discussed.

However, one of these occurring interaction types is represented by cell fusion, a rare event, which has been demonstrated in several publications. Thereby, merging of MSC with cancer cells ended up in hybrid cells which acquired characteristics from both parental cell populations.

Nevertheless, profound suggestions about potential cellular mechanisms underlying MSC-cancer cell fusion are missing. In addition, characterization and functional studies of hybrid cells are scarce.

Therefore, the aim of the doctoral thesis was on the one hand to better characterize the hybrid cells resulting from fusion between human umbilical cord-derived MSC with different breast (and ovarian) cancer cells with regard to their proliferation potential, chromosomal stability, stem cell marker expression, their ability to induce primary tumor growth in vivo and their responsiveness to chemotherapeutics. On the other hand, the mechanisms underlying MSC-cancer cell fusion should be investigated for potential involvement of established fusogens and other factors.

A detailed characterization of hybrid cells in combination with potential cellular mechanisms of cell fusion might help to further describe the role of mesenchymal stem cells during tumorigenesis.

2. Publications

This thesis is based on the publications listed below. All publications were accepted in peer reviewed journals except for 2.4 which has been submitted for revision.

The publications are attached in the following sections:

2.1 In vitro fusion of normal and neoplastic breast epithelial cells with human mesenchymal stroma/stem cells partially involves tumor necrosis factor receptor signaling.

Melzer C, von der Ohe J, Hass R.

Stem Cells. 2018 Mar 23. doi: 10.1002/stem.2819. [Epub ahead of print]

2.2 Enhanced metastatic capacity of breast cancer cells after interaction and hybrid formation with mesenchymal stroma/stem cells (MSC).

Melzer C, von der Ohe J, Hass R.

Cell Commun Signal. 2018 Jan 5;16(1):2. doi: 10.1186/s12964-018-0215-4.

2.3 MSC stimulate ovarian tumor growth during intercellular communication but reduce tumorigenicity after fusion with ovarian cancer cells.

Melzer C, von der Ohe J, Hass R.

Cell Commun Signal. 2018 Oct 13;16(1):67. doi: 10.1186/s12964-018-0279-1.

2.4 In vivo cell fusion between mesenchymal stroma/stem-like cells and breast cancer cells.

Melzer C, von der Ohe J, Hass R.

Manuscript

2.1 In vitro fusion of normal and neoplastic breast epithelial cells with human mesenchymal stroma/stem cells partially involves tumor necrosis factor receptor signaling

Catharina Melzer, Juliane von der Ohe and Ralf Hass

published in

Stem Cells

2018 Jul;36(7):977-989.

doi: 10.1002/stem.2819.

Epub 2018 Mar 28.

Author contribution statement:

Catharina Melzer (CM) performed the experiments (Fig. 1, 2, 3B-D, 4, 5B-D, 6B, 7 and table 1) and analyzed the data. CM co-wrote the manuscript.

STEM CELLS

CANCER STEM CELLS

In Vitro Fusion of Normal and Neoplastic Breast Epithelial Cells with Human Mesenchymal Stroma/Stem Cells Partially Involves Tumor Necrosis Factor Receptor Signaling

CATHARINA MELZER, JULIANE VON DER OHE, RALF HASS

Key Words. Hybrid cells • Mesenchymal stem cells • Breast and ovarian cancer • Tumor microenvironment • Tumor necrosis factor receptor

Biochemistry and Tumor Biology Lab, Department of Obstetrics and Gynecology, Hannover Medical School, Hannover, Germany

Correspondence: Ralf Hass, Ph.D., Biochemistry and Tumor Biology Lab, Department of Obstetrics and Gynecology (OE 6410), Hannover Medical School, Carl-Neuberg-Str. 1, Hannover D–30625, Germany. Telephone: +49 511 532 6070; e-mail: hass.ralf@mh-hannover.de

Received August 24, 2017; accepted for publication February 24, 2018; first published online in STEM CELLS *EXPRESS* March 23, 2018.

http://dx.doi.org/10.1002/stem.2819

ABSTRACT

Formation of hybrid cells by "accidental cell fusion" of normal and neoplastic breast epithelial cells with local tissue-associated mesenchymal stroma/stem-like cells (MSC) in an inflammatory microenvironment can generate new cancer cell populations whereby molecular signaling mechanisms of this process remain unclear. Fusions of lentiviral enhanced green fluorescent protein-labeled MSC with mcherry-labeled breast epithelial cells were quantified and effects of tumor necrosis factor alpha (TNF-α) and receptor downstream signaling were investigated. Cocultures of MSC with normal human mammary epithelial cells, with neoplastic MCF10A, or with MDA-MB-231 or MCF7 breast cancer cells demonstrated hybrid cell formation between 0.1% and about 2% of the populations within 72 hours, whereby the fusion process occurred in less than 5 minutes. Addition of the pro-inflammatory cytokine TNF-α significantly enhanced MCF10A-MSC cell fusion. Small-interfering RNA (siRNA) knockdown experiments revealed an involvement of tumor necrosis factor (TNF) receptor-1 and -2 in this process. This was also substantiated by siRNA knockdown of tumor necrosis factor receptor type 1-associated death domain which abolished TNF-α-stimulated fusion. While TNF receptor signaling can be relayed via the Mitogen-activated protein kinase 8 (MAPK8), NF-κB or cell death pathways, examination of further downstream signaling exhibited little if any effects of MAPK8 or RelA (p65) on TNF-α-mediated cell fusion, respectively. These data suggested that cell fusion between MSC and MCF10A breast epithelial cells can be stimulated by TNF-α involving TNF receptor-activated cell death pathways or additional NF-κB signaling. STEM CELLS *2018; 00:000–000*

SIGNIFICANCE STATEMENT

Mesenchymal stroma/stem cells play a pivotal role during tumorigenesis by direct and indirect interactions with cancer cells. This study shows that direct interactions can spontaneously fuse stroma/stem cells and breast cancer cells leading to hybrid cells carrying cancer cell and stroma/stem cell-like characteristics. Importantly, the pro-inflammatory cytokine tumor necrosis factor alpha, which is abundant in the tumor microenvironment, reinforced certain cell fusions involving tumor necrosis factor receptor 1 and tumor necrosis factor receptor 2 signaling with downstream tumor necrosis factor receptor type 1-associated death domain and certain NF-κB or apoptosis pathways. Thus, mesenchymal stroma/stem cells contribute to tumor heterogeneity via new hybrid cell formation exhibiting altered properties.

INTRODUCTION

Cell fusion usually represents a rare process in the course of cellular interactions, nevertheless, its importance is documented during development of certain tissues such as (a) muscle fiber formation by repetitive fusion of myoblasts to multinucleated myocytes, (b) bone metabolism and turnover by fusion of osteoclasts, (c) placenta formation by fusion of fetal trophoblasts to syncytiotrophoblasts. Likewise, a merge of gamete genomes by rearrangement of haploid chromosomes to a diploid embryonic stem cell is achieved by fusion of egg and sperm [1, 2].

Cell fusion results in the formation of hybrid cells either by homotypic (fusion of cells from the same population = autofusion) or by heterotypic processes (hybrid formation of different cell types = heterofusion) [3]. Previous work has identified some factors with

©AlphaMed Press 2018

fusogenic properties which include truncated genes in the mammalian genome originating from HERV-W retroviral envelope genes and encoding the proteins syncytin-1 and -2 predominantly found in placental syncytiotrophoblasts [4, 5]. Moreover, formation of multinucleated myocytes and macrophage fusion can involve the Dock180 (dedicator of cytokinesis) guanine nucleotide exchange factor associated with members of the ELMO (Engulfment and Cell Motility) protein family for subsequent Rac1 activation and disproportional regulation of the actin cytoskeleton [6, 7].

Besides these normal development-associated and tightly regulated fusion processes, hybrid cell formation can also occur spontaneously by "accidental cell fusion" which is favorized by a fusion-permissive environment including acidic pH, hypoxia, accumulation of damage-associated molecular patterns, and membrane lipids destabilizing ions and peptides [8, 9]. Accordingly, cell fusion can generate aneuploidy, chromosomal instability, and DNA damage, all of which cause multiple genetic aberrations and potentially neoplastic development [10]. Indeed, cell fusion can be also detected in existing cancers including tumors of the breast [11, 12], whereby endothelial alanine, serine and cysteine selective transporter-2 (ASCT2) can function as a syncytin receptor allowing heterofusion of breast cancer cells with endothelial cells [13]. However, the underlying regulatory interplay for hybrid cell formation by spontaneous breast cancer cell fusion is unknown.

A tumor site is also characterized by an inflammatory microenvironment including elevated levels of pro-inflammatory cytokines such as tumor necrosis factor alpha (TNF-α). Multifunctional mesenchymal stroma/stem-like cells (MSC) are recruited to modulate this inflammatory process following interaction with immune cells and breast cancer cells within the tumor microenvironment. These eventually close and tight cell-cell interactions can result in the formation of breast cancer hybrid cells [14] although associated molecular mechanisms for these events remain unclear.

In the present work, homo- and heterotypic fusion events between normal and neoplastic breast epithelial cells and MSC were investigated. Moreover, potential molecular mechanisms demonstrated little if any involvement of known fusogenic partners such as syncytins, MFSD2A, and ASCT2. Alternatively, the data demonstrated that activation of the tumor necrosis factor (TNF) receptors within the inflammatory tumor microenvironment contributed to hybrid cell formation by neoplastic breast epithelial cell fusion with MSC.

Materials and Methods

The use of primary human MSC following explant culture from umbilical cord tissue was approved by the Ethics Committee of Hannover Medical School, Project #443 on February 26th, 2009, respectively, and informed written consent was obtained from each patient.

Cell Culture

All cells were tested for mycoplasma by the luminometric MycoAlert Plus mycoplasma detection kit (Lonza, Inc., Rockland, ME) according to the manufacturer's recommendations.

Mesenchymal Stroma/Stem Cells. MSC-like cells were derived from umbilical cord tissue and isolated as previously described [15, 16]. MSC were cultured at 37°C in a humidified atmosphere with 5% CO_2 in minimum essential medium (αMEM) supplemented with 10% allogenic human AB-serum (commercially obtained from University Campus Lübeck, Germany), 100 U/ml penicillin, 100 μg/ml streptomycin and 2 mM L-glutamine (Sigma Chemie GmbH, Steinheim, Germany). For the experiments, primary MSC cultures were used from six donors with different passages ranging from P4 to P8 (MSC100314, MSC290115, MSC300415, MS280416, MSC060616, and MSC180816).

Breast Cancer Cells. Human breast carcinoma cell lines MCF10A, MCF7, and MDA-MB-231 were obtained from ATCC. The benign breast cancer cell line MCF10A was grown in phenol red-free Mammary Epithelial Cell Basal Medium (MECBM) with appropriate supplement mix (PromoCell, Heidelberg, Germany). MCF7 breast cancer cells were cultivated in Dulbecco's modified Eagle's medium supplemented with 10% (vol/vol) fetal calf serum (FCS), 100 U/ml penicillin, 100 μg/ml streptomycin and 2 mM L-glutamine (Sigma). Triple negative breast cancer cell line MDA-MB-231 was cultured in Leibovitz's L-15-medium (Life Technologies, Darmstadt, Germany) with medium supplements [10% (vol/vol) FCS, 100 U/ml penicillin, 100 μg/ml streptomycin and 2 mM L-glutamine (Sigma)]. Authentication of the human breast carcinoma cell lines was performed by short tandem repeat (STR) fragment analysis using the GenomeLab human STR primer set (Beckman Coulter, Inc., Fullerton, CA).

Primary human breast cancer-derived epithelial cells (HBCEC) were isolated from explant cultures of human breast cancer biopsies tested negative for HIV-1, hepatitis B and C, bacteria, yeast and fungi and grown in phenol red-free MECBM with supplements (PromoCell) as described previously [17].

Human Mammary Epithelial Cells. Primary normal human mammary epithelial cells (HMEC) were isolated from a 50-year-old caucasian female and commercially provided by Bio-Whittaker, Inc. (Walkersviell, MD) as culture passage 7 (Lot #1F1012). HMEC were also cultured in MECBM with appropriate supplements (PromoCell) as indicated [18].

Cocultures. In order to discriminate between MSC and breast cancer cell lines in coculture, both cell types were stably transduced with a third generation lentiviral SIN vector carrying either the enhanced green fluorescent protein (eGFP) gene (MSC^{GFP}) or the mCherry gene ($MCF10A^{cherry}$, $MCF7^{cherry}$, $MDA\text{-}MB\text{-}231^{cherry}$). Moreover, for evaluation of autofusion data, also MSC^{cherry}, $MCF10A^{GFP}$, $MCF7^{GFP}$, and $MDA\text{-}MB\text{-}231^{GFP}$ were generated by stable transduction.

Coculture between MSC^{GFP} and primary HMEC or HBCEC was performed after transient labeling of the primary human breast epithelial cells with a PKH26 red fluorescent dye (Sigma) according to the manufacturer's recommendation.

Cocultures of 50% of GFP-labeled MSC and 50% of cherry-labeled breast epithelial cells were incubated up to 4 days in 24-well plates at an initial cell density between 3,000 and 8,000 cells/cm^2. Whereas cocultures of MSC with MCF7 or

©AlphaMed Press 2018

with MDA-MB-231 were cultivated in MSC medium, cocultures with MCF10A, HBCEC, and HMEC were grown in mix-medium consisting of 40% of MSC medium and 60% of MECBM (PromoCell).

Proliferation Measurement

Proliferation of monoculture and coculture cells was analyzed by Fluoroskan measurements. Briefly, mono-cultures (2,000 cells/well) and cocultures (4,000 cells/well) were initiated in flat bottom 96-well plates (Nunc, Thermo Fisher Scientific, Roskilde, Denmark). At indicated time points, the medium was removed and cells were lysed with 10% SDS following detection of fluorescence intensity of mCherry (excitation 584 nm, emission 612 nm) and eGFP (excitation 485 nm, emission 520 nm) using the Fluoroskan Ascent FL (Thermo Fisher Scientific, Schwerte, Germany) since the fluorescence intensity is proportional to the cell number.

Fluorescence Time Lapse Imaging

Initially, 1,000 cells/cm^2 of cocultures between MSC^{GFP} and MCF10A^{cherry} or HBCEC$^{PKH26\ red}$ were incubated overnight to allow attachment. Thereafter, time lapse fluorescence video microscopy was applied using Leica microscope AF6000 with fluorochrome settings for GFP and mCherry. Single-channel pictures were taken every 5 minutes for up to 3 days and overlayed using LAS AF (Leica Application Suite Advanced Fluorescence) software.

Quantification of Hybrid Cells

To quantify the amount of hybrid cells, cocultures were initiated and cultivated for up to 96 hours in appropriate medium in 24-well plates with a defined cell number. At indicated time points, each well was quantified for dual fluorescent cells (GFP- and cherry-positive fluorescence revealing a yellowish color) using a fluorescence microscope (Olympus IX50) with green and red fluorescence filters and an additional fluorescein isothiocyanate (FITC)/tetramethylrhodamine (TRIC) fluorescence dual band filter. After counting the amount of double fluorescent cells/well, the cocultures were trypsinized and the total cell number was evaluated in a hemocytometer to calculate the percentage of hybrid cells. All experiments were performed with different individual MSC cocultures whereby hybrid cells were counted in three replicates of each experiment.

Small-Interfering RNA Transfection

A reverse transfection was applied for each knockdown experiment using small-interfering RNAs (siRNAs) according to the manufacturer's protocol (Dharmacon, GE Healthcare, Uppsala, Sweden). Cocultures of MCF10A^{cherry} with MSC^{GFP} were transfected with 25 nM of the following listed target siRNA, respectively, using DharmaFECT1 transfection reagent (cat. #T-2001-02) diluted 1:1,000 in transfection medium (antibiotic-free mix medium) for 24 hours:

- siGENOME Human ERVW-1 siRNA SMARTpool, cat. #M-010573-00
- siGENOME Human SLC1A5 siRNA SMARTpool, cat. #M-007429-01
- siGENOME Human ERVFRD-1 siRNA SMARTpool, cat. #M-032206-00
- siGENOME Human MFSD2A siRNA SMARTpool, cat. #M-014999-00
- siGENOME Human TNFRSF1A siRNA SMARTpool, cat. #M-005197-00
- siGENOME Human TNFRSF1B siRNA SMARTpool, cat. #M-003934-00
- siGENOME Human TRADD siRNA SMARTpool, cat. #M-004452-01
- siGENOME Human MAPK8 siRNA SMARTpool, cat. #M-003514-04
- siGENOME Human RELA siRNA SMARTpool, cat. #M-003533-02-0005 or
- nontargeting siRNA siGENOME Nontargeting siRNA #3, cat.# D-001210-03

Thereafter, cocultures were washed with phosphate buffered saline (PBS) and cultured in normal mix-medium. The transfection efficiency was either validated by flow cytometry and Western Blot analysis or by transfection of 25 nM siGLO-^{Green} (cat. #D001630-01).

Flow Cytometry Analysis and Fluorescence Activated Cell Sorting

For validation of transfection efficiency, monocultures and cocultures were harvested and analyzed via flow cytometry. After washing with PBS, cells were incubated with labeled monoclonal CD120a-PE antibody (clone REA252, IgG1; Miltenyi Biotec; PE, phycoerythrin) at 4°C for 30 minutes. A PE-labeled REA control S antibody (clone REA293; Miltenyi Biotec) served as a control. After antibody staining, cells were washed twice with PBS and analyzed by a flow cytometer using FACSCalibur (BD Biosciences, Singapore) and FlowJo V10 analysis software.

In a separate experimental approach, MSC^{GFP} were incubated with labeled monoclonal CD120a-PE antibody and sorted via fluorescence activated cell sorting (FACS) into CD120a-PE positive and CD120a-PE negative cells.

Immunoblot Analysis

Cell lysates of fluorescence-labeled MSC and normal and neoplastic breast epithelial cells in monoculture and coculture were prepared in reswelling buffer (8 M urea [Carl Roth GmbH Co KG, Karlsruhe, Germany]), 1% CHAPS (3-[(3-Cholamidopropyl)-dimethylammonio]-1- propanesulfonate) (Carl Roth GmbH Co KG), 0.002% (wt/vol) bromophenol blue (SERVA Electrophoresis GmbH, Heidelberg, Germany) and freshly prepared 0.4% (wt/vol) Dithiothreitol (Carl Roth GmbH Co KG)) or lysis buffer as described previously [15]. Protein concentration was determined using the colorimetric BCA-assay (BCA, bicinchoninic acid; Thermo Fisher Scientific) and 40 μg protein were applied to SDS-polyacrylamide gel electrophoresis and subsequent Western blotting. Membranes were incubated at 4°C overnight with: monoclonal anti-GAPDH (clone 6C5, mouse, dilution 1:200, Santa Cruz Biotechnology, Inc.; GAPDH, glyceraldehyde 3-phosphate dehydrogenase), polyclonal anti-TRADD (TNF receptor type 1-associated death domain protein) (rabbit, dilution 1:1,000, Cell Signaling Technology) and monoclonal anti-JNK1 (clone 2C6, mouse, dilution 1:1,000, Cell Signaling Technology). After washing six times with tris-buffered saline (TBS)/Tween-20, blots were incubated with the appropriate horseradish peroxidase-conjugated anti-mouse IgG (dilution 1:5,000) or anti-rabbit IgG (dilution 1:5,000)

©AlphaMed Press 2018

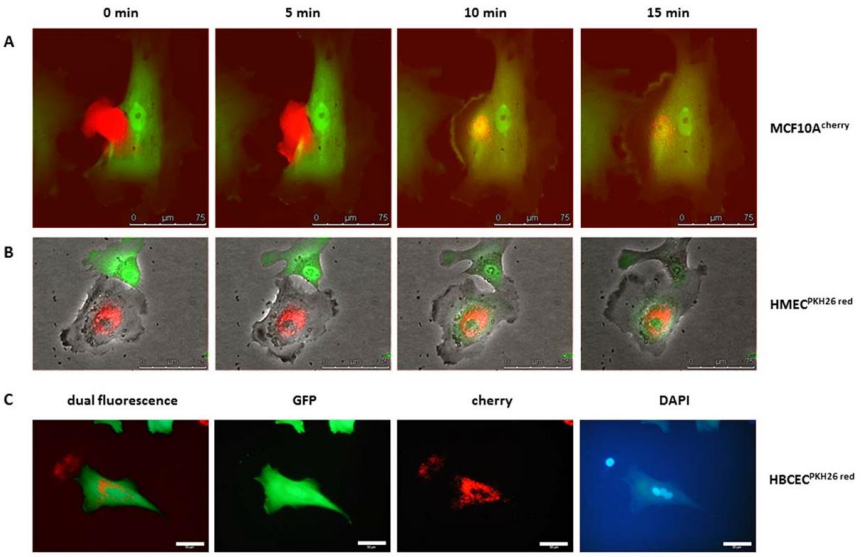


Figure 1. Fluorescence microscopy of hybrid cells. Images from time lapse fluorescence video microscopy revealed formation of hybrid cells in cocultures between MSC^{GFP} and $MCF10A^{cherry}$ **(A)** and between MSC^{GFP} and primary $HMEC^{PKH26\ red}$ **(B)**, respectively. This event proceeded within 5 minutes. Scale bars: 75 μm. **(C):** Fluorescence microscopy of cocultures between MSC^{GFP} and primary $HBCEC^{PKH26\ red}$ demonstrated multinuclear hybrid cells as documented after DAPI staining (1:50,000 for 5 minutes, Invitrogen, Carlsbad, CA). Scale bars: 50 μm. Abbreviations: DAPI, 4′,6-diamidino-2-phenylindole; GFP, green fluorescent protein.

secondary antibody (both from GE Healthcare) for 1 hour at room temperature. After repeated washing, membranes were visualized by autoradiography using WesternBright Chemiluminescent Substrate Quantum (Biozym Scientific, Hess. Oldendorf, Germany).

Transcript Analysis by Reverse Transcription Polymerase Chain Reaction

Total cellular RNA was isolated using RNeasy Mini Kit (Qiagen, Hilden, Germany) according to manufacturer's protocol. Thereafter, 1 μg of RNA was reverse transcribed into cDNA using 0.5 mM of NTP, 5 μM of Random Hexan primer, 5 μM of Oligo$(dT)_{18}$ primer, 1 U of RiboLock RNase Inhibitor and 5 U of Reverse Transcriptase in appropriate reaction buffer (all reagents from Thermo Scientific). The cDNA reactions were performed for 10 minutes at 25°C, followed by 1 hour at 42°C and 10 minutes at 72°C. As a template, 2.5 μl of cDNA were used for standard polymerase chain reaction (PCR) with following specific primers (all primers were customized by Eurofins MWG GmbH, Ebersberg, Germany):

- eGFP (sense: 5′-CTA TAT CAT GGC CGA CAA GCA GA-3′; antisense: 5′-GGA CTG GGT GCT CAG GTA GTG G-3′; amplification product 165 bp)
- mcherry (sense: 5′-TTC ATG TAC GGC TCC AAG GC-3′; antisense: 5′-CTG CTT GAT CTC GCC CTT CA-3′; amplification product 297 bp)
- syncytin-1 (sense: 5′-AGG AGC TTC GAA ACA CTG GA-3′; antisense: 5′-GTG AGC TAA GTT GCA AGC CC-3′; amplification product 494 bp [19])
- ASCT2 (sense: 5′-GAC CGT ACG GAG TCG AGA AG-3′; antisense: 5′-GGG ACG CAG CAG AAC ATT AT-3′; amplification product 445 bp [20])
- syncytin-2 (sense: 5′-AGC AGC CGT AGT CCT TCA AA-3′; antisense: 5′-AGG GGA AGA ACC CAA GAG AA-3′; amplification product 231 bp [21])
- MFSD2A (sense: 5′-CTC CTG GCC ATC ATG CTC TC-3′; antisense: 5′-GGC CAC CAA GAT GAG AAA-3′; amplification product 129 bp)
- TNF-α (sense: 5′-AGT GAC AAG CCT GTA GCC C-3′; antisense: 5′-GCA ATG ATC CCA AAG TAG ACC-3′; amplification product 443 bp [22])
- TNFR1 (sense: 5′-TGC CAG GAG AAA CAG AAC A-3′; antisense: 5′-AAC CAA TGA AGA GGA GGG AT-3′; amplification product 223 bp [22])
- TNFR2 (sense: 5′-TCC CAA GCC AGC TCC ACA ATG-3′; antisense: 5′-AGG GGC AGG GGC TTC TCT TC-3′; amplification product 158 bp [23])
- GAPDH as a control (sense: 5′-ACC ACA GTC CAT GCC ATC AC-3′; antisense: 5′-TCC ACC ACC CTG TTG CTG TA-3′; amplification product 452 bp [24]).

Aliquots of 25 μl of the PCR products were separated on a 2% agarose gel including the standard GeneRuler 100 bp DNA Ladder (Thermo Scientific) and were visualized by GelRed (Biotium, Inc., Fremont, CA) staining.

Real-Time PCR (qPCR)

RNAs from MSC^{GFP}/$MCF10A^{cherry}$ cocultures double-transfected with siRNAs of either syncytin-1 and ASCT2 or syncytin-2 and MFSD2A were isolated and reverse transcribed into cDNA. Real-time PCR was performed for:

©AlphaMed Press 2018

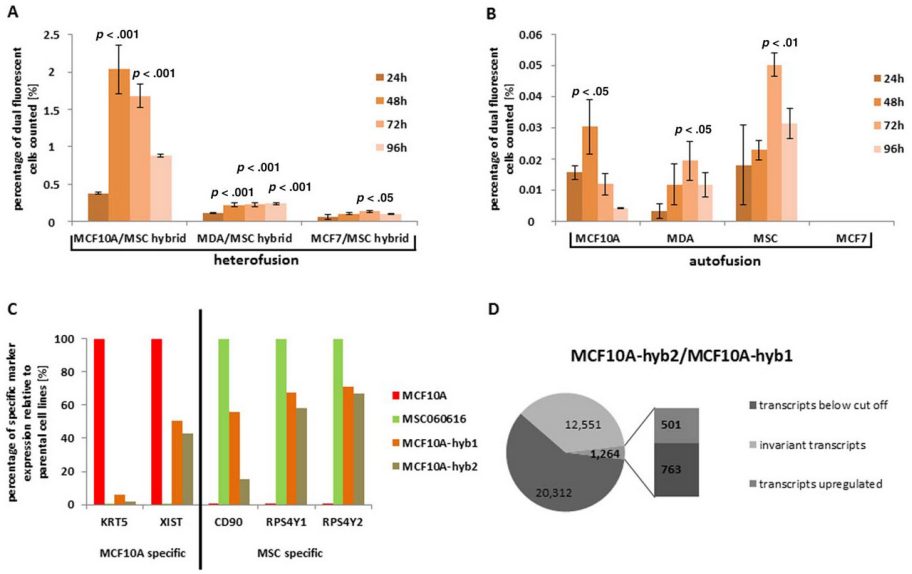


Figure 2. Quantification of hybrid cell formation and characterization of MCF10A-hybrids. Cocultures were performed for up to 96 hours (cell ratio 50:50) and quantified for dual fluorescent (green fluorescent protein and cherry positive) cells. **(A):** Heterofusions were quantified in cocultures of MSC^{GFP} with $MCF10A^{cherry}$ (5,000 cells/cm^2), MSC^{GFP} with $MDA\text{-}MB\text{-}231^{cherry}$ (5,000 cells/cm^2), or MSC^{GFP} with $MCF7^{cherry}$ (3,000 cells/cm^2). **(B):** For quantification of autofusion, $MCF10A^{cherry}$ were cocultured with $MCF10A^{GFP}$ (8,000 cells/cm^2), $MDA\text{-}MB\text{-}231^{cherry}$ with $MDA\text{-}MB\text{-}231^{GFP}$ (8,000 cell/cm^2), MSC^{cherry} with MSC^{GFP} (3,000 cells/cm^2) or $MCF7^{cherry}$ with $MCF7^{GFP}$ (3,000 cells/cm^2). Both hetero- and autofusion events occurred time-dependent whereby heterofusion events were detectable up to 10-fold more often than autofusion events. The relative percentage of dual fluorescent cells was calculated by the mean ± SD from cocultures in triplicate and significance (p) was calculated by ANOVA followed by Dunnett's multiple comparisons test. **(C):** Relative expression analysis of specific markers for MCF10A (KRT5 = cytokeratin 5, XIST = X interactive-specific transcript [female-specific gene]) and specific markers for MSC (CD90, RPS4Y1 = ribosomal protein S4, Y-linked-1; RPS4Y2 = ribosomal protein S4, Y-linked-2 [male-specific genes]) was calculated for MCF10A-hyb1 and MCF10A-hyb2 cells in comparison to their parental cell populations. For relative evaluations, the expression levels of MCF10A or MSC were used as a control (set to 100%). **(D):** Microarray analysis followed by quantification and comparison of transcripts with altered expression levels in MCF10A-hyb1 and MCF10A-hyb2 cell populations was performed revealing 1,264 differences in gene expression (501 upregulated and 763 downregulated transcripts). Changes in transcript levels of more than twofold were considered as up- or downregulated. Abbreviations: ANOVA, analysis of variance; MSC, mesenchymal stroma/stem-like cells.

- SLC1A5 TaqMan Gene Expression Assay, FAM-MGB, Hs0105642_m1
- MFSD2A TaqMan Gene Expression Assay, FAM-MGB, Hs00293017_m1
- RELA TaqMan Gene Expression Assay, FAM-MGB, Hs01042014_m1
- GAPDH TaqMan Gene Expression Assays, FAM-MGB, Hs99999905_m1 (all from Applied Biosystems)

A total of 50 ng of cDNA was used for each 20 μl reaction using StepOnePlus Real-Time PCR System (Thermo Fisher Scientific) by incubating the reactions at 95°C for 2 minutes, followed by 40 cycles of 95°C for 5 seconds and 60°C for 20 seconds. Relative quantities (RQs) were calculated with the comparative cycle threshold (C_T) method.

Real-Time RT PCR TaqMan Array, Human Tumor Necrosis Factor Receptor 1 Pathway

Cocultures of $MCF10A^{cherry}$ and MSC^{GFP} were stimulated for 72 hours with 100 U/ml TNF-α and thereafter, total RNA was isolated and reverse transcribed (s. transcript analysis by reverse transcription PCR). Unstimulated cocultures served as a control. Complementary DNA (50 ng/well) from both cocultures was amplified using TaqMan Array Human tumor necrosis factor receptor 1 (TNFR1) Pathway Fast 96-well (Thermo Fisher Scientific) and StepOnePlus Real-Time PCR System according to manufacturer's protocol. RQs were calculated with the comparative cycle threshold (C_T) method.

Microarray-Based mRNA Expression Analysis

RNA microarray analysis was performed according to the previously described details [14]. The parental cells $MSC060616^{GFP}$ and $MCF10A^{cherry}$ were investigated and likewise the resulting two hybrid populations $MCF10A\text{-}hyb1^{GFP/cherry}$ and $MCF10A\text{-}hyb2^{GFP/cherry}$. Alterations in transcript levels were compared between parental cells and hybrid cells displaying a more than twofold difference in gene expression. Microarray data are uploaded at NCBI database with accession no. GSE106756.

Gene Ontology Enrichment Analysis

Expression levels of genes from the microarray mRNA analysis that were more than twofold upregulated or downregulated

©AlphaMed Press 2018

Table 1. Gene Ontology analysis of MCF10A-hyb1 and MCF10A-hyb2 cells.

Compared populations	Up- or downregulation	Over- or underrepresentation of gene ontologies	Biological processes according to gene ontology enrichment analysis
hyb1/MCF10A hyb2/MCF10A hyb1/MSC hyb2/MSC	Upregulated	Under-represented	RNA / mRNA processing RNA splicing mRNA metabolic process DNA replication DNA metabolic process
hyb1/MSC hyb2/MSC	Upregulated	Over-represented	Small molecule metabolic process Organic acid metabolic process Oxidation-reduction process Carboxylic acid metabolic process Lipid metabolic process
hyb1/MCF10A hyb2/MCF10A	Upregulated	Over-represented	Regulation of cell migration Extracellular matrix organization Regulation of cell differentiation Lipid metabolic process Regulation of angiogenesis Positive regulation of cell death Cell adhesion
hyb1/MCF10A hyb2/MCF10A hyb1/MSC hyb2/MSC	Downregulated	Over-represented	Cell cycle Mitotic cell cycle Chromosome segregation Cell division DNA replication

Comparison of more than twofold changed expression levels between the different populations (MCF10A-hyb1 vs. MCF10A; MCF10A-hyb1 vs. MSC; MCF10A-hyb2 vs. MCF10A; MCF10A-hyb2 vs. MSC) were analyzed to obtain a list of GOs for biological processes. This list was sorted by *p* values which are determined by the binomial statistics according to the PANTHER Classification System whereby the most significant and relevant GOs are displayed.
Abbreviations: GOs, gene ontologies; MSC, mesenchymal stroma/stem-like cells.

within a specific set of data comparison (e.g., Hyb1/MCF10A or Hyb2/MSC) were processed online at the Gene Ontology Consortium website: http://www.geneontology.org/page/go-enrichment-analysis with focus on biological processes. Using the analysis tool from the PANTHER Classification System, a list of gene ontologies (GOs) was obtained demonstrating over- or underrepresentation in a specific set of data comparison.

Quantification of TNF-α Levels

The secretion of TNF-α in mono- and separated cocultures of MSC^{GFP} with $MCF10A^{cherry}$ was quantified using Human TNF-α Quantikine HS ELISA according to manufacturer's instructions (R&D Systems, Minneapolis, MN). Separated cocultures were obtained by FACS of GFP- and cherry-positive cells from a 3d MSC^{GFP}/$MCF10A^{cherry}$ coculture (cell ratio 50:50 at a density of 5,000 cells/cm^2). Following FACS, the separated cells were incubated as mono-cultures for further 24 hours. Thereafter, medium supernatant was collected and analyzed as separated cocultures by ELISA.

Results

MSC Fuse with a Variety of Breast Cancer Cells

Recent data suggested cell fusion between MSC and different breast (MDA-MB-231 and MCF7) and ovarian (NIH:OVCAR-3, SK-OV-3, and SCCOHT-1) cancer cells, respectively [25]. Here, we demonstrate that in addition to malignant breast cancer cell lines, MSC also form fusion cells with benign breast epithelial cells (MCF10A) and with normal HMEC strengthening the general occurrence of stem cell fusion with a plethora of malignant and nonmalignant cell types. Fluorescence time lapse imaging revealed hybrid formations between MSC and either MCF10A or HMEC within a short period of time (Fig. 1A, 1B, Supporting Information Figs. S1, S2, Videos S1–S7). The two different fusion partners directly interacted over a longer time frame of several hours, however, the actual fusion process involving connections of the cell membranes from both interaction partners proceeded within less than 5 minutes (Fig. 1A, 1B, Supporting Information Videos S1–S7). Likewise, patient-derived primary HBCEC demonstrated formation of hybrid cells following coculture with MSC (Fig. 1C) indicating similar effects in cell lines and primary breast cancer cells.

The amount of hybrid cells in cocultures of MSC^{GFP} with different breast cancer cell lines including $MCF10A^{cherry}$, MDA-MB-231^{cherry}, and $MCF7^{cherry}$ was quantified and all cocultures revealed a time-dependent hybrid formation with the highest percentage of dual fluorescent cell appearance between 48 and 72 hours (Fig. 2A). The amount of hybrid cell formation varied strongly between benign or malignant breast cancer cells as fusion partner for MSC. Thus, cocultures of MSC with $MCF10A^{cherry}$ revealed an up to 10-fold increased amount of hybrid cells (>2% after 48 hours) compared with cocultures of MSC with MDA-MB-231^{cherry} (0.2% after 48 hours) or MSC with $MCF7^{cherry}$ (0.1% after 48 hours) (Fig. 2A). Fluorescence microscopy images of these three cocultures substantiated the different percentages in cell fusion formation whereby distinct hybrid cells are exemplarily highlighted with a yellow arrow for each coculture and appropriate time points (Supporting Information Figs. S3–S5).

In addition to heterofusion events between MSC and various breast cancer populations, autofusion events among corresponding cell types themselves were observed and quantified (Fig. 2B). Likewise, hybrid formation in all auto cocultures was time-dependent with maximal appearance after 48 hours (0.03% for MCF10A) to 72 hours (0.02% for MDA and 0.05% for MSC). Of interest, cocultures of

©AlphaMed Press 2018

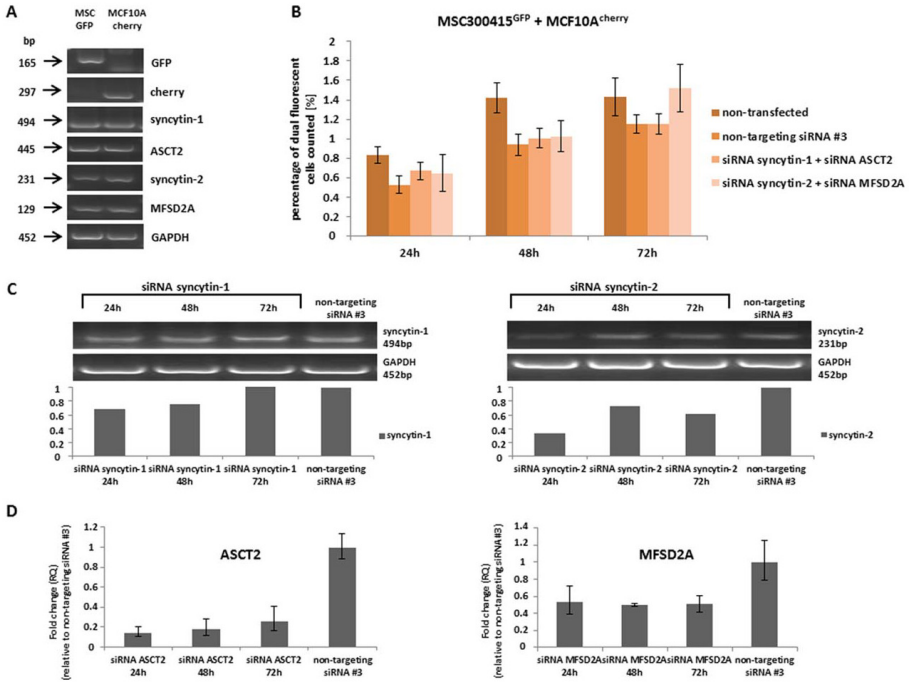


Figure 3. Effects of fusogenic factors during hybrid cell formation. **(A):** PCR analysis was performed with mcherry, eGFP, and the fusion-associated transcripts syncytin-1, ASCT2, syncytin-2, and MFSD2A in MSC300415^{GFP} and MCF10A^{cherry} cells, respectively. Unaltered GAPDH mRNA served as a control. **(B):** Significance of fusion cell formation by MCF10A^{cherry} and MSC300415^{GFP} was examined and quantified following double knock down with siRNAs targeting either syncytin-1 and ASCT2 or syncytin-2 and MFSD2A for 24 hours. The relative percentage of hybrid cells was calculated by the mean ± SD from cocultures in triplicate and significance (p) was calculated by ANOVA followed by Dunnett's multiple comparisons test. **(C):** Successful down-modulation of syncytin-1 and syncytin-2 was demonstrated by RT-PCR following siRNA transfection. Intensities were quantified using ImageJ with corresponding GAPDH expression as a reference. **(D):** Similarly, ASCT2 and MFSD2A siRNA knockdown was verified in cocultures between MCF10A^{cherry} and MSC^{GFP} for up to 72 hours by quantitative PCR. Gene expressions were normalized to the GAPDH and relative quantification was calculated via the comparative C_T method. Abbreviations: ANOVA, analysis of variance; ASCT2, alanine, serine and cysteine selective transporter 2; eGFP, enhanced fluorescent protein; GAPDH, glyceraldehyde 3-phosphate dehydrogenase; MSC, mesenchymal stroma/stem-like cells; PCR, polymerase chain reaction; RT-PCR, reverse transcription polymerase chain reaction; siRNAs, small-interfering RNAs.

MCF7^{cherry} with MCF7^{GFP} revealed little if any detectable autohybrids within 96 hours. Autofusion plays a pivotal role during physiological processes including the immune response with macrophages fusion to generate giant cells or muscle development to form multinucleated muscle fibers. However, the percentage of dual fluorescent cells resulting from autofusion events was at least 10-fold lower compared to the amount of heterofusion cells indicating that a fusion-permissive environment is increased by distinct molecular structures on different cell types compared with homotypic hybrid cell formation.

To confirm the formation of stable hybrid cells during coculture of MCF10A^{cherry} and MSC^{GFP}, a two time FACS of double fluorescing cells (GFP and cherry) followed by single cell cloning revealed two different hybrid populations, termed MCF10A-hyb1 and MCF10A-hyb2 with an altered spindle-like cell morphology (Supporting Information Fig. S6). RNA microarray analysis was performed for MCF10A-hyb1 and MCF10A-hyb2 cells in comparison to the parental MSC and MCF10A cells and revealed marked differences in transcript levels indicating the generation of two newly stable cell populations (Supporting Information Fig. S7). Indeed, the MCF10A-associated transcripts cytokeratin-5 (KRT5) and XIST appeared in both hybrid populations although undetectable in MSC. Vice versa, MSC-associated genes CD90, RPS4Y1 and RPS4Y2 were likewise expressed in the two hybrid populations but undetectable in MCF10A cells (Fig. 2C). Together, these findings substantiated MCF10A-hyb1 and MCF10A-hyb2 cells as new cell populations carrying selective markers from both originating parental cell types. In addition, MCF10A-hyb1 compared to MCF10A-hyb2 cells displayed only 1,264 differences in gene expression demonstrating more similarities between the two hybrid populations than to their parental cells (>5,340 differences in gene expression) (Fig. 2D, Supporting Information Fig. S7).

Further characterization of MCF10A-hyb1 and MCF10A-hyb2 cells was performed by gene ontology enrichment

 ©AlphaMed Press 2018

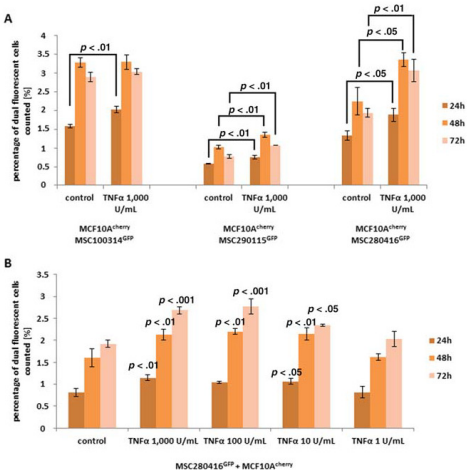


Figure 4. TNF-α increased hybrid cell formation. **(A):** Cocultures of MCF10A^{cherry} with three different MSC^{GFP} were initiated at a cell density of 3,000 cells/cm^2 (ratio 50:50) and hybrid cell formation was quantified in these three different cocultures in the presence of 1,000 U/ml TNF-α for up to 72 hours. The significance was calculated by the mean ± SD from each coculture in triplicate and significance (p) was calculated by Student's t test. **(B):** Different concentrations of TNF-α on fusion events were investigated in cocultures between MCF10A^{cherry} and MSC280416^{GFP} (3,000 cells/cm^2, ratio 50:50) stimulated with 1,000, 100, 10, and 1 U/ml TNF-α. The relative percentage of hybrid cells was calculated by the mean ± SD from cocultures in triplicate and significance (p) was calculated by ANOVA followed by Dunnett's multiple comparisons test. Abbreviations: ANOVA, analysis of variance; TNF-α, tumor necrosis factor alpha.

analysis (Table 1). Whereas decreased transcripts of both hybrid populations in comparison to the parental counterparts revealed an overrepresentation of gene ontology terms involved in cell cycle and cell division, gene ontologies covering DNA and RNA processes such as RNA splicing or DNA replication were underrepresented in increased transcripts of MCF10A-hyb1 and MCF10A-hyb2. Moreover, increased genes in MCF10A-hyb1 and MCF10A-hyb2 compared to MSC demonstrated an enrichment of GOs encompassing metabolic processes (e.g., redox processes or lipid metabolism). By contrast, increased transcripts in relation to MCF10A resulted in GO terms including cell migration and cell motility as well as regulation of cell differentiation or regulation of angiogenesis (Table 1). Taken together, these data suggested that both hybrid populations exhibit reduced proliferative capacity and altered metabolic activities compared to the parental MCF10A and MSC. Moreover, transcripts associated with migratory activity are increased in the hybrid populations compared to MCF10A cells.

Fusogenic Syncytins Play a Minor Role in MSC-Cancer Cell Fusion

For a potential mechanism of this cell fusion, further analysis was performed with the known fusogenic proteins syncytin-1 and syncytin-2 and the corresponding receptors ASCT2 and MFSD2A which are involved in formation of syncytiotrophoblasts [26]. Remarkably, these fusogenic proteins are also linked to pathologic developments such as preeclampsia and cancer whereby downregulation of syncytin-1 inhibited cell fusion between breast cancer cells and endothelial cells [20]. To validate a potentially similar involvement in the fusion of breast cancer cells with MSC, reverse transcription polymerase chain reaction (RT-PCR) analysis revealed expression of the fusogenic genes syncytin-1, ASCT2, syncytin-2, and MFSD2A in the two fusion partners MCF10A^{cherry} with MSC^{GFP}. Moreover, appropriately selective transcript levels of the cherry and GFP genes were expressed together with GAPDH as a control (Fig. 3A). Following down-modulation of syncytin-1 and ASCT2 or syncytin-2 and MFSD2A in the coculture by appropriate siRNA transfections, the amount of dual fluorescent cells was quantified after 24, 48, and 72 hours whereby nontransfected cocultures and nontargeting siRNA #3-transfected cocultures served as relevant controls. The transfection efficiency was tested using siGLO^{Green} in appropriate wild-type mono-cultures (MSC^{wt} and MCF10A^{wt}) (Supporting Information Fig. S8). Cell counting of green fluorescent cells, flow cytometric analysis and fluorescence microscopy revealed about 95% of transfected cells (Supporting Information Fig. S8).

Surprisingly, neither double knockdown of syncytin-1 and ASCT2 nor double knockdown of syncytin-2 and MFSD2A demonstrated any significant differences in hybrid cell formation compared to the nontargeting siRNA #3 control (Fig. 3B). A partial knock down of syncytin-1 and syncytin-2 was demonstrated by RT-PCR (Fig. 3C) and successful down-modulation of the corresponding fusion factors ASCT2 and MFSD2A was confirmed by qPCR (Fig. 3D). These findings suggested only minor involvement of the known fusogenic factors in the formation of tumor cell hybrids.

TNF-α Increases Hybrid Cell Formation and Decreases Proliferation of MCF10A^{cherry} and MSC^{GFP}

According to a permanent inflammation process within the tumor tissue microenvironment, we asked the question whether certain pro-inflammatory cytokines such as TNF-α may contribute to fusion-permissive conditions. Thus, stimulation of cocultures (MCF10A^{cherry} and MSC^{GFP}) with TNF-α (1,000 U/ml) for up to 72 hours revealed a significant elevation in hybrid cell formation compared to control cultures (Fig. 4A). These findings were reproducible and were substantiated using cocultures with MSC primary cultures from three different donors (MSC100314 in P6, MSC290115 in P5, and MSC280416 in P4). Moreover, the TNF-α-mediated increase in cell fusion was paralleled by a significant increase in dual fluorescent cells after stimulation with 1,000 U/ml to 10 U/ml TNF-α while 1 U/ml TNF-α exhibited no detectable effects (Fig. 4B). The TNF-α-mediated increase in hybrid cell formation could be blocked by simultaneous incubation with a TNF-α antibody (Supporting Information Fig. S9). Of interest, further cytokines like TNF-β or CCL2 and lipids like oleate demonstrated little if any effect on hybrid cell formation (Supporting Information Fig. S9).

The pro-fusogenic effects of TNF-α were accompanied by reduced cell growth. Fluorescence measurements of MSC^{GFP} in both, monocultures (Supporting Information Fig. S10A) and cocultures (Supporting Information Fig. S10C) demonstrated a marked

©AlphaMed Press 2018

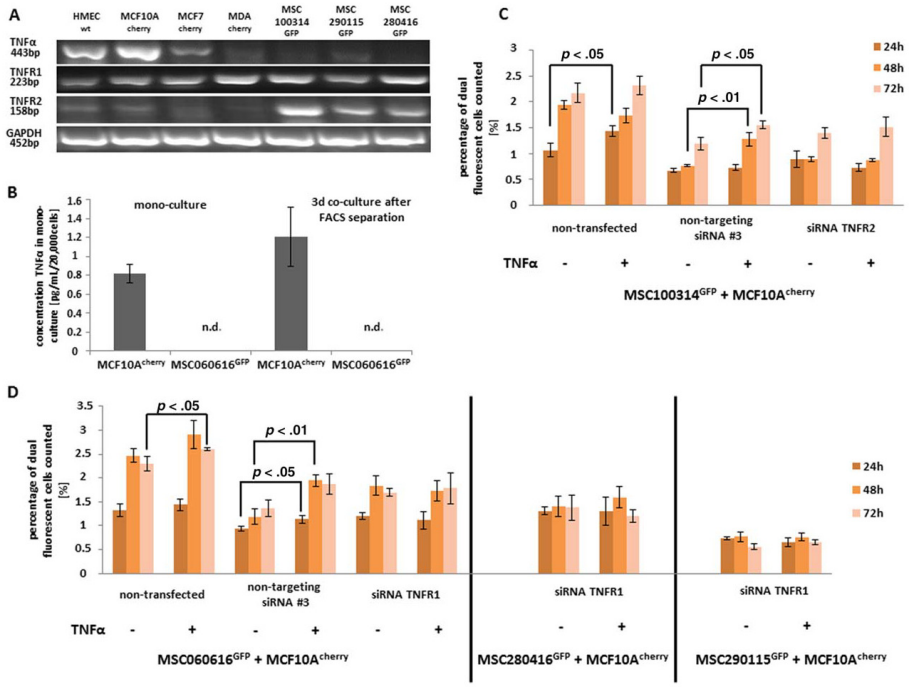


Figure 5. TNF-α-enhanced cell fusion occurs via TNFR1 and TNFR2. **(A):** PCR analysis was performed with TNF-α, TNFR1, and TNFR2 in primary HMEC^{wt}, three neoplastic breast cell lines (MCF10A^{cherry}, MCF7^{cherry}, MDA-MB-231^{cherry}), and three different primary MSC (MSC100314^{GFP}, MSC290115^{GFP}, and MSC280416^{GFP}). Unaltered GAPDH transcripts served as a control. **(B):** Secretion of TNF-α in mono-culture and in 3d cocultured FACS-separated cell populations was quantified by ELISA. Data represent the mean ± SD ($n = 3$). **(C, D):** Significance (p) of hybrid cell formation by MCF10A^{cherry} with MSC^{GFP} was examined and quantified following siRNA-mediated down-modulation of TNFR2 and TNFR1 for 24 hours, respectively. Nontransfected cocultures and a nontargeting siRNA served as controls. TNF-α (100 U/ml) was added to cocultures after 24 hours of transfection. The relative percentage of hybrid cells was calculated by the mean ± SD from cocultures in triplicate and significance (p) was calculated by Student's t test. Abbreviations: FACS, fluorescence activated cell sorting; GAPDH, glyceraldehyde 3-phosphate dehydrogenase; MSC, mesenchymal stroma/stem-like cells; PCR, polymerase chain reaction; siRNA, small-interfering RNA; TNF-α, tumor necrosis factor alpha; TNFR1, tumor necrosis factor receptor 1; TNFR2, tumor necrosis factor receptor 2.

decrease in the proliferation rate during TNF-α stimulation. Cell numbers of mono-culture MSC^{GFP} were significantly reduced in the presence of 100 U/ml and 1,000 U/ml TNF-α (Supporting Information Fig. S10A) and MSC^{GFP} in the coculture were even affected by 10 U/ml TNF-α (Supporting Information Fig. S10C).

Likewise, proliferation of mono-cultured MCF10A^{cherry} was inhibited at TNF-α concentrations between 1,000 U/ml and 10 U/ml (Supporting Information Fig. S10B) and in coculture MCF10A^{cherry} exhibited sensitivity to all TNF-α concentrations (Supporting Information Fig. S10D).

TNF-α Signals via TNFR1 and Tumor Necrosis Factor Receptor 2

To further analyze the pro-fusogenic role of TNF-α, we examined the expression of TNF-α and the corresponding receptors TNFR1 and tumor necrosis factor receptor 2 (TNFR2). PCR analysis was performed with mono-cultures of normal HMEC, breast cancer cell lines MCF10A, MCF7, and MDA-MB-231 and with mono-cultures of MSC from three different donors (Fig. 5A). The transcript of GAPDH served as a control. HMEC, MCF10A, and MCF7 cells exhibited transcripts for TNF-α in contrast to undetectable mRNA levels in MDA-MB-231 and all three MSC cultures (Fig. 5A). While all investigated cell populations demonstrated TNFR1 expression, transcripts of TNFR2 were strongly expressed exclusively in all MSC with low mRNA levels in HMEC, MCF10A, MCF7, and MDA-MB-231 (Fig. 5A). Supportive evidence for TNFR1 (CD120a) expression was obtained by flow cytometry analysis of MSC and MCF10A monocultures and cocultures (Supporting Information Fig. S11A). MCF10A mono-culture expressed about 46% of TNFR1 and MSC mono-culture revealed approximately 73% of TNFR1 expression. Consequently, coculture of MSC with MCF10A exhibited 65% of TNFR1 protein. Production of TNF-α by ELISA quantification also confirmed the RT-PCR data demonstrating release of 0.8 ± 0.1 pg/ml/24 hours by 20,000 MCF10A cells in contrast to undetectable TNF production by MSC (Fig. 5B). Moreover, FACS separation of a 3d MSC^{GFP} and MCF10A^{cherry} coculture and subsequent 24 hours culture of the two

 ©AlphaMed Press 2018

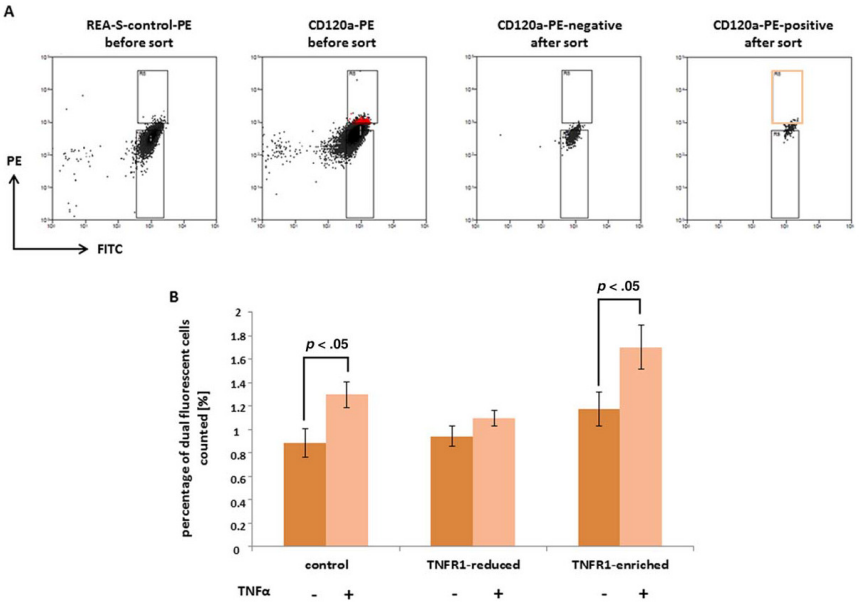


Figure 6. TNFR1-enriched cocultures show higher responsiveness to TNF-α. **(A):** MSC^{GFP} were sorted via FACS after staining with CD120a-PE revealing CD120a-PE-negative (TNFR1-reduced) and CD120a-PE-positive (TNFR1-enriched) cells. REA-S-control-PE-stained MSC^{GFP} were used as negative control. **(B):** Hybrid cell formation between $MCF10A^{cherry}$ and FACS-separated TNFR1-reduced or TNFR1-enriched MSC^{GFP} subpopulations was quantified after stimulation with 100 U/ml TNF-α for 24 hours. Cocultures of $MCF10A^{cherry}$ with nonsorted MSC^{GFP} served as a control. Significance (p) was calculated by the mean ± SD from cocultures in triplicate using Student's t test. Abbreviations: FACS, fluorescence activated cell sorting; FITC, fluorescein isothiocyanate; PE, phycoerythrin; TNF-α, tumor necrosis factor alpha; TNFR1, tumor necrosis factor receptor 1.

separated populations likewise revealed 1.2 ± 0.3 pg/ml/24 hours TNF-α by 20,000 MCF10A cells and no detectable TNF-α release by MSC (Fig. 5B). Together, these findings suggested that TNF-α-stimulated hybrid formation involves both, TNFR1 and TNFR2, whereby MCF10A-released TNF-α can bind to the corresponding receptor on the MSC fusion partner.

To further substantiate an involvement of TNF receptor signaling in the MCF10A/MSC hybrid cell formation, siRNA knock downs of TNFR1 and TNFR2 in the absence or presence of TNF-α (100 U/ml) stimulation did not result in markedly altered hybrid cell formation in contrast to significantly elevated hybrid cell numbers in nontransfected cocultures and cultures transfected with nontargeting siRNA #3 after TNF-α treatment (Fig. 5C, 5D). Moreover, these findings were further reproduced in cocultures with TNF receptor knockdown using MSC from two other donors to exclude donor specific effects (Fig. 5D). The successful knock down of TNFR1 was confirmed in siRNA TNFR1-transfected cells by flow cytometric analysis demonstrating a continuous down-regulation of the receptor for at least 72 hours after transfection in contrast to a normal TNFR1 expression in nontargeting siRNA #3-transfected cells (Supporting Information Fig. S11B). Analysis of TNF-associated gene expression by real-time RT-PCR array of 44 genes involved in TNFR1 signaling with cDNA from cocultures stimulated for 72 hours with TNF-α did not reveal significant changes in relative expression pattern compared to nonstimulated cocultures (Supporting Information Fig. S12).

To further substantiate involvement of predominantly TNFR1 during MSC fusion with neoplastic breast epithelial cells staining of MSC^{GFP} was performed with CD120a-PE followed by FACS separation into TNFR1-reduced and TNFR1-enriched MSC^{GFP} (Fig. 6A). Subsequent initiation of cocultures between these two different TNFR1-carrying MSC^{GFP} subpopulations and $MCF10A^{cherry}$ demonstrated marked differences in hybrid cell formation compared with steady-state cocultures which served as a control (Fig. 6B). Thus, cocultures of $MCF10A^{cherry}$ cells with TNFR1-enriched MSC^{GFP} subpopulation revealed an increase in dual fluorescent hybrid cell formation after a 24 hours TNF-α stimulation which was even more pronounced compared with control cocultures. In contrast, no significant increase in the amount of hybrid cells was detectable after a 24 hours TNF-α exposure to a coculture with TNFR1-reduced MSC^{GFP} (Fig. 6B) demonstrating an elevated capability of hybrid cell formation in the TNFR1-enriched MSC^{GFP} subpopulation.

TNF-α Activates Apoptosis and NF-κB Pathway via Tumor Necrosis Factor Receptor Type 1-Associated Death Domain

Downstream signaling via TNFR1 involves three different major pathways: (a) apoptosis/necrosis/necroptosis, (b) NF-κB

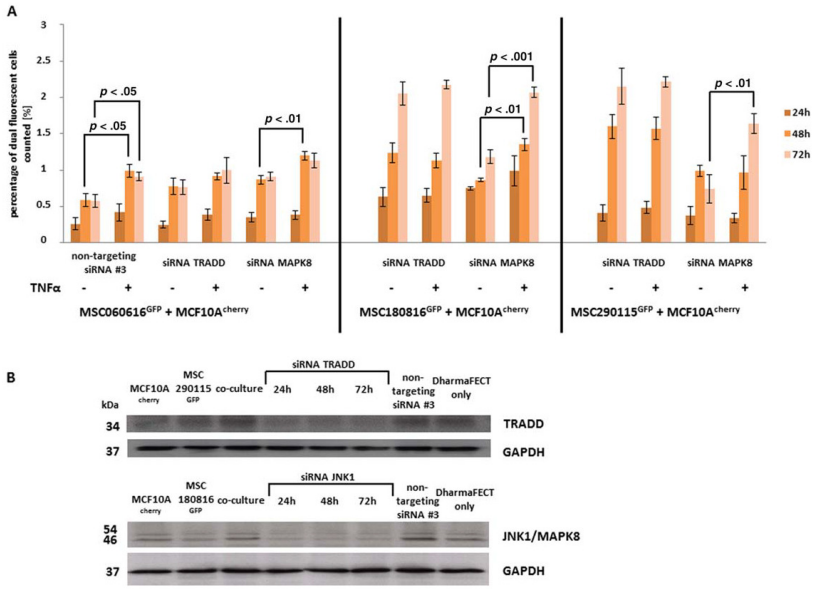


Figure 7. Effects of TRADD and MAPK8 during TNF-α-mediated fusion. **(A):** Hybrid cell formation between MCF10A^{cherry} and three different MSC^{GFP} was quantified after siRNA treatment targeting either TRADD or JNK1/MAPK8 for 24 hours followed by stimulation with 100 U/ml TNF-α. Cocultures transfected with nontargeting siRNA #3 served as controls. Significance (p) of hybrid cell formation was calculated by the mean ± SD from cocultures in triplicate using Student's t test. **(B):** Successful down-modulation of TRADD and JNK1/MAPK8 by siRNA transfection and subsequent cocultures of MCF10A^{cherry} with MSC^{GFP} for up to 72 hours was verified by immunoblot analysis whereby GAPDH protein expression was applied as a control. Abbreviations: GAPDH, glyceraldehyde 3-phosphate dehydrogenase; MSC, mesenchymal stroma/stem-like cells; siRNA, small-interfering RNA; TNF-α, tumor necrosis factor alpha; TNFR1, tumor necrosis factor receptor 1; TRADD, tumor necrosis factor receptor type 1-associated death domain.

activation, and (c) c-Jun N-terminal kinase 1 (JNK1)/Mitogen-activated protein kinase 8 (MAPK8) activation [27]. Tumor necrosis factor receptor type 1-associated death domain (TRADD) (TNFR1-associated death domain protein) acts as downstream molecule of TNFR1 and can recruit additional adaptor proteins like RIP, TRAF2, and FADD to relay activation signals for all three pathways. Knock down of TRADD by siRNA targeting in three different MCF10A/MSC cocultures abolished the pro-fusogenic effects of TNF-α substantiating the necessity of TNFR1 downstream signaling via TRADD for augmentation of hybrid cell formation (Fig. 7A). To further examine the three different TRADD pathways and a potential involvement in pro-fusogenic TNFR1 signaling, knock down of JNK1/MAPK8 did not abolish the effects of TNF-α to increase the hybrid formation (Fig. 7A). These findings suggested little if any contribution of the JNK1/MAPK8 pathway to the formation of hybrid cells.

Effective down-modulation of TRADD and JNK1/MAPK8 with siRNA was confirmed by immunoblot analysis (Fig. 7B). Likewise, no significant alterations of hybrid cell formation after TNF-α stimulation were observed after siRNA knock down of p65 (RelA) (Supporting Information Fig. S13). However, NF-κB is constituted of seven proteins whereby TNFR1 via TRADD activates canonical NF-κB signaling leading to activation of NF-κB1 (p50), RelA (p65), and c-Rel [28] indicating signal transduction via a dimer combination without involving RelA.

Discussion

Interaction of normal or neoplastic breast cancer cells with certain MSC are multimodal and can last for several hours or even days [29–31]. During those interactions, accidental hybrid cell formation is observed within less than 5 minutes whereby the fused cells acquired fluorescence from both parental cell types. Generation of hybrid cells can occur by engulfment of a target cell via entosis which also includes degradation of the target cell genome. In contrast, fusion-associated MSC hybrid cell formation is accompanied by a recombination of genomic parts from both parental donors in a nuclear hetero-to-synkaryon transition during subsequent cell division [32]. This is also demonstrated by a homogenous distribution of mcherry and GFP in the hybrids of normal and neoplastic breast epithelial cells. However, the significant differences of autofusion compared with the 10- to 50-fold elevated heterofusion events suggested the involvement of different molecular signals between the fusion partners. Although the known fusogenic factors including syncytin-1 and −2 and corresponding receptors such as ASCT2 and MFSD2A were detectable in MSC and MCF10A cells, respectively, double knockdown with siRNA (syncytin-1 + ASCT2) or siRNA (syncytin-2 + MFSD2A) demonstrated little if any effects on the cell fusion. These findings suggested altered or

©AlphaMed Press 2018

additional molecular fusion signaling during the spontaneously accidental cell fusion of MSC with neoplastic breast epithelial cells compared with the normal developmental cell fusion also known from syncytiotrophoblast formation.

Following the search for alternative fusion mechanisms based on the idea of a continuous inflammatory tumor microenvironment, we found that increasing levels of TNF-α demonstrated progressively elevated fusion events which were reproducible with different MSC populations suggesting involvement of the corresponding TNF receptors. Indeed, TNF receptor-1 and -2 were detectable predominantly in different MSC populations with low expression level of TNFR2 in normal HMEC and in breast cancer cells and successful siRNA knockdown of TNF receptor-1 or TNF receptor-2 could abolish the TNF-α-mediated enhanced cell fusion. Further analysis of this fusion signal revealed a markedly elevated production and release of TNF-α by MCF10A cells in contrast to MSC suggesting that TNF-α released by MCF10A contributes to heterofusion by triggering the TNF receptors in MSC. Low to undetectable TNF-α production by MSC is in line with previous findings [33] and other work has demonstrated that TNF-α stimulation of MSC can enhance formation of breast cancer metastases [34].

TNF-α-mediated stimulation of TNFR1 further activates TRADD which in turn can relay downstream signaling to the activation of jun kinase (JNK), the NF-κB family, and/or the cell death pathway [27, 35, 36]. Our data are in accordance with these findings demonstrating that siRNA knockdown of TRADD also blocked the TNF-α-mediated fusion which further substantiated involvement of TNFR1 and TNFR2 activation in this process. Interference with downstream signaling by successful siRNA knockdown of JNK1 and p65 (RelA) revealed no detectable effects on TNF-α-induced cell fusion suggesting that other NF-κB molecules and/or the apoptosis/necroptosis pathways eventually trigger fusion. This is also supported by other studies demonstrating an involvement of apoptosis signaling in cell fusion [37] and that TNF-α-stimulated MSC activate apoptosis/necroptosis and NF-κB signaling but not JNK-mediated factor production [38]. Moreover, TNFR1 signaling also activates phospholipase A2 leading to enhanced lipid metabolism and phospholipid turnover in the plasma membrane [39] which may create further fusion-permissive conditions.

Whereas TNF-α demonstrated selective effects on hybrid cell formation when compared to TNF-β and further substances, other pro-inflammatory cytokines may also contribute to this process, however, immune-modulatory properties of MSC could interfere with those signals [40].

Distinct therapeutic effects of cell fusion have been suggested in previous work [41] including regeneration and maintenance of skeletal muscle by hybrid cell formation of satellite cells with existing muscle fibers [42]. Likewise, fusion of MSC with neoplastic cells can alter the functionality of the cancer cells in various directions. In case of MCF10A-hyb1 and -hyb2 cells, expression of proliferation- and cell cycle-associated genes was down-modulated suggesting the acquisition of certain antitumorigenic properties.

Conclusion

Together, these findings demonstrate marked differences in autofusion compared with heterofusion of benign and malignant breast epithelial cells with MSC. Hybrid cell formation revealed the stable generation of new cell populations including neoplastic breast cells with altered properties obtained from both parental cell types. Molecular signals involved in this fusion process include pro-inflammatory cytokines such as TNF-α and signaling via TNFR1 and TNFR2, TRADD, certain NF-κB or apoptosis/necroptosis pathways among others. Compared to normal developmental fusion processes such as myotube or syncytiotrophoblast formation, these data indicate that accidental cell fusion like tumor cell hybrid generation can involve pro-inflammatory cytokine activation such as TNF-α and corresponding receptor signaling pathways.

Acknowledgments

We are grateful to colleagues from Hannover Medical School including Dr. Detlef Neumann and Dr. Bastian Schirmer for assistance with qPCR analysis, to Dr. Thomas Rothämel and PD Dr. Gudrun Göhring for support with the STR fragment analysis, to Dr. Matthias Ballmaier (FACS core unit) for cell separation and to Dr. Oliver Dittrich-Breiholz (research core unit Transcriptomics) for microarray analysis. This work was supported by a grant from the Erich und Gertrud Roggenbuck-Stiftung for Cancer Research to Ralf Hass.

Author Contributions

R.H.: conception and design, financial support, data analysis and interpretations, manuscript writing; J.v.d.O.: collection and assembly of data, data analysis and interpretations; C.M.: collection and assembly of data, data analysis and interpretations, manuscript writing. All authors approved the final version of the manuscript.

Disclosure of Potential Conflicts of Interest

The authors indicated no potential conflicts of interest.

References

1 Duelli D, Lazebnik Y. Cell fusion: A hidden enemy? Cancer Cell 2003;3:445–448.

2 Ogle BM, Cascalho M, Platt JL. Biological implications of cell fusion. Nat Rev Mol Cell Biol 2005;6:567–575.

3 Aguilar PS, Baylies MK, Fleissner A et al. Genetic basis of cell-cell fusion mechanisms. Trends Genet 2013;29:427–437.

4 Blaise S, de Parseval N, Benit L et al. Genomewide screening for fusogenic human endogenous retrovirus envelopes identifies syncytin 2, a gene conserved on primate evolution. Proc Natl Acad Sci USA 2003;100:13013–13018.

5 Mi S, Lee X, Li X et al. Syncytin is a captive retroviral envelope protein involved in human placental morphogenesis. Nature 2000;403:785–789.

6 Lu M, Ravichandran KS. Dock180-ELMO cooperation in Rac activation. Methods Enzymol 2006;406:388–402.

7 Pajcini KV, Pomerantz JH, Alkan O et al. Myoblasts and macrophages share molecular components that contribute to cell-cell fusion. J Cell Biol 2008;180:1005–1019.

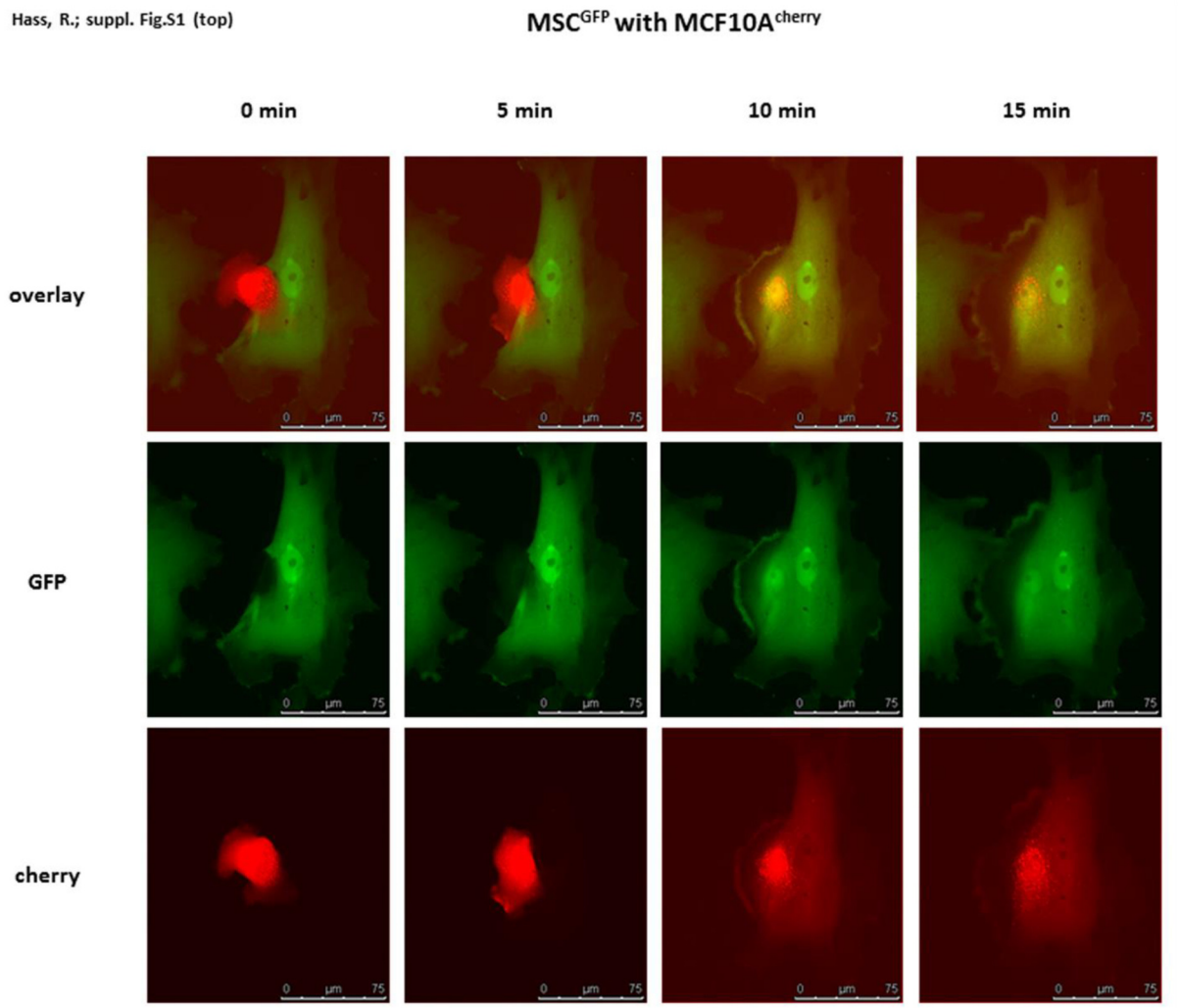
8 Freeman BT, Jung JP, Ogle BM. Single-cell RNA-seq reveals activation of unique gene groups as a consequence of stem cell-

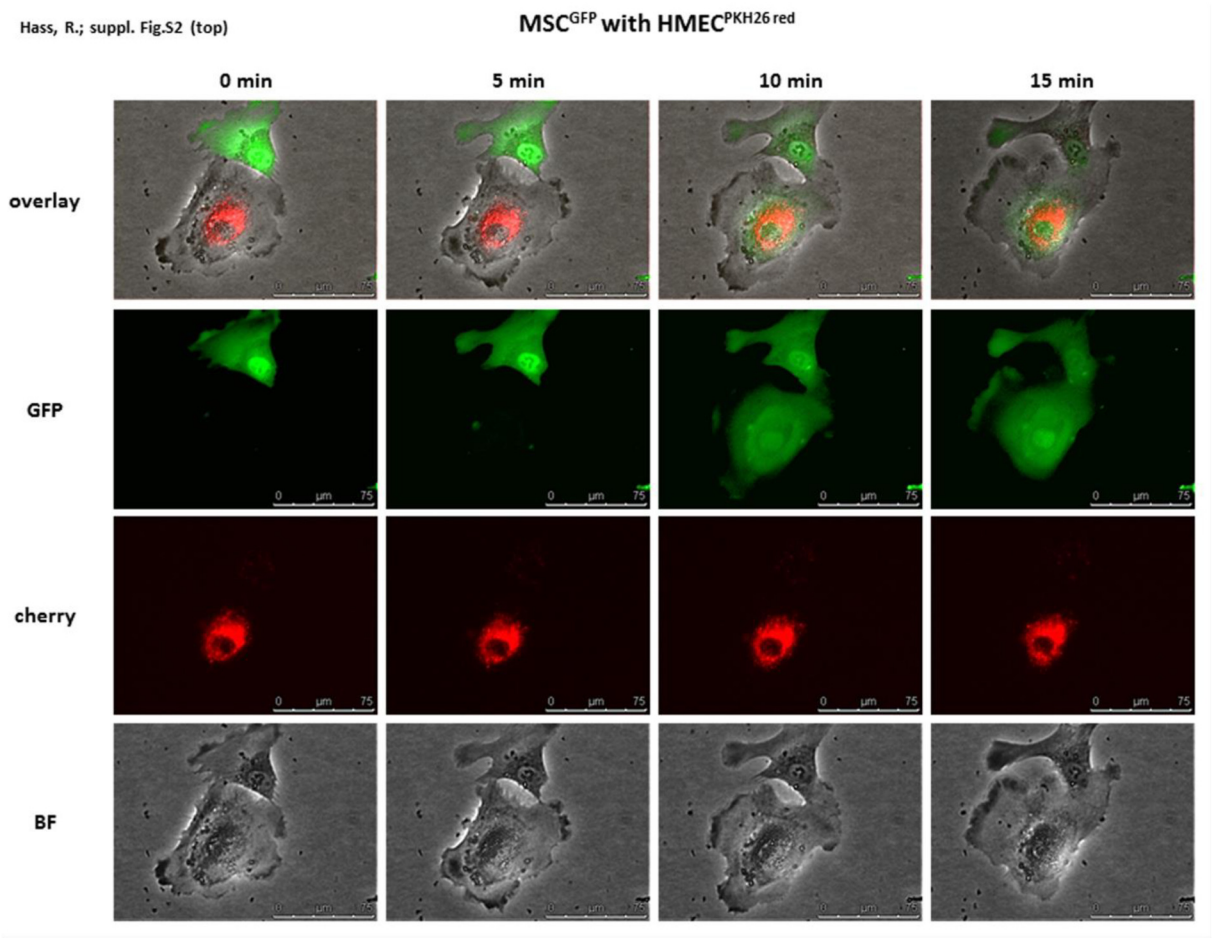
©AlphaMed Press 2018

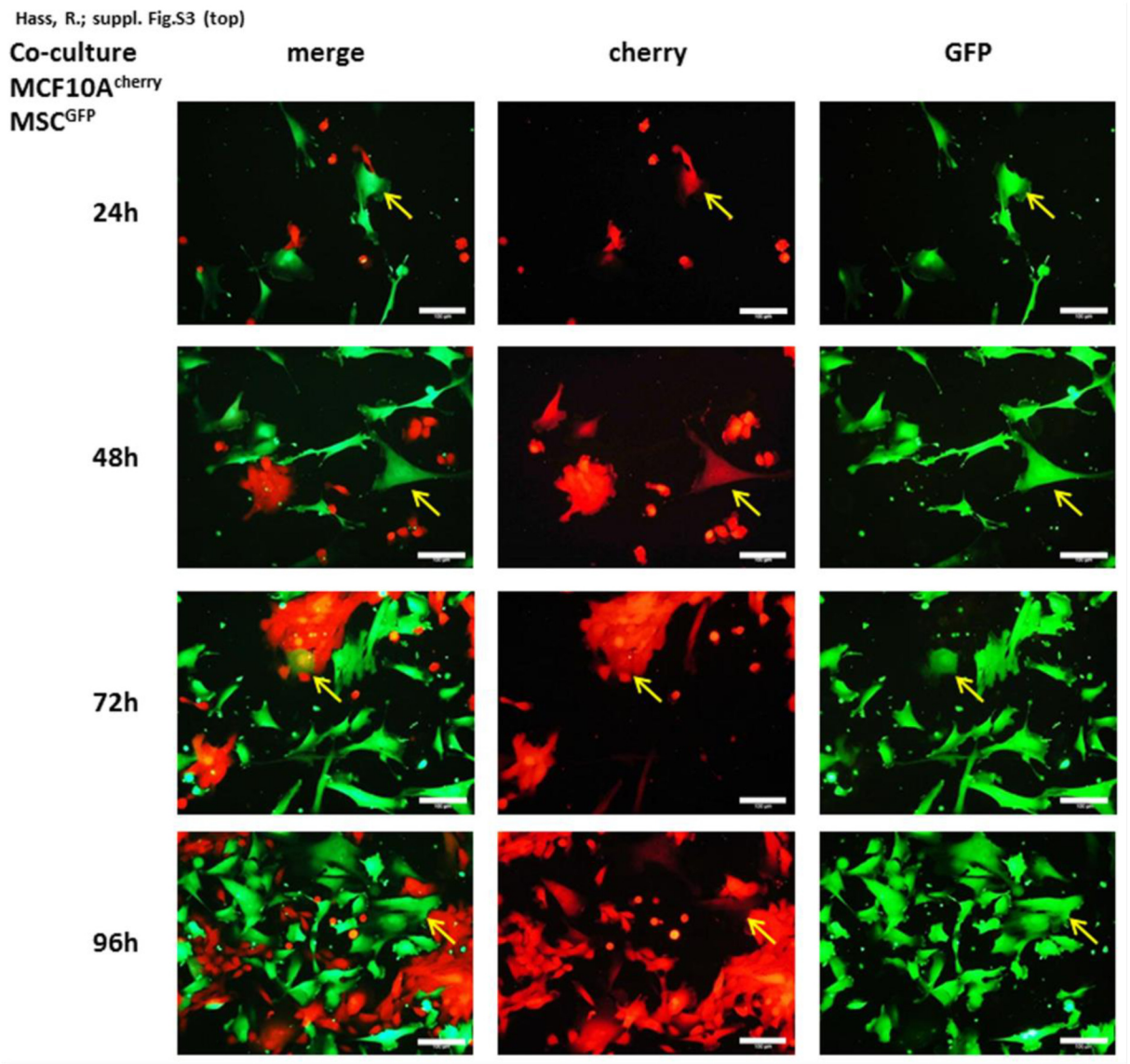
parenchymal cell fusion. Sci Rep 2016;6:23270.
9 Mondal Roy S, Sarkar M. Membrane fusion induced by small molecules and ions. J Lipids 2011;2011:528784.
10 Berndt B, Zanker KS, Dittmar T. Cell fusion is a potent inducer of aneuploidy and drug resistance in tumor cell/normal cell hybrids. Crit Rev Oncog 2013;18:97–113.
11 Lazova R, Laberge G, Duvall S et al. A melanoma brain metastasis with a donor-patient hybrid genome following bone marrow transplantation: First evidence for fusion in human cancer. PLoS One 2013;8:e66731.
12 Noubissi FK, Ogle BM. Cancer cell fusion: Mechanisms slowly unravel. Int J Mol Sci 2016;17:1587.
13 Larsson LI, Bjerregaard B, Wulf-Andersen L et al. Syncytin and cancer cell fusions. ScientificWorldJournal 2007;7:1193–1197.
14 Melzer C, von der Ohe J, Hass R. Enhanced metastatic capacity of breast cancer cells after interaction and hybrid formation with mesenchymal stroma/stem cells (MSC). Cell Commun Signal 2018;16:2.
15 Lavrentieva A, Majore Kasper IC, Hass R. Effects of hypoxic culture conditions on umbilical cord-derived human mesenchymal stem cells. Cell Commun Signal 2010;8:18.
16 Otte A, Bucan V, Reimers K et al. Mesenchymal stem cells maintain long-term in vitro stemness during explant culture. Tissue Eng Part C Methods 2013;19:937–948.
17 Hass R, Bertram C. Characterization of human breast cancer epithelial cells (HBCEC) derived from long term cultured biopsies. J Exp Clin Cancer Res 2009;28:127.
18 Bertram C, Hass R. MMP-7 is involved in the aging of primary human mammary epithelial cells (HMEC). Exp Gerontol 2008;43:209–217.
19 Kudo Y, Boyd CA, Sargent IL et al. Hypoxia alters expression and function of syncytin and its receptor during trophoblast cell fusion of human placental BeWo cells: Implications for impaired trophoblast syncytialisation in pre-eclampsia. Biochim Biophys Acta 2003;1638:63–71.
20 Bjerregaard B, Holck S, Christensen IJ et al. Syncytin is involved in breast cancer-endothelial cell fusions. Cell Mol Life Sci 2006;63:1906–1911.
21 Delidaki M, Gu M, Hein A et al. Interplay of cAMP and MAPK pathways in hCG secretion and fusogenic gene expression in a trophoblast cell line. Mol Cell Endocrinol 2011;332:213–220.
22 Zhu G, Du Q, Wang X et al. TNF-alpha promotes gallbladder cancer cell growth and invasion through autocrine mechanisms. Int J Mol Med 2014;33:1431–1440.
23 Derouich-Guergour D, Aldebert D, Vigan I et al. *Toxoplasma gondii* infection can regulate the expression of tumour necrosis factor-alpha receptors on human cells in vitro. Parasite Immunol 2002;24:271–279.
24 Marconi C, Peppicelli S, Bianchini F et al. TNFα receptor1 drives hypoxia-promoted invasiveness of human melanoma cells. Exp Oncol 2013;35:187–191.
25 Yang Y, Otte A, Hass R. Human mesenchymal stroma/stem cells exchange membrane proteins and alter functionality during interaction with different tumor cell lines. Stem Cells Dev 2015;24:1205–1222.
26 Esnault C, Priet S, Ribet D et al. A placenta-specific receptor for the fusogenic, endogenous retrovirus-derived, human syncytin-2. Proc Natl Acad Sci USA 2008;105:17532–17537.
27 Wajant H, Pfizenmaier K, Scheurich P. Tumor necrosis factor signaling. Cell Death Differ 2003;10:45–65.
28 Vallabhapurapu S, Karin M. Regulation and function of NF-kappaB transcription factors in the immune system. Annu Rev Immunol 2009;27:693–733.
29 Mandel K, Yang Y, Schambach A et al. Mesenchymal stem cells directly interact with breast cancer cells and promote tumor cell growth in vitro and in vivo. Stem Cells Dev 2013;22:3114–3127.
30 Melzer C, von der Ohe J, Lehnert H et al. Cancer stem cell niche models and contribution by mesenchymal stroma/stem cells. Mol Cancer 2017;16:28.
31 Melzer C, Yang Y, Hass R. Interaction of MSC with tumor cells. Cell Commun Signal 2016;14:20.
32 Sottile F, Aulicino Theka FI, Cosma MP. Mesenchymal stem cells generate distinct functional hybrids in vitro via cell fusion or entosis. Sci Rep 2016;6:36863.
33 van den Berk LC, Jansen BJ, Siebers-Vermeulen KG et al. Mesenchymal stem cells respond to TNF but do not produce TNF. J Leukoc Biol 2010;87:283–289.
34 Yu PF, Huang Y, Han YY et al. TNFα-activated mesenchymal stromal cells promote breast cancer metastasis by recruiting CXCR2+ neutrophils. Oncogene 2017;36:482–490.
35 Pobezinskaya YL, Kim YS, Choksi S et al. The function of TRADD in signaling through tumor necrosis factor receptor 1 and TRIF-dependent Toll-like receptors. Nat Immunol 2008;9:1047–1054.
36 Pobezinskaya YL, Liu Z. The role of TRADD in death receptor signaling. Cell Cycle 2012;11:871–876.
37 Noubissi FK, Harkness T, Alexander CM et al. Apoptosis-induced cancer cell fusion: A mechanism of breast cancer metastasis. FASEB J 2015;29:4036–4045.
38 Crisostomo PR, Wang Y, Markel T et al. Human mesenchymal stem cells stimulated by TNF-alpha, LPS, or hypoxia produce growth factors by an NF kappa B- but not JNK-dependent mechanism. Am J Physiol Cell Physiol 2008;294:C675–C682.
39 Schutze S, Machleidt T, Kronke M. Mechanisms of tumor necrosis factor action. Semin Oncol 1992;19:16–24.
40 Casiraghi F, Noris M, Remuzzi G. Immunomodulatory effects of mesenchymal stromal cells in solid organ transplantation. Curr Opin Organ Transplant 2010;15:731–737.
41 Sullivan S, Eggan K. The potential of cell fusion for human therapy. Stem Cell Rev 2006;2:341–349.
42 Buckingham M. Myogenic progenitor cells and skeletal myogenesis in vertebrates. Curr Opin Genet Dev 2006;16:525–532.

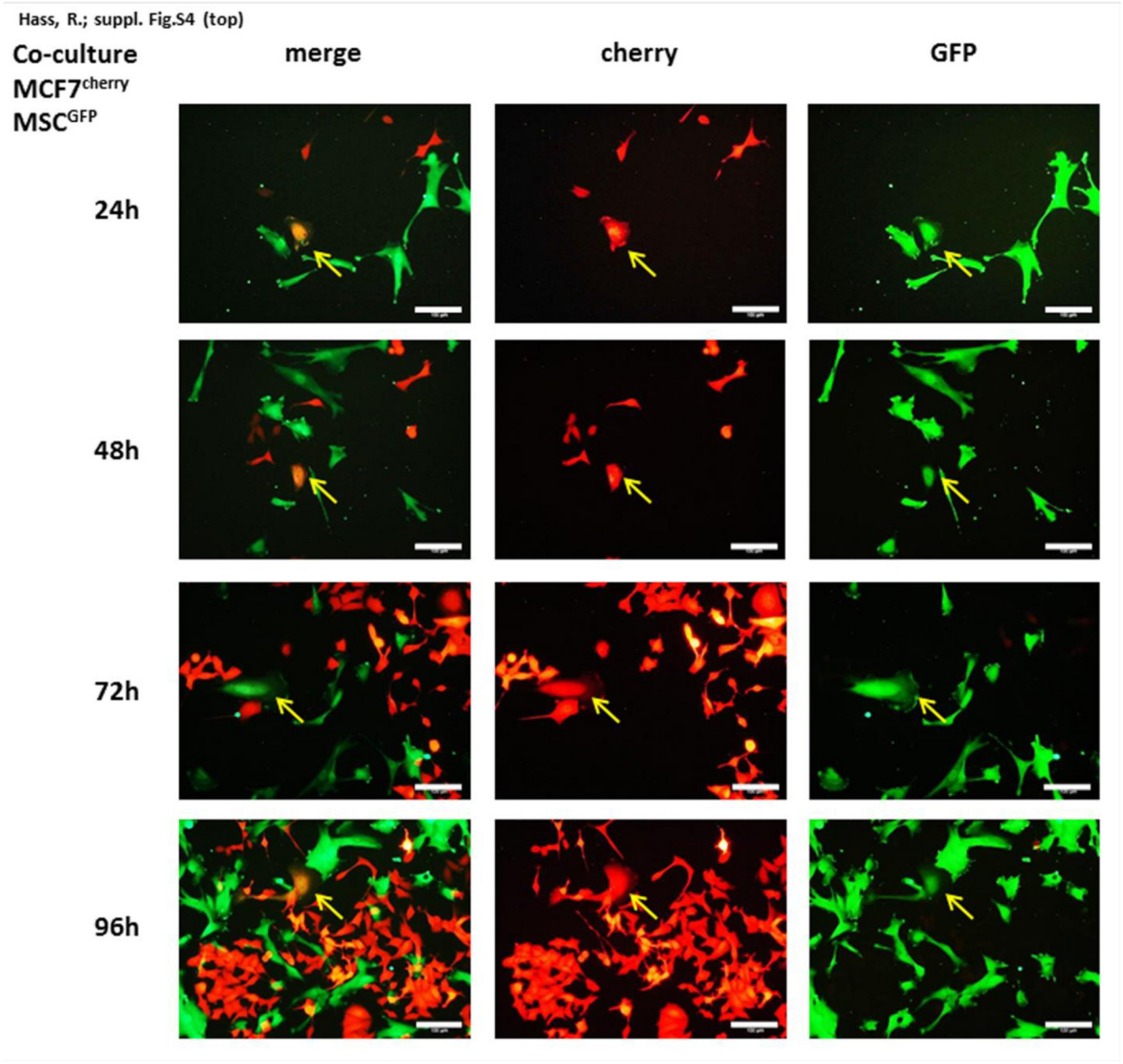

See www.StemCells.com for supporting information available online.

©AlphaMed Press 2018

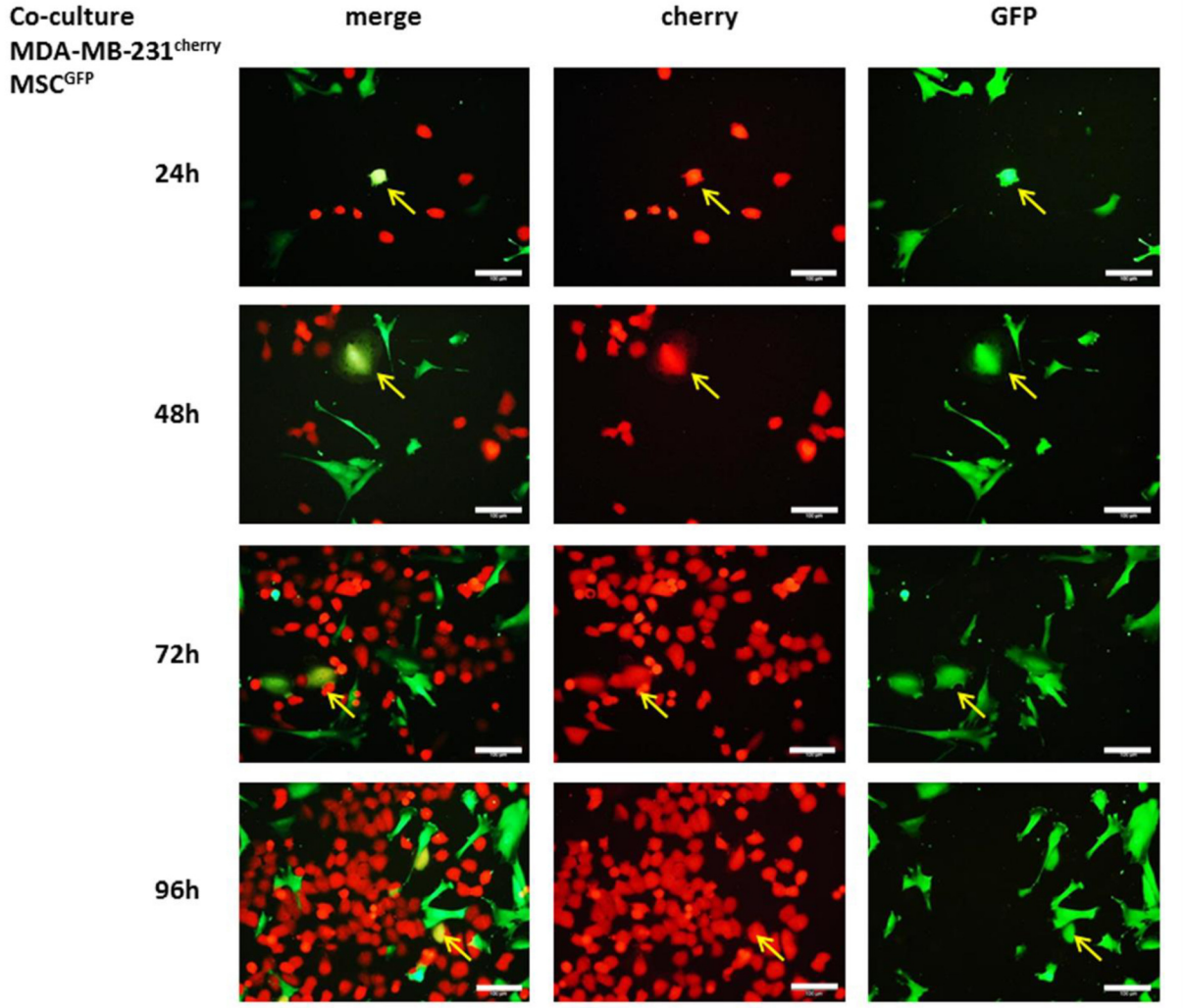

Hass, R.; suppl. Fig.S1 (top)
MSC^GFP with MCF10A^cherry
0 min
5 min
10 min
15 min
overlay
GFP
cherry
0 µm 75


Hass, R.; suppl. Fig.S2 (top)
MSC^GFP with HMEC^PKH26 red
0 min
5 min
10 min
15 min
overlay
GFP
cherry
BF

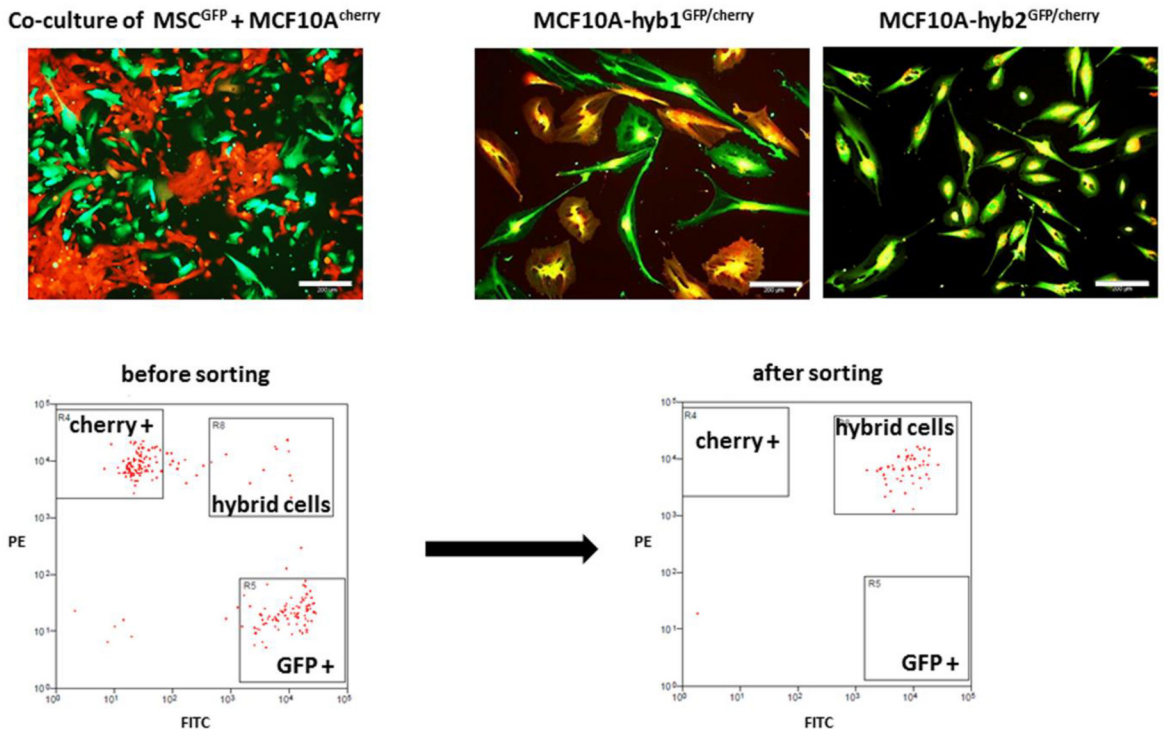

Hass, R.; suppl. Fig.S3 (top)
Co-culture
MCF10A cherry
MSC GFP
merge
cherry
GFP
24h
48h
72h
96h


Hass, R.; suppl. Fig.S4 (top)
Co-culture
MCF7cherry
MSCGFP
merge
cherry
GFP
24h
48h
72h
96h

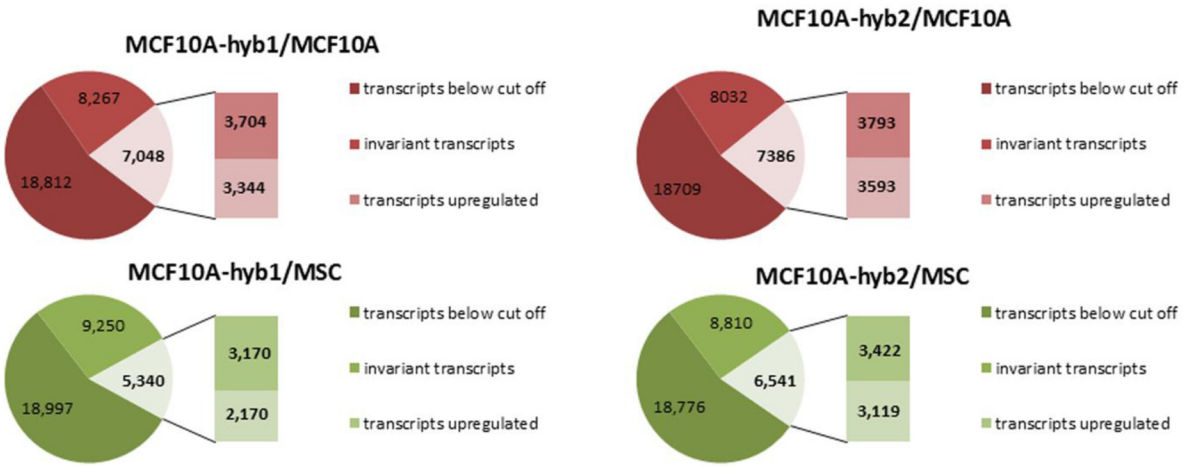
Hass, R.; suppl. Fig.S5 (top)



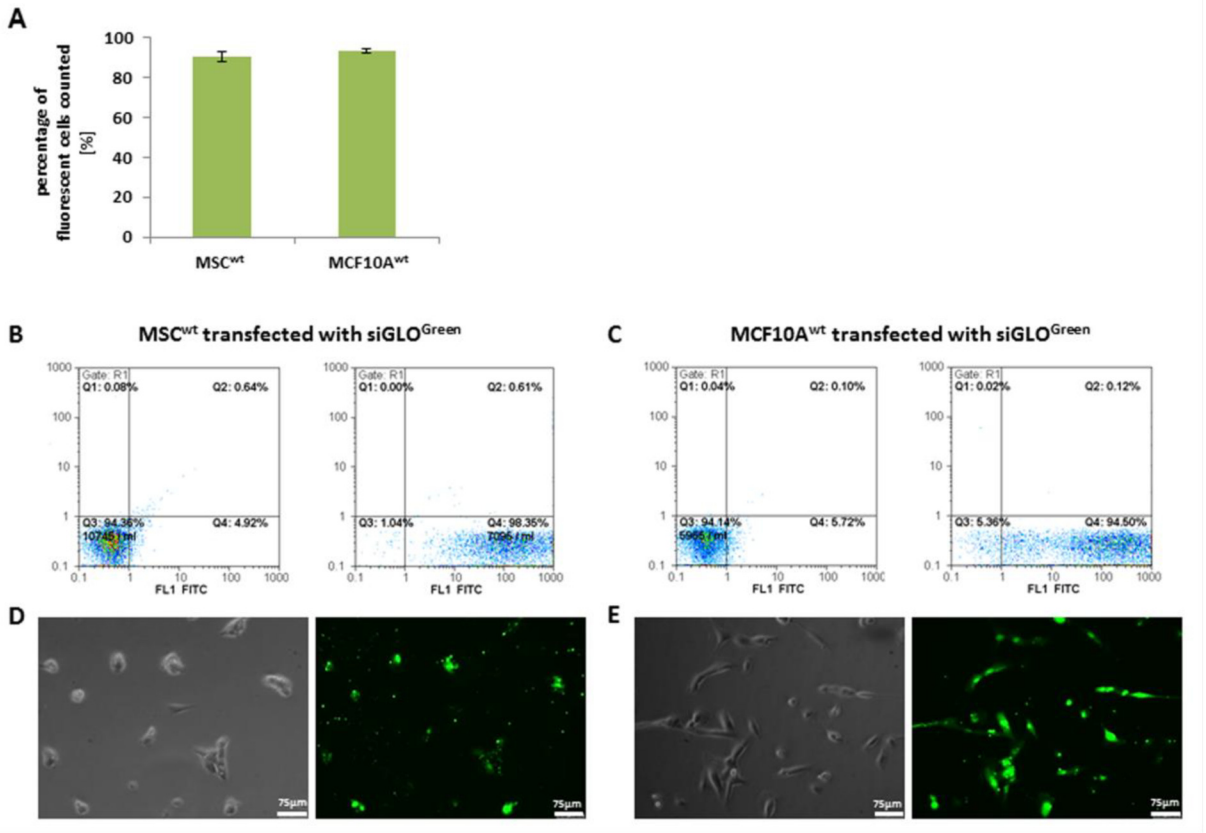
Hass, R.; suppl. Fig.S6 (top)



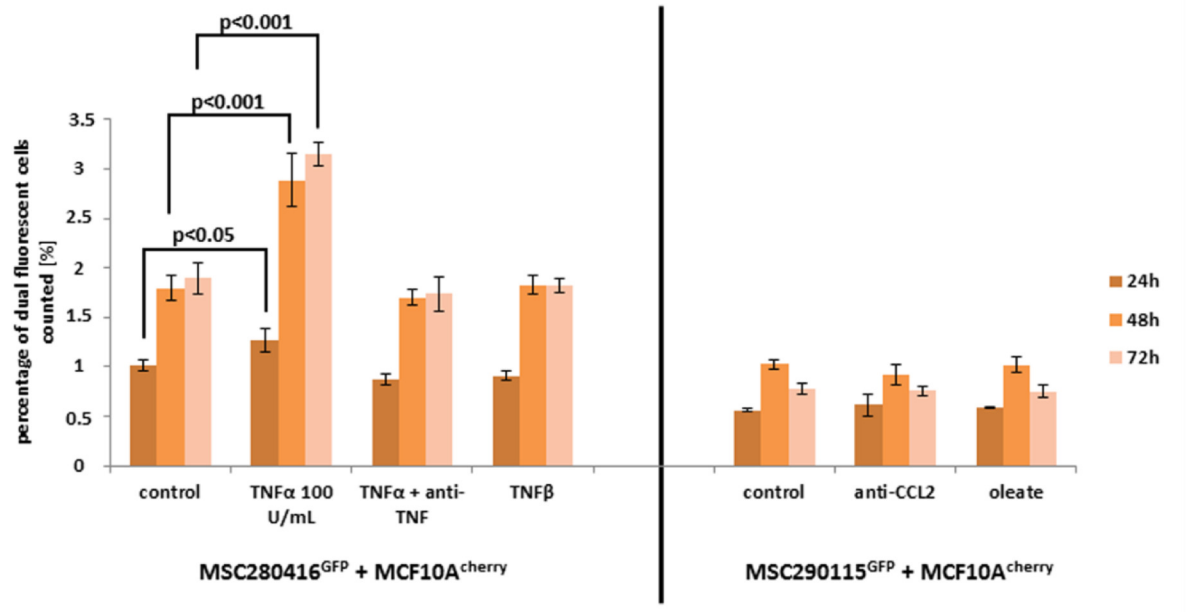
Hass, R.; suppl. Fig.S7 (top)



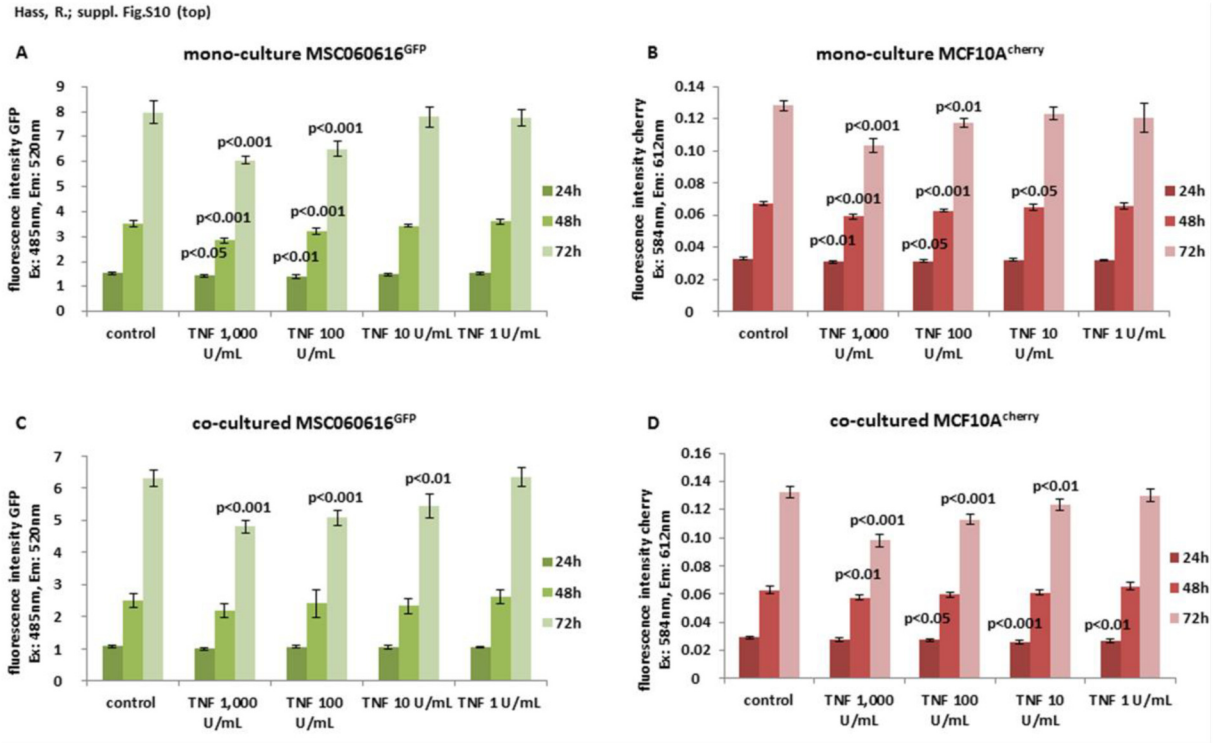
Hass, R.; suppl. Fig.S8 (top)

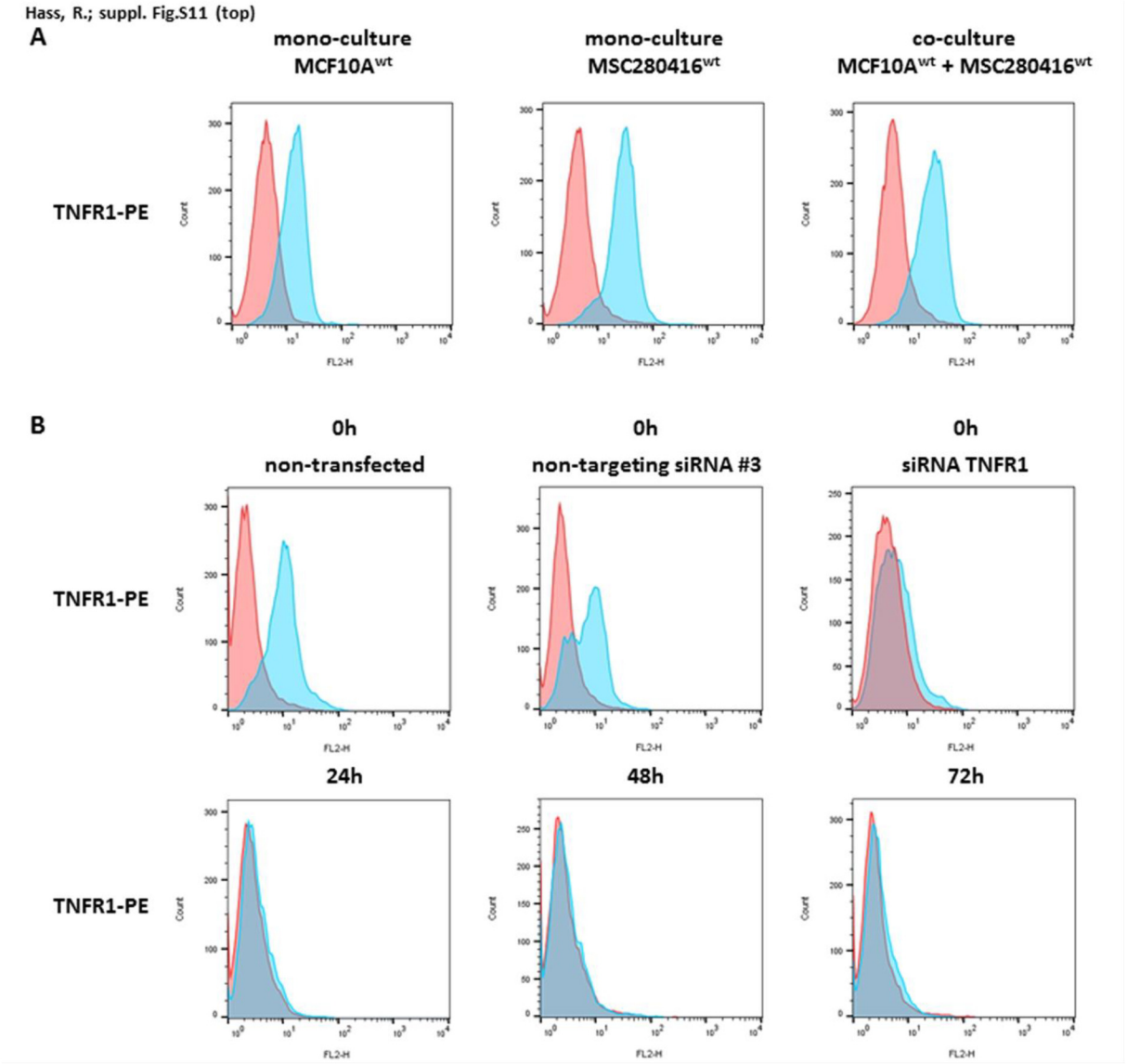


Hass, R.; suppl. Fig.S9 (top)

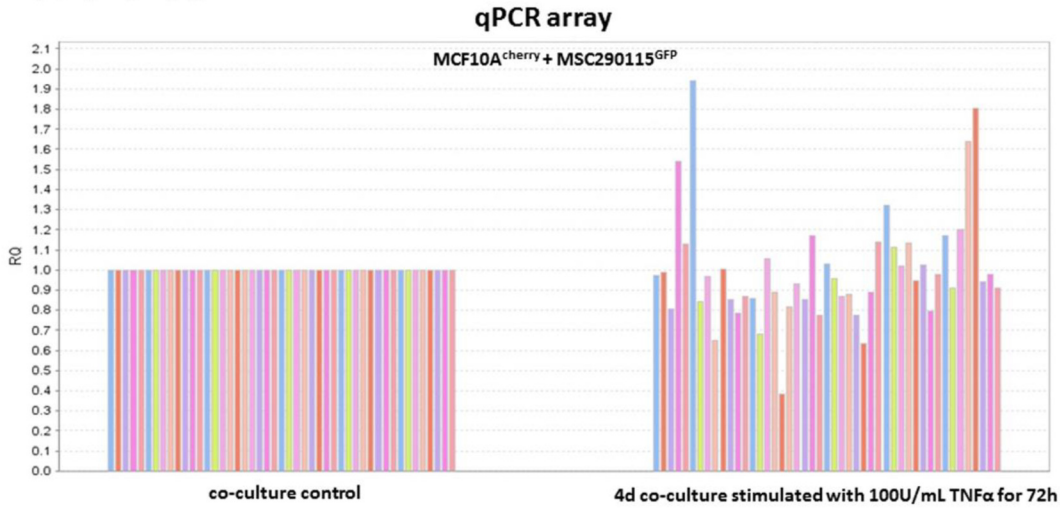


Hass, R.; suppl. Fig.S10 (top)




Hass, R.; suppl. Fig.S11 (top)
A
mono-culture
MCF10A^wt
mono-culture
MSC280416^wt
co-culture
MCF10A^wt + MSC280416^wt
TNFR1-PE
B
0h
non-transfected
0h
non-targeting siRNA #3
0h
siRNA TNFR1
TNFR1-PE
24h
48h
72h
TNFR1-PE
Count
FL2-H

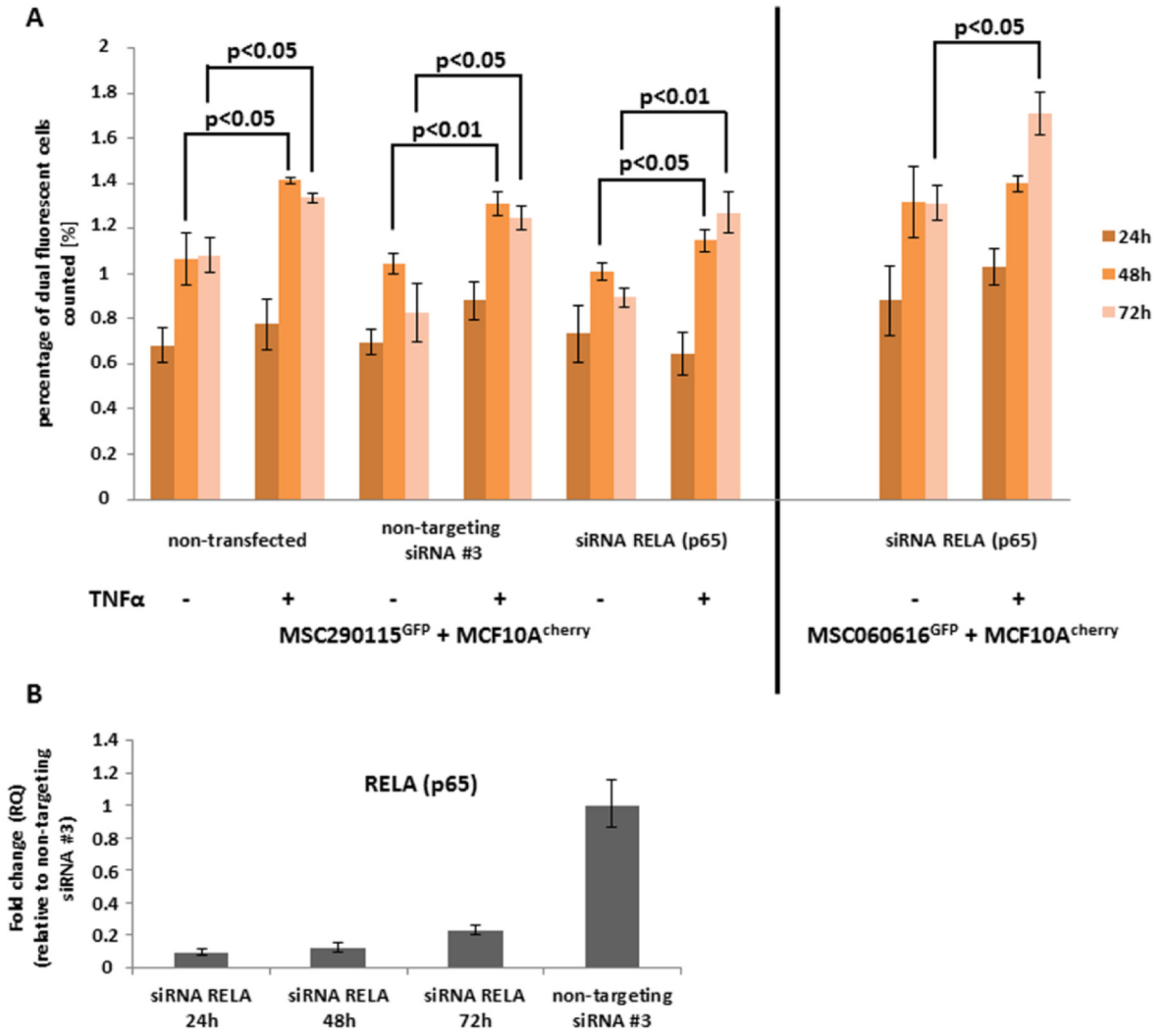
Hass, R.; suppl. Fig.S12 (top)



genes quantified:

18S	0.97	APAF1	0.99	BAG4	0.81	BID	1.54	BIRC2	1.13	BIRC3	1.94
CASP2	0.84	CASP3	0.96	CASP8	0.65	CASP7	1.00	CASP8	0.85	CASP9	0.79
CDC42	0.87	CHUK	0.86	CRADD	0.68	CYCS	1.06	FADD	0.89	FOS	0.39
IKBKB	0.85	IKBKE	1.17	IKBKG	0.77	JUN	1.03	MADD	0.96	MAP2K4	0.87
MAP3K1	0.88	MAP3K14	0.63	MAP3K7	0.78	MAPK8	0.89	NFKB1	1.14	NFKB2	1.32
NFKBIA	1.11	NFKBIB	1.02	NFKBIE	1.14	PAK1	0.94	PAK2	1.02	REL	0.80
RELA	0.98	RELB	1.17	RIPK1	0.91	TANK	1.20	TNF	1.64	TNFAIP3	1.81
TNFRSF1A	0.94	TRADD	0.98	TRAF2	0.91						

Hass, R.; suppl. Fig.S13 (top)



2.2 Enhanced metastatic capacity of breast cancer cells after interaction and hybrid formation with mesenchymal stroma/stem cells (MSC)

Catharina Melzer, Juliane von der Ohe and Ralf Hass

published in

Cell Communication and Signaling

2018 Jan 5;16(1):2.

doi: 10.1186/s12964-018-0215-4.

Author contribution statement:

Catharina Melzer (CM) performed the experiments (Fig. 1b+c, 3a+c, 4, 5, 6 ,7) and analyzed the data. CM critically read and approved the final manuscript.

Melzer et al. Cell Communication and Signaling (2018) 16:2
DOI 10.1186/s12964-018-0215-4

Cell Communication and Signaling

RESEARCH Open Access

Enhanced metastatic capacity of breast cancer cells after interaction and hybrid formation with mesenchymal stroma/stem cells (MSC)

Catharina Melzer, Juliane von der Ohe and Ralf Hass*

Abstract

Background: Fusion of breast cancer cells with tumor-associated populations of the microenvironment including mesenchymal stroma/stem-like cells (MSC) represents a rare event in cell communication whereby the metastatic capacity of those hybrid cells remains unclear.

Methods: Functional changes were investigated in vitro and in vivo following spontaneous fusion and hybrid cell formation between primary human MSC and human MDA-MB-231 breast cancer cells. Thus, lentiviral eGFP-labeled MSC and breast cancer cells labeled with mcherry resulted in dual-fluorescing hybrid cells after co-culture.

Results: Double FACS sorting and single cell cloning revealed two different aneuploid male hybrid populations (MDA-hyb1 and MDA-hyb2) with different STR profiles, pronounced telomerase activities, and enhanced proliferative capacities as compared to the parental cells. Microarray-based mRNA profiling demonstrated marked regulation of genes involved in epithelial-mesenchymal transition and increased expression of metastasis-associated genes including S100A4. In vivo studies following subcutaneous injection of the breast cancer and the two hybrid populations substantiated the in vitro findings by a significantly elevated tumor growth of the hybrid cells. Moreover, both hybrid populations developed various distant organ metastases in a much shorter period of time than the parental breast cancer cells.

Conclusion: Together, these data demonstrate spontaneous development of new tumor cell populations exhibiting different parental properties after close interaction and subsequent fusion of MSC with breast cancer cells. This formation of tumor hybrids contributes to continuously increasing tumor heterogeneity and elevated metastatic capacities.

Keywords: Mesenchymal stem cells, Breast cancer, Tumor microenvironment, Cell fusion, Hybrid cells

Background

In many cases removal of the tumor mass by surgery and subsequent treatment after early detection of primary tumors such as breast cancer reveal a favorable outcome and good prognosis for the patients. In contrast, spreading of cancer cells in the circulation (blood or lymph vessels) and formation of metastases significantly complicate a therapeutic regimen with predominantly bad prognosis. Properties of cancer cells to liberate from the primary tumor followed by trans-endothelial migration and attachment to distant tissues require a certain plasticity and adaption to a new microenvironment associated with maintenance of self-renewal capacity [1–3]. Consequently, such metastasizing cancer cells acquire new functional properties which simultaneously alter their chemotherapeutic responsiveness as compared to the local cancer cells of the primary tumor. Various mechanisms contribute to functional alterations of cancer cells including release of soluble factors (cytokines, chemokines, enzymes, metabolites), microvesicles and exosomes, induction of a retrodifferentiation program for potential formation of cancer stem-like cells (CSCs), and close

* Correspondence: hass.ralf@mh-hannover.de
Biochemistry and Tumor Biology Laboratory, Department of Obstetrics and Gynecology, Hannover Medical School, Carl-Neuberg-Str. 1, Hannover D–30625, Germany

BioMed Central

© The Author(s). 2018 **Open Access** This article is distributed under the terms of the Creative Commons Attribution 4.0 International License (http://creativecommons.org/licenses/by/4.0/), which permits unrestricted use, distribution, and reproduction in any medium, provided you give appropriate credit to the original author(s) and the source, provide a link to the Creative Commons license, and indicate if changes were made. The Creative Commons Public Domain Dedication waiver (http://creativecommons.org/publicdomain/zero/1.0/) applies to the data made available in this article, unless otherwise stated.

interaction with adjacent neighboring cell populations within the heterogeneous tumor tissue such as immune cells, endothelial cells or local tissue-associated mesenchymal stroma/stem cells (MSC).

Although MSC express diverse and multi-functional plasticity according to tissue-specific origin/homing, these heterogenic populations share a variety of common properties including regenerative potential, protection of stemness and tissues, regulation of stem cell homeostasis, support of repair and neovascularization, immune modulation, and differentiation capacity [4–6]. Similar properties are evolved by MSC at tumor sites by interacting with cancer cells [7]. Previous work has demonstrated that different breast and ovarian cancer cells at least transiently acquire new functional properties following interaction with MSC via gap junctional intercellular communication or notch signaling in vitro and in vivo [8, 9]. Moreover, receptor interactions such as the intercellular adhesion molecule ICAM-1 expressed on MSC can directly associate with the transmembrane heterodimeric glycoprotein MUC-1 (CD227, DF3, CA15–3) on the cell surface of breast cancer cells to promote an actin-based cell invasive motility in the tumor cells [10–12]. Furthermore, MSC release a large panel of trophic factors including different interleukins, CCLs, CXCLs, FGFs, EGFs, all forms of TGF-β, and PDGFs [13–17]. In response, breast cancer cells express appropriate receptors such as CCR5 and CXCR4 which promote proliferation and migration signals for further corresponding stimuli like CCL5 and SDF-1 [7, 18–23]. Additionally, interactions of breast cancer cells with populations of perivascular regions including pericytes and MSC contribute to tumor cell dormancy [24]. Such changes of cancer cell properties and function by transient stimulation and interaction with MSC can also be induced permanently e.g. by fusion processes and the generation of new cancer cell hybrid populations.

Cell fusions represent rare processes although important during development of certain tissues such as formation of placenta (fusion of fetal trophoblasts to syncytiotrophoblasts), formation of muscle fibers (repeated fusion of myoblasts to multi-nucleated myocytes), or bone metabolism (fusion of osteoclasts). Moreover, fertilization (fusion of sperm and egg) as a merge of gamete genomes displays a special form of cell fusion [25, 26].

The underlying mechanisms for cell fusion including homo- (fusion of cells from the same population) and heterofusion (hybrid formation of different cell types) are not fully understood yet. However, previous work suggested cell fusion as a rare event which appears to be tightly regulated by involving multiple pathways [27]. Factors identified with fusogenic properties include sequestered or truncated genes originating from viral functions such as the HERV-W retroviral envelope genes that have been domesticated in the mammalian genome and evolving proteins termed syncytin-1 and -2 are predominantly found in syncytiotrophoblasts in placenta tissue [28, 29] but also in tumors including tumors of the breast. Moreover, ASCT-2 (alanine, serine and cysteine selective transporter-2) present on endothelial cells and functioning as a syncytin receptor demonstrated fusion of breast cancer cells with endothelial cells [30]. Alternatively, macrophage fusion and myoblast formation may involve the Dock180 (dedicator of cytokinesis) guanine nucleotide exchange factor in cooperation with ELMO for subsequent Rac1 activation and disproportional regulation of the actin cytoskeleton [31, 32].

Cell fusion can be also detected in existing cancers [33]. Thus, cell fusion can generate aneuploidy, chromosomal instability, and DNA damage, all of which might cause multiple genetic changes and cancer [34, 35].

In the present work, we isolated and characterized different cancer hybrid cell populations following interaction and fusion of MDA-MB-231 breast cancer cells with MSC. These hybrid cells revealed alterations in tumorigenicity, metastatic properties and chemotherapeutic responsiveness when compared to their originating parental populations and to each other.

Methods

Cell culture

Human MSC were isolated from umbilical cord explant cultures as reported previously [36] and cultured in αMEM (Sigma Chemie GmbH, Steinheim, Germany) supplemented with 10% of allogeneic human AB-serum (commercially obtained from blood bank, University Campus Lübeck, Germany), 100 U/ml penicillin, 100 μg/ml streptomycin and 2 mM L-glutamine (Sigma). For subculture, MSC were harvested by accutase (Sigma) treatment for 3 min at 37 °C. Although limited by clonal convergence during in vitro expansion [37] neo-natal umbilical cord explanted MSC in low passage numbers (P1 to P4) were used due to their superior capabilities as compared to a heterogeneous local tissue-associated MSC population [5].

Human MDA-MB-231 breast cancer cells were obtained from the ATCC (#HTB-26) and cultivated initially at 1500 cells/cm^2 in Leibovitz's L-15-medium (Invitrogen) supplemented with 10% (v/v) FCS, 2 mM L-glutamin and 1 mM penicillin/streptomycin.

Cell line testing and authentication

All cells were tested for mycoplasma by the luminometric MycoAlert Plus mycoplasma detection kit (Lonza Inc., Rockland, ME, USA) according to the manufacturer's recommendations. Moreover, authentication of MDA-MB-231 and MDA-hybrid populations was performed by short tandem repeat (STR) fragment analysis

using the GenomeLab human STR primer set (Beckman Coulter Inc., Fullerton, CA, USA). The STR pattern of MDA-MB-231 cell line demonstrated similar results according to the STR database provided by the ATCC, Manassas, VA, USA.

Co-culture of MSC with human cancer cell lines and isolation of hybrid cells

For co-culture experiments with MSC populations, MDA-MB-231 breast cancer cells were previously adapted to MSC culture medium. In order to distinguish the different cell types and newly formed hybrid cells within the co-culture, the MSC and the cancer cells have been transduced with a 3rd generation lentiviral SIN vector containing the eGFP and the mcherry gene, respectively, as indicated in previous work [9]. Following 6d of MSC^{GFP}/MDA-MB-231^{cherry} co-culture (cell ratio 60:40 at a density of 2000 cells/cm^2) in MSC medium, the cells were separated by repeated fluorescence-activated cell sorting (FACS) of double-labeled (mcherry and GFP) cells into microtiter plates with one to two hybrid cells/well for subsequent cell cloning. Two resulting hybrid clones of MDA-MB-231 co-culture (MDA-hyb1 and MDA-hyb2) were further analyzed.

Telomerase assay

The activity of this nuclear enzyme was detected by TRAPeze telomerase detection kit (Millipore, Beverly, MA, USA) in a radioactive assay as previously described [38]. Briefly, homogenates of 10^6 cells were prepared in CHAPS lysis buffer and combined with the reaction mixture including a [γ-32P] ATP radiolabeled TS primer which has been previously labelled with T4-polynucleotide kinase (NEB, Beverly, MA, USA). Evaluation and adjustment of equal amount of protein was performed using the Bradford assay (Bio-Rad Inc., Richmond, CA, USA). The different cell samples were subjected to PCR amplification according to the manufacturer's instructions using Taq DNA polymerase (NEB, Beverly, MA, USA). Thereafter, loading dye was added to the amplified DNA and the samples were separated in a 10% non-denaturing polyacrylamide gel electrophoresis. The gel was dried and the radioactive bands were visualized in a PhosphorImager (Storm 820, Amersham Biosciences).

Transcript analysis by RT-PCR

Total RNA was isolated using RNeasy Mini Kit (Qiagen, Hilden, Germany) according to the manufacturer's instructions. One μg RNA was reverse transcribed into cDNA using 500 μM of dNTP (R0193), 5 μM Oligo(dT)18 primer (S0132), 5 μM Random Hexan primer (S0142), 1 U RiboLockTM RNase Inhibitor (E00381) and 5 U RevertAidTM M-MuLV Reverse Transcriptase (EP0441) in the supplied reaction buffer (all reagents from Thermo Scientific, Schwerte, Germany). The cDNA reactions were performed for 10 min/25 °C, 1 h/37 °C and stopped at 72 °C for 10 min. As a template 2.5 μl of cDNA was used with primers specific for

- mcherry (sense: 5`-TTC ATG TAC GGC TCC AAG GC-3´; antisense: 5`-CTG CTT GAT CTC GCC CTT CA-3´; amplification product 297 bp)
- eGFP (sense: 5`-CTA TAT CAT GGC CGA CAA GCA GA-3´; antisense: 5`-GGA CTG GGT GCT CAG GTA GTG G-3´; amplification product 165 bp)
- CD73 (sense: 5'-CGC AAC AAT GGC ACA ATT AC-3´; antisense: 5'-CTC GAC ACT TGG TGC AAA GA-3´; amplification product 241 bp) [9];
- CD90 (sense: 5´-GGA CTG AGA TCC CAG AAC CA-3´; antisense: 5'-ACG AAG GCT CTG GTC CAC TA-3´; amplification product 124 bp) [9];
- CD105 (sense: 5´-TGT CTC ACT TCA TGC CTC CAG CT-3´; antisense: 5´-AGG CTG TCC ATG TTG AGG CAG T-3´; amplification product 378 bp) [9]
- MFSD-2A (sense: 5`-CTC CTG GCC ATC ATG CTC TC-3´; antisense: 5`-GGC CAC CAA GAT GAG AAA-3´; amplification product 129 bp)
- syncytin-2 (sense: 5`-AGC AGC CGT AGT CCT TCA AA-3´; antisense: 5`-AGG GGA AGA ACC CAA GAG AA-3´; amplification product 231 bp) [39]
- Ki67 (sense: 5`-TAT CAA AAG GAG CGG GGT CG-3´; antisense: 5`-TTG AGC TTT TCT CAT CAG GGT CA-3´; amplification product 389 bp) [40]
- GAPDH as a control (sense: 5'-ACC ACA GTC CAT GCC ATC AC-3´; antisense: 5'-TCC ACC ACC CTG TTG CTG TA-3´; amplification product 452 bp) [41]

(all primers customized by Eurofins, MWG GmbH, Ebersberg, Germany). PCR reactions included 0.2 μM of each primer, 200 μM of dNTP (R0193, Thermo Scientific) and 0.03 U One Taq Hot Start DNA polymerase (New England Biolabs GmbH, Frankfurt am Main, Germany) in the supplied reaction buffer. PCR cycling conditions were performed 30 s at 94 °C, 1 min at 60 °C and 68 °C for 1 min respectively, including an initial 30 s denaturation step at 94 °C and a final 5 min extension step at 68 °C (35 cycles). Aliquots of 25 μl of each RT-PCR product were separated on a 2% agarose gel including the standard GeneRuler 100 bp DNA Ladder (Thermo Scientific) and visualized by GelRedTM (Biotium Inc., Hayward, CA, US) staining.

Microarray-based mRNA expression analysis (single color mode)

This Microarray study has been performed by use of a refined version of the Whole Human Genome Oligo Microarray 4x44K v2 (AMADID 026652, Agilent Technologies), called '026652AsQuintuplicatesOn180k'

(AMADID 054261) developed by the Research Core Unit Transcriptomics of Hannover Medical School. Microarray design was defined at Agilent's eArray portal using a 4x180k design format for mRNA expression as template. All non-control probes of AMADID 026652 have been selected to be printed five times onto one 180 k Microarray (on-chip quintuplicates). Control probes required for proper Feature Extraction software algorithms were determined and placed automatically by eArray using recommended default settings.

Synthesis of Cy3-labeled cRNA was performed with the 'Quick Amp Labeling kit, one color' (#5190–0442, Agilent Technologies) according to the manufacturer's recommendations. cRNA fragmentation, hybridization and washing steps were carried-out exactly as recommended in the 'One-Color Microarray-Based Gene Expression Analysis Protocol V5.7'.

Slides were scanned on the Agilent Micro Array Scanner G2565CA (pixel resolution 3 μm, bit depth 20). Data extraction was performed with the 'Feature Extraction Software V10.7.3.1' by using the recommended default extraction protocol file 'GE1_107_Sep09.xml', except that the minimal number of replicates used to calculate population outliers was set to 5.

Measurements of on-chip replicates were averaged using the geometric mean of processed intensity values of the green channel, 'gProcessedSignal' (gPS) to retrieve one resulting value per unique non-control probe. Single Features were excluded from averaging, if they i) were manually flagged, ii) were identified as Outliers by the Feature Extraction Software, iii) lay outside the interval of '1.42 x interquartile range'regarding the normalized gPS distribution of the respective on-chip replicate population, or, iv) showed a coefficient of variation of pixel intensities per Feature that exceeded 0.5.

Averaged gPS values were normalized by global linear scaling. For this, all gPS values of one sample were multiplied by an array-specific scaling factor. This factor was calculated by dividing a 'reference 75th Percentile value' (set as 1500 for the whole series) by the 75th Percentile value of the particular Microarray to be scaled ('Array i' in the formula shown below). Accordingly, normalized gPS values for all samples (microarray data sets) were calculated by the following formula:

$$\text{normalized gPS}_{\text{Array i}} = \text{gPS}_{\text{Array i}} \times \left(1500/75^{\text{th}}\ \text{Percentile}_{\text{Array i}}\right).$$

A lower intensity threshold (surrogate value) was defined based on intensity distribution of negative control features. This value was fixed at 10 normalized gPS units. All of those measurements that fell below this intensity cutoff were substituted by the respective surrogate value of 10. Gene expression levels of more than 2-fold difference were compared between parental MSC and hybrid cells as well as between corresponding cancer and hybrid cells and the data file are included as Additional file 1: Figure S9 and stored with the accession no. #GSE100551 at the NCBI-GEO database.

Cell cycle analysis

For cell cycle analysis in the MDA-hybrid cells and the parental cell lines, 10^5 cells were fixed in 70% (v/v) ice-cold ethanol at 4 °C for 24 h. Thereafter, the fixed cells were stained with 500 μL of DNAse-free RNase (200 U/mL) and 500 μL of propidium iodide (PI) buffer (10 mL PBS + 100 μL Triton-X-100 + 500 μL 0.5 mg/mL propidium iodide in water) in the dark at room temperature for 30 min. The stained cells were analyzed for DNA content in a FACSCalibur (BD Biosciences) using FlowJo software.

siRNA knock-down

A reverse transfection was applied for knock-down according to the manufacturer's protocol (Dharmacon, GE Healthcare) using S100A4 small-interfering RNA (siRNA). The breast cancer cell line MDA-MB-231 was transfected with 25 nM S100A4 siRNA (siGENOME Human S100A4 siRNA SMARTpool, cat. #M-004792-01) or non-targeting siRNA (siGENOME Non-Targeting siRNA #3, cat. #D-001210-03, Dharmacon, GE Healthcare) using DharmaFECT1 transfection reagent (cat. #T-2001-02, Dharmacon, GE Healthcare) diluted 1:2000 in transfection medium (antibiotic-free medium) for 24 h. After 24 h transfection, the cells were washed and cultured in normal growth medium. Examination of transfection efficiency was analyzed by flow cytometry following transfection of MDA-MB-231 cells with 25 nM of the green fluorescing siGLOGreen (cat. #D-001630-01, Dharmacon) for 24 h.

For quantification of fusion cells, lentiviral transduced MDA-MB-231^{cherry} cells were transfected for 24 h in 24-well plates with a cell density of 3500 cells/cm^2 in triplicate. After transfection with siRNA S100A4 and non-targeting siRNA, respectively, the same amount of lentiviral transduced MSC^{GFP} was added and co-cultures were initiated for up to 72 h. At indicated time points, each well was screened for dual fluorescent cells (double positive for GFP and cherry) with green and red fluorescence filters, and a FITC/TRIC fluorescence dual band filter using a fluorescence microscope (Olympus IX50). Following quantification of hybrid cells in the wells, all co-cultures were trypsinized and counted in a hemocytometer to calculate the percentage of dual fluorescent cells.

In vivo experiments

Animal research using NOD/scid mice was carried out by following the internationally recognized guidelines on animal welfare and has been approved by the

institutional licensing committee (Nieders. Landesamt für Verbraucherschutz und Lebensmittelsicherheit) ref. # 33.19–42,502–04-15/1992 on Dec. 18th, 2015.

About 2×10^6 GFP-labeled MDA-MB-231 cells and in separate groups, 2×10^6 MDA-hyb1 and MDA-hyb2 cells were injected subcutaneously into 5 animals of 5 to 6 weeks old female NOD/scid mice, respectively. After 18d post injection, all 15 mice had developed subcutaneous tumors and the animals were sacrificed by CO_2 anesthesia and cervical dislocation. For a comparable tumor size, additional 4 NOD/scid mice were injected with 2×10^6 GFP-labeled MDA-MB-231 cells and the mice were sacrificed after 34d post injection when the tumor size had reached the range of MDA-hyb1 tumors after 18d post injection.

In vivo treatment experiments were carried out after subcutaneous injection of MDA-MB-231^{GFP} cells and MDA-hyb1 cells into 6 animals, respectively. Four days after tumor cells injection oral therapy (200 μL) was started twice a week with 25 mg/kg taxol in 3 mice and a solvent control (25% ethanol in PBS (*v*/v)) in the other 3 mice of both tumor cell populations. All gavage treatments were carried out using sterile straight 18-gauge, 30 mm plastic feeding tubes (Instech Laboratories Inc., Plymouth, PA, USA). Following tumor cell injection, all 12 mice had developed subcutaneous tumors and the animals were sacrificed by cervical dislocation.

Primary tumor tissues were dissected under UV light and weighted. Organs were also dissected from the mice and thin sections were analyzed by fluorescence microscopy for presence and accumulation of metastatic cells.

Cytotoxicity measurements of chemotherapeutic-treated cell cultures by fluoroskan assay

The proliferative capacities of MDA-MB-231^{GFP}, MDA-hyb1, and MDA-hyb2 cells were compared by fluorescence measurement using the fluoroskan assay as previously described [42, 43]. Briefly, 3000 cells/well were seeded with standard culture medium (100 μL/well) in flat bottom 96-well plates (Nunc/ThermoFischer Scientific, Roskilde, Denmark) and incubated overnight to allow attachment. Thereafter, 100 μL of culture medium was added to the cells as a control and in further wells 100 μL of culture medium containing different chemotherapeutics were added to the cells. Following incubation for up to 72 h, the medium was removed and the cells were lysed with 5% (*w*/*v*) SDS. Afterwards, the fluorescence intensities of mcherry and eGFP in the cell homogenate which corresponded to the appropriate cell number of cancer cells were measured at excitation 485 nm / emission 520 nm (for MDA-MB-231 and MDA-hyb2) or at excitation 584 nm / emission 612 nm (for MDA-hyb1) using the Fluoroskan Ascent Fl (ThermoFisher Scientific).

Results

Co-culture of different human MSC^{GFP} with mcherry-labeled breast cancer cells was accompanied by formation of hybrid cells via spontaneous cell fusions. Two resulting hybrid clones of MSC^{GFP}/MDA-MB-231^{cherry} co-culture (MDA-hyb1 and MDA-hyb2) were selected by subsequent two step cell sorting (Additional file 2: Figure S1). One of these clones lost the GFP gene during the selection process (MDA-hyb1) while the other clone remained double-labeled (MDA-hyb2).

Proliferative capacity of the three different breast cancer populations was tested by cell counting of initially seeded 2.5×10^3 cells in 24-well plates after 72 h to 120 h, respectively (Fig.1a). All tumor cell cultures progressively increased in cell number over time. A significantly elevated hybrid cell population was observed with a 10-fold enhanced proliferation for MDA-hyb1 and a 4-fold increased cell growth for MDA-hyb2 as compared to their wildtype MDA-MB-231 tumor counterpart (Fig.1a).

A sustained telomerase activity substantiated a persistent cell growth of the fused hybrid cell populations as detected for MDA-hyb1 (Fig.1b) and MDA-hyb2 (Fig.1c) in comparison to prominent telomere adducts in the immortalized parental MDA-MB-231 cell line and a weak telomerase activity in the parental MSC (Fig.1b, c).

Characterization of the different populations by STR fragment analysis confirmed the known patterns of the parental MDA-MB-231 cell line and revealed some significant differences in the corresponding MDA-hyb1 and MDA-hyb2 cells after spontaneous fusion with individual MSC populations during co-culture (Fig.2). To provide parental populations of different gender, MSC from a male donor were selected for co-culture with the female breast cancer cells and chromosomal rearrangements in the hybrid cells revealed an acquisition of the MSC-derived XY configuration in the analyzed hybrid populations (Fig.2). Karyotype analysis confirmed the male sex of MDA-hyb1 whereby some MDA-hyb2 cells lost the Y-chromosome. Both hybrid populations displayed a pseudo-triploid karyotype like in the parental MDA-MB-231 cells (Additional file 3: Figure S2). Supportive evidence was obtained from steady state cell cycle analysis. DNA fluorescence measurements of normal diploid chromosomes in G1 phase of MSC was enhanced by nearly 50% in MDA-MB-231 cells with a shift in G1 peak and the whole cell cycle demonstrating aneuploidy (Additional file 4: Figure S3). Similar results were obtained for MDA-hyb1 and MDA-hyb2 cells with a pseudo-triploid G1 peak as observed for MDA-MB-231 cells (Additional file 4: Figure S3). Moreover, MDA-hyb1 and MDA-hyb2 cells exhibited a markedly elevated S and G2/M phase, respectively, in contrast to the parental MSC or MDA-MB-231 cells further substantiating a

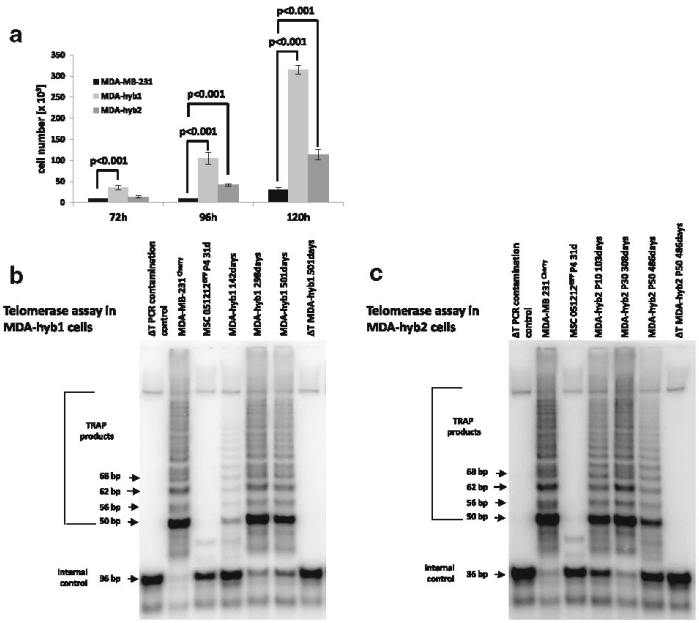


Fig. 1 Elevated proliferative potential and sustained telomerase activity in MDA-hyb1 and MDA-hyb2 cells. **a** Proliferative capacity of the different breast cancer populations was tested by cell counting of initially seeded 2.5×10^3 cells in 24-well plates after 72 h to 120 h, respectively. All tumor cell cultures progressively increased in cell number over time. A significantly elevated 10-fold enhanced proliferation for MDA-hyb1 and a 4-fold increased cell growth for MDA-hyb2 hybrid cell population were observed as compared to their wildtype MDA-MB-231 tumor counterpart. Data represent the mean ± s.d. of 3 independent experiments. **b** and **c** Telomerase activity was measured in hybrid populations at different ages including MDA-hyb1 after 142d, 298d, or 501d in culture, respectively and MDA-hyb2 in passage 10 (P10), P30, or P50, respectively, in comparison to the parental $MSC051212^{GFP}$ P4 and $MDA\text{-}MB\text{-}231^{cherry}$ cells. A primer/dimer control and a heat-inactivated telomerase in MSC samples served as an appropriate negative control in the assays

more active proliferation of these hybrid cells (Additional file 4: Figure S3). Interestingly, Ki67 staining (Additional file 5: Figure S4 upper panel) and overall expression of Ki67 (Additional file 5: Figure S4 lower panel) remained at reduced or unaltered levels in MDA-hyb1 and MDA-hyb2 cells suggesting that only parts of these populations exhibit high proliferative capacity.

Together with the appearance of various different STR fragments as compared to the parental cells, these findings demonstrated the generation of heterogeneously proliferating and completely altered hybrid breast cancer cell populations.

More detailed analysis of these newly-formed hybrid cell types was performed by RNA microarray profiling (Additional file 1: Figure S9). MDA-hyb1 cells revealed a different expression of 4011 genes compared to MDA-MB-231 cells and 5742 altered expression levels compared to the corresponding MSC (Fig.3a). An even more pronounced alteration was observed in MDA-hyb2 cells with 4592 altered gene expressions compared to the parental MDA-MB-231 cells and 6201 varied mRNA levels compared to the parental MSC, whereby about half of them were up- or down-modulated (Fig.3a).

Exclusive expression of mcherry was detectable in $MDA\text{-}MB\text{-}231^{cherry}$ and eGFP in MSC^{GFP} cells (Fig.3b). Analysis of the two hybrid population revealed both fluorescence transcripts in MDA-hyb2 cells whereas MDA-hyb1 cells only demonstrated mcherry. The MSC-characteristic stemness markers CD73 and CD90 were differentially expressed in all cell types as evaluated by PCR and RNA microarray analysis, respectively (Fig.3b, Additional file 6: Figure S5). Thus, mRNA levels of the GPI-anchored ecto-5′-nucleotidase (CD73) were significantly enhanced in MDA-hyb1 and even further elevated in MDA-hyb2 cells (Fig.3b, Additional file 6: Figure S5). CD90 was undetectable in the MDA-MB-231 and MDA-hyb1 cells. In contrast, low mRNA levels of CD90 were expressed by MDA-hyb2 when compared to MSC controls (Fig.3b, Additional file 6: Figure S5). Regarding potential fusion properties, all four cell

	parental cell populations		hybrid cell populations	
STR fragment	MDA-MB 231	MSC051212 IV P1 29d	MDA-hyb1 426d	MDA-hyb2 P42 397d
	pseudo-triploid	diploid	pseudo-triploid	pseudo-triploid
Penta D A1	11	11	14	11
Penta D A2	14	11	14	14
Penta E A1	11	7	11	7
Penta E A2	11	13	11	11
AMEL A1	X-chr	X-chr	X-chr	X-chr
AMEL A2	X-chr	Y-chr	Y-chr	Y-chr
CSF1PO A1	12	10	12	12
CSF1PO A2	13 + 14	10	13 + 14	13 + 14
D13S317 A1	13	11	13	12
D13S317 A2	13	12	13	13
D16S539 A1	12	12	12	12
D16S539 A2	12	12	12	12
D18S51 A1	11	15	11	11
D18S51 A2	11	19	11	15
D3S1358 A1	16	14	16	14
D3S1358 A2	16	16	16	16
D7S820 A1	8	10	8	8
D7S820 A2	9	12	9	9 + 10
D8S1179 A1	13	14	13	13
D8S1179 A2	13	14	13	14
TH01 A1	7	6	7	9,3
TH01 A2	9,3	9,3	10	9,3
TPOX A1	8	8	8	8
TPOX A2	9	8	9	9

Fig. 2 STR fragment analysis of MDA-hyb1 and MDA-hyb2 cells. Characterization by short tandem repeat (STR) fragment analysis was performed for the parental breast cancer MDA-MB-231 cells and MSC051212 in comparison to their spontaneous fusion products MDA-hyb1 and MDA-hyb2. Changes in the STR fragment pattern of the hybrid populations compared to the corresponding parental counterparts are labeled in red

populations expressed transcripts of some fusogenic factors including MFSD-2A and syncytin-2 whereby MFSD-2A has been described as the receptor for syncytin-2 during trophoblast fusion [44].

Further marker, such as CD29 exhibited higher levels in the hybrid cells as compared to MDA-MB-231. In contrast, the hyaluronan receptor CD44 like CD146 and CD166 displayed lower mRNA transcripts in the hybrids compared to both parental populations (Additional file 6: Figure S5). CD105 expression remained nearly unchanged in MDA-MB-231 and the two hybrid populations although significantly lower as compared to MSC (Additional file 6: Figure S5). Together, these findings further characterized the two hybrid populations as completely different cell types whereby MDA-hyb1 exhibited more similarities to MDA-MB-231 cells in contrast to MDA-hyb2 cells expressing certain properties associated with MSC.

Liberation from the primary tumor site, followed by trans-epithelial and trans-endothelial migration as circulating tumor cells in blood or lymphatic vessels represents a necessity for breast cancer cells to form disseminated distant metastasis [45]. This development is predominantly associated with an epithelial-mesenchymal transition (EMT) of the cancer cells although EMT is not absolutely required for tumor dissemination but dispensable in certain kinds of metastasizing tumors [46, 47]. A variety of genes are up-regulated during EMT in parallel to a down-modulation of other genes to enable development of a mesenchymal phenotype. Expression analysis in MDA-hyb1 and even more pronounced in MDA-hyb2 revealed appropriate up-regulation of EMT-associated genes including SNAI2, collagen and fibronectin (Fig. 3c). Moreover, expression of N-cadherin was increased along with matrix metalloproteinases MMP3 and MMP9 (Fig. 3c). In addition, down-regulation was detected for certain genes such as cytokeratin 19, desmoplakin, and some basic helix-loop-helix-associated transcription factors such as MITF (Fig. 3d). These data suggested potential metastatic properties of MDA-hyb1 and MDA-hyb2 cells.

Supportive evidence for this suggestion was obtained by the expression profile of metastasis-related gene expression in the two hybrid populations versus the parental MDA-MB-231 breast cancer cell line which revealed a significant up-regulation of a majority of metastasis genes in MDA-hyb1 compared to MDA-MB-231 and likewise in MDA-hyb2 compared to MDA-MB-231 cells (Fig. 4). Together, these findings suggested an enhanced

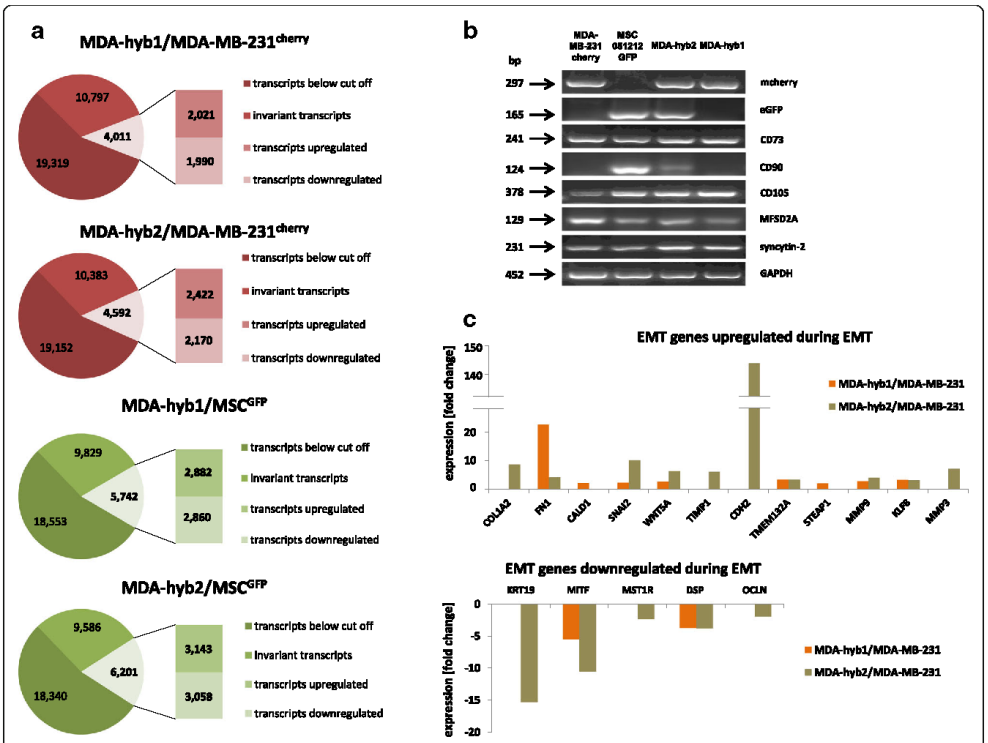


Fig. 3 Microarray and PCR analysis of the two hybrid populations in comparison to the parental cell lines. **a** Quantification of genes with changed expression levels (up-regulation = numbers in upper rectangular; down-regulation = numbers in lower rectangular) in MDA-hyb1 (upper panels, red and green) and MDA-hyb2 cells (lower panels, red and green) was performed following microarray analysis with comparison to the parental MDA-MB-231^{cherry} cells (red panels) and to the parental MSC051212^{GFP} (green panels) respectively. Changes in expression levels of more than 2-fold were considered as up- or down-regulated. **b** PCR analysis was performed with mcherry, eGFP, fusion-associated factors syncytin-2 and MFSD-2A, and MSC stem-like markers CD73, CD90, and CD105 expression in the parental MDA-MB-231 and MSC populations as compared to the two hybrid populations. Unaltered GAPDH transcripts served as loading control. **c** Comparison of EMT-related gene expression in MDA-hyb1 relative to MDA-MB-231 (orange-colored bars) and in MDA-hyb2 relative to the parental MDA-MB-231 cells (kaki-colored bars). A variety of genes are up-regulated during EMT (upper panel) in parallel to a down-modulation of other genes (lower panel) to enable development of a mesenchymal phenotype

metastatic capacity of the hybrid populations over the parental MDA-MB-231 cells. Indeed, evaluation and comparison of certain disease- and function-associated gene clusters in MDA-hyb1 and MDA-hyb2 hybrid cells as compared to the parental MDA-MB-231 and MSC051212 revealed a significantly elevated expression level of gene clusters accompanied with certain malignancies including different kinds of cancer, migratory capacity, and formation of metastasis (Additional file 7: Figure S6).

Although MDA-hyb1 cells demonstrated increased transcripts associated with metastatic capacity, MDA-hyb2 cells revealed further enhanced expression of EMT genes and more metastasis-associated mRNAs. A direct comparison of all elevated metastasis genes in the microarray data of MDA-hyb1 with those of the MDA-hyb2 expression profile revealed 31 identical and 7 different genes in MDA-hyb1, among them S100A4 which encodes a member of the S100 calcium-binding protein family supporting tumorigenic proliferation by stimulating angiogenesis and by promoting metastases [48]. Calcium-binding induces a conformational change in S100A4 to enable interaction with other proteins such as p53, liprin-β1 or factors involved in cell migration including actins, non-muscle myosin heavy chain IIA, and tropomyosin [49]. Based upon these functionalities, the

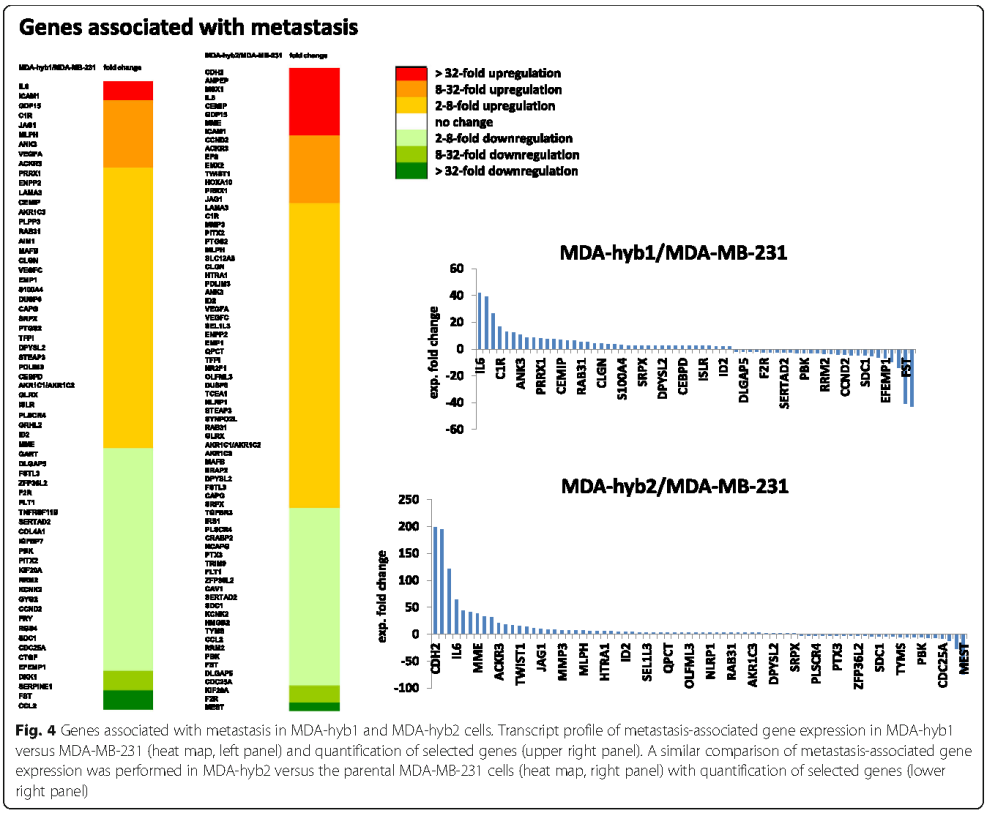


Fig. 4 Genes associated with metastasis in MDA-hyb1 and MDA-hyb2 cells. Transcript profile of metastasis-associated gene expression in MDA-hyb1 versus MDA-MB-231 (heat map, left panel) and quantification of selected genes (upper right panel). A similar comparison of metastasis-associated gene expression was performed in MDA-hyb2 versus the parental MDA-MB-231 cells (heat map, right panel) with quantification of selected genes (lower right panel)

role of S100A4 in MDA-MB-231 cells and hybrid formation with MSC was elucidated by siRNA knockdown experiments. S100A4 targeting in MDA-MB-231 cells with a transfection efficiency of 92.5% (Additional file 8: Figure S7) was associated with a significantly reduced formation of hybrid cells following co-culture with MSC as compared to a non-targeting siRNA after 48 h (Fig. 5a). These findings suggested that blocking S100A4 signaling reduces the formation of high proliferative active breast cancer hybrid cells also carrying metastatic properties. Supportive evidence is presented by recent work demonstrating reduced migration and metastases of breast cancer cells following down-modulation of S100A4 [50].

To substantiate potentially enhanced tumorigenicity of MDA-hybrid cells and corresponding knowledge in an in vivo system, testing of metastatic capacity was performed after subcutaneous injection of 2×10^6 MDA-MB-231^{GFP}, MDA-hyb1, and MDA-hyb2 cells into NODscid mice, respectively. Following simultaneous injection, the hybrid populations developed a substantially increased tumor growth as compared to the parental MDA-MB-231 cells after 18d post injection (Fig. 5b). Using the parental MDA-MB-231-generated tumors (n = 5) as a reference, tumor weight was significantly elevated by 18.1-fold in MDA-hyb1 (n = 5) and by 2.4-fold in MDA-hyb2 (n = 5) tumors following 18d after tumor cell injection (Fig. 6a). Similarly, the relationship of tumor weight / mouse weight of 0.25 ± 0.13 in MDA-MB-231^{GFP} mice increased by 17.7-fold to 4.42 ± 1.31 in MDA-hyb1 and by 2.4-fold to 0.60 ± 0.16 in MDA-hyb2 (Fig. 6b). To reach an approximately equivalent tumor size like MDA-hyb1-induced tumors, the parental MDA-MB-231 required 34d after tumor cell injection (Fig. 5b).

Four out of the five mice from each tumor cell population were randomly chosen and screened for potential metastases. Formation of distant organ metastases was analyzed by removal of organs from all 12 mice followed by tissue thin section phase contrast

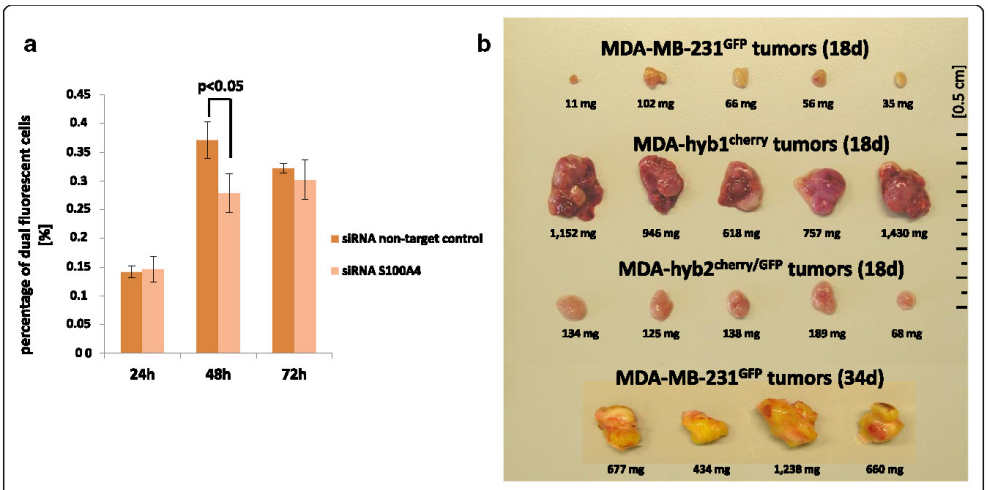


Fig. 5 Effects of S100A4 knock-down in hybrid cell formation and in vivo tumor development of hybrid cells. **a** Efficiency and significance of hybrid cell formation by MDA-MB-231^{cherry} and MSC^{GFP} fusion was examined and quantified following siRNA targeted down-modulation of S100A4 versus a non-targeting siRNA. The relative amount of hybrid cells was calculated by the mean ± s.d. from 3 different co-cultures and significance was calculated by student's-t-test. **b** In vivo tumor development was tested after simultaneous subcutaneous injection of 2×10^6 cells of MDA-MB-231^{GFP}, MDA-hyb1, or MDA-hyb2 cells into 5 NODscid mice respectively. The fifteen mice were euthanized after 18d and dissected tumors were compared for tumor size. In addition, 2×10^6 cells of MDA-MB-231^{GFP} cells were injected subcutaneously into 4 NODscid mice. to achieve a comparable tumor size like MDA-hyb1 cells after 34d

/ fluorescence microscopy. None of the organs of previously MDA-MB-231^{GFP}–injected cells displayed any detectable GFP fluorescence in the 4 mice after 18d. In contrast, 3 out of 4 mice exhibited metastases to the lung, liver, spleen, and heart, and all (4/4) to the kidney in MDA-hyb1-induced tumors (Fig. 6c). Likewise, organ metastases of MDA-hyb2-derived tumors were detectable in spleen (1/4), heart (1/4), and kidney (3/4). An appropriate size of MDA-MB-231^{GFP}-induced tumors after 34d of xeno-transplantation (Fig. 5b) revealed distant organ metastases in the lung (4/4), spleen (1/4), heart (1/4), and kidney (1/4) whereby GFP-positive cells in the liver remained undetectable (Fig. 6c).

While MDA-MB-231 cells as triple negative breast cancer cell line (negative for estrogen, progesterone, and Her2/neu receptors) are long time known for metastatic tumor growth [51] this capability is significantly enhanced and much more accelerated in the MDA-hyb1 and MDA-hyb2 populations.

Taken together, these data demonstrated an expression profile with elevated EMT- and metastasis-associated genes in MDA-hybrid populations which was functionally substantiated in vivo by significantly enhanced tumor growth and much faster formation of multiple organ metastases.

Of interest, MDA-hyb1 and MDA-hyb2 cells demonstrated increased chemotherapeutic sensitivity to a variety of compounds including taxol, cisplatin, methotrexate (MTX), epirubicin, and foretinib after in vitro incubation for 24 h up to 72 h when compared to the parental MDA-MB-231 cells (Additional file 9: Figure S8). To substantiate these findings in vivo, taxol was chosen to evaluate the responsiveness of MDA-hyb1-induced and parental MDA-MB-231-generated NODscid mice tumors (Fig. 7). Whereas MDA-hyb1-mediated tumors developed heterogeneously with different types of metastases, an increased sensitivity to taxol was detectable and this treatment was also associated with no detectable metastases. Parental MDA-MB-231-induced tumors also developed various organ metastases and displayed a certain taxol-sensitivity, however, some organ metastases in kidney (1/3) and spleen (1/3) remained detectable (Fig. 7).

Discussion

Invasive tumor growth and development of solid tumors is associated with an inflammatory environment, acidic pH, hypoxia and reduced nutrient availability which favor the accumulation of damage products and cell death [52]. Apoptotic, necrotic/necroptotic, and autophagic cells within the tumor microenvironment release

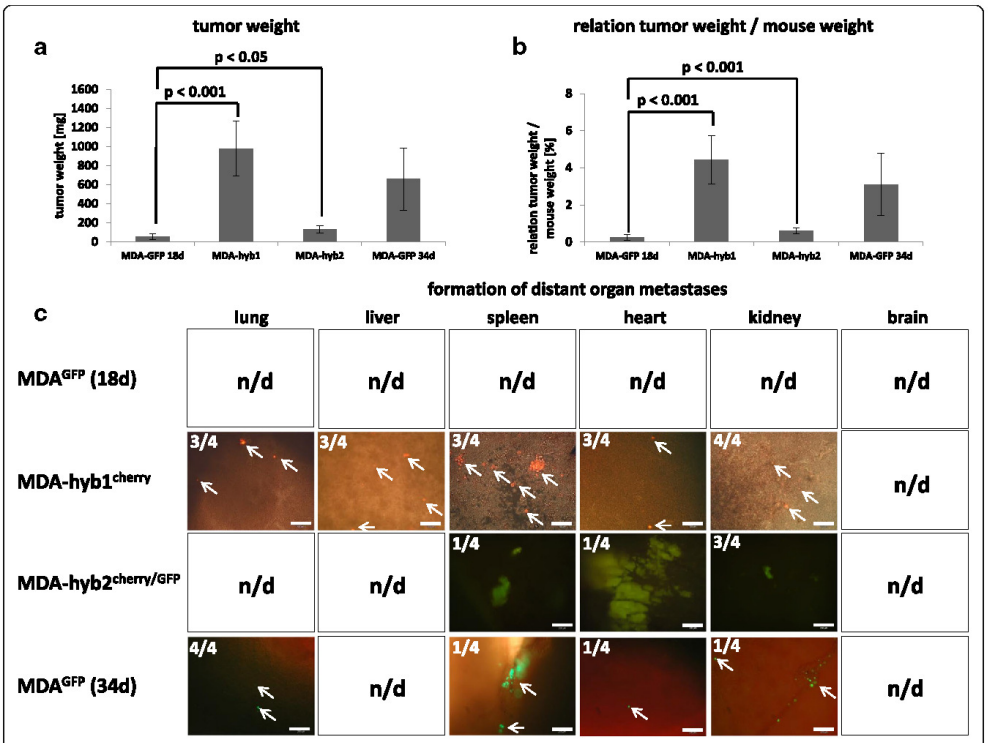


Fig. 6 Tumor and metastases formation of MDA-hyb1 and MDA-hyb2 cells. **a** Quantification of the tumor weight was performed after dissection of the solid subcutaneous primary tumors only (disregard of metastatic tumor tissue) derived from the parental MDA-MB-231^{GFP} cells (MDA-GFP) in comparison to mcherry-labeled MDA-hyb1 and mcherry/GFP-labeled MDA-hyb2 populations. Data were obtained by the mean ± s.d. from 5 different tumors of each cell type after 18d. Moreover, additional 4 different MDA-GFP tumors were analysed after 34d. Significance was calculated by student's-t-test. **b** Quantification of the relationship of tumor weight / mouse weight was calculated with tumors of the parental MDA-MB-231^{GFP} cells (MDA-GFP) in comparison to mcherry-labeled MDA-hyb1 and mcherry/GFP-labeled MDA-hyb2 populations. Data were obtained from 5 different tumors of each cell type after 18d. Moreover, additional 4 different MDA-GFP tumors were analysed after 34d. Significance was calculated by student's-t-test. **c** Organs from four mice from each injected tumor cell population were dissected after euthanization and evaluated by fluorescence microscopy whereby appropriate fluorescence should indicate formation of distant metastases. Appearance of organ metastases from all of these 16 mice was quantified and exemplary pictures from tissue thin section phase contrast / fluorescence microscopy of organ metastases were documented. n.d. = not detectable. Bars represent 100 μm

damage-associated molecular patterns (DAMPs) which represent mediators including S100 proteins, ATP, heat shock proteins, hyaluronan, HMGB1 (high mobility group box 1), and calcireticulin [53] and are sensed by pattern recognition receptors (PRRs) such as toll-like receptors [54]. Such damage products in the presence of an acidified and hypoxic microenvironment can act as fusogenic triggers for aberrant spontaneous cell fusion or a so-called process of "accidental cell fusion" [55]. Previous work has demonstrated that hypoxia-induced apoptosis stimulates fusion between MSCs and breast tumor cells and generated hybrids accompanied by enhanced migratory capacity [56]. Peptides and proteins as well as small molecular metabolites and ions can destabilize the lipid bilayer of adjacent cell membranes and thereby contribute to spontaneous cell fusion by different mechanisms [57]. Similar effects of accidental cell fusion appear to be involved during spontaneous formation of hybrid cells following close interaction of MDA-MB-231 cells with MSC. The appearance of yellow fluorescing cells during co-culture of eGFP-transduced MSC with mcherry-transduced breast cancer cells suggested hybrid cell formation by cell fusion. Further confirmation was obtained by synchronous expression of both fluorescence genes at least in MDA-hyb2 cells. Moreover, MDA-hyb1 and MDA-hyb2

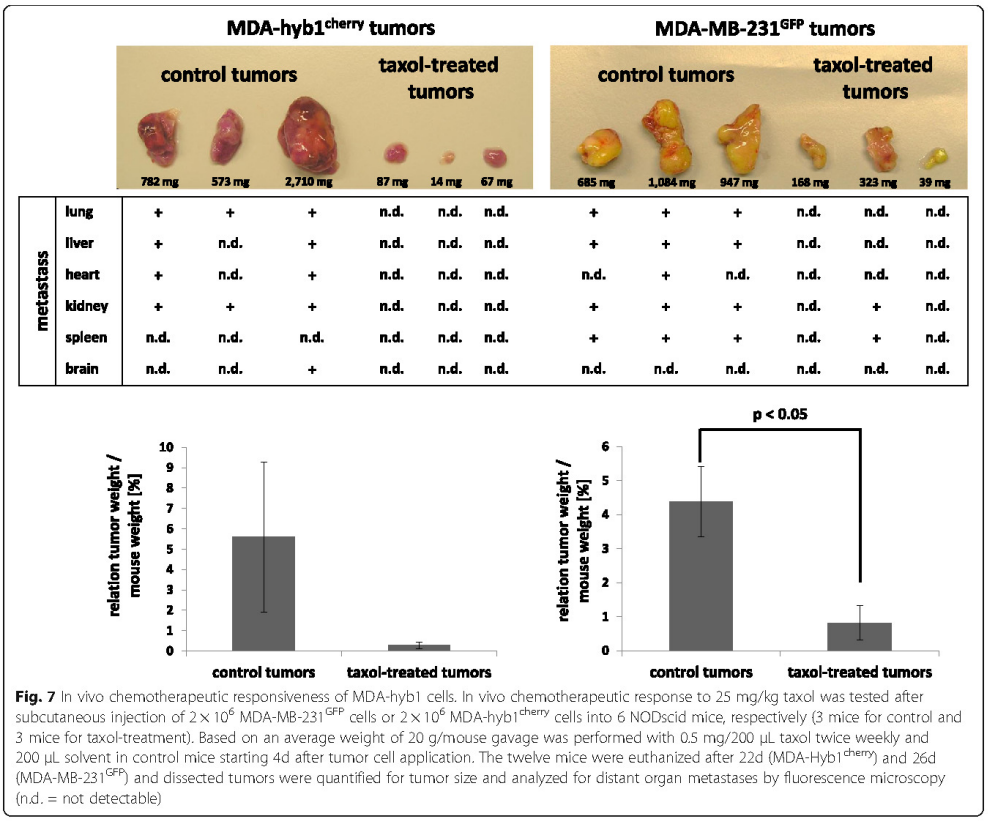


Fig. 7 In vivo chemotherapeutic responsiveness of MDA-hyb1 cells. In vivo chemotherapeutic response to 25 mg/kg taxol was tested after subcutaneous injection of 2×10^6 MDA-MB-231^{GFP} cells or 2×10^6 MDA-hyb1^{cherry} cells into 6 NODscid mice, respectively (3 mice for control and 3 mice for taxol-treatment). Based on an average weight of 20 g/mouse gavage was performed with 0.5 mg/200 μL taxol twice weekly and 200 μL solvent in control mice starting 4d after tumor cell application. The twelve mice were euthanized after 22d (MDA-Hyb1^{cherry}) and 26d (MDA-MB-231^{GFP}) and dissected tumors were quantified for tumor size and analyzed for distant organ metastases by fluorescence microscopy (n.d. = not detectable)

cells display a pseudo-triploid karyotype similar to MDA-MB-231 cells and a male phenotype acquired from MSC thus representing a combined genome from both parental cell types. Together, these effects support a mechanism via cell fusion rather than hybrid formation via entosis which includes degradation of the target cell genome. Fusion-driven hybrid cell formation combines the genomic parts from both parental donors by a hetero-to-synkaryon transition during subsequent cell division [58].

Although this breast cancer cell / MSC fusion process itself represents a rare event, only few of the resulting hybrid cells are capable of cell cycle progression due to regulatory impairments and replicative stress of the two different nuclei. Following initial aneuploidy and chromosomal instability of proliferative active hybrid cells, however, an immediate post-fusion selection process developed different genetically stable pseudo-triploid clones including MDA-hyb1 and MDA-hyb2 populations. Similar findings of rapid genomic post-fusion stabilization of hybrid cells without continuing prominent genetic and phenotypic plasticity were also obtained following PEG-induced xenogenic fusion of the small intestinal rat epithelial crypt cell line IEC-6 with human HeLa cervical carcinoma cells [59]. Spontaneous fusion of human bone marrow–derived multipotent stromal cells with breast carcinoma cell lines demonstrated mixed gene expression profiles and increased DNA ploidy [60]. Moreover, cancer cells can undergo homofusion to generate highly tumorigenic polyploid giant cancer cells. Previous work reported spontaneous fusion of the eGFP-Neo-transfected M13SV1 breast epithelial cell line with MDA-MB-231-Hyg [61] and with MDA-MB-435-Hyg breast cancer cells [62] which was accompanied by increased migratory activity and malignancy. Likewise, in vitro proliferative capacity and prominent telomerase activity paralleled by markedly elevated expression levels of genes associated with migration,

EMT, and metastatic behavior were detectable in MDA--hyb1 and MDA-hyb2 hybrids in contrast to the parental MDA-MB-231 cells. Our data were further substantiated in vivo by the significantly enhanced MDA-hyb1- and MDA-hyb2-induced tumor growth and the rapid formation of organ metastases suggesting substantial increase in breast cancer metastatic capacity and malignancy of these hybrid cells. These findings are also in line with previous concepts suggesting that cancer cell fusion represents a potential mechanism of tumor metastases [63]. However, chemotherapeutic sensitivity was elevated in the hybrid populations compared to the parental MDA-MB-231 breast cancer cells.

Differences in malignancy are observed by correlating the properties of the two hybrid populations themselves. Thus, MDA-hyb1 presented higher in vitro proliferation as compared to MDA-hyb2 and accordingly, a faster tumor growth in vivo associated with a larger network of distant organ metastases which may be related in part to elevated S100A4 and more MDA-MB-231-like properties in MDA-hyb1. Together with the characteristics of the hybrid cells these data indicated that MDA-hyb2 cells carry more MSC-like properties and express a less aggressive tumor phenotype than MDA-hyb1.

Although previous work suggested that tumor-associated aberrant MSC contribute to tumor cell protection either directly by expression of protective extracellular matrix proteins and/or indirectly by promoting a carcinoma stem cell niche [41, 64, 65], the involvement of MSC in MDA-hyb1 and MDA-hyb2 cell formation displays increased sensitivity to various chemotherapeutic compounds.

Conclusions

Altogether, tumor cell fusion by breast cancer/MSC hybrid cell formation enhanced the diversity of the tumor, accelerated tumor growth, increased metastases formation, and progressively altered the chemotherapeutic responsiveness whereby hybrid cells exhibited tumorigenic differences according to the acquisition of certain parental cell characteristics and properties.

Additional files

Additional file 1: Figure S9. RNA microarray analysis. Gene expression data file for comparison between parental MSC and hybrid cells as well as between corresponding cancer and hybrid cells. Data are also stored at the NCBI-GEO database with the accession no. #GSE100551. (XLS 3897 kb)

Additional file 2: Figure S1. Isolation of MDA-hyb1 and MDA-hyb2 cells. Co-culture was performed between human MSC051212^{GFP} P3 20d and MDA-MB-231^{cherry} breast cancer cells for 6 days in MSC medium (cell ratio 60:40) resulted in the appearance of yellow-colored hybrid cells. These hybrid cells were separated for double-labeled (mcherry and eGFP) cells in two steps by repeated fluorescence-activated cell sorting (FACS). Hybrid cells were collected in microtiter plates with one to two hybrid cells/well and subsequent cell cloning. (PDF 252 kb)

Additional file 3: Figure S2. Karyotype analysis of MDA-hyb1 and MDA-hyb2 cells. Following preparation of metaphase chromosomes by colchicine treatment and Giemsa staining karyotype analysis was performed in MSC051212^{GFP} and MDA-MB-231^{cherry} cells as compared to MDA-hyb1 and MDA-hyb2 cells. (PDF 315 kb)

Additional file 4: Figure S3. Cell cycle analysis of MDA-hyb1 and MDA-hyb2 cells. Cell cycle analysis was performed by DNA labeling and subsequent FACS measurements in steady state MSC^{GFP} and MDA-MB-231^{cherry} cells as compared to MDA-hyb1 and MDA-hyb2 cells. The cell cycle shift of MDA-MB-231^{cherry}, MDA-hyb1, and MDA-hyb2 cells towards increased fluorescence intensities as compared to MSC^{GFP}-demonstrated an increased amount of DNA and accordingly, aneuploidy in these three cell populations in contrast to a normal diploid set of chromosomes in MSC^{GFP}. Quantification of cell cycle phases was performed using FlowJo software. (PDF 192 kb)

Additional file 5: Figure S4. Ki67 expression in MDA-hyb1 and MDA--hyb2 cells. Cell cultures of MDA-MB-231^{cherry}, MDA-hyb1 and MDA-hyb2 cells were fixed and stained with Ki67 (upper panel). Quantification was performed by cell counting of four independent specimen and calculated as percentage of Ki67-positive cells. Data represent the mean ± s.d. (n = 4). Expression of Ki67 was performed in MSC051212^{GFP}, MDA-MB-231^{cherry}, MDA-hyb1, and MDA-hyb2 cells by RT-PCR analysis (lower panel). Unaltered mRNA levels of GAPDH served as a control. (PDF 368 kb)

Additional file 6: Figure S5. MSC characteristic markers. Relative expression analysis based on the RNA microarray data of some characteristic mesenchymal stem-like markers was calculated for MDA-MB-231 cells and the hybrid populations MDA-hyb1 and MDA-hyb2. For relative evaluations the expression levels of MSC were used as a control (set to 100%). (PDF 175 kb)

Additional file 7: Figure S6. Analysis of disease and function genes. Relative dominance and importance of certain disease- and function-associated gene clusters in hybrid cells and the parental MDA-MB-231 and MSC051212 were calculated as –log(p-values). Evaluation was performed by relative expression levels of these disease- and function-associated genes in MDA-hyb1 cells in relationship to both parental MDA-MB-231 and MSC051212, respectively, and in MDA-hyb2 cells in relationship to both parental MDA-MB-231 and MSC051212, respectively (left panel). In further summarizing disease- and function-associated clusters obtained from Ingenuity pathway analysis, the relationship of MDA-hyb1 to MDA-MB-231 cells (right upper panel) and the relationship of MDA-hyb2 to MDA-MB-231 cells (right lower panel) are presented. (PDF 501 kb)

Additional file 8: Figure S7. Transfection efficiency. Transfection efficiency for the siRNA knock-down experiments was evaluated following transfection of MDA-MB-231 cells with 25 nM of the green fluorescing siGLO^{green} control vector. (PDF 172 kb)

Additional file 9: Figure S8. Chemotherapeutic responsiveness of MDA-hyb1 and MDA-hyb2 cells. Compared to the parental MDA-MB-231 cells, MDA-hyb1 and MDA-hyb2 cells were treated with 1 μM of the chemotherapeutic compounds taxol, cisplatin, methotrexate (MTX), epirubicin, and foretinib for 24 h up to 72 h, respectively. Relative fluorescence was evaluated by fluoroskan assay representing the mean ± s.d. (n = 10). (PDF 96 kb)

Abbreviations

ASCT-2: Alanine serine and cysteine selective transporter-2; ATP: Adenosine triphosphate; CCL: Chemokine (C-C motif) ligand; CCR5: C-C chemokine receptor type 5; CSC: Cancer stem-like cells; CXCL: Chemokine (C-X-C motif) ligand; CXCR4: C-X-C chemokine receptor type 4; EGF: Epidermal growth factor; eGFP: Enhanced green fluorescent protein; EMT: Epithelial-mesenchymal transition; FACS: Fluorescence-activated cell sorting; FCS: Fetal calf serum; FGF: Fibroblast growth factor; HMGB1: High mobility group box 1; ICAM-1: Intercellular adhesion molecule 1; MFSD-2A: Major facilitator superfamily domain containing 2A; MSC: Mesenchymal stroma/stem cells; MUC-1: Mucin-1; PDGF: Platelet-derived growth factor; PRR: Pattern recognition receptor; RT-PCR: Reverse transcription polymerase chain reaction; SDF-1: Stromal cell-derived factor-1; siRNA: Small-interfering RNA; STR: Short tandem repeat; TGF-β: Transforming growth factor beta; TRAP: Telomeric repeat amplification protocol

Acknowledgements
The authors are grateful to colleagues from Hannover Medical School including Dr. Thomas Rothämel for support with the STR fragment analysis, to Prof. Konstantin Miller for assistance with the karyotyping, to Dr. Matthias Ballmaier (FACS core unit) for cell separation, and to Dr. Oliver Breiholz-Dittrich (research core unit Transcriptomics) for microarray analysis. This work was supported by a grant from the Erich und Gertrud Roggenbuck-Stiftung for Cancer Research to RH.

Funding
This work was supported by a grant from the Erich und Gertrud Roggenbuck-Stiftung for Cancer Research to RH.

Availability of data and materials
NCBI-GEO database with the accession no. #GSE100551.

Authors' contributions
CM, JvO and RH performed the experiments. RH designed the study, and drafted the manuscript. All authors critically read and approved the final manuscript.

Ethics approval and consent to participate
The use of primary human MSC following explant culture from umbilical cord tissue has been approved by the Ethics Committee of Hannover Medical School, Project #443 on February 26th, 2009, respectively, and informed written consent was obtained from each patient.

Consent for publication
All authors have critically read and approved this work.

Competing interests
The authors declare no financial, personal, or professional conflict of interest.

Publisher's Note

Springer Nature remains neutral with regard to jurisdictional claims in published maps and institutional affiliations.

Received: 26 July 2017 Accepted: 2 January 2018
Published online: 05 January 2018

References

1. Hanahan D, Weinberg RA. Hallmarks of cancer: the next generation. Cell. 2011;144(5):646–74.
2. Mani SA, Guo W, Liao MJ, Eaton EN, Ayyanan A, Zhou AY, Brooks M, Reinhard F, Zhang CC, Shipitsin M, Campbell LL, Polyak K, Brisken C, Yang J, Weinberg RA. The epithelial-mesenchymal transition generates cells with properties of stem cells. Cell. 2008;133(4):704–15.
3. Ungefroren H, Sebens S, Seidl D, Lehnert H, Hass R. Interaction of tumor cells with the microenvironment. Cell Commun Signal. 2011;9:18.
4. De Miguel MP, Fuentes-Julian S, Blazquez-Martinez A, Pascual CY, Aller MA, Arias J, Arnalich-Montiel F. Immunosuppressive properties of mesenchymal stem cells: advances and applications. Curr Mol Med. 2012;12(5):574–91.
5. Hass R, Kasper C, Bohm S, Jacobs R. Different populations and sources of human mesenchymal stem cells (MSC): a comparison of adult and neonatal tissue-derived MSC. Cell Commun Signal. 2011;9:12.
6. Hilfiker A, Kasper C, Hass R, Haverich A. Mesenchymal stem cells and progenitor cells in connective tissue engineering and regenerative medicine: is there a future for transplantation? Langenbeck's Arch Surg. 2011;396(4):489–97.
7. Hass R, Otte A. Mesenchymal stem cells as all-round supporters in a normal and neoplastic microenvironment. Cell Commun Signal. 2012;10(1):26.
8. Mandel K, Yang Y, Schambach A, Glage S, Otte A, Hass R. Mesenchymal stem cells directly interact with breast cancer cells and promote tumor cell growth in vitro and in vivo. Stem Cells Dev. 2013;22(23):3114–27.
9. Yang Y, Otte A, Hass R. Human mesenchymal stroma/stem cells exchange membrane proteins and alter functionality during interaction with different tumor cell lines. Stem Cells Dev. 2015;24(10):1205–22.
10. Kufe D, Inghirami G, Abe M, Hayes D, Justi-Wheeler H, Schlom J. Differential reactivity of a novel monoclonal antibody (DF3) with human malignant versus benign breast tumors. Hybridoma. 1984;3(3):223–32.
11. Rahn JJ, Dabbagh L, Pasdar M, Hugh JC. The importance of MUC1 cellular localization in patients with breast carcinoma: an immunohistologic study of 71 patients and review of the literature. Cancer. 2001;91(11):1973–82.
12. Shen Q, Rahn JJ, Zhang J, Gunasekera N, Sun X, Shaw AR, Hendzel MJ, Hoffman P, Bernier A, Hugh JC. MUC1 initiates Src-CrkL-Rac1/Cdc42-mediated actin cytoskeletal protrusive motility after ligating intercellular adhesion molecule-1. Mol Cancer Res. 2008;6(4):555–67.
13. Caplan AI, Correa D. The MSC: an injury drugstore. Cell Stem Cell. 2011;9(1):11–5.
14. Hatlapatka T, Moretti P, Lavrentieva A, Hass R, Marquardt N, Jacobs R, Kasper C. Optimization of culture conditions for the expansion of umbilical cord-derived mesenchymal stem or stromal cell-like cells using xeno-free culture conditions. Tissue Eng Part C Methods. 2011;17(4):485–93.
15. Haynesworth SE, Baber MA, Caplan AI. Cytokine expression by human marrow-derived mesenchymal progenitor cells in vitro: effects of dexamethasone and IL-1 alpha. J Cell Physiol. 1996;166(3):585–92.
16. Majore I, Moretti P, Stahl F, Hass R, Kasper C. Growth and differentiation properties of mesenchymal stromal cell populations derived from whole human umbilical cord. Stem Cell Rev. 2011;7(1):17–31.
17. Ren G, Zhang L, Zhao X, Xu G, Zhang Y, Roberts AI, Zhao RC, Shi Y. Mesenchymal stem cell-mediated immunosuppression occurs via concerted action of chemokines and nitric oxide. Cell Stem Cell. 2008;2(2):141–50.
18. Johnson-Holiday C, Singh R, Johnson E, Singh S, Stockard CR, Grizzle WE, Lillard JW Jr. CCL25 mediates migration, invasion and matrix metalloproteinase expression by breast cancer cells in a CCR9-dependent fashion. Int J Oncol. 2011;38(5):1279–85.
19. Liu J, Liao S, Huang Y, Samuel R, Shi T, Naxerova K, Huang P, Kamoun W, Jain RK, Fukumura D, Xu L. PDGF-D improves drug delivery and efficacy via vascular normalization, but promotes lymphatic metastasis by activating CXCR4 in breast cancer. Clin Cancer Res. 2011;17(11):3638–48.
20. Lu X, Kang Y. Chemokine (C-C motif) ligand 2 engages CCR2+ stromal cells of monocytic origin to promote breast cancer metastasis to lung and bone. J Biol Chem. 2009;284(42):29087–96.
21. Patsialou A, Wyckoff J, Wang Y, Goswami S, Stanley ER, Condeelis JS. Invasion of human breast cancer cells in vivo requires both paracrine and autocrine loops involving the colony-stimulating factor-1 receptor. Cancer Res. 2009;69(24):9498–506.
22. Shin SY, Nam JS, Lim Y, Lee YH. TNFalpha-exposed bone marrow-derived mesenchymal stem cells promote locomotion of MDA-MB-231 breast cancer cells through transcriptional activation of CXCR3 ligand chemokines. J Biol Chem. 2010;285(40):30731–40.
23. Zhang Y, Yao F, Yao X, Yi C, Tan C, Wei L, Sun S. Role of CCL5 in invasion, proliferation and proportion of CD44+/CD24- phenotype of MCF-7 cells and correlation of CCL5 and CCR5 expression with breast cancer progression. Oncol Rep. 2009;21(4):1113–21.
24. Ghajar CM, Peinado H, Mori H, Matei IR, Evason KJ, Brazier H, Almeida D, Koller A, Hajjar KA, Stainier DY, Chen EI, Lyden D, Bissell MJ. The perivascular niche regulates breast tumour dormancy. Nat Cell Biol. 2013;15(7):807–17.
25. Duelli D, Lazebnik Y. Cell fusion: a hidden enemy? Cancer Cell. 2003;3(5):445–8.
26. Noubissi FK, Ogle BM. Cancer cell fusion: mechanisms slowly unravel. Int J Mol Sci. 2016;17(9).
27. Aguilar PS, Baylies MK, Fleissner A, Helming L, Inoue N, Podbilewicz B, Wang H, Wong M. Genetic basis of cell-cell fusion mechanisms. Trends Genet. 2013;29(7):427–37.
28. Blaise S, de Parseval N, Benit L, Heidmann T. Genomewide screening for fusogenic human endogenous retrovirus envelopes identifies syncytin 2, a gene conserved on primate evolution. Proc Natl Acad Sci U S A. 2003;100(22):13013–8.
29. Mi S, Lee X, Li X, Veldman GM, Finnerty H, Racie L, LaVallie E, Tang XY, Edouard P, Howes S, Keith JC Jr, McCoy JM. Syncytin is a captive retroviral envelope protein involved in human placental morphogenesis. Nature. 2000;403(6771):785–9.
30. Larsson LI, Bjerregaard B, Wulf-Andersen L, Talts JF. Syncytin and cancer cell fusions. ScientificWorldJournal. 2007;7:1193–7.
31. Lu M, Ravichandran KS. Dock180-ELMO cooperation in Rac activation. Methods Enzymol. 2006;406:388–402.
32. Pajcini KV, Pomerantz JH, Alkan O, Doyonnas R, Blau HM. Myoblasts and macrophages share molecular components that contribute to cell-cell fusion. J Cell Biol. 2008;180(5):1005–19.
33. Lazova R, Laberge GS, Duvall E, Spoelstra N, Klump V, Sznol M, Cooper D, Spritz RA, Chang JT, Pawelek JM. A melanoma brain metastasis with a

donor-patient hybrid genome following bone marrow transplantation: first evidence for fusion in human cancer. PLoS One. 2013;8(6):e66731.
34. Berndt B, Zanker KS, Dittmar T. Cell fusion is a potent inducer of aneuploidy and drug resistance in tumor cell/ normal cell hybrids. Crit Rev Oncog. 2013;18(1–2):97–113.
35. Ogle BM, Cascalho M, Platt JL. Biological implications of cell fusion. Nat Rev Mol Cell Biol. 2005;6(7):567–75.
36. Majore I, Moretti P, Hass R, Kasper C. Identification of subpopulations in mesenchymal stem cell-like cultures from human umbilical cord. Cell Commun Signal. 2009;7:6.
37. Selich A, Daudert J, Hass R, Philipp F, von Kaisenberg C, Paul G, Cornils K, Fehse B, Rittinghausen S, Schambach A, Rothe M. Massive Clonal selection and transiently contributing clones during expansion of Mesenchymal stem cell cultures revealed by Lentiviral RGB-barcode technology. Stem Cells Transl Med. 2016;5(5):591–601.
38. Otte A, Gohring G, Steinemann D, Schlegelberger B, Groos S, Langer F, Kreipe HH, Schambach A, Neumann T, Hillemanns P, Park-Simon TW, Hass R. A tumor-derived population (SCCOHT-1) as cellular model for a small cell ovarian carcinoma of the hypercalcemic type. Int J Oncol. 2012;41(2):765–75.
39. Delidaki M, Gu M, Hein A, Vatish M, Grammatopoulos DK. Interplay of cAMP and MAPK pathways in hCG secretion and fusogenic gene expression in a trophoblast cell line. Mol Cell Endocrinol. 2011;332(1–2):213–20.
40. Garreis F, Schroder A, Reinach PS, Zoll S, Khajavi N, Dhandapani P, Lucius A, Pleyer U, Paulsen F, Mergler S. Upregulation of transient receptor potential Vanilloid Type-1 channel activity and Ca2+ influx dysfunction in human Pterygial cells. Invest Ophthalmol Vis Sci. 2016;57(6):2564–77.
41. Otte A, Yang Y, von der Ohe J, Melzer C, Hillemanns P, Feuerhake F, Hass R. SCCOHT tumors acquire chemoresistance and protection by interacting mesenchymal stroma/stem cells within the tumor microenvironment. Int J Oncol. 2016;49(6):2453–63.
42. Otte A, Rauprich F, Hillemanns P, Park-Simon TW, von der Ohe J, Hass R. Vitro and in vivo therapeutic approach for a small cell carcinoma of the ovary hypercalcaemic type using a SCCOHT-1 cellular model. Orphanet J Rare Dis. 2014;9:126.
43. Bertram C, Hass R. Cellular senescence of human mammary epithelial cells (HMEC) is associated with an altered MMP-7/HB-EGF signaling and increased formation of elastin-like structures. Mech Ageing Dev. 2009; 130(10):657–69.
44. Toufaily C, Vargas A, Lemire M, Lafond J, Rassart E, Barbeau B. MFSD2a, the Syncytin-2 receptor, is important for trophoblast fusion. Placenta. 2013;34(1): 85–8.
45. Kang Y, Pantel K. Tumor cell dissemination: emerging biological insights from animal models and cancer patients. Cancer Cell. 2013;23(5):573–81.
46. Fischer KR, Durrans A, Lee S, Sheng J, Li F, Wong ST, Choi H, El Rayes T, Ryu S, Troeger J, Schwabe RF, Vahdat LT, Altorki NK, Mittal V, Gao D. Epithelial-to-mesenchymal transition is not required for lung metastasis but contributes to chemoresistance. Nature. 2015;527(7579):472–6.
47. Zheng X, Carstens JL, Kim J, Scheible M, Kaye J, Sugimoto H, Wu CC, LeBleu VS, Kalluri R. Epithelial-to-mesenchymal transition is dispensable for metastasis but induces chemoresistance in pancreatic cancer. Nature. 2015; 527(7579):525–30.
48. Fei F, Qu J, Zhang M, Li Y, Zhang S. S100A4 in cancer progression and metastasis: a systematic review. Oncotarget. 2017;8(42):73219–39.
49. Bresnick AR, Weber DJ, Zimmer DB. S100 proteins in cancer. Nat Rev Cancer. 2015;15(2):96–109.
50. Chen A, Wang L, Li BY, Sherman J, Ryu JE, Hamamura K, Liu Y, Nakshatri H, Yokota H. Reduction in migratory phenotype in a metastasized breast cancer cell line via Downregulation of S100A4 and GRM3. Sci Rep. 2017;7(1):3459.
51. Price JE, Polyzos A, Zhang RD, Daniels LM. Tumorigenicity and metastasis of human breast carcinoma cell lines in nude mice. Cancer Res. 1990;50(3): 717–21.
52. Quail DF, Joyce JA. Microenvironmental regulation of tumor progression and metastasis. Nat Med. 2013;19(11):1423–37.
53. Hernandez C, Huebener P, Schwabe RF. Damage-associated molecular patterns in cancer: a double-edged sword. Oncogene. 2016;35(46):5931–41.
54. Hou W, Zhang Q, Yan Z, Chen R, Zeh Iii HJ, Kang R, Lotze MT, Tang D. Strange attractors: DAMPs and autophagy link tumor cell death and immunity. Cell Death Dis. 2013;4:e966.
55. Freeman BT, Jung JP, Ogle BM. Single-cell RNA-seq reveals activation of unique gene groups as a consequence of stem cell-parenchymal cell fusion. Sci Rep. 2016;6:23270.
56. Noubissi FK, Harkness T, Alexander CM, Ogle BM. Apoptosis-induced cancer cell fusion: a mechanism of breast cancer metastasis. FASEB J. 2015;29(9): 4036–45.
57. Mondal Roy S, Sarkar M. Membrane fusion induced by small molecules and ions. J Lipids. 2011;2011:528784.
58. Sottile F, Aulicino F, Theka I, Cosma MP. Mesenchymal stem cells generate distinct functional hybrids in vitro via cell fusion or entosis. Sci Rep. 2016;6: 36863.
59. Zhou X, Merchak K, Lee W, Grande JP, Cascalho M, Platt JL. Cell fusion connects Oncogenesis with tumor evolution. Am J Pathol. 2015;185(7): 2049–60.
60. Rappa G, Mercapide J, Lorico A. Spontaneous formation of tumorigenic hybrids between breast cancer and multipotent stromal cells is a source of tumor heterogeneity. Am J Pathol. 2012;180(6):2504–15.
61. Dittmar T, Schwitalla S, Seidel J, Haverkampf S, Reith G, Meyer-Staeckling S, Brandt BH, Niggemann B, Zanker KS. Characterization of hybrid cells derived from spontaneous fusion events between breast epithelial cells exhibiting stem-like characteristics and breast cancer cells. Clin Exp Metastasis. 2011; 28(1):75–90.
62. Ozel C, Seidel J, Meyer-Staeckling S, Brandt BH, Niggemann B, Zanker KS, Dittmar T. Hybrid cells derived from breast epithelial cell/breast cancer cell fusion events show a differential RAF-AKT crosstalk. Cell Commun Signal. 2012;10(1):10.
63. Pawelek JM, Chakraborty AK. Fusion of tumour cells with bone marrow-derived cells: a unifying explanation for metastasis. Nat Rev Cancer. 2008; 8(5):377–86.
64. Melzer C, von der Ohe J, Hass R. Breast carcinoma: from initial tumor cell detachment to settlement at secondary sites. Biomed Res Int. 2017;2017: 8534371.
65. Melzer C, von der Ohe J, Lehnert H, Ungefroren H, Hass R. Cancer stem cell niche models and contribution by mesenchymal stroma/stem cells. Mol Cancer. 2017;16(1):28.

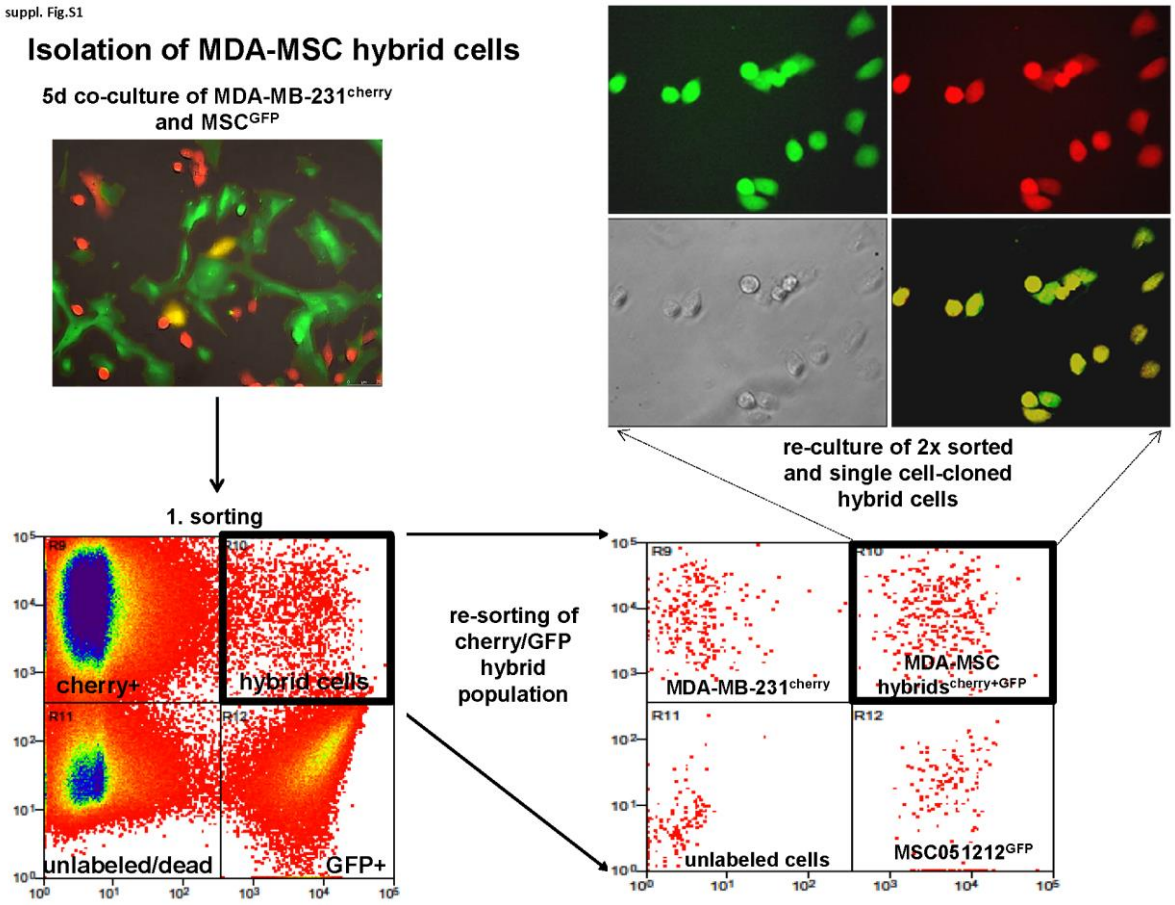
Submit your next manuscript to BioMed Central and we will help you at every step:

- We accept pre-submission inquiries
- Our selector tool helps you to find the most relevant journal
- We provide round the clock customer support
- Convenient online submission
- Thorough peer review
- Inclusion in PubMed and all major indexing services
- Maximum visibility for your research

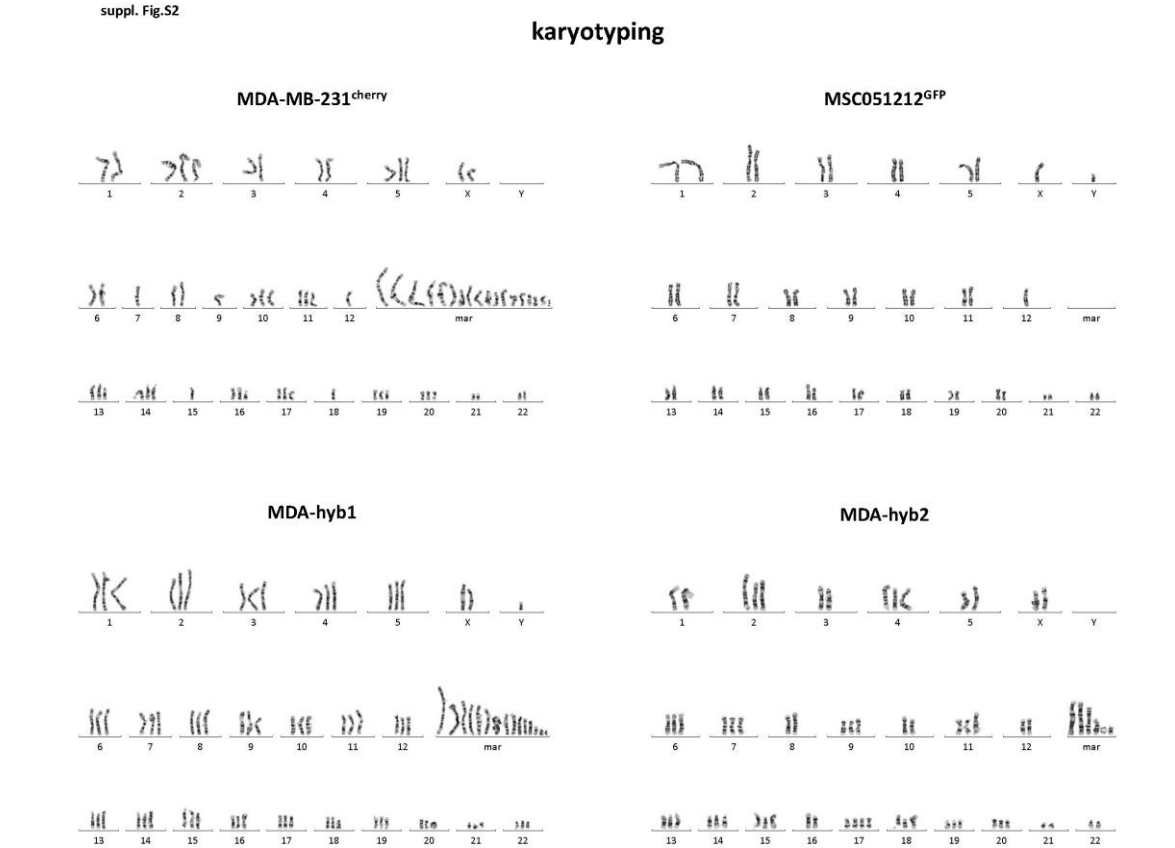
Submit your manuscript at
www.biomedcentral.com/submit

BioMed Central

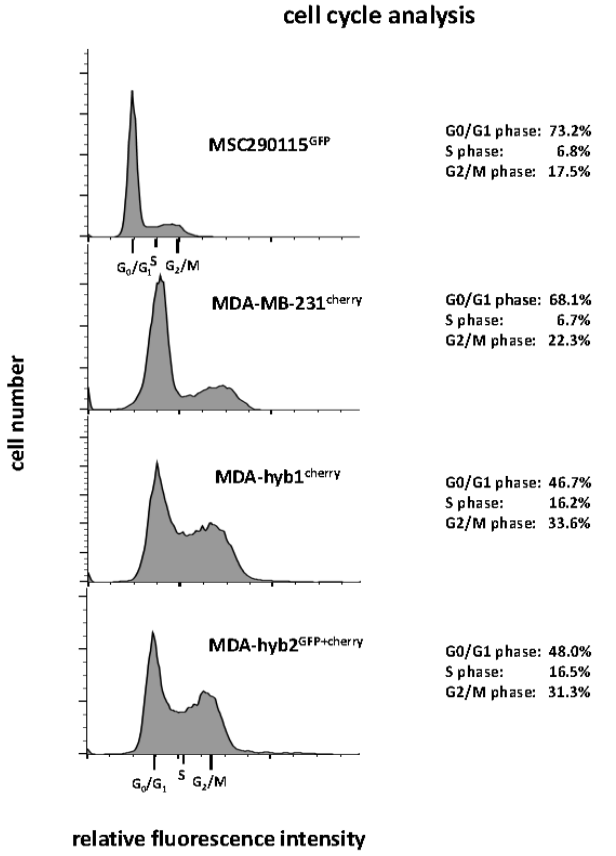
suppl. Fig.S1



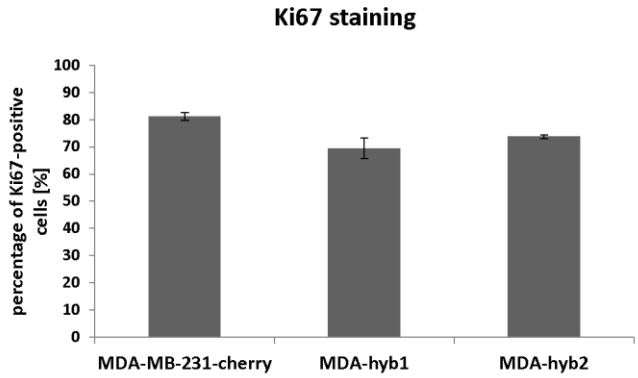
suppl. Fig.S2

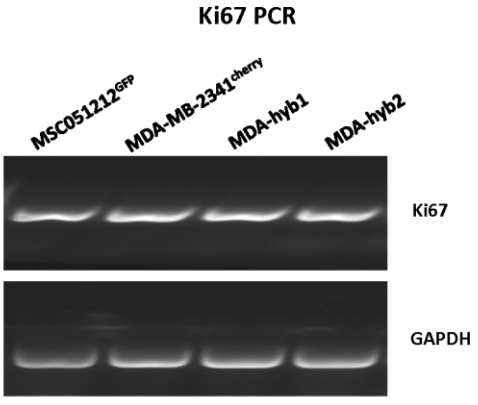


suppl. Fig.S3

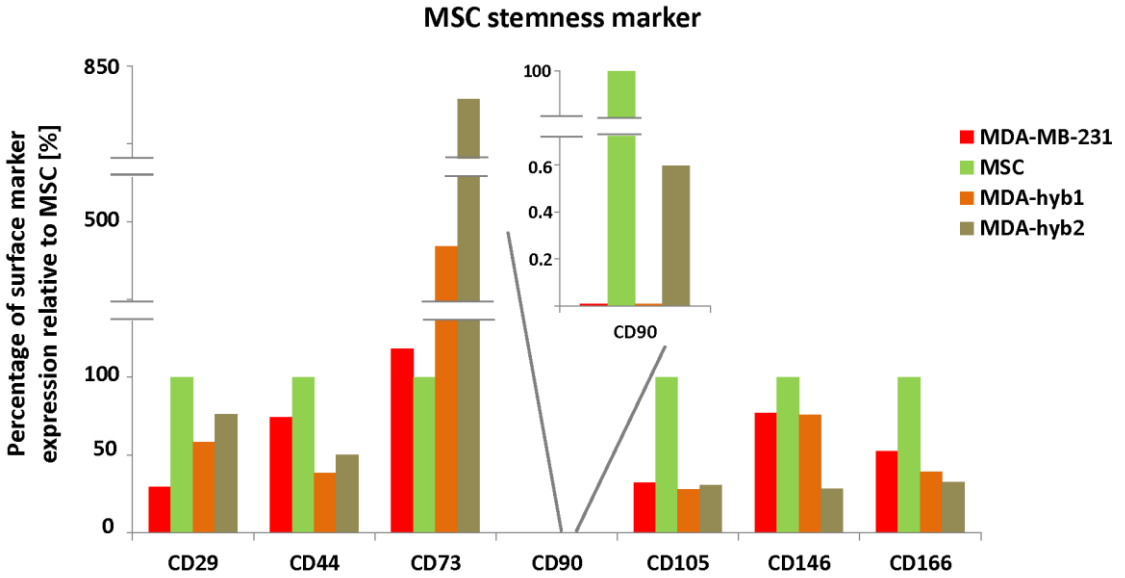


suppl. Fig.S4

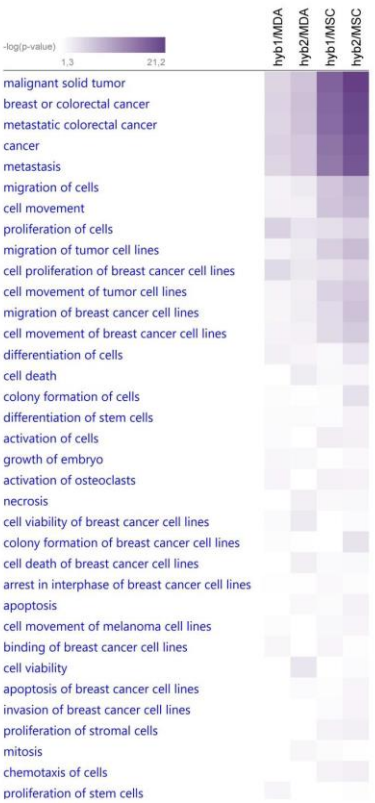


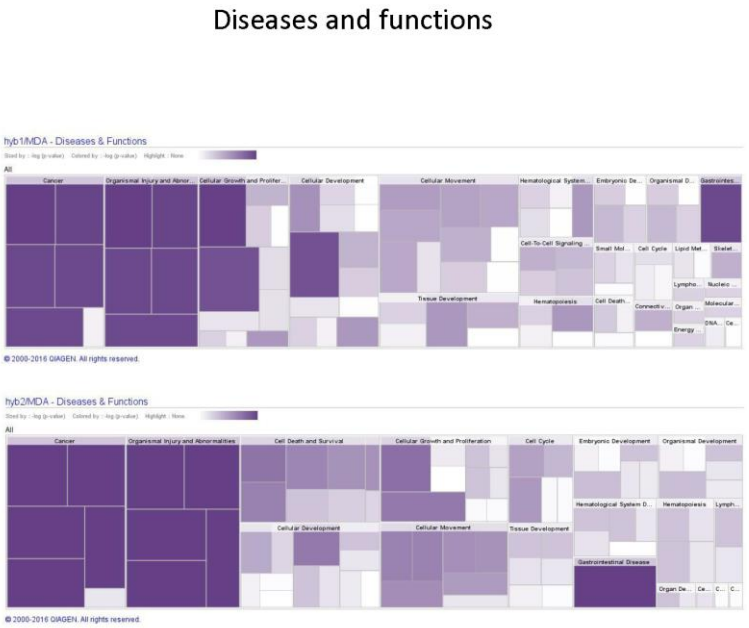


suppl. Fig.S5

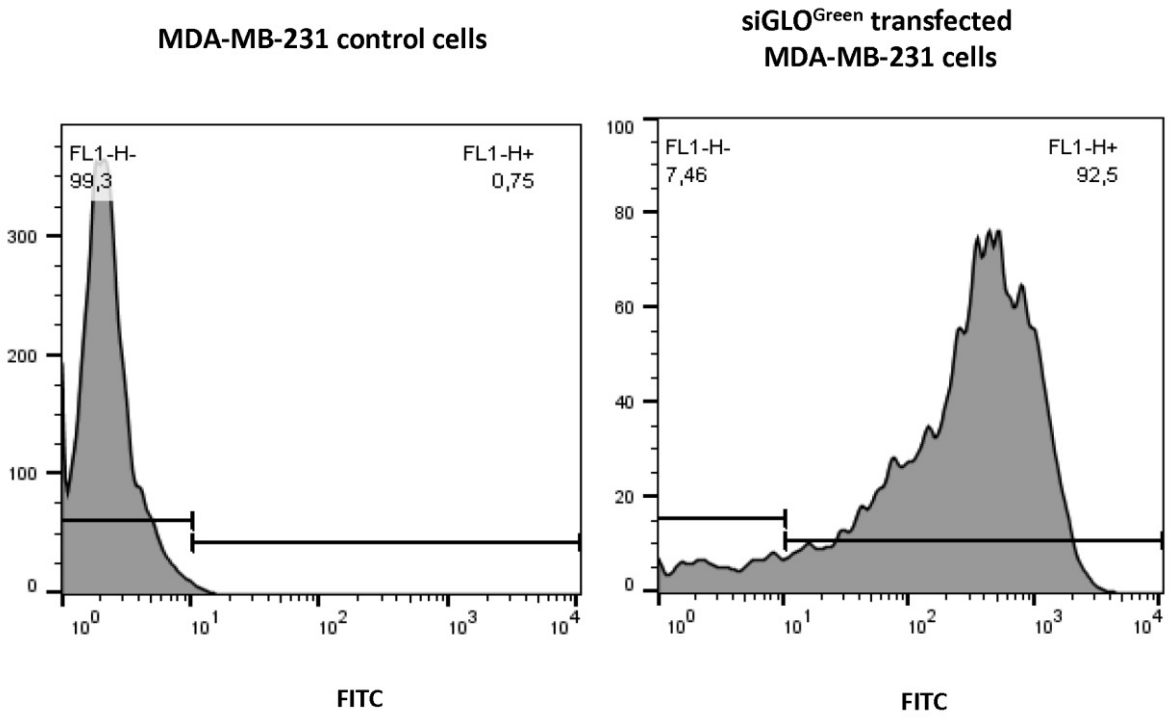


suppl. Fig.S6

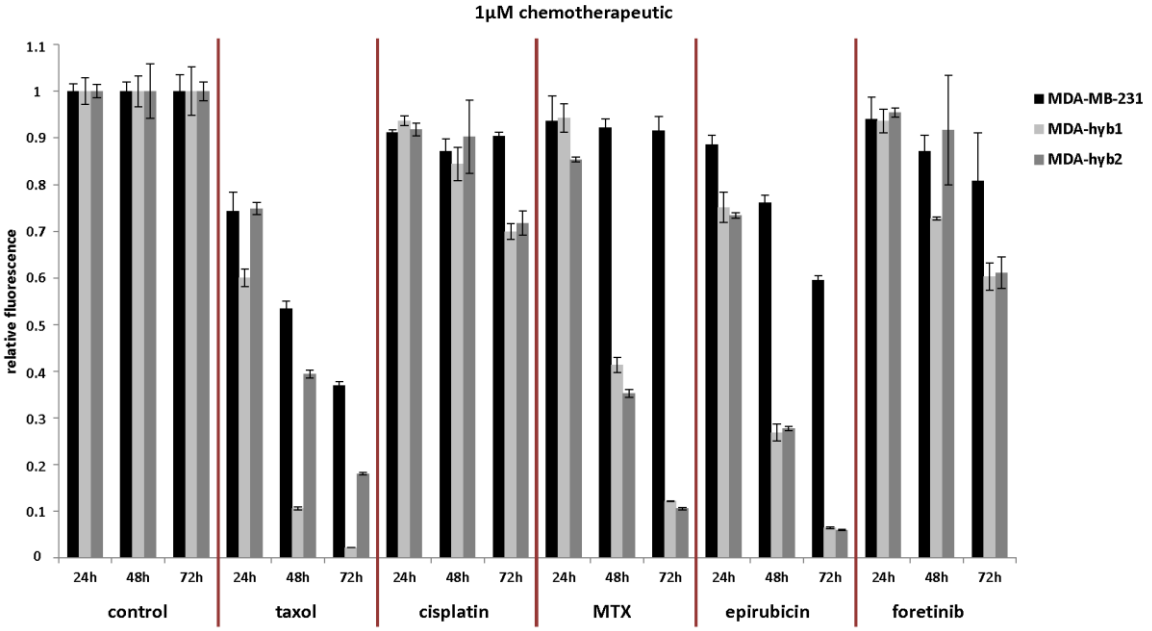




suppl. Fig.S7



suppl. Fig.S8



2.3 MSC stimulate ovarian tumor growth during intercellular communication but reduce tumorigenicity after fusion with ovarian cancer cells

Catharina Melzer, Juliane von der Ohe and Ralf Hass

published in

Cell Communication and Signaling

2018 Oct 13;16(1):67.

doi: 10.1186/s12964-018-0279-1.

Author contribution statement:

Catharina Melzer (CM) performed the experiments (Fig. 1, 3, 4C+D) and analyzed the data. CM critically read and approved the final manuscript.

Melzer et al. Cell Communication and Signaling (2018) 16:67
https://doi.org/10.1186/s12964-018-0279-1

Cell Communication and Signaling

SHORT REPORT Open Access

MSC stimulate ovarian tumor growth during intercellular communication but reduce tumorigenicity after fusion with ovarian cancer cells

Catharina Melzer, Juliane von der Ohe and Ralf Hass*

Abstract

The tumor microenvironment enables important cellular interactions between cancer cells and recruited adjacent populations including mesenchymal stroma/stem cells (MSC). In vivo cellular interactions of primary human MSC in co-culture with human SK-OV-3 ovarian cancer cells revealed an increased tumor growth as compared to mono-cultures of the ovarian cancer cells. Moreover, the presence of MSC stimulated formation of liver metastases. Further interactions of MSC with the ovarian cancer cells resulted in the formation of hybrid cells by cell fusion. Isolation and single cell cloning of these hybrid cells revealed two differentially fused ovarian cancer cell populations termed SK-hyb1 and SK-hyb2. RNA microarray analysis demonstrated expression profiles from both parental partners whereby SK-hyb1 were attributed with more SK-OV-3 like properties and SK-hyb2 cells displayed more similarities to MSC. Both ovarian cancer hybrid populations exhibited reduced proliferative capacity compared to the parental SK-OV-3 cells. Moreover, the fused populations failed to develop tumors in NODscid mice. Together, these data suggested certain stimulatory effects on ovarian tumor growth in the presence of MSC. Conversely, fusion of MSC with SK-OV-3 cells contributed to the generation of new cancer hybrid populations displaying a significantly reduced tumorigenicity.

Keywords: Mesenchymal stem cells, Breast and ovarian cancer, Tumor microenvironment

Background

One of the most lethal gynecologic malignancies is caused by ovarian cancer. The majority of epithelial ovarian cancers is categorized into two types. Type I ovarian tumors include low-grade serous, endometrioid, clear cell and mucinous carcinomas carrying gene mutations of KRAS, BRAF, ERBB2, PTEN, CTNNB1, and PIK3CA among others which appear clinically indolent. Conversely, type II tumors often display genetic instabilities with a high frequency of TP53 mutations and cyclin E1 amplifications and are characterized as high-grade serous, high-grade endometrioid or undifferentiated carcinomas [1, 2]. Moreover, malignant mixed mesodermal tumors (carcinosarcomas) with papillary, glandular, and solid patterns are predominantly observed in advanced ovarian tumor stages and display highly aggressive cancer cells [3–5].

Development and progression of ovarian cancer represents a complex multistep cascade during malignant conversion and interactions with adjacent cell types in the tumor microenvironment including mesenchymal stroma/stem-like cells (MSC) [6]. MSC preferentially reside in perivascular niches of nearly all kinds of human tissues [7, 8]. Despite functional differences according to their tissue-specific origins, heterogenic MSC populations share distinct surface marker expressions such as CD73, CD90, and CD105, and they maintain the capability to differentiate at least along certain phenotypes of the mesodermal lineage [9–12]. Moreover, MSC contribute to regulate stem cell homeostasis, migrate towards damaged or injured tissues to utilize repair processes [13], support angiogenesis [14] and modulate immune cell functions [15].

* Correspondence: hass.ralf@mh-hannover.de
Biochemistry and Tumor Biology Lab, Department of Obstetrics and Gynecology (OE 6410), Hannover Medical School, Carl-Neuberg-Str. 1, D – 30625 Hannover, Germany

© The Author(s). 2018 **Open Access** This article is distributed under the terms of the Creative Commons Attribution 4.0 International License (http://creativecommons.org/licenses/by/4.0/), which permits unrestricted use, distribution, and reproduction in any medium, provided you give appropriate credit to the original author(s) and the source, provide a link to the Creative Commons license, and indicate if changes were made. The Creative Commons Public Domain Dedication waiver (http://creativecommons.org/publicdomain/zero/1.0/) applies to the data made available in this article, unless otherwise stated.

According to this multi-functional plasticity, intracellular expression levels of several miRs contribute to alter the MSC state of activation and susceptibility [16]. Consequently, MSC are considered cellular all-round supporters and exhibit a significant sensitivity to mutual extracellular signaling with normal and carcinoma cell populations [17–20]. Distinct functions within this unique panel of MSC biodiversity can be triggered by alterations of the microenvironment such as the threshold of cytokines/chemokines to induce MSC adherence [21], changes in the extracellular matrix composition, and determination of a direct cell-to-cell contact.

Although MSC and their multi-functionality play an important role in combination with several different types of carcinoma cells such as breast and ovarian cancer cells, little is known about the mechanisms involved and resulting effects can be controversial. Thus, cellular interactions of MSC can develop opposite effects in ovarian cancer cells, whereby the underlying mechanisms remain unclear. Previous work has demonstrated that MSC extracts derived from either MSC lysates or supernatants inhibit cell growth of a variety of carcinoma cell lines including breast, ovarian, and osteosarcoma cells [22]. Conversely, human MSC were suggested to promote ovarian cancer growth and support proliferation and survival [23]. In fact, intercellular communication of MSC with different carcinoma cells is associated with mutual functional alteration including enhanced tumor growth and elevated metastatic potential [24, 25]. Moreover, studies in breast cancer cells revealed that interaction with MSC can also generate new cancer hybrid populations by cellular fusion [26–28].

To address this controversial issue, the present study in ovarian carcinoma models offers some new data to potential tumor-supportive and tumor-inhibitory effects of MSC. The results demonstrate that initial ovarian tumor growth is enhanced by cellular communication in the presence of MSC. However, tight interaction and subsequent fusion of MSC with ovarian cancer cells generate new populations displaying reduced tumorigenicity.

Materials and methods

Cell culture

Isolation of primary human MSC was performed from umbilical cord explant cultures as reported previously [29] and cultured in αMEM (Sigma Chemie GmbH, Steinheim, Germany) supplemented with 10% of allogeneic human AB-serum (commercially obtained from blood bank, University Campus Lübeck, Germany), 100 U/ml penicillin, 100 μg/ml streptomycin and 2 mM L-glutamine (Sigma). The use of primary human mesenchymal stem cells following explant culture from umbilical cord tissue has been approved by the Ethics Committee of Hannover Medical School, Project #443 on February 26th, 2009, respectively, and informed written consent was obtained from the patient.

MSC were subcultured following accutase (Sigma) treatment for 3 min at 37 °C. MSC from different donors and passages (MSC060616 P5 and MSC081113 P6) were used in the experiments.

Human SK-OV-3 ovarian cancer cells (ATCC® #HTB-77TM) were commercially obtained in P25 from the ATCC, Manassas, VA, USA. These cells were originally established from the malignant ascites of a patient with progressive adenocarcinoma of the ovary. SK-OV-3 cells were cultivated at about 1,750 cells/cm^2 in RPMI 1640 supplemented with 10% (v/v) fetal calf serum, 100 U/ml L-glutamine, 100 U/ml penicillin and 100 μg/ml streptomycin. Subculture was performed by trypsin/EDTA (Biochrom GmbH, Berlin, Germany) treatment for 5 min at 37 °C.

Cell line testing and authentication

All cells were tested for mycoplasma by the luminometric MycoAlert Plus mycoplasma detection kit (Lonza Inc., Rockland, ME, USA) according to the manufacturer's recommendations. Cell line authentication was performed by short tandem repeat (STR) fragment analysis using the GenomeLab human STR primer set (Beckman Coulter Inc., Fullerton, CA, USA). The STR pattern of SK-OV-3 ovarian cancer cells was confirmed in previous work [30] according to the STR database provided by the ATCC, Manassas, VA, USA.

Co-culture of MSC with human ovarian cancer cells and isolation of hybrid cells

For co-culture experiments with MSC populations, SK-OV-3 ovarian cancer cells were previously adapted to MSC culture medium. In order to distinguish the different cell types and newly formed hybrid cells within the in vitro co-culture, MSC and ovarian cancer cells have been transduced with a 3rd generation lentiviral SIN vector containing the eGFP and the mcherry gene, respectively, as indicated in previous work [25]. Following 7d co-culture of MSC081113^{GFP} P6 with SK-OV-3^{cherry} P90 (cell ratio 60:40 at a density of 2,000 cells/cm^2) in MSC medium, a total amount of 5.7×10^7 co-cultured cells was subjected to repeated separation by fluorescence-activated cell sorting (FACS). The first separation step yielded 2.4×10^4 cells identified as double positive for mcherry and GFP. However, this population still contained false positive and doublet cells and therefore, a second FACS separation was performed with this population resulting in 150 double positive for mcherry and GFP. These hybrid cells were cultured as single cell per well in 96-well microtiter

plates (Nunc) and from these 150 clones, two initially proliferating hybrid clones of MSC/SK-OV-3 co-culture termed SK-hyb1 and SK-hyb2 were isolated and further analyzed.

In vivo experiments

Animal research using NOD/scid mice was carried out by following the internationally recognized guidelines on animal welfare and has been approved by the institutional licensing committee ref. # 33.19–42502–04-15/1992 on Dec. 18th, 2015.

About 4.5×10^5 GFP-labeled SK-OV-3^{GFP} cells as both mono- or co-culture (together with 4.5×10^5 MSC060616) were injected subcutaneously into 5 animals of 5 to 6 weeks old female NOD/scid mice, respectively. After 38d post injection, all 10 mice had developed subcutaneous tumors and the animals were sacrificed by cervical dislocation. Primary tumor tissues were dissected under UV light, weighted, washed in PBS, and subsequently cultured in vitro for explant culture of the tumor cells. Organs were also dissected from the mice and thin sections were analyzed by fluorescence microscopy for presence and accumulation of metastatic cells.

In a separate set of experiments, 4.5×10^5 SK-hyb1, and SK-hyb2 cells were injected subcutaneously into NOD/scid mice, respectively, and tumor development was compared to that of 4.5×10^5 SK-OV-3^{GFP} parental control cells.

Transcript analysis by RT-PCR

Total RNA was isolated using RNeasy Mini Kit (Qiagen, Hilden, Germany) according to the manufacturer's instructions. One μg RNA was reverse transcribed into cDNA using 500 μM of dNTP (R0193), 5 μM Oligo(dT)18 primer (S0132), 5 μM Random Hexan primer (S0142), 1 U RiboLockTM RNase Inhibitor (E00381) and 5 U RevertAidTM M-MuLV Reverse Transcriptase (EP0441) in the supplied reaction buffer (all reagents from Thermo Scientific, Schwerte, Germany). The cDNA reactions were performed for 10 min/25 °C, 1 h/37 °C and stopped at 72 °C for 10 min. cDNA (2.5 μl) was used as a template with following specific primers (customized by Eurofins, MWG GmbH, Ebersberg, Germany) as described previously [27, 28, 31].

PCR reactions included 0.2 μM of each primer, 200 μM of dNTP (R0193, Thermo Scientific) and 0.03 U One Taq Hot Start DNA polymerase (New England Biolabs GmbH, Frankfurt am Main, Germany) in the supplied reaction buffer. PCR cycling conditions were performed 30s at 94 °C, 1 min at 60 °C and 68 °C for 1 min respectively, including an initial 30s denaturation step at 94 °C and a final 5 min extension step at 68 °C (35 cycles). Aliquots of 25 μl of each RT-PCR product were separated on a 2% agarose gel including the standard GeneRuler 100 bp DNA Ladder (Thermo Scientific) and visualized by GelRedTM (Biotium Inc., Hayward, CA, US) staining.

Microarray-based mRNA expression analysis (single color mode)

RNA microarray analysis was performed according to the previously described details [27]. The parental cells SK-OV-3^{cherry} and MSC081113^{GFP} were investigated and likewise the resulting two hybrid populations SK-hyb1 and SK-hyb2. Alterations in transcript levels were compared between parental cells and hybrid cells displaying a more than 2-fold difference in gene expression. Microarray data are uploaded at NCBI database with accession no. GSE117411.

Cell cycle analysis

The cell cycle analysis in the ovarian cancer cells, MSC, and SK-hybrid cells was performed as described previously [32]. Briefly, 10^5 cells were fixed in 70% (*v*/v) ice-cold ethanol at 4 °C for 24 h. Thereafter, the fixed cells were stained with propidium-iodide for 30 min at room temperature. The samples were then measured in a FACSCalibur (BD Biosciences, Singapore) flow cytometer and analyzed using the FlowJo V10 software.

Cytotoxicity measurements of explant tumor cultures by fluoroscan assay

The proliferative capacity in the absence and presence of different chemotherapeutic compounds was tested in steady-state SK-OV-3^{GFP} in vitro cell cultures compared to ex vivo explant cultures from SK-OV-3^{GFP}-induced NODscid mouse tumors and MSC + SK-OV-3^{GFP} co-cultured tumors. Fluorescence measurement using the fluoroscan assay was performed as previously described [33]. Briefly, 3,000 cells/well were seeded with standard culture medium (100 μl/well) in flat bottom 96-well plates (Nunc/ThermoFischer Scientific, Roskilde, Denmark) and incubated overnight to allow attachment. Thereafter, 100 μl of culture medium with drug solvent was added to the cells as a control and in further wells 100 μl of culture medium containing different chemotherapeutics were added to the cells. Following incubation for up to 72 h, the medium was removed and the cells were lysed with 5% (*w*/*v*) SDS. Afterwards, the fluorescence intensities of GFP in the cell homogenate which corresponded to the appropriate cell number of cancer cells was measured at excitation 485 nm/emission 520 nm using the Fluoroscan Ascent Fl (ThermoFisher Scientific).

Results

In vivo co-injection of human SK-OV-3 ovarian cancer cells with human MSC exhibited a significantly enhanced tumor growth in NODscid mice (Fig. 1a). Tumor weight was increased by 4.2-fold in the presence of MSC

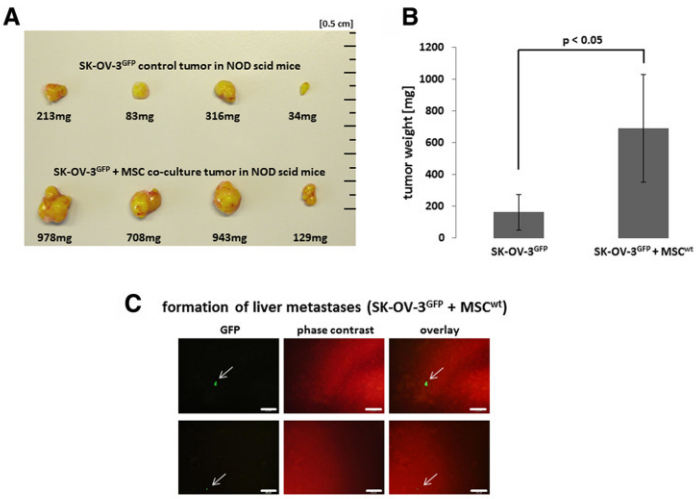


Fig. 1 **a** NODscid mouse tumors were derived following injection of human SK-OV-3^{GFP} ovarian cancer cells in comparison to a co-injection of SK-OV-3^{GFP} and MSC060616^{wt} in MSC medium. **b** Tumor weight of SK-OV-3^{GFP}-induced mouse tumors was compared to tumors after co-injection. Significance (p) was calculated by the mean ± s.d. ($n = 4$) using student's t-test. **c** Formation of distant metastases was detected by GFP-fluorescence evaluation in thin sections from organ tissues and exemplary pictures from tissue thin section phase contrast/fluorescence microscopy of liver metastases are documented (arrows). Bars represent 200 μm

(Fig. 1b). All organs were tested for potential metastases whereby lung, spleen, heart, kidney, and brain revealed no detectable metastatic cells. However, MSC-mediated enhanced tumor development was associated with appearance of GFP-labeled tumor cells in the liver in contrast to SK-OV-3 cells-induced tumors without MSC co-injection (Fig. 1c).

Histopathological evaluation of the mouse tumors in 4 μm thick and formalin-fixed tissue sections by hematoxylin/eosin (HE) staining demonstrated various filament structures in MSC co-injected tumors which were not observed in SK-OV-3-induced tumors alone (Fig. 2a, upper panel). Staining of the tumor tissues with the proliferation marker Ki67 revealed 41.2 ± 0.5% positive cells ($n = 3$) in MSC + SK-OV-3 co-injected tumors as compared to 31.3 ± 3.6% in SK-OV-3-induced tumors alone (Fig. 2a, lower panel, Fig. 2b).

Ex vivo explant culture was performed with SK-OV-3-induced tumors and MSC + SK-OV-3 co-injected tumors to obtain corresponding primary cultures for chemotherapeutic comparison to the steady-state SK-OV-3 in vitro cell culture. While exposure to 1 μM taxol reduced the viability of SK-OV-3 in vitro cell culture down to 6.7 $\pm$ 1.1% after 24 h, both ex vivo explant tumor cultures were significantly less sensitive with remaining 56.1 $\pm$ 2.2% viable SK-OV-3 and 48.2 $\pm$ 3.1% viable co-injected tumor explants after 24 h. Similar effects were observed after 48 h and 72 h. Of interest, epothilone B (epo B), a tubulin inhibitor similar to taxol, demonstrated less differences between SK-OV-3 in vitro cell culture and the two ex vivo explant tumor cultures although a significantly reduced sensitivity was still observed in the tumor cultures (Fig. 2c). Treatment with 1 μM carboplatin revealed relative resistance of all three cell populations after 72 h (Additional file 1: Figure S1). Higher concentration of 10 μM carboplatin progressively decreased the viability of steady-state SK-OV-3 control tumor cells, however, the tumor explant cultures remained unaffected (Additional file 1: Figure S1). Moreover, exposure to 100 μM carboplatin demonstrated cytotoxity in all populations with fewer effects in the explant cultures (Additional file 1: Figure S1). Together, these data further substantiated a reduced chemosensitivity in the ex vivo cultured tumors.

SK-OV-3-derived tumors and MSC co-injected tumors from three mice were examined for expression of MSC markers in comparison to their corresponding explant cell cultures, respectively. All tissue samples and cell populations expressed the MSC markers CD44, CD73, and CD105 with unaltered GAPDH levels as a loading control. However, little if any CD90 expression was detectable in either sample (Additional file 2: Figure S2).

During interaction of SK-OV-3^{cherry} ovarian cancer cells with different MSC^{GFP} the generation of hybrid populations was observed displaying the fluorescence of

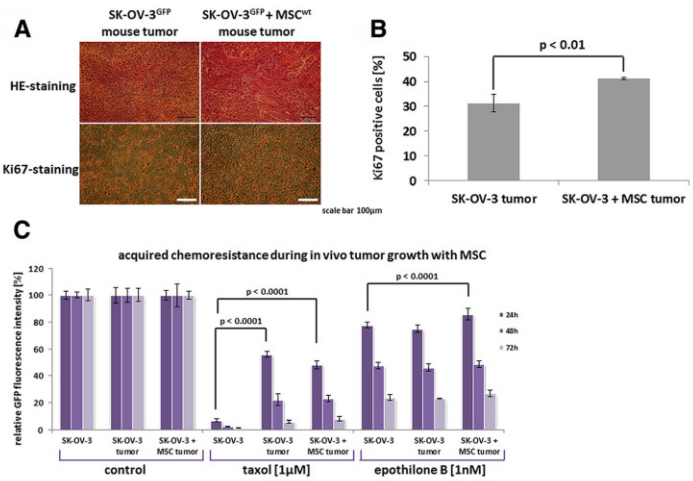


Fig. 2 **a** Tissue sections (4 µm thick) of SK-OV-3^{GFP} control tumors and SK-OV-3^{GFP}/MSC060616^{wt} co-injected tumors were stained for HE and Ki67 following fixation in paraformaldehyde. A representative selection of tumor areas is shown. (Bars = 100 µm). **b** Ki67 positive cells in the histopathologic tissue samples were counted and the percentage was calculated in SK-OV-3^{GFP} control tumors compared to SK-OV-3^{GFP}/MSC060616^{wt} co-injected tumors. Significance (p) was calculated by the mean ± s.d. using student's t-test. **c** Chemotherapeutic response was tested in SK-OV-3^{GFP} control cells and cell populations derived from tumor explant cultures of SK-OV-3^{GFP} tumors and SK-OV-3^{GFP}/MSC060616^{wt} co-injected tumors. Relative proliferative capacity from steady state SK-OV-3^{GFP} cells and the mouse tumor-derived explant populations was evaluated in a fluoroscan assay following exposure to appropriate concentrations of different chemotherapeutics for 24 h up to 72 h. Data were calculated as the mean ± s.d. ($n = 5$) whereby fluorescence values were set = 100% for the corresponding cells in control medium. Significance (p) was calculated using ANOVA followed by Dunnett's multiple comparisons test

both partners (Additional file 3: Figure S3). While cell fusion represents a rare event in general, most hybrid cells died during the post-fusion selection process and two initially proliferating clones were obtained yielding about 1 hybrid cell clone per 2.85×10^7 cells in co-culture. These findings substantiate previous observations [25] and the two different hybrid cell clones SK-hyb1 and SK-hyb2 were isolated and further characterized. RNA microarray analysis of these SK-hyb1 and SK-hyb2 cells was performed in comparison to the parental populations SK-OV-3^{cherry} and MSC081113^{GFP}, respectively (Fig. 3a). While the majority of genes referred to invariant and below cutoff transcripts, SK-hyb1 cells displayed a more SK-OV-3-like phenotype with 1,072 up- and 1,227 down-regulated transcripts, however, about 3,656 to 3,811 genes were differentially expressed compared to the parental MSC (Fig. 3a, left panel). Conversely, SK-hyb2 cells exhibited slightly less changes in mRNA expression levels versus MSC than versus SK-OV-3 cells indicating a more MSC-like phenotype (Fig. 3a, right panel).

These results were substantiated for the expression of different cell surface markers associated with MSC stemness. In particular, the markers CD73, CD90, CD105 and CD146 revealed a similar expression pattern for SK-OV-3 and SK-hyb1 on one side and for parental MSC and SK-hyb2 on the other side (Fig. 3b). Of interest, prominent expression of telomerase in SK-OV-3 cells was significantly reduced in the SK-hyb1 and SK-hyb2 cells and only slightly increased in relation to MSC (Fig. 3c). Moreover, E-cadherin was down-modulated by 8.8-fold in SK-hyb1 and by 246.3-fold in SK-hyb2 compared to SK-OV-3 cells, and up-regulated compared to MSC. Vice versa, N-cadherin was slightly up-regulated in the hybrid cells in relation to SK-OV-3 cells paralleled by a down-modulation compared to MSC (Fig. 3c). Again, the findings suggest increasing mesenchymal-like characteristics in both hybrid populations whereby SK-hyb2 cells displayed more similarities to the parental MSC as compared to SK-hyb1.

Hybrid cell formation was also supported by RT-PCR demonstrating simultaneous expression of both fluorescence genes in SK-hyb2 cells while the SK-hyb1 population lost the eGFP plasmid. mRNA transcripts of the MSC markers CD73, CD90, CD105 revealed low to undetectable levels of CD90 and CD105 in SK-OV-3 and SK-hyb1 cells. All four cell populations expressed the fusion-associated gene syncytin-2 and the corresponding fusion receptor MFSD-2A suggesting a fusion-permissive environment (Fig. 4a).

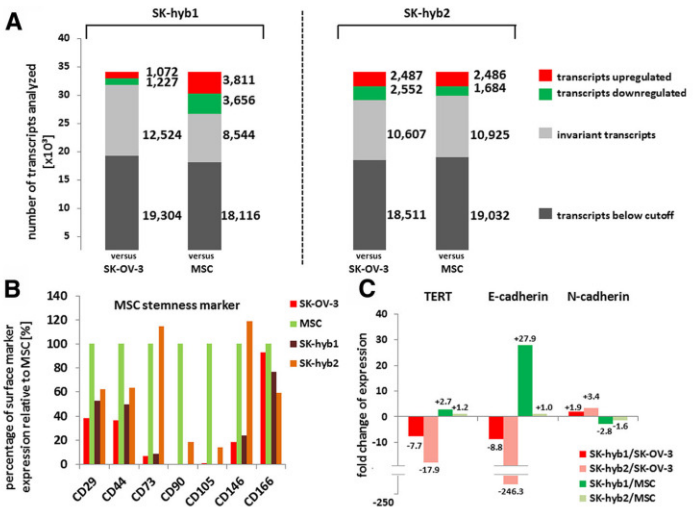


Fig. 3 **a** Following RNA microarray analysis, changes in gene expression levels were quantified in SK-hyb1 (left panel) and SK-hyb2 cells (right panel) versus the corresponding parental cell populations SK-OV-3^{cherry} P90 and MSC081113^{GFP} P6, respectively. Changes in transcript levels of more than 2-fold were considered as up- or down-regulated. The entire set of microarray data is stored with the accession no. GSE117411 at the NCBI-GEO database. **b** Relative expression analysis based on the RNA microarray data of some characteristic mesenchymal stem-like markers was calculated for SK-OV-3 cells and the hybrid populations SK-hyb1 and SK-hyb2. For relative evaluations the expression levels of MSC were used as a control (set to 100%). **c** Functional changes of SK-hyb1 and SK-hyb2 cells by altered expression of telomerase (TERT) and cadherins when compared to the parental cell populations SK-OV-3^{cherry} P90 and MSC081113^{GFP} P6, respectively. Numbers indicate the fold changes of increased (+) or decreased (–) transcript levels

Further characterization of the hybrid populations was performed by evaluation of the proliferation rate. Compared to the exponential cell division potential of the parental SK-OV-3 cells only a linear increase in SK-hyb1 cells was observed which continued to proliferate at a low level. In contrast, the cell number of SK-hyb2 cells which was propagated until passage 7, remained nearly unaltered after 72 h indicating little if any proliferative advancement and thus, an eventual cessation of proliferation either due to insufficient growth conditions or post-fusion alteration processes. Together, these data suggested a significantly reduced growth capacity of the ovarian cancer hybrid cell population (Fig. 4b).

Cell cycle analysis demonstrated a pronounced distribution of MSC, SK-OV-3 and SK-hyb1 cells throughout the different cell cycle phases. However, a progressive shift to higher fluorescence intensities was detectable in the different histograms which corresponded to elevated DNA content (Fig. 4c). Compared to a normal diploid set of chromosomes in MSC, the shift to increased DNA content in SK-OV-3 represents aneuploidy which is known for this ovarian cancer cell line displaying a heterogeneous set of chromosomes [34]. Further increase in DNA fluorescence intensity continued in SK-hyb1 cells reaching a level for cells in G_0/G_1 nearly to that observed for MSC in G_2/M phase (Fig. 4c, dotted line). Supportive evidence was obtained from karyotype analysis of SK-hyb1 cells displaying a hypertriploid set of chromosomes. This effect is equivalent to additional chromosomes acquired by SK-hyb1 cells and consequently, supports furthermore the previous cell fusion with MSC.

For in vivo analysis of the proliferative capacity and accompanying tumorigenicity, 4.5×10^5 SK-hyb1 and SK-hyb2 cells were injected subcutaneously into 4 NOD/scid mice, respectively, and tumor development was compared to the application of 4.5×10^5 parental SK-OV-3^{GFP} control cells in 4 NOD/scid mice. Tumor growth of SK-OV-3 cells was detectable already after 20d post injection in (1/4) NODscid mice and was continuously growing. Conversely, no tumor development was detectable in mice transplanted with either SK-hyb1 (0/4) or SK-hyb2 cells (0/4). The average tumor weight induced by SK-OV-3^{GFP} cells reached 161.5 ± 110 mg ($n = 4$) after 38d post inoculation and those mice were sacrificed by cervical dislocation according to animal welfare (Fig. 4d). In contrast, application of SK-hyb1 and SK-hyb2 cells was associated with no detectable tumor development at any time and the

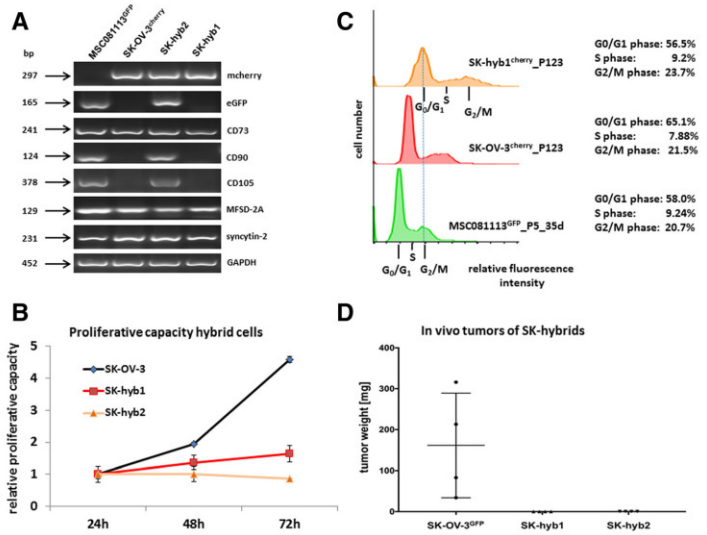


Fig. 4 **a** PCR analysis was performed with mcherry, eGFP, MSC stem-like markers CD73, CD90, CD105, and fusion-associated factors syncytin-2 and MFSD-2A expression in the parental SK-OV-3^{cherry} and MSC^{GFP} populations as compared to the two hybrid populations SK-hyb1 and SK-hyb2, respectively. Unaltered GAPDH transcripts served as loading control. **b** Proliferative capacity of the parental SK-OV-3^{cherry} cells was compared to the SK-hyb1 and SK-hyb2 hybrid populations by cell counting of initially seeded 10^4 cells/well in 24-well plates for 24 h up to 72 h, respectively. Data represent the mean ± s.d. ($n = 3$). **c** Cell cycle analysis was performed in steady state SK-hyb1 cells and compared to the parental control populations SK-OV-3^{cherry} and MSC^{GFP} using the FlowJo V10 software. Cell cycle sub-populations of similar relative fluorescence intensities were matched by the dotted line indicating that the DNA content of MSC in G_2/M corresponded to SK-hyb cells in G_0/G_1 phase. **d** Tumor weight of SK-OV-3^{GFP}-induced tumors ($n = 4$) was measured following dissection of the solid subcutaneous primary tumors. No tumors were detectable after transplantation of either SK-hyb1 or SK-hyb2 cell populations

mice ($n = 4$ for each SK hybrid cell population) subsequently died of age latest after 346d post injection (Fig. 4d).

Discussion

Previous work has demonstrated that MSC promote enhanced proliferative capacity in different breast and ovarian cancer cells during in vitro co-culture [18, 25]. Likewise, MSC populations also enhanced initial tumor growth of ovarian cancer cells in vivo by displaying a filamentous tumor environment with an increased amount of Ki67-positive cells. These findings were substantiated in co-cultures of ovarian cancer cells with adipose tissue-derived MSC whereby MSC developed altered properties and were therefore characterized as carcinoma-associated (CA-)MSC [23, 35]. Moreover, evidence was presented that distinct bone morphogenic proteins contribute to the capability of CA-MSC to enhance tumor heterogeneity by further promoting tumor growth and by increasing the number of cancer stem cells.

Elevated tumorigenicity in the presence of MSC is also demonstrated by the detection of distant organ metastases in the liver and by a reduced chemosensitivity of explant tumor cells after MSC co-culture when compared to the original SK-OV-3 ovarian cancer cells. MSC-mediated chemoresistance of a drug combination was previously observed in the rare small cell ovarian carcinoma (SCCOHT) [36]. This "chemoresistance" was partially based on tumor-protective effects by enhanced CA-MSC-mediated filament expression including collagen, laminin, elastin, and fibronectin [37] which may explain similar effects in the filamentous tumor microenvironment of MSC co-cultured SK-OV-3 cells.

Increased ovarian tumor heterogeneity is also achieved by fusion of MSC with ovarian cancer cells to generate new hybrid cell populations. Fusion of MSC with cancer cells was previously observed with the MDA-MB-231 breast cancer cell line [26, 27]. Although the resulting fusion populations MDA-hyb1 and MDA-hyb2 demonstrated enhanced tumor growth and elevated formation of metastases compared to the parental MDA-MB-231 cells, these hybrid cells exhibited increased chemosensitivity [27]. Moreover, fusion of MSC with neoplastic MCF10A breast epithelial cells generated hybrid cells which have

lost their autonomous growth capacity during post-fusion modifications and underwent aging with cessation of proliferation after a couple of doublings in passage 3 to 4 [28] supporting evidence for anti-tumorigenic effects of MSC during fusion with cancer cells.

Formation of MSC/cancer hybrid cells represents a rare event which can occur by different mechanisms via a certain type of entosis like cancer cell cannibalism [38] or via cell fusion. Previous work suggested the requirement of two coordinated processes for either directed or accidental cell fusion. These include a reorganization of the actin cytoskeleton by different adhesion molecules to generate membrane protrusions with appropriate placement of a transmembrane fusogenic protein [39, 40]. Thus, local membrane protrusions allow the two cell membranes coming into close proximity, whereby such contacts create microdomains that favor exchanges between the adjacent cells. Moreover, certain cell type-specific fusogenic proteins are required, e.g. syncytin-1 and -2 which are predominantly detectable in syncytiotrophoblasts of placenta tissue but also in certain solid tumors [28]. In the course of heterofusion, ASCT-2 (alanine, serine and cysteine selective transporter-2) and MFSD-2A (major facilitator superfamily domain containing 2A) can function as corresponding syncytin receptor on the fusion partner cell [41]. Accordingly, SK-OV-3 cells and the fusion cell partner MSC081113 demonstrated expression of both, syncytin-2 and MFSD-2A suggesting the availability of a fusogenic environment.

The resulting new hybrid cells acquired genomic parts from both parental cells during cell fusion. Consequently, the new karyotype of the fused cell displays more DNA content as compared to the parental cells. Corresponding observations are obtained from SK-hyb1 cell cycle analysis suggesting the acquisition of certain SK-OV-3 and MSC properties. Moreover, the reduced proliferative capacity of the hybrid populations as compared to the parental tumor cell line further supported potential functional alterations mediated by MSC. Together with the observed changes in telomerase, N-, and E-cadherin expression, these data supported a reduced tumorigenicity of the ovarian cancer cell hybrid populations. Indeed, in vivo observations in NOD/scid mice further substantiated the in vitro data demonstrating no detectable tumor development of the SK-hyb1 and SK-hyb2 populations.

In summary, the bipolar MSC functionalities are associated with the all-round supportive regenerative properties and the unique biodiverse capabilities of MSC contributing to increased ovarian cancer growth and potentially enhanced formation of metastases during intercellular communication processes. However, MSC fusion with ovarian cancer cells was associated with the generation of new hybrid cell populations also displaying normal MSC-like properties with reduced proliferative capacity in conjunction with a loss of tumorigenic potential.

Additional files

Additional file 1: Figure S1. Dose-dependent response to carboplatin was tested in SK-OV-3^{GFP} control cells and compared to cells derived from SK-OV-3^{GFP}-induced tumor explants and ex vivo tumor cultures from SK-OV-3^{GFP}/MSC060616$^{wt.}$ co-injections. Relative proliferative capacity was evaluated in a fluoroscan assay following exposure to 1 μM, 10 μM, and 100 μM carboplatin for up to 72 h, respectively. Data represent the mean ± s.d. ($n = 5$) whereby fluorescence values were set to 100% for the corresponding cells in control medium. (TIF 962 kb)

Additional file 2: Figure S2. Expression of MSC stem-like markers CD44, CD73, and CD105 was analyzed by RT-PCR in three SK-OV-3^{GFP}-derived tumors (mouse tumor 1.1 to 1.3) and SK-OV-3^{GFP}/MSC060616$^{wt.}$ co-injected tumors (mouse tumor 2.1 to 2.3) as well as in corresponding SK-OV-3^{GFP} tumor explant cultures and in SK-OV-3^{GFP}/MSC060616$^{wt.}$ tumor explant cultures. GAPDH transcripts served as loading control. (TIF 448 kb)

Additional file 3: Figure S3. Hybrid cell formation was observed after fusion of the parental cell populations SK-OV-3^{cherry} P90 and MSC081113^{GFP} P6 by appearance of double-labeled (mcherry and GFP)-expressing yellow fluorescing cells. Separation of this hybrid cell population was performed in two steps by repeated fluorescence-activated cell sorting (FACS). Hybrid cells were collected in microtiter plates with one to two hybrid cells/well and subsequent cell cloning. Two different clones (SK-hyb1 and SK-hyb2) were isolated. (TIF 1151 kb)

Abbreviations

ASCT-2: Alanine, serine and cysteine selective transporter-2; BRAF: v-Raf murine sarcoma viral oncogene homolog B; CTNNB1: Catenin Beta 1; eGFP: Enhanced green fluorescent protein; epoB: Epothilone B; ERBB2: Erythroblastic oncogene B (=Her2/neu); FACS: Fluorescence-activated cell sorting; HE: Hematoxylin/eosin; KRAS: Kirsten RAt Sarcoma virus gene; MFSD-2A: Major facilitator superfamily domain 2A; MSC: Mesenchymal stroma/stem cells; PIC3CA: Phosphatidylinositol-4,5-bisphosphate 3-kinase catalytic subunit alpha.; PTEN: Phosphatase and tensin homolog.; STR: Short tandem repeat.; TERT: Telomerase reverse transcriptase.; TP53: Tumor protein 53.

Acknowledgements

The authors are grateful to colleagues from Hannover Medical School including Dr. Thomas Rothämel for support with the STR fragment analysis, to Dr. Matthias Ballmaier (FACS core unit) for cell separation, and to Dr. Oliver Breiholz-Dittrich (research core unit Transcriptomics) for microarray analysis.

Availability of data and materials

NCBI-GEO database with the accession no. # GSE117411.

Authors' contributions

CM, JvO and RH performed the experiments. RH designed the study, and drafted the manuscript. All authors critically read and approved the final manuscript.

Ethics approval and consent to participate

The use of primary human MSC following explant culture from umbilical cord tissue has been approved by the Ethics Committee of Hannover Medical School, Project #443 on February 26th, 2009, respectively, and informed written consent was obtained from each patient.

Consent for publication

All authors have critically read and approved this work.

Competing interests

The authors declare no financial, personal, or professional conflict of interest.

Publisher's Note

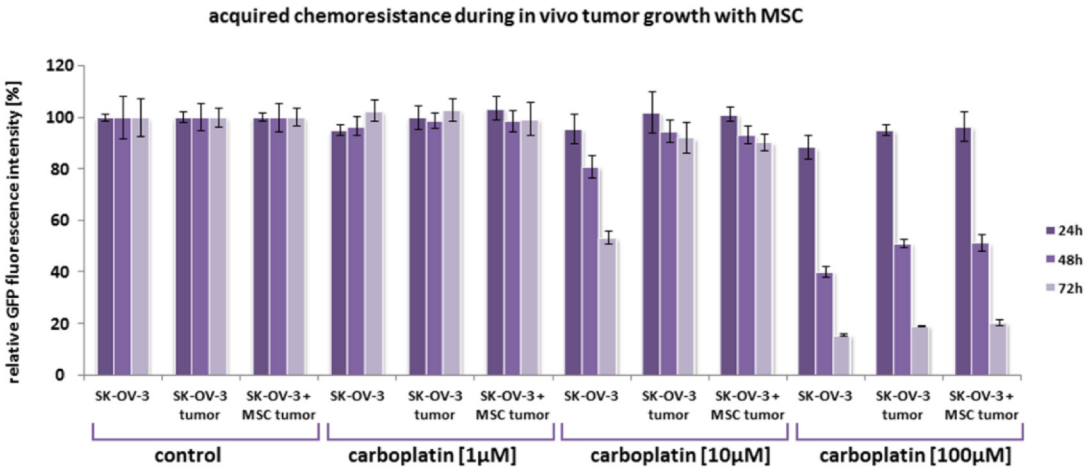
Springer Nature remains neutral with regard to jurisdictional claims in published maps and institutional affiliations.

Received: 24 July 2018 Accepted: 1 October 2018
Published online: 13 October 2018

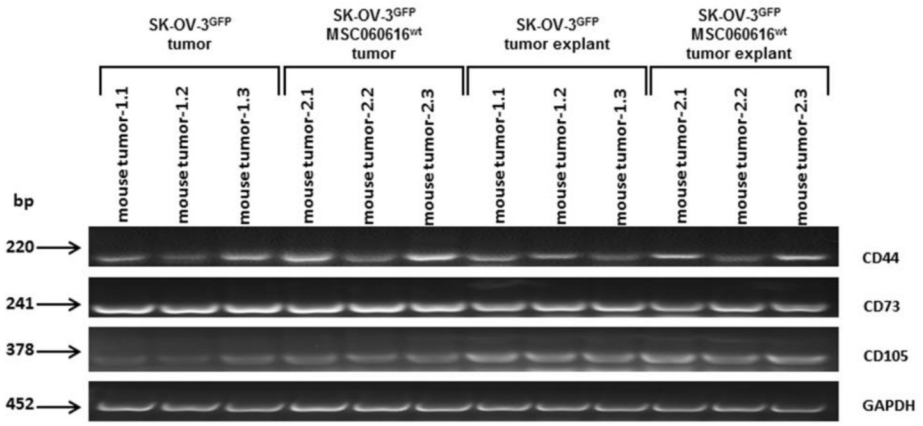
References

1. Dubeau L. The cell of origin of ovarian epithelial tumours. Lancet Oncol. 2008;9(12):1191–7.
2. Hafner N, Nicolaus K, Weiss S, Frey M, Diebolder H, Rengsberger M, Durst M, Runnebaum IB. p53-autoantibody may be more sensitive than CA-125 in monitoring microscopic and macroscopic residual disease after primary therapy for epithelial ovarian cancer. J Cancer Res Clin Oncol. 2013;139(7): 1207–10.
3. Kurman RJ, Visvanathan K, Roden R, Wu TC, Shih Ie M. Early detection and treatment of ovarian cancer: shifting from early stage to minimal volume of disease based on a new model of carcinogenesis. Am J Obstet Gynecol. 2008;198(4):351–6.
4. Kurman RJ, Shih Ie M. The origin and pathogenesis of epithelial ovarian cancer: a proposed unifying theory. Am J Surg Pathol. 2010;34(3):433–43.
5. Kim A, Ueda Y, Naka T, Enomoto T. Therapeutic strategies in epithelial ovarian cancer. J Exp Clin Cancer Res. 2012;31:14.
6. Ungefroren H, Sebens S, Seidl D, Lehnert H, Hass R. Interaction of tumor cells with the microenvironment. Cell Commun Signal. 2011;9:18.
7. Caplan AI. Mesenchymal stem cells. J Orthop Res. 1991;9(5):641–50.
8. Friedenstein A, Kuralesova AI. Osteogenic precursor cells of bone marrow in radiation chimeras. Transplantation. 1971;12(2):99–108.
9. Bianco P. "mesenchymal" stem cells. Annu Rev Cell Dev Biol. 2014;30: 677–704.
10. Hass R, Kasper C, Bohm S, Jacobs R. Different populations and sources of human mesenchymal stem cells (MSC): a comparison of adult and neonatal tissue-derived MSC. Cell Commun Signal. 2011;9:12.
11. Phinney DG. Building a consensus regarding the nature and origin of mesenchymal stem cells. J Cell Biochem Suppl. 2002;38:7–12.
12. Pittenger MF, Mackay AM, Beck SC, Jaiswal RK, Douglas R, Mosca JD, Moorman MA, Simonetti DW, Craig S, Marshak DR. Multilineage potential of adult human mesenchymal stem cells. Science. 1999;284(5411):143–7.
13. Sasaki M, Abe R, Fujita Y, Ando S, Inokuma D, Shimizu H. Mesenchymal stem cells are recruited into wounded skin and contribute to wound repair by transdifferentiation into multiple skin cell type. J Immunol. 2008;180(4): 2581–7.
14. Ghajar CM, Kachgal S, Kniazeva E, Mori H, Costes SV, George SC, Putnam AJ. Mesenchymal cells stimulate capillary morphogenesis via distinct proteolytic mechanisms. Exp Cell Res. 2010;316(5):813–25.
15. De Miguel MP, Fuentes-Julian S, Blazquez-Martinez A, Pascual CY, Aller MA, Arias J, Arnalich-Montiel F. Immunosuppressive properties of mesenchymal stem cells: advances and applications. Curr Mol Med. 2012;12(5):574–91.
16. Torne M, Lopez-Romero P, Albo C, Sepulveda JC, Fernandez-Gutierrez B, Dopazo A, Bernad A, Gonzalez MA. miR-335 orchestrates cell proliferation, migration and differentiation in human mesenchymal stem cells. Cell Death Differ. 2011;18(6):985–95.
17. Hass R, Otte A. Mesenchymal stem cells as all-round supporters in a normal and neoplastic microenvironment. Cell Commun Signal. 2012;10(1):26.
18. Mandel K, Yang Y, Schambach A, Glage S, Otte A, Hass R. Mesenchymal stem cells directly interact with breast cancer cells and promote tumor cell growth in vitro and in vivo. Stem Cells Dev. 2013;22(23):3114–27.
19. Melzer C, von der Ohe J, Lehnert H, Ungefroren H, Hass R. Cancer stem cell niche models and contribution by mesenchymal stroma/stem cells. Mol Cancer. 2017;16(1):28.
20. Melzer C, Yang Y, Hass R. Interaction of MSC with tumor cells. Cell Commun Signal. 2016;14(1):20.
21. Ciuculescu F, Giesen M, Deak E, Lang V, Seifried E, Henschler R. Variability in chemokine-induced adhesion of human mesenchymal stromal cells. Cytotherapy. 2011;13(10):1172–9.
22. Gauthaman K, Yee FC, Cheyyatraivendran S, Biswas A, Choolani M, Bongso A. Human umbilical cord Wharton's jelly stem cell (hWJSC) extracts inhibit cancer cell growth in vitro. J Cell Biochem. 2012;113(6):2027–39.
23. McLean K, Gong Y, Choi Y, Deng N, Yang K, Bai S, Cabrera L, Keller E, McCauley L, Cho KR, Buckanovich RJ. Human ovarian carcinoma-associated mesenchymal stem cells regulate cancer stem cells and tumorigenesis via altered BMP production. J Clin Invest. 2011;121(8):3206–19.
24. Yang Y, Bucan V, Baehre H, von der Ohe J, Otte A, Hass R. Acquisition of new tumor cell properties by MSC-derived exosomes. Int J Oncol. 2015; 47(1):244–52.
25. Yang Y, Otte A, Hass R. Human mesenchymal stroma/stem cells exchange membrane proteins and alter functionality during interaction with different tumor cell lines. Stem Cells Dev. 2015;24(10):1205–22.
26. Noubissi FK, Harkness T, Alexander CM, Ogle BM. Apoptosis-induced cancer cell fusion: a mechanism of breast cancer metastasis. FASEB J. 2015;29(9): 4036–45.
27. Melzer C, von der Ohe J, Hass R. Enhanced metastatic capacity of breast cancer cells after interaction and hybrid formation with mesenchymal stroma/stem cells (MSC). Cell Commun Signal. 2018;16(1):2.
28. Melzer, C., J. von der Ohe, and R. Hass, In Vitro fusion of Normal and neoplastic breast epithelial cells with human mesenchymal stroma/stem cells partially involves tumor necrosis factor receptor signaling. Stem cells, 2018.
29. Majore I, Moretti P, Hass R, Kasper C. Identification of subpopulations in mesenchymal stem cell-like cultures from human umbilical cord. Cell Commun Signal. 2009;7:6.
30. Otte A, Rauprich F, von der Ohe J, Yang Y, Kommoss F, Feuerhake F, Hillemanns P, Hass R. C-met inhibitors attenuate tumor growth of small cell hypercalcemic ovarian carcinoma (SCCOHT) populations. Oncotarget. 2015; 6(31):31640–58.
31. Kim MH, Kim MH, Kim KS, Park MJ, Jeong JH, Park SW, Ji YH, Kim KI, Lee TS, Ryu PY, Kang JH, Lee YJ. In vivo monitoring of CD44+ cancer stem-like cells by gamma-irradiation in breast cancer. Int J Oncol. 2016;48(6):2277–86.
32. Bertram C, Hass R. Cellular senescence of human mammary epithelial cells (HMEC) is associated with an altered MMP-7/HB-EGF signaling and increased formation of elastin-like structures. Mech Ageing Dev. 2009; 130(10):657–69.
33. Otte A, Rauprich F, Hillemanns P, Park-Simon TW, von der Ohe J, Hass R. In vitro and in vivo therapeutic approach for a small cell carcinoma of the ovary hypercalcaemic type using a SCCOHT-1 cellular model. Orphanet J Rare Dis. 2014;9:126.
34. Buick RN, Pullano R, Trent JM. Comparative properties of five human ovarian adenocarcinoma cell lines. Cancer Res. 1985;45(8):3668–76.
35. Coffman LG, Choi YJ, McLean K, Allen BL, di Magliano MP, Buckanovich RJ. Human carcinoma-associated mesenchymal stem cells promote ovarian cancer chemotherapy resistance via a BMP4/HH signaling loop. Oncotarget. 2016;7(6):6916–32.
36. Otte A, Gohring G, Steinemann D, Schlegelberger B, Groos S, Langer F, Kreipe HH, Schambach A, Neumann T, Hillemanns P, Park-Simon TW, Hass R. A tumor-derived population (SCCOHT-1) as cellular model for a small cell ovarian carcinoma of the hypercalcemic type. Int J Oncol. 2012;41(2):765–75.
37. Otte A, Yang Y, von der Ohe J, Melzer C, Hillemanns P, Feuerhake F, Hass R. SCCOHT tumors acquire chemoresistance and protection by interacting mesenchymal stroma/stem cells within the tumor microenvironment. Int J Oncol. 2016;49(6):2453–63.
38. Bartosh TJ, Ullah M, Zeitouni S, Beaver J, Prockop DJ. Cancer cells enter dormancy after cannibalizing mesenchymal stem/stromal cells (MSCs). Proc Natl Acad Sci U S A. 2016;113(42):E6447–56.
39. Shilagardi K, Li S, Luo F, Marikar F, Duan R, Jin P, Kim JH, Murnen K, Chen EH. Actin-propelled invasive membrane protrusions promote fusogenic protein engagement during cell-cell fusion. Science. 2013;340(6130):359–63.
40. Melzer C, von der Ohe J, Hass R. Concise review: crosstalk of mesenchymal stroma/stem-like cells with Cancer cells provides therapeutic potential. Stem Cells. 2018. https://doi.org/10.1002/stem.2829. [Epub ahead of print].
41. Mi S, Lee X, Li X, Veldman GM, Finnerty H, Racie L, LaVallie E, Tang XY, Edouard P, Howes S, Keith JC Jr, McCoy JM. Syncytin is a captive retroviral envelope protein involved in human placental morphogenesis. Nature. 2000;403(6771):785–9.

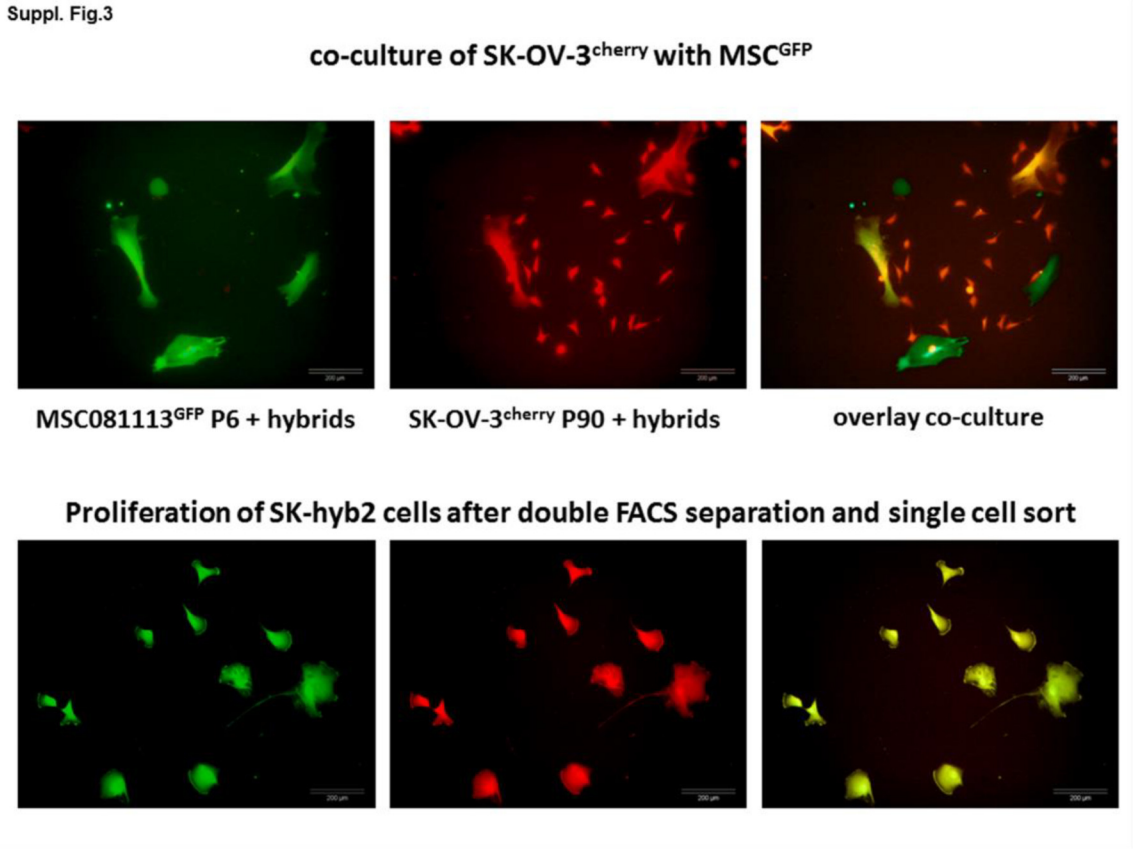
Suppl. Fig.1



Suppl. Fig.2



Suppl. Fig.3


co-culture of SK-OV-3cherry with MSCGFP
MSC081113GFP P6 + hybrids
SK-OV-3cherry P90 + hybrids
overlay co-culture
Proliferation of SK-hyb2 cells after double FACS separation and single cell sort

2.4 In vivo cell fusion between mesenchymal stroma/stem-like cells and breast cancer cells

Catharina Melzer, Juliane von der Ohe and Ralf Hass

Manuscript

Author contribution statement:

Catharina Melzer (CM) performed the experiments and analyzed the data. CM co-wrote the manuscript.

In vivo cell fusion between mesenchymal stroma/stem-like cells and breast cancer cells

Catharina Melzer [1], Juliane von der Ohe [1] and Ralf Hass [1,*]

[1] Biochemistry and Tumor Biology Lab, Department of Obstetrics and Gynecology, Hannover Medical School
* Correspondence: hass.ralf@mh-hannover.de Tel.: +49-511-532-6070

Abstract: Cellular communication within the tumor microenvironment enables important interactions between cancer cells and recruited adjacent populations including mesenchymal stroma/stem-like cells (MSC). These interactions were monitored in vivo following co-injection of GFP-labeled human MSC together with mcherry-labeled MDA-MB-231 breast cancer cells in NODscid mice. Within 14d of tumor development the number of initially co-injected MSC had significantly declined and spontaneous formation of breast cancer/MSC hybrid cells was observed by appearance of double fluorescing cells. This in vivo fusion displayed a rare event and occurred in less than 0.5% of the tumor cell population. Similar findings were observed in a parallel in vitro co-culture. Characterization of the new cell fusion products obtained after two consecutive flow cytometry cell sorting and single cell cloning revealed two populations, termed MDA-hyb3 and MDA-hyb4. The breast cancer fusion cells expressed both, GFP and mcherry and displayed more characteristics of the MDA-MB-231 cells than of the parental MSC. While little if any differences were determined in the proliferative capacity, a significant delay of MDA-hyb3 cells in tumor formation was observed when compared to the parental MDA-MB-231 cells. Moreover, MDA-hyb3 cells developed an altered pattern of distant organ metastases. These findings demonstrated in vivo and in vitro fusion with the development of new breast cancer hybrid cells carrying altered tumorigenic properties and contributing to progressively increasing tumor heterogeneity.

Keywords: in vivo fusion; cancer hybrid cells; mesenchymal stem cells; breast cancer; metastases; tumor microenvironment

1. Introduction

Cell fusion in general represents a rare biological process which requires close proximity between fusogenic cell partners and is tightly regulated by multiple pathways which, however, are not fully understood yet [1]. This process of hybrid cell formation besides entosis or cell cannibalism is associated with a proper alignment of certain glycoproteins and a permissive lipid composition of the involved parts of the cell membranes to facilitate the initiation of a fusion event. Moreover, an acidified and hypoxic microenvironment detectable in several tumors can act as fusogenic triggers for aberrant spontaneous cell fusion or a so-called process of "accidental cell fusion" [2, 3]. Indeed, previous work has demonstrated that hypoxia-induced apoptosis stimulates fusion between breast cancer cells and mesenchymal stroma/stem-like cells whereby the newly formed hybrids demonstrated enhanced migratory capacity [4]. Physiologically observed cell fusions include the generation of muscle fibers by a continuous homo- or autofusion of myoblasts to form multi-nucleated myocytes. Moreover, autofusion of osteoclasts contribute to bone regeneration and metabolic activity. Furthermore, fusion of fetal trophoblasts create syncytiotrophoblasts which are involved in placenta formation. In addition, heterofusion between egg and sperm combines their haploid gamete genomes and form a diploid embryonic stem cell [5, 6].

Cell fusion also occurs within the tumor microenvironment between cancer cells and neighboring non-malignant cells including MSC [7, 8]. These stroma/stem-like cells represent a heterogenous population preferentially residing in perivascular niches of nearly all kinds of human tissues [9, 10]. Despite biological differences according to their tissue-specific origins, MSC share distinct surface

protein expressions such as CD73, CD90, and CD105, and they exhibit the capability to differentiate at least along certain phenotypes of the mesodermal lineage [11-14]. Physiological functions of MSC include among others the regulation of stem cell homeostasis in the bone marrow and an accumulation at damaged or injured tissues to utilize repair processes [15], support angiogenesis [16] and modulate immune cell functions [17], preferably also at tumor sites.

Interaction between cancer cells and MSC in the tumor microenvironment represents a complex multistep cascade whereby an accidental merger e.g. between breast cancer cells and MSC as a rare event can be observed within less than five minutes [18]. This is associated with the generation of cancer hybrid cells displaying new cancer cell populations with altered biological properties [19, 20].

Molecular mechanisms of cell fusion processes include a reorganization of the actin cytoskeleton by different adhesion molecules to generate membrane structures with appropriate accumulation of transmembrane fusogenic proteins [21, 22]. Focal membrane protrusions containing lamellipodia and/or filopodia allow the two adjacent cell membranes to localize in close proximity, whereby contacts create microdomains that favor exchange of membrane patches and cytosolic parts between the attached cells. Moreover, certain cell type-specific fusogenic proteins are required, e.g. syncytin-1 and -2 which originate as truncated viral genes such as the HERV-W retroviral envelope genes [23] and are predominantly detectable in syncytiotrophoblasts of placenta tissue but also in certain solid tumors [18]. Previous findings have demonstrated that heterofusion of breast cancer cells with endothelial cells involves endothelial cell associated ASCT2 (alanine, serine and cysteine selective transporter-2) which functions as a syncytin receptor present on breast cancer cells [24].

However, the underlying regulatory interplay and physiological relevance for hybrid cell formation by spontaneous breast cancer cell fusion with MSC remains unclear. The present work extends existing knowledge about the in vitro data by providing evidence for breast cancer / MSC fusion in vivo. Moreover, newly generated hybrid cell populations from previous fusion processes between human breast cancer cells and MSC are characterized.

2. Materials and Methods

Cell culture

Primary human MSC were isolated from umbilical cord tissue as described previously [25]. MSC were cultured at 37 °C with 5 % CO2 in αMEM (Sigma Chemie GmbH, Steinheim, Germany) supplemented with 10 % of allogeneic human AB-serum (blood from 31 male AB donors was commercially obtained from blood bank, Hannover Medical School, Germany, and processed to serum), 100 U/mL penicillin, 100 µg/mL streptomycin and 2 mM L-glutamine (Sigma). The study was conducted in accordance with the Declaration of Helsinki, and the Ethics Committee of Hannover Medical School has approved the isolation and culturing of primary human MSC, Project #443 on February 26th, 2009, and informed written consent was obtained from each patient.

Subculture of MSC was performed by accutase (Sigma) treatment for 3 min at 37 °C. For the experiments, MSC from two different donors (MSC290115 and MSC300415) were applied.

Human breast carcinoma cell line MDA-MB-231 was commercially obtained from ATCC, Manassas, VA, USA. This breast cancer cell line was cultured in Leibovitz´s L-15-medium (Life technologies, Darmstadt, Germany) supplemented with 10% (v/v) FCS, 100 U/mL penicillin, 100 µg/mL streptomycin and 2 mM L-glutamine (Sigma). Subculture was performed by trypsin/EDTA (Biochrom GmbH, Berlin, Germany) treatment for 5 min at 37°C.

Cells were tested for mycoplasma by the luminometric MycoAlert Plus mycoplasma detection kit (Lonza Inc., Rockland, ME, USA) according to the manufacturer's recommendations. Cell line authentication was performed by short tandem repeat (STR) fragment analysis using the GenomeLab human STR primer set (Beckman Coulter Inc., Fullerton, CA, USA). For fluorescence labeling and discrimination of the cell populations in co-culture, MSC and the cancer cells have been transduced

with a 3rd generation lentiviral SIN vector containing the eGFP and the mcherry gene, respectively, as indicated in previous work [20].

In vivo experiments

Animal experiments using NOD/scid mice have been approved by the institutional licensing committee ref. # 33.19-42502-04-15/1992 on Dec. 18th, 2015 and were performed by obeying the internationally recognized guidelines on animal welfare.

In a first set of in vivo experiments, $2x10^6$ GFP-labeled MSC300415^{GFP} together with $2x10^6$ cherry-labeled MDA-MB-231^{cherry} were co-injected subcutaneously into 5 female NOD/scid mice (5 to 6 weeks old), respectively. After 4d post injection, all 5 mice had developed subcutaneous tumors. Mice were sacrificed by cervical dislocation at different time points, 4d, 8d, 14d, 45d and 51d post injection. Tumors developed after 8d and 14d were dissected, washed in PBS and incubated in tumor dissociation buffer (a mixture of 50% (v/v) reconstituted tumor dissociation enzyme reagent (DCS Innovative Diagnostik-Systeme GmbH, Hamburg, Germany) and 50% (v/v) serumfree medium) for 5h at 37°C. Liberated cells from digested tumor tissue in the supernatant were harvested by centrifugation (360g/5min), counted in a hemocytometer, and analyzed by flow cytometry.

In parallel to the in vivo study, a similar 2D in vitro co-culture of MSC300415^{GFP} and MDA-MB-231^{cherry} (same cell ratio) was performed for 8d and 14d, respectively. Organs from mice sacrificed after 45d and 51d were analyzed for metastasis by fluorescence microscopy.

In a second set of in vivo experiments, $1x10^6$ MSC290115^{GFP} together with $1x10^6$ MDA-MB-231^{cherry} cells were co-injected subcutaneously into the left and the right flank of 3 female NOD/scid mice (5 to 6 weeks old). After 7d post injection, all 3 mice had developed subcutaneous tumors on both sides. Mice were sacrificed by cervical dislocation 14d after cell co-injection. All tumors were dissected, washed in PBS and incubated in tumor dissociation buffer for 5h at 37°C. Liberated cells from digested tumor tissue in the supernatant were harvested by centrifugation (360g/5min), counted in a hemocytometer, documented by fluorescence microscopy, and analyzed by flow cytometry.

In a third in vivo experiment, a population of $1x10^6$ MDA-hyb3$^{GFP/cherry}$ cells was injected subcutaneously into the left and the right flank of 3 female NOD/scid mice (5 to 6 weeks old) and tumor development was compared to $1x10^6$ MDA-MB-231^{GFP} similarly injected on both sides of 2 female NOD/scid mice. Tumor progression of MDA-hyb3 tumor was measured using a digital caliper (VWR International) and corresponding tumor volumes (V) were calculated as previously described [26]. Organs from mice sacrificed after 48d with MDA-MB-231^{GFP} tumors and after 70d with MDA-hyb3$^{GFP/cherry}$-induced tumors were analyzed for metastasis by fluorescence microscopy.

Flow cytometric analysis

For detection and quantification of in vivo-generated hybrid cells, flow cytometry analysis was performed by using the LSRII (BD Bioscience) and FlowJo V10 analysis software.

Proliferation measurement by fluoroskan assay

Proliferation of MDA-hyb3$^{GFP/cherry}$ and MDA-hyb4$^{GFP/cherry}$ was analyzed by fluoroskan measurements as described previously [27]. Briefly, 1,000 cells/well were incubated in flat bottom 96-well plates (Nunc, Thermo Fisher Scientific, Rokslide, Denmark) at appropriate time points for 24h up to 96h. After removal of the medium supernatant, cells were lysed with 10% (w/v) SDS and fluorescence was measured by detection of fluorescence intensity of mCherry (excitation: 584nm, emission: 612nm) and eGFP (excitation: 485nm, emission: 520nm) using the Fluoroskan Ascent FL (Thermo Fisher Scientific, Schwerte, Germany).

Cell cycle analysis

Analysis of cell cycle distribution was performed as indicated elsewhere [28]. Briefly, $1x10^5$ cells were fixed in 70% ice-cold Ethanol at 4°C for 24h. After washing with PBS, fixed cells were stained with 500 µL of DNAse-free RNase (200 U/mL) and 500 µL of propidium-iodide (PI) staining solution (500 µL 0.5 mg/mL propidium iodide in 10mL PBS + 100 µL Trition-X-100) at room temperature protected from light for 30 min and subsequently analyzed by FACScalibur (BD Biosciences) and FlowJo V10 analysis software.

Transcript analysis by RT-PCR

Total RNA was isolated using RNeasy Mini Kit (Qiagen, Hilden, Germany) according to manufacturer´s instructions. One µg RNA was reverse transcribed into cDNA using 500 µM of dNTP (R0193), 5 µM Oligo(dT)18 primer (S0132), 5 µM Random Hexan primer (S0142), 1 U RiboLockTM RNase Inhibitor (E00381) and 5 U RevertAidTM M-MuLV Reverse Transcriptase (EP0441) in the supplied reaction buffer (all reagents obtained from Thermo Scientific, Schwerte, Germany). The cDNA reactions were performed for 10 min at 25°C followed by 1h at 37°C and stopped at 72 °C for 10 min. cDNA (2.5µl) was used as a template and amplified by PCR with following specific primers (customized by Eurofins, MWG GmbH, Ebersberg, Germany) as described previously [19].

3. Results

In vivo co-injection of MSC300415^{GFP} with MDA-MB-231^{cherry} demonstrated tumor development already after 4 days (Fig. 1A). Tumor weight of 44 mg after 4d increased to 743 mg after 51d post injection (Fig. 1A+B). Distant organ metastases in liver, heart, lung, spleen or brain remained undetectable whereas metastasized mcherry-positive fluorescing cancer cells exclusively appeared in kidney sections of the two mice after 45 and 51 days post injection (Fig. 1C). Of interest, these metastases demonstrated only mcherry fluorescence without any traceable GFP fluorescence. This is also supported by fluorescence microscopy demonstrating that in parallel to the increasing tumor development, the amount of detectable MSC^{GFP} decreased over time (Fig. 1D). Indeed, after initiating the 2D in vitro co-culture and the 3D in vivo co-injection with both cell populations in equal amounts, fluorescence microscopy images of tumor tissues from mice sacrificed after 4, 8 and 14 days clearly documented the decline of cells expressing GFP fluorescence (Fig. 1D, middle and lower panel). Concomitantly, the amount of cherry fluorescence was continuously increasing over time. These in vivo observations were substantiated by 2D in vitro co-cultures with decreasing numbers of GFP-expressing MSC (Fig. 1D upper panel).

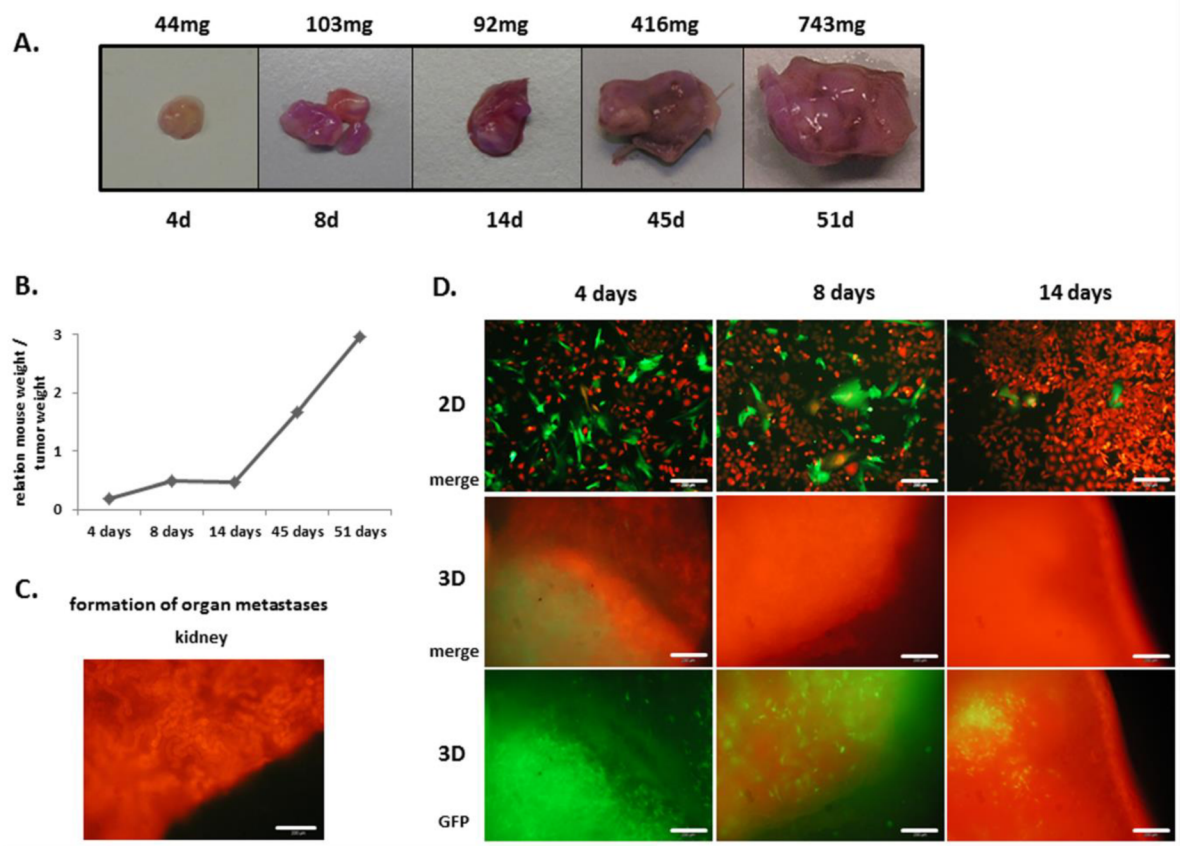
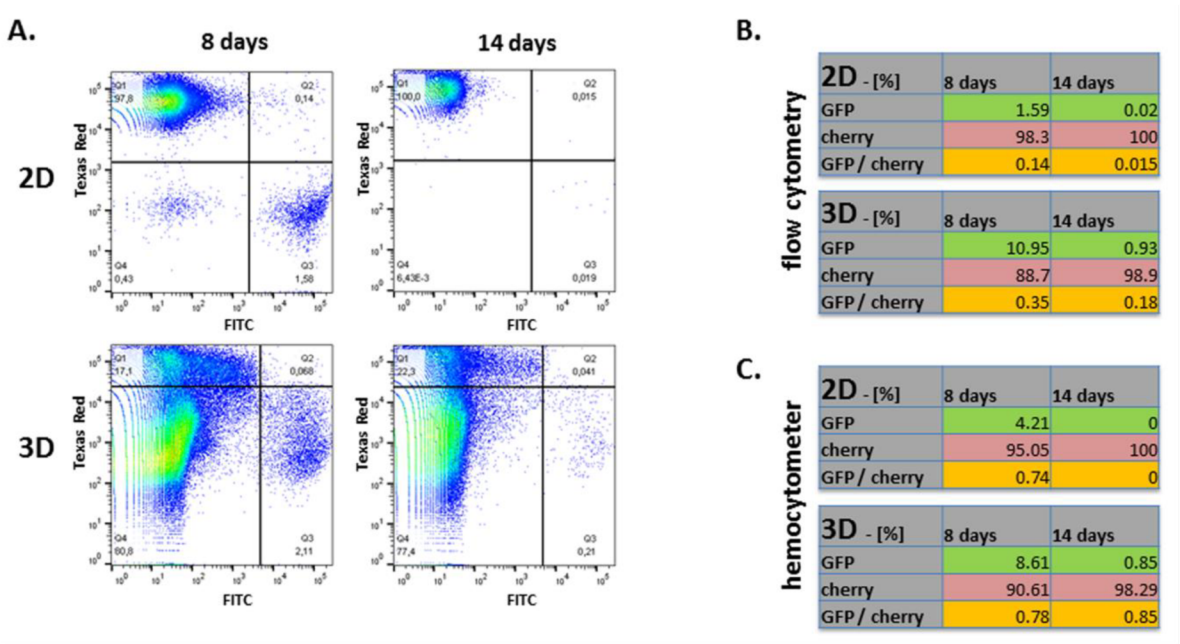


Figure 1. (**a**) NOD/scid mouse tumors were derived following subcutaneous co-injection of $2x10^6$ human MSC300415^{GFP} with $2x10^6$ MDA-MB-231^{cherry} breast cancer cells for different time points (4d, 8d, 14d, 45d and 51d). (**b**) Ratio of mouse weight to tumor weight was compared within different time points. (**c**) Formation of distant metastases was evaluated in mice after 45d and 51d of tumor development by investigation of cherry- and GFP-fluorescence in organs. One exemplary picture from kidney metastasis is documented. Bars represent 200µm. (**d**) Morphology and cell ratio of 2D co-cultures between MSC300415^{GFP} and MDA-MB-231^{cherry} was compared to appropriate 3D tumor tissues after 4d, 8d and 14d as documented by GFP fluorescence microscopy (GFP) and by a merge of mcherry and GFP fluorescence (merge). Bars represent 200µm.

Following trysinization of the 2D co-cultures and dissociation of 3D tumor tissues after 8d and 14d, respectively, the collected cell populations were quantified by flow cytometry for mcherry, GFP and double fluorescing cells whereby all non-fluorescing cells were excluded as negative populations (Fig. 2A). From 100% of the fluorescing populations which initially equals 50% of mcherry and GFP cells, the amount of GFP-positive cells within the tumor tissue declined to about 11% after 8d and further dropped to 0.93% after 14d (Fig. 2B, lower panel). In contrast, the percentage of mcherry-positive cells increased from 88.7% after 8d up to 98.9% after 14d. A small population of dual fluorescent cells was detectable at both time points (0.35% at 8d and 0.18% at 14d) (Fig. 2B, lower panel). Even more stringent effects were observed in corresponding 2D co-cultures. About 1.6% of GFP-positive cells remained detectable after 8d of co-culture and were largely overgrown by the mcherry breast cancer cells with a remaining population of 0.02% after 14d. Similarly, the amount of double positive hybrid cells dropped from 0.14% after 8d to about 0.015% after 14d (Fig. 2B, upper panel).

Similar findings were obtained in an independent cell counting evaluation of both, previously co-injected 3D tumor tissue-dissociated cell populations and 2D co-cultures by using a hemocytometer (Fig. 2C).



2D - [%]	8 days	14 days
GFP	1.59	0.02
cherry	98.3	100
GFP / cherry	0.14	0.015

3D - [%]	8 days	14 days
GFP	10.95	0.93
cherry	88.7	98.9
GFP / cherry	0.35	0.18

2D - [%]	8 days	14 days
GFP	4.21	0
cherry	95.05	100
GFP / cherry	0.74	0

3D - [%]	8 days	14 days
GFP	8.61	0.85
cherry	90.61	98.29
GFP / cherry	0.78	0.85

Figure 2. Analysis of GFP, cherry and GFP+cherry fluorescence in 8d and 14d tumors (3D) was (**a**) examined by flow cytometric analysis and (**b**) proportions were adjusted to 100% after exclusion of unlabeled cell populations. (**c**) In addition, percentages of GFP and cherry fluorescence were quantified by cell counting in a hemocytometer. All results were compared to appropriate 2D co-cultures.

In a further in vivo approach, tumor development and potential in vivo cell fusion was examined following subcutaneous co-injection of MDA-MB-231^{cherry} breast cancer cells with MSC from a different donor (MSC290115) into 6 NOD/scid mice. The mice were sacrificed after 14 days post injection and tumor tissues were documented and weighted (Fig. 3A). Differences in tumor size compared to the data in Fig. 1A after 14 days resulted from the reduced initial number of co-injected cells. Calculations of the relationship of tumor weight to mouse weight revealed a distribution between 0.05 and 0.24 % (Fig. 3B). Following dissociation of all 6 tumor tissues, the appearance of dual fluorescent cells was documented by fluorescence microscopy in one dissociated representative tumor population (Fig. 3C middle panel, yellow arrows). Appropriate 2D co-cultures were performed in parallel and likewise demonstrated the presence of double fluorescing hybrid cells (Fig. 3C upper panel, yellow arrows). Control fluorescence pictures of tumor tissue thin sections revealed the presence of both, mcherry-labeled breast cancer cells and GFP-expressing MSC (Fig. 3C lower panel).

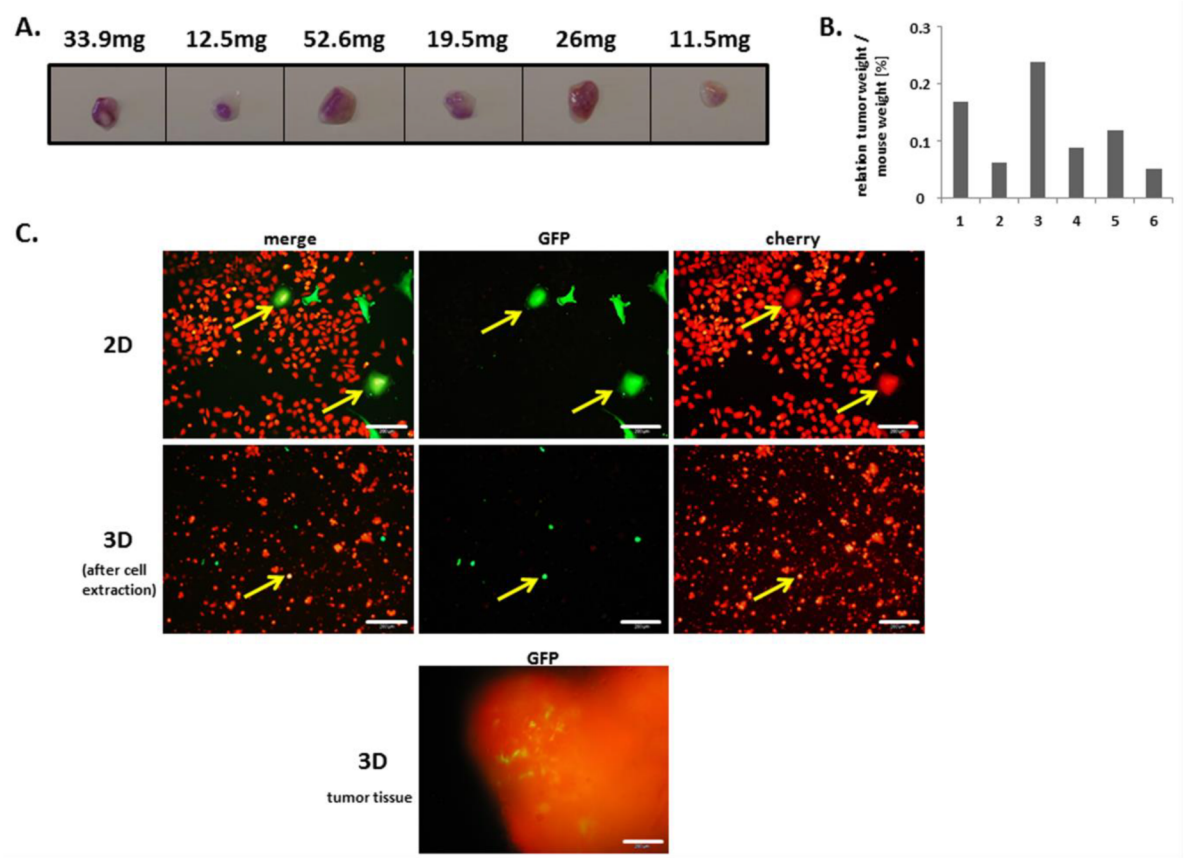


Figure 3. (**a**) In vivo formation of hybrid cells during tumor development was tested after subcutaneous co-injection of 10^6 human MSC290115^{GFP} together with 10^6 MDA-MB-231^{cherry} breast cancer cells in NOD/scid mice for 14d. (**b**) Ratio of mouse weight to tumor weight was compared between 6 tumors from 3 NOD/scid mice. (**c**) Formation of hybrid cells as indicated by yellow arrows was detectable by fluorescence microscopy in both, 2D in vitro co-cultures (upper panel) and in 3D ex vivo tumor tissues following extracellular matrix digestion and cell isolation (middle panel). In vivo presence of MSC290115^{GFP} in tumor tissues after 14d is exemplarily documented (lower micrograph). Bars represent 200µm.

Isolated cells from dissociated tumor tissues were further examined by flow cytometry for the existence of dual fluorescent fusion cells after co-injection. Indeed, in vivo fusion cells were confirmed in the FACS dot plots (Fig. 4A). While most cells were unlabeled, the vast majority of fluorescing cells was represented by the mcherry breast cancer population. Still, MSC^{GFP} and in vivo fusion cells carrying mcherry and GFP double fluorescence displayed a detectable population in all tumor tissues (Fig. 4A). Quantification of the fluorescing cells from FACS analysis revealed about 98% of mcherry breast cancer cells after 14d in vivo (Fig. 4B). Conversely, the amount of MSC^{GFP} had decreased from initially 50% to almost 1% after 14d. At the same time formation of GFP and cherry positive breast cancer fusion cells acquired 0.41% (Fig. 4B).

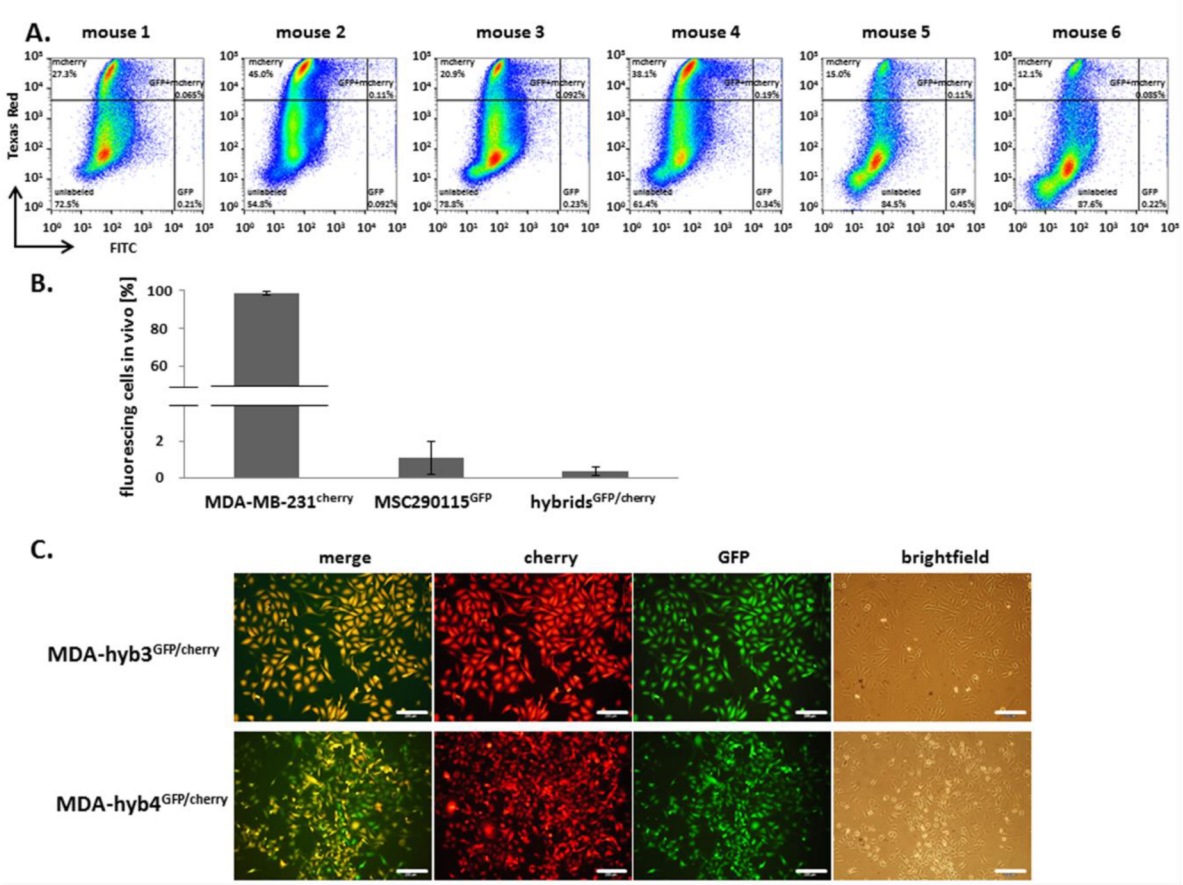


Figure 4. After dissociation of 6 in vivo tumor tissues, supernatants were analyzed by flow cytometry (**a**) and quantified for MDA-MB-231^{cherry}, MSC290115^{GFP} and hybrid cells$^{GFP/cherry}$ fluorescence. Data represent the mean ± s.d. from all 6 tumor tissue supernatants (**b**). Hybrid cell formation was observed in 2D co-cultures between MSC290115^{GFP} and MDA-MB-231^{cherry} resulting in GFP and cherry positive yellow fluorescing cells. Separation of hybrid cells was performed by fluorescence-activated cell sorting (FACS) and subsequent single cell cloning. Two different clones (MDA-hyb3 and MDA-hyb4) were isolated (**c**).

While corresponding 2D co-cultures revealed a similarly detectable amount of hybrid cells, repeated fluorescence activated cell sorting (FACS) was performed after 7d co-culture with subsequent single cell cloning for dual fluorescent cells. Following culture of 5,473 double-sorted dual fluorescing cell clones, 2 different hybrid clones termed MDA-hyb3$^{GFP/cherry}$ and MDA-hyb4$^{GFP/cherry}$ initiated proliferative capacity and were selected for further analysis (Fig. 4C).

Cell cycle analysis of these two hybrid populations demonstrated a similar cell cycle distribution as compared to MDA-MB-231^{cherry} breast cancer cells. While the parental MSC290115^{GFP} displayed a cell cycle with normal diploid DNA content, the pronounced cell cycle shift towards an elevated fluorescence intensity and accordingly, increased DNA content suggests aneuploidy / hyperdiploidy of MDA-hyb3 and MDA-hyb4, respectively, like the mixed MDA-MB-231^{cherry} karyotype carrying 52 to 68 chromosomes (Fig. 5A, dotted line). Moreover, the proliferation rate assessed by fluoroskan assay revealed little if any differences of MDA-hyb3 in comparison to the parental MDA-MB-231^{cherry} cells while the proliferative potential of MDA-hyb4 was slightly decreased after 24h up to 96h (Fig. 5B).

RT-PCR analysis substantiated hybrid cell formation of MDA-hyb3 and MDA-hyb4 by simultaneous expression of both fluorescence genes mcherry and GFP whereby exclusive expression of mcherry was detectable in MDA-MB-231^{cherry} and eGFP in MSC290115^{GFP} (Fig. 5C). mRNA transcript levels of MSC stemness marker CD44, CD73 and CD105 were expressed in all 4 cell

populations. By contrast, CD90 expression was limited to MSC^{GFP} further supporting a more MDA-MB-231-like phenotype of the two hybrid populations MDA-hyb3 and MDA-hyb4.

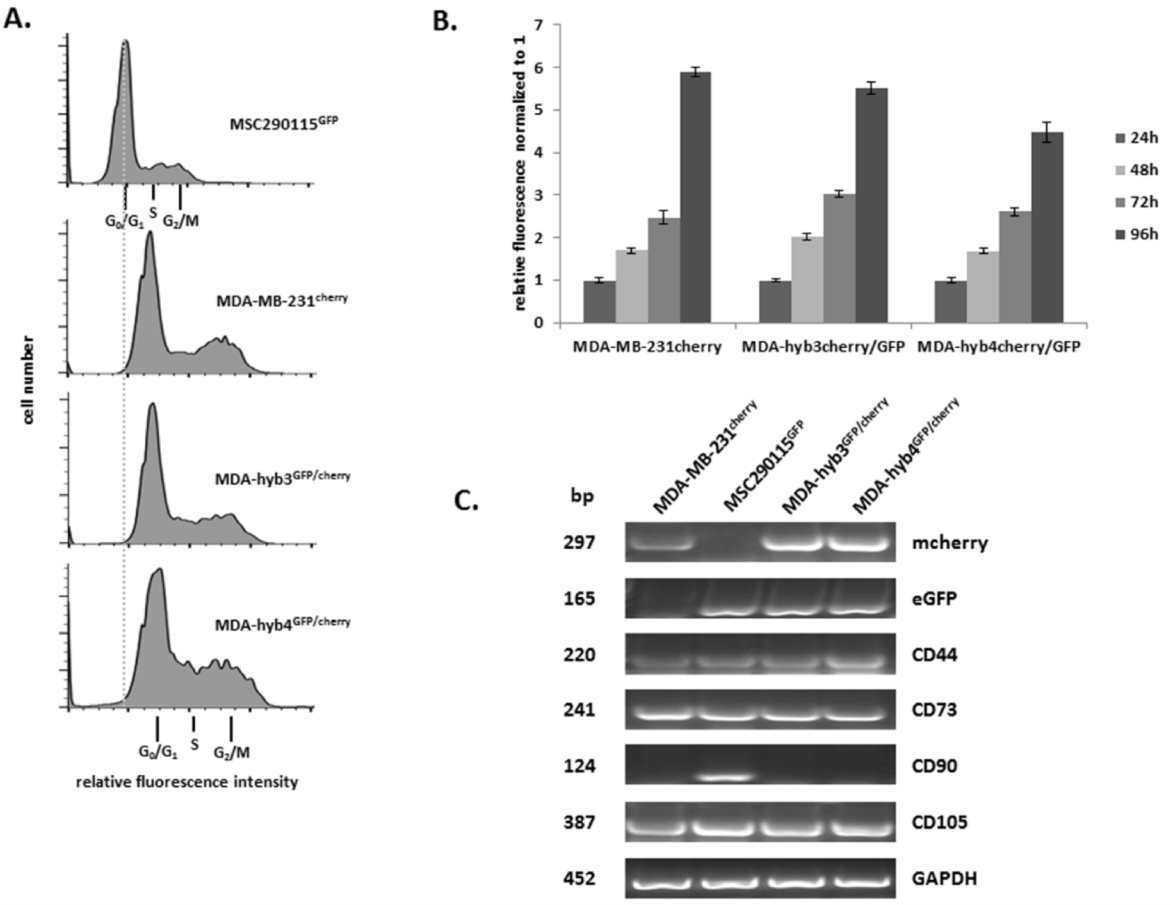


Figure 5. (**a**) Cell cycle analysis of MDA-hyb3 and MDA-hyb4 in contrast to the parental cell populations revealed hyperdiploidy of both hybrid cell populations. (**b**) Proliferation of hybrid cell lines was examined in a fluoroskan assay for 24h up to 96h and compared to proliferation capacity of the parental MDA-MB-231^{cherry} breast cancer cells. Data represent the mean ± s.d. (n=10) whereby fluorescence values after 24h were set to 1. (**c**) PCR analysis was performed for mcherry, eGFP and MSC stem-like markers CD44, CD73, CD90 and CD105. Expression of parental MDA-MB-231^{cherry} and MSC290115^{GFP} populations was compared to the two hybrid populations. Expression levels of GAPDH served as control.

Together, these data suggested the isolation of two new cell populations after spontaneous fusion of MSC290115^{GFP} with MDA-MB-231^{cherry} with congruous proliferative capacity and cell cycle pattern as compared to the parental MDA-MB-231^{cherry}.

According to the similar proliferation rate of MDA-hyb3 and MDA-MB-231, these cell populations were compared for their capability to develop in vivo tumors and potential organ metastases in NODscid mice (Fig, 6). While MDA-MB-231^{GFP} cells promoted subcutaneous tumors with an average weight of 1,356mg within 48 days, this tumor development was significantly delayed in MDA-hyb3-induced tumors reaching an average weight of 1,221mg after 70 days (Fig. 6A). Likewise, the MDA-MB-231^{GFP} cell-associated tumor volume of about 781 mm^3 was paralleled by a tumor volume of 14 mm^3 in MDA-hyb3-induced tumors after 48d (Fig. 6B, inserted bar diagram). Thereafter, the MDA-hyb3 tumors progressively increased to an average volume of 478mm^3 after 70d (Fig. 6B). Distant organ metastases were detectable in all investigated organs in MDA-MB-231^{GFP}-induced tumors after 48d. In contrast, double fluorescing cells of MDA-hyb3 remained undetectable in

lung and kidney after 70d. Moreover, metastatic cells in the heart were identified only in 1 out of 3 MDA-hyb3 tumor mice (Fig. 6C). Together, these data indicated a retarded tumor development with reduced formation of metastases in MDA-hyb3 cells when compared to the parental MDA-MB-231^{GFP} cells.

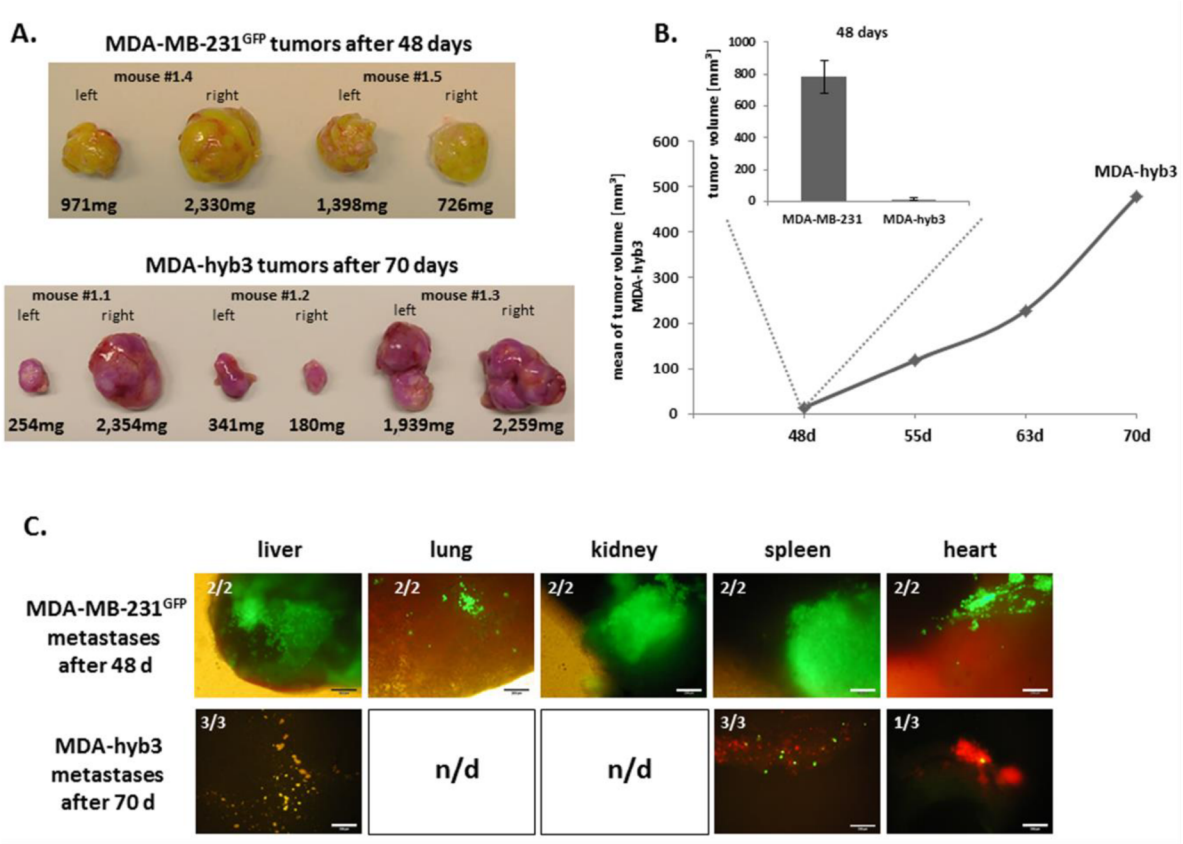


Figure 6. (**a**) MDA-MB-231^{GFP} cells-induced tumors in both flanks of two NODscid mice were harvested after 48d whereas MDA-hyb3-induced tumors from three mice were collected after 70d displaying a similar average tumor size. (**b**) Progressively increasing tumor volumes of MDA-hyb3-induced tumors were monitored and evaluated from 48d to 70d when the tumor volume reached an average size of that observed for parental MDA-MB-231^{GFP} cells after 48d (inserted bar diagram). (**c**) Formation and quantification of distant organ metastases in representative fluorescence pictures is demonstrated for MDA-MB-231^{GFP} cells after 48d as compared to MDA-hyb3-mediated metastases after 70d. n/d = not detectable. Bars represent 200μm.

4. Discussion

A variety of mechanisms contribute to indirect interaction of breast cancer cells with MSC including release of soluble factors (cytokines, chemokines, enzymes, metabolites), microvesicles and exosomes, which can induce among others cancer cell alteration and a retrodifferentiation program for potential formation of cancer stem-like cells [29, 30]. Moreover, interaction of breast cancer cells with populations of perivascular regions such as pericytes and MSC can also contribute to tumor cell dormancy [31]. Furthermore, during indirect interaction with ovarian cancer cells, human MSC were suggested to promote tumor growth and support proliferation and survival [32]. Indeed, co-culture of different breast and ovarian carcinoma cells with MSC is associated both, in vitro and in vivo with progressive reduction of MSC by overgrowing cancer cells while intercellular communication of MSC with these cancer cells promotes mutual functional alteration including enhanced tumor growth and elevated metastatic potential [20, 33].

Alternatively, more close and direct interaction of cancer cells with adjacent neighboring cell populations such as immune cells, adipose tissue cells, endothelial cells or local tissue-associated MSC involve nanotube formation, trogocytosis, or cell fusion including cannibalism or entosis. Spontaneous or accidental cell fusion between neoplastic breast epithelial cells and MSC represents a rare event while the fusion process itself occurs rapidly within a few minutes [18]. Successful cell fusion with the generation of viable hybrid cells requires a coordinated chromosomal restructure and a coherent nuclear rearrangement and reprogramming [34, 35]. Otherwise, cell fusion and associated post-fusion selection processes can generate aneuploidy, chromosomal instability, and DNA damage, all of which cause multiple genetic changes including genetic aberrations and a potentially neoplastic development [6, 36]. Indeed, previous work suggested that natural progression of cancer is accompanied by cell fusion between cancer cells and non-tumorigenic adjacent cells leading to massive genomic alterations, enhanced clonal diversity and thus, increasing tumor heterogeneity [37]. Consequently, detection of mcherry and GFP double fluorescing breast cancer fusion cells in vivo add to the tumor heterogeneity and may contribute to facilitated development of distant tissue metastases which is also supported by the findings of Chitwood et al. [38].

The generation of new cancer hybrid populations in breast cancer [4, 18, 19, 38] and ovarian cancer [39] was documented by cellular fusion with interacting MSC. In addition, previous work has demonstrated that spontaneous fusion of certain human breast epithelial with breast cancer cells generated five different hybrid populations exhibiting cancer stem cell-like properties [40]. Although distinct stem cell markers are also acquired during heterotypic fusion of breast or ovarian cancer cells with MSC, the resulting hybrid populations displayed altered or reduced tumorigenic potential. While recent studies demonstrated enhanced tumor growth and formation of metastases in fusion populations of MDA-MB-231 breast cancer with human MSC051212, termed MDA-hyb1 and MDA-hyb2, these tumor hybrid populations had acquired increased sensitivity to various chemotherapeutic compounds in contrast to their parental breast cancer counterparts [19]. The presently new established MDA-hyb3 and MDA-hyb4 breast cancer hybrid populations were derived after fusion with MSC from a different donor (MSC290115) whereby MDA-hyb3 cells displayed retarded tumor development and reduced metastatic potential unlike the parental MDA-MB-231 cells. These findings indicate overall increased tumor heterogeneity, however, the involvement of MSC in these fusion processes reflects certain physiologically beneficial contributions e.g. by elevated drug response [41] and/or reduced tumorigenicity of the cancer hybrid cells. Indeed, this conclusion is also supported by in vivo data obtained with the SK-OV-3 / MSC fused ovarian cancer hybrid populations SK-hyb1 and SK-hyb2 demonstrating that the ovarian cancer fusion cells had completely lost the capacity of tumor formation [39]. While molecular signaling mechanims remain to be elucidated, these findings further underscore the heterogenic and diverse functionalities of in vivo MSC during tumor development by direct and/or indirect interaction including fusion with cancer cells.

Author Contributions: CM, JvO and RH performed the experiments. CM and RH drafted the manuscript. RH conceived and oversaw the study. All authors critically read and approved the final manuscript.

Acknowledgments: The authors are grateful to colleagues from Hannover Medical School including Dr. Matthias Ballmaier (FACS core unit) for cell separation. This work was supported by a grant from the Erich und Gertrud Roggenbuck-Stiftung for Cancer Research to Ralf Hass.

Conflicts of Interest: The authors declare no conflict of interest.

References

1. Aguilar, P.S., Baylies, M.K., Fleissner, A., Helming, L., Inoue, N., Podbilewicz, B., Wang, H., and Wong, M. Genetic basis of cell-cell fusion mechanisms. *Trends Genet.* **2013**, *29*, 427-37.
2. Freeman, B.T., Jung, J.P., and Ogle, B.M., Single-cell RNA-seq reveals activation of unique gene groups as a consequence of stem cell-parenchymal cell fusion. *Sci Rep* **2016**, *6*, 23270.

3. Mondal Roy, S. and Sarkar, M., Membrane fusion induced by small molecules and ions. *J Lipids* **2011**, *2011*, 528784.
4. Noubissi, F.K., Harkness, T., Alexander, C.M., and Ogle, B.M., Apoptosis-induced cancer cell fusion: a mechanism of breast cancer metastasis. *FASEB J*. **2015**, *29*, 4036-45.
5. Duelli, D. and Lazebnik, Y., Cell fusion: a hidden enemy? *Cancer Cell*. **2003**, *3*, 445-8.
6. Ogle, B.M., Cascalho, M., and Platt, J.L., Biological implications of cell fusion. *Nat Rev Mol Cell Biol* **2005**, *6*, 567-75.
7. Rappa, G., Mercapide, J., and Lorico, A., Spontaneous formation of tumorigenic hybrids between breast cancer and multipotent stromal cells is a source of tumor heterogeneity. *Am J Pathol* **2012**, *180*, 2504-15.
8. Sottile, F., Aulicino, F., Theka, I., and Cosma, M.P., Mesenchymal stem cells generate distinct functional hybrids in vitro via cell fusion or entosis. *Sci Rep* **2016**, *6*, 36863.
9. Caplan, A.I., Mesenchymal stem cells. *J Orthop Res* **1991**, *9*, 641-50.
10. Friedenstein, A. and Kuralesova, A.I., Osteogenic precursor cells of bone marrow in radiation chimeras. *Transplantation* **1971**, *12*, 99-108.
11. Bianco, P., "Mesenchymal" stem cells. *Annu Rev Cell Dev Biol* **2014**, *30*, 677-704.
12. Hass, R., Kasper, C., Bohm, S., and Jacobs, R., Different populations and sources of human mesenchymal stem cells (MSC): A comparison of adult and neonatal tissue-derived MSC. *Cell Commun Signal* **2011**. *9*, 12.
13. Phinney, D.G., Building a consensus regarding the nature and origin of mesenchymal stem cells. *J Cell Biochem Suppl* **2002**, *38*, 7-12.
14. Pittenger, M.F., Mackay, A.M., Beck, S.C., Jaiswal, R.K., Douglas, R., Mosca, J.D., Moorman, M.A., Simonetti, D.W., Craig, S., and Marshak, D.R., Multilineage potential of adult human mesenchymal stem cells. *Science* **1999**, *284*, 143-7.
15. Sasaki, M., Abe, R., Fujita, Y., Ando, S., Inokuma, D., and Shimizu, H., Mesenchymal stem cells are recruited into wounded skin and contribute to wound repair by transdifferentiation into multiple skin cell type. *J Immunol* **2008**, *180*, 2581-7.
16. Ghajar, C.M., Kachgal, S., Kniazeva, E., Mori, H., Costes, S.V., George, S.C., and Putnam, A.J., Mesenchymal cells stimulate capillary morphogenesis via distinct proteolytic mechanisms. *Exp Cell Res* **2010**, *316*, 813-25.
17. De Miguel, M.P., Fuentes-Julian, S., Blazquez-Martinez, A., Pascual, C.Y., Aller, M.A., Arias, J., and Arnalich-Montiel, F., Immunosuppressive properties of mesenchymal stem cells: advances and applications. *Curr Mol Med* **2012**, *12*, 574-91.
18. Melzer, C., von der Ohe, J., and Hass, R., In Vitro Fusion of Normal and Neoplastic Breast Epithelial Cells with Human Mesenchymal Stroma/Stem Cells Partially Involves Tumor Necrosis Factor Receptor Signaling. *Stem Cells* **2018**.
19. Melzer, C., von der Ohe, J., and Hass, R., Enhanced metastatic capacity of breast cancer cells after interaction and hybrid formation with mesenchymal stroma/stem cells (MSC). *Cell Commun Signal* **2018**, *16*, 2.
20. Yang, Y., Otte, A., and Hass, R., Human mesenchymal stroma/stem cells exchange membrane proteins and alter functionality during interaction with different tumor cell lines. *Stem Cells Dev* **2015**, *24*, 1205-22.
21. Melzer, C., von der Ohe, J., and Hass, R., Concise Review: Crosstalk of Mesenchymal Stroma/Stem-Like Cells with Cancer Cells Provides Therapeutic Potential. *Stem Cells* **2018**.
22. Shilagardi, K., Li, S., Luo, F., Marikar, F., Duan, R., Jin, P., Kim, J.H., Murnen, K., and Chen, E.H., Actin-propelled invasive membrane protrusions promote fusogenic protein engagement during cell-cell fusion. *Science* **2013**, *340*, 359-63.
23. Mi, S., Lee, X., Li, X., Veldman, G.M., Finnerty, H., Racie, L., LaVallie, E., Tang, X.Y., Edouard, P., Howes, S., Keith, J.C., Jr., and McCoy, J.M., Syncytin is a captive retroviral envelope protein involved in human placental morphogenesis. *Nature* **2000**, *403*, 785-9.
24. Larsson, L.I., Bjerregaard, B., Wulf-Andersen, L., and Talts, J.F., Syncytin and cancer cell fusions. *ScientificWorldJournal* **2007**, *7*, 1193-7.
25. Majore, I., Moretti, P., Hass, R., and Kasper, C., Identification of subpopulations in mesenchymal stem cell-like cultures from human umbilical cord. *Cell Commun Signal* **2009**, *7*, 6.

26. Geran, R.I., Greenberg, N.H., Macdonald, M.M., and Abbott, B.J., Modified protocol for the testing of new synthetics in the L1210 lymphoid leukemia murine model in the DR&D program, DCT, NCI. *Natl Cancer Inst Monogr* **1977**, *45*, 151-3.
27. Otte, A., Rauprich, F., Hillemanns, P., Park-Simon, T.W., von der Ohe, J., and Hass, R., In vitro and in vivo therapeutic approach for a small cell carcinoma of the ovary hypercalcaemic type using a SCCOHT-1 cellular model. *Orphanet J Rare Dis* **2014**, *9*, 126.
28. Bertram, C. and Hass, R., Cellular senescence of human mammary epithelial cells (HMEC) is associated with an altered MMP-7/HB-EGF signaling and increased formation of elastin-like structures. *Mech Ageing Dev* **2009**, *130*, 657-69.
29. Melzer, C., Yang, Y., and Hass, R., Interaction of MSC with tumor cells. *Cell Commun Signal* **2016**, *14*, 20.
30. Ungefroren, H., Sebens, S., Seidl, D., Lehnert, H., and Hass, R., Interaction of tumor cells with the microenvironment. *Cell Commun Signal* **2011**, *9*, 18.
31. Ghajar, C.M., Peinado, H., Mori, H., Matei, I.R., Evason, K.J., Brazier, H., Almeida, D., Koller, A., Hajjar, K.A., Stainier, D.Y., Chen, E.I., Lyden, D., and Bissell, M.J., The perivascular niche regulates breast tumour dormancy. *Nat Cell Biol* **2013**, *15*, 807-17.
32. McLean, K., Gong, Y., Choi, Y., Deng, N., Yang, K., Bai, S., Cabrera, L., Keller, E., McCauley, L., Cho, K.R., and Buckanovich, R.J., Human ovarian carcinoma-associated mesenchymal stem cells regulate cancer stem cells and tumorigenesis via altered BMP production. *J Clin Invest* **2011**, *121*, 3206-19.
33. Yang, Y., Bucan, V., Baehre, H., von der Ohe, J., Otte, A., and Hass, R., Acquisition of new tumor cell properties by MSC-derived exosomes. *Int J Oncol* **2015**, *47*, 244-52.
34. Palermo, A., Doyonnas, R., Bhutani, N., Pomerantz, J., Alkan, O., and Blau, H.M., Nuclear reprogramming in heterokaryons is rapid, extensive, and bidirectional. *FASEB J* **2009**, *23*, 1431-40.
35. Yamanaka, S. and Blau, H.M., Nuclear reprogramming to a pluripotent state by three approaches. *Nature* **2010**, *465*, 704-12.
36. Berndt, B., Zanker, K.S., and Dittmar, T., Cell fusion is a potent inducer of aneuploidy and drug resistance in tumor cell/ normal cell hybrids. *Crit Rev Oncog* **2013**, 18, 97-113.
37. Searles, S.C., Santosa, E.K., and Bui, J.D., Cell-cell fusion as a mechanism of DNA exchange in cancer. *Oncotarget* **2018**, *9*, 6156-6173.
38. Chitwood, C.A., Dietzsch, C., Jacobs, G., McArdle, T., Freeman, B.T., Banga, A., Noubissi, F.K., and Ogle, B.M. Breast tumor cell hybrids form spontaneously in vivo and contribute to breast tumor metastases. *APL Bioengineering* **2018**, 2, 031907.
39. Melzer, C., von der Ohe, J., and Hass, R., MSC stimulate ovarian tumor growth during intercellular communication but reduce tumorigenicity after fusion with ovarian cancer cells. *Cell Commun Signal* **2018**, 16, 67.
40. Gauck, D., Keil, S., Niggemann, B., Zanker, K.S., and Dittmar, T., Hybrid clone cells derived from human breast epithelial cells and human breast cancer cells exhibit properties of cancer stem/initiating cells. *BMC Cancer* **2017**, 17, 515.
41. Kucerova L, Durinikova E, Toro L, Cihova M, Miklikova S, Poturnajova M, Kozovska Z, Matuskova M. Targeted antitumor therapy mediated by prodrug-activating mesenchymal stromal cells. *Cancer Lett.* **2017**, 408, 1-9

3. Summary and discussion of results

Human life begins by fusion of a sperm cell with an egg and is continued by more cell fusions including the fusion of fetal trophoblasts to syncytiotrophoblasts during the placenta formation, the fusion of myoblasts to multinucleated muscle fibers, or the generation of giant cells by macrophage fusion. As this merging of cell membranes occurs under physiological conditions during development, cell fusion processes must be tightly regulated [181, 212]. Despite the crucial importance of physiological fusion events, the formation of hybrid cells under pathophysiological conditions and during disease plays an equally relevant role. Especially the role of cancer cell autofusion involving two cancer cells as well as heterofusion of cancer cells with non-cancer cells during tumor development and tumorigenesis is of interest. Although previous work identified some fusogenic factors including syncytin-1 and -2, OC- and DC-stamp or soluble cytokines [169, 195-197, 200], firstly, the molecular mechanisms underlying cancer cell fusion still need to be unraveled and secondly, the role of the generated hybrid cells by cell fusion in conjunction with their characteristics and functions needs to be further investigated to estimate their impact on tumor heterogeneity.

The focus of this thesis therefore addresses the role of MSC during tumor development by their fusion with cancer cells and aims to unveil distinct factors that mediate cell fusion events.

3.1 MSC fuse with breast (and ovarian) cancer cells in vitro and in vivo

The fusion of MSC with cancer cells has been demonstrated in several tumor entities like breast, ovarian, gastric and lung cancer in vitro [158, 161-164]. However, there exist various methods to observe cell fusion events whereby all methods use fluorescence-based systems to track MSC-cancer interactions comprising Cre-LoxP recombination techniques, bimolecular fluorescence complementation, or the distinct fluorescent labeling of interacting cell partners [161, 163, 188, 213]. In this doctoral thesis, stably lentiviral transduced MSC with eGFP and cancer cells with mCherry were used for hybrid cell formation studies. Of interest, cell fusion events between GFP-labeled MSC and cherry-labeled benign MCF10A or red dye-labeled normal HMEC were documented by time lapse fluorescence video microscopy. Membrane fusion is thought to proceed in three steps: inter membrane contact, lipid mixing with pore opening and mixing of inner contents [214]. Although interactions between MSC and cancer cells contain various direct and indirect types taking place over longer periods of time [143,

158, 161], the actual hybrid cell formation whereby MSC membranes fused with normal and neoplastic breast epithelial membranes was observed within a very short time frame, mainly within less than 5 minutes suggesting merging of two interacting membranes as rapid event. Cell fusion may be a result of cannibalism or so-called entosis which has been demonstrated by breast cancer cells engulfing MSC with subsequent degradation of the entosed cell including the genome [215]. However, entosis can be excluded from the observed events since time lapse fluorescence video microscopy documented a homogenous distribution of GFP and cherry which was later verified by the characterization of different hybrid clones that acquired genomic parts from both parental cell partners. Moreover, the time frame of cell fusion is in concordance with a recent publication that quantified cell fusion products albeit among lymphocytes between 3 and 8 minutes after stimulation with PEG (polyethylene glycol) [216]. In addition to the fusion of normal and neoplastic breast epithelial cells with MSC, co-cultures of MSC with various malignant breast cancer cells including HBCEC, MCF7 and MDA-MB-231, or with ovarian carcinoma cells like SK-OV-3 resulted in spontaneous hybrid cell formation as well substantiating the general occurrence of MSC-cancer cell fusion. Since these events have been shown in vitro in a 2D culture model which might not necessarily reflect the in vivo situation, co-injection of GFP-labeled MSC with cherry-labeled MDA-MB-231 breast cancer cells in NODscid mice demonstrated the appearance of dual fluorescent cells in a 3D approach. Of interest, the percentage of 3D in vivo fusion events was similar to the observed 2D in vitro fusion products accompanied by a progressive decline of MSC and by tremendously overgrowing cancer cells. Thus, hybrid cell numbers were only detectable in the presence of MSC. These data are in line with previous reports that were able to record in vivo fusion events, for instance the fusion of mouse stromal cells with breast cancer cells, macrophages with tumor cells, the fusion of MSC with mouse cells in the murine heart or the fusion of melanoma cells and non-cancer cells [217-220]. Likewise, a very recent publication proposed the occurrence of MSC murine mammary cancer cell fusion in vivo with a higher number of hybrids in metastases [221].

Consequently, these findings of MSC-cancer cell fusion which takes place in vitro and in vivo substantiate the contribution of MSC to tumor heterogeneity. To what extent these intimate direct interactions impact tumor growth and tumorigenesis was further investigated.

3.2 MSC promote ovarian tumor growth in vivo

Due to the fact that MSC are involved in tissue repair and wound healing, MSC are also attracted and migrate towards tumors which can be regarded as invasive tissues causing an inflammatory microenvironment [94, 143].

In co-cultures in vitro, MSC promote and enhance proliferative potential of breast and ovarian tumor cells [158, 222]. In addition, previous work also reported growth-inhibitory effects of MSC on cancer cell proliferation [223]. Of interest, one publication demonstrated on the one hand inhibitory effects of MSC on various tumor cell lines of hematopoietic and non-hematopoietic origin in vitro and on the other hand the MSC-mediated promotion on tumor growth in vivo proposing the ability of MSC to contribute to a cancer stem cell niche formation in vivo facilitating cancer cell proliferation [157].

In the present thesis, in vivo experiments of co-injected MSC with ovarian SK-OV-3 carcinoma cells resulted in elevated primary tumor growth accompanied by metastasis formation in contrast to injection of ovarian cancer cells alone. These data are substantiated by the presence of MSC in human ovarian tumor samples increasing tumor growth whereby these MSC exhibited altered properties and were therefore described as carcinoma-associated MSC (CA-MSC). Moreover, CA-MSC were suggested to promote tumor growth by raising the number of cancer stem cells [224]. Since in vivo results showed a progressive decrease of MSC with an overgrowing of cancer cells, it seems likely that co-injected MSC boosted ovarian tumor growth only initially via different types of interaction.

Likewise, explant SK-OV-3 tumors of mono- and MSC co-cultures exhibited higher chemoresistance in contrast to original SK-OV-3 cultures. In particular, 1µM of taxol (paclitaxel) which is used in combination with cis- or carboplatin for the treatment of ovarian cancer patients showed significant inhibitory effects on original SK-OV-3 in contrast to reduced effects on explant cultures. Protection of MSC on ovarian carcinoma cells during drug treatment was recently observed with the small cell carcinoma of the ovary hypercalcemic type (SCCOHT-1) [225]. Furthermore, during carboplatin treatment elevation in IC50 of ovarian cancer cell lines SK-OV-3, OVCAR-3 and IGROV-1 was achieved in the presence of MSC [226] and CA-MSC promoted chemoresistance to CAOV3 ovarian carcinoma cells [227] substantiating protective effects of MSC on ovarian tumor cells. Concomitant with MSC-mediated enhanced ovarian cancer proliferation these data claim a tumor-promoting role of MSC.

3.3 MSC-cancer cell fusion represents a rare event

Apart from the actual fusion process which proceeded within less than 5 minutes, the appearance of dual fluorescent cells was already observed after 24h after co-culturing (MSC with HMEC, MCF10A, MCF7, HBCEC, or MDA-MB-231, respectively) which is in accordance with a variety of other studies [158, 161, 162, 188]. Interestingly, the amount of dual fluorescent cells that was analyzed between 24h and 96h consisted of less than 2 % strengthening the rareness of this event. Similar percentages were gained in other studies with a quantification after 24h and 48h, respectively. Spontaneous fusion of gastric cancer cell with human umbilical cord-derived MSC showed around 1.1 % [162] and fusion of breast cancer cell lines with breast epithelial cells resulted in less than 0.5 % [213]. However, both studies could increase the amount by PEG to more than 4% in MSC-gastric cancer fusion and about 2% in breast cancer-breast epithelial cell fusion. Older publications reported a fusion frequency in tumors with around 1% [228-230].

Nevertheless, the percentage of dual fluorescent cells in this thesis was time-dependent and much higher in benign MCF10A-MSC co-cultures in contrast to malignant MDA-MB-231-MSC co-cultures, though contrary to a recent publication [188]. Time-dependency can be explained by the initial cell density of co-culturing. As observed in time lapse fluorescence video microcopy MSC and breast cancer cells need to be in close proximity for a potential cell fusion. Starting with a very low cell density, co-cultures will need more time to come into close proximity in comparison to co-cultures with a high cell density already harboring the requirement for a potential direct interaction. Thus, a medium cell density was chosen to be able to detect dual fluorescent cells after 24h. From 24h up to 96h the number of hybrid cells was continuously growing, however, the parental cell types were proliferating much faster in an exponential manner giving an explanation for the overall numerical decrease in the percentage of hybrid cells after 72h due to the ability of only a small fraction of hybrid cells to proliferate. The difference of hybrid cell formation between benign (2%) and malignant (<0.5%) co-cultures may result from various sources and has not been addressed in other publications so far. Since all co-cultures were incubated with MSC, the discrepancy likely originates from the diverse breast cancer cell partners (MCF10A, MDA-MB-231, MCF7). Based on lacking knowledge of the mechanisms underlying cell fusion, it can only be speculated why co-cultured benign MCF10A cells give rise to higher numbers of hybrid cells in contrast to malignant breast cancer cells. Aside the distinct soluble factors secretion profile which might stimulate MSC in various ways and the differential expression of potential

fusogens also represented by e.g. more than 4,000 up- and 3,000 downregulated transcripts in MDA-MB-231 versus MCF10A by microarray analysis, one possible explanation lies in the karyotype of the breast cancer cells. While MCF10A cells are nearly diploid with 48 chromosomes, MDA-MB-231 are near triploid and MCF7 are even hypertriploid to hypotetraploid suggesting already the possibility of previous fusion events. Although cancer is caused by the accumulation of mutations and hallmarks of cancer include sustaining proliferative capacity, evasion of apoptosis, angiogenesis, invasion and metastasis [231], previous work proposed cell fusion as another cause for tumor development since it induces mutations and aneuploidy by genomic instability [232]. Thus, regarding aneuploid MDA-MB-231 and MCF7 cells as populations that putatively arose by cellular fusion, neoplastic MCF10A cells with a near diploid karyotype are likely in a more fusion permissive state representing the pre-stage of cancer development. This hypothesis also provides an explanation for the distinct amounts of hybrid cell formation in autofusion which was the highest among MSC, followed by MCF10A and MDA-MB-231 and no detectable autofusion events among MCF7. The large disparity between hetero- and autofusion being 10- to 50-fold higher in hetero co-cultures indicates the involvement of distinct molecular signals between the fusion partners.

3.4 MSC-cancer cell fusion gives rise to more aggressive, but also to non-tumorigenic hybrid cells

In contrast to indirect interactions such as the exchange of soluble factors and extracellular vesicles and direct interactions like the transfer of small molecules and organelles via gap junctions and nanotubes, cellular fusion enables the exchange of DNA possibly leading to an altered genotype with newly acquired functional properties contributing to elevated tumor heterogeneity [220].

A repeated fluorescence-activated cell sorting (FACS) of these dual fluorescent cells followed by single cell cloning resulted in the isolation of distinct hybrid cell clones which were named according to their parental cell types. MDA-hyb1, MDA-hyb2, MDA-hyb3 and MDA-hyb4 were generated from fusion of MSC^{GFP} with malignant MDA-MB-231^{cherry} breast cancer cells whereby hyb1 and hyb2 were produced from $MSC051212^{GFP}$ and hyb3 and hyb4 from $MSC290115^{GFP}$, respectively. The two hybrid clones MCF10A-hyb1 and MCF10A-hyb2 arose from fusion of neoplastic $MCF10A^{cherry}$ with $MSC060616^{GFP}$. Hybrid cell formation

between SK-OV-3^{cherry} and MSC081113^{GFP} later led to SK-hyb1 and SK-hyb2. Interestingly, the isolation and expansion was accompanied by a post-fusion selection process involving nuclear fusion followed by chromosomal rearrangement from hetero- to synkaryons (loss and re-sorting of chromosomes) and cell death of clones due to chromosomal instability, DNA damage and aneuploidy [233-235]. This is demonstrated by the high number of more than 5,400 clones which were derived after FACS of co-cultures between MDA-MB-231^{cherry} and MSC290115^{GFP}. Indeed, only a small amount of these initially sorted clones was able to proliferate whereby the rest failed to transit from hetero- to synkaryons and was unable to overcome chromosomal rearrangements, respectively. These data are supported by the hypothesis of Duelli and Lazebnik who suggested that the majority (99%) of fusion cells will die or remain in a quiescent state whereas only 1% of hybrid cells will proliferate and exhibit new properties probably encompassing metastatic potential, a higher proliferation rate and drug resistance [236]. Thus, it can be proposed that cell fusion implicates a two-step fusion process that starts with a merging of two adjacent membranes leading to heterokaryons with multiple distinct nuclei (≥2) [234]. In a post-fusion selection process merging of the 2 nuclei from both parental cell types results in mononuclear hybrid cells that are able to proliferate. Remaining heterokaryons do not proliferate and keep multiple nuclei [234]. Therefore, nuclei after nuclear fusion consisted of a double chromosomal set 4n (MCF10A-MSC fusion) or after fusion of MSC with e.g. MDA-MB-231 of 5n. Consequently, a rearrangement of chromosomes gave rise to unique new clones with properties of both parental cell types which excluded the possibility of a total loss of one nucleus and rather suggested a mixture and rearrangement of chromosomes after nuclear fusion. Indeed, the various established hybrid cell lines exhibited an aneuploid karyotype detected by cell cycle analysis, STR fragment analysis and karyotype analysis. However, the karyotype did not equal the sum of both fused nuclei. All MDA-hybrid cell lines (hyb1 to hyb4) and SK-hyb1 demonstrated a pronounced shift to higher fluorescence intensities which correlates to an increased DNA content as compared to the parental diploid MSC rendering these hybrids pseudo-triploid. Of interest, tetraploidy of normal diploid cells was associated with a more malignant cell type [237] strengthening the hypothesis that cancer can arise from cell fusion, but also that aneuploid hybrid cells can promote tumor development.

Moreover, STR fragment analysis of MDA-hyb1 and -hyb2 displayed the acquisition of the MSC-derived XY configuration further substantiating the genomic generation of hybrid cells with characteristics from both parental cell populations and excluding the possibility of entosis [215]. Similar results were observed by microarray analysis of MCF10A-hyb1

and -hyb2 that showed expression levels of X- and Y-linked transcripts. The fact that the various hybrid cell populations were obtained by initial cell fusion was further confirmed by the expression of MSC-derived GFP and cancer cell-derived cherry except for MDA-hyb1 and SK-hyb1 which lost the eGFP gene during post-fusion selection. As a consequence, it was not surprising that the hybrid clones acquired certain MSC-specific stemness markers such as CD73, CD90 and CD105 equipping these clones with mesenchymal traits. These more mesenchymal characteristics potentially facilitate migration and invasion of the hybrid populations which are prerequisite for metastatic spread like in the course of EMT [238-240] as for instance confirmed with MDA-hyb1 and -hyb2.

With regard to the role of MSC on tumorigenesis, plenty of publications investigated the proliferative capacity of tumor cells in co-cultures with MSC. Whereas the majority of studies attributes a tumor growth promoting role to MSC on breast and ovarian cancer cell lines [145, 146, 158, 163, 222, 241, 242], some reports also indicate tumor inhibitory effects of MSC [148, 223, 243] allocating a dual role to MSC. Albeit to a low percentage, MSC contribute to tumor heterogeneity by fusion with cancer cells accompanied by the formation of hybrid cells with altered properties. To what extent these hybrid cells could impact tumorigenesis was examined by proliferation studies with distinct hybrid cell lines in this thesis. As diverse as data of MSC on cancer cell growth are, proliferation capacity of isolated hybrids is similarly varying. Interestingly, MDA-hyb1 and -hyb2 were proliferating much faster than the parental MDA-MB-231. By contrast, MDA-hyb3 demonstrated little, if any differences in proliferative behavior when compared to MDA-MB-231 while the proliferation rate of MDA-hyb4 was slightly decreased. Reduced proliferative capacity was observed in SK-hyb1 and -hyb2 as well as in MCF10A-hyb1 and -hyb2. Accordingly, fusion of MSC with breast and ovarian cancer cells generates hybrid cells with higher and lower proliferative potential.

Based on previous results announcing the acquisition of higher motility by hybrid cells after fusion of breast cancer cells with MSC [161, 188] and based on microarray analysis of MDA-hyb1 and -hyb2 suggesting metastatic potential, tumorigenicity of MDA-hyb1, -hyb2 and -hyb3 as well as SK-hyb1 and -hyb2 was verified in vivo. The results were in line with in vitro proliferation studies. In contrast to no detectable tumor growth of SK-hyb1 and -hyb2 populations, tumor development of MDA-hyb3 was delayed by more than 20 days when compared to the parental MDA-MB-231. However, MDA-hyb1 and -hyb2 populations significantly enhanced primary tumor growth accompanied by a rapid formation of tumor metastases proposing profound elevation in malignancy and breast cancer metastatic potential

of MDA-hyb1 and -hyb2. These findings coincide with the hypothesis that cancer cell fusion provides an explanation for the cause of metastasis [244]. Moreover, cancer cell fusion has been suggested as mechanism for higher chemoresistance [171, 220, 245] and chemotherapy has been recently correlated to promote cancer cell hybrid formation [246]. Nevertheless, sensitivity to several chemotherapeutics was elevated in MDA-hyb1 and -hyb2 when compared to the parental MDA-MB-231. However, these data can be explained by the molecular mechanism of chemotherapeutics commonly affecting cell division, in particular highly proliferating cells that are in this case represented by hyb1 and hyb2 and to a lesser extent by MDA-MB-231.

The fact that not all, but only a few hybrid cells exhibited increased tumorigenic capacities, raises the question why some fusion products display higher malignancies than the others. Considering that hybrid cells developed from fusion between MSC and various breast and ovarian cancer cell lines followed by nuclear fusion resulting in a mixed genome profile, it is unambiguous that some hybrids are equipped with more mesenchymal characteristics while others have acquired more cancer cell-like properties. With regard to RNA microarray profiling, mRNA expression levels of MDA-hyb1 and -hyb2 were more altered (up- and down-regulated) in comparison to parental MSC than versus MDA-MB-231 suggesting the parental breast cancer cell as leading cell during cellular fusion which is further confirmed by the morphology of MDA-hyb1 and -hyb2 being more epithelial than mesenchymal-like. As opposed to this, SK-hyb2 for instance showed slightly less differences in transcript levels versus MSC than versus ovarian SK-OV-3 cells and exhibited a rather fibroblast-like morphology proposing MSC as leading cell. Thus, it can be speculated that hybrid cells with MSC as leading cell during cellular fusion will display anti-tumorigenic properties possibly accompanied by a downmodulation of proliferation and cell cycle associated genes with a potential senescent phenotype as observed in MCF10A-hyb1 and -hyb2. Consequently, cellular fusion with a cancer leading cell will generate hybrid cells with more tumorigenic and feasible high invasive and metastatic functions. This theory is substantiated by a recent publication whereby less than 1,300 genes were altered between high-tumorigenic hybrids versus parental MDA-MB-231 in contrast to more than 5,300 differentially expressed genes between these hybrids and the parental MSC [161].

Although microarray data of SK-hyb1 assume ovarian cancer SK-OV-3 as leading cell, this hybrid population demonstrated decreased proliferation capacity in vitro with no detectable tumor development in vivo diminishing that theory. Karyotype analysis revealed a

hypertriploid set of chromosomes as compared to diploid MSC and hypodiploid to hypotetraploid SK-OV-3 [247]. However, cell cycle analysis manifested a pronounced shift to an even higher DNA content of SK-hyb1 when compared to parental SK-OV-3. Therefore, this larger set of chromosomes in SK-hyb1 might cause replicative stress giving an explanation for the reduced proliferative potential and the non-tumorigenic properties.

3.5 TNF-α increases neoplastic MCF10A-MSC cell fusion

Certain factors contribute to a fusion-permissive environment including soluble factors, acidic pH and hypoxia [188, 206-211]. Moreover, reorganization of the actin cytoskeleton by adhesion molecules for the generation of membrane protrusions and the accumulation of potential transmembrane fusogens is thought to drive cell fusion [150, 190].

Although the prominent fusogenic proteins syncytin-1 and -2 and the appropriate receptors have been reported in physiological cell fusion events like the generation of syncytiotrophoblasts during the placenta formation [195-197], these fusogenic factors demonstrated little, if any involvement on MCF10A-MSC cell fusion after a double-knockdown (syncytin-1 and ASCT2, syncytin-2 and MFSD2A) assuming differential or additional molecular signaling in pathophysiological fusion of MSC with MCF10A.

Considering the tumor microenvironment which consists of a plethora of soluble factors constantly causing an inflammatory milieu, exogenous levels of the pro-inflammatory cytokine TNF-α increased the cell fusion rate in a dose-dependent manner suggesting an involvement of the appropriate TNF receptors. In particular, TNF receptor 1 (TNFR1) was similarly expressed on normal HMEC, in breast cancer cell lines and on various MSC, and a knock-down of TNFR1 and TNFR2, respectively, by siRNA abolished the pro-fusogenic effect of TNF-α. Of interest, production and release of TNF-α was markedly enhanced in MCF10A as compared to MSC proposing that MCF10A-derived TNF-α stimulates TNFR1 and TNFR2 on MSC for cellular fusion. These data are in accordance with previous findings postulating that MSC respond to TNF-α but are not able to release this pro-inflammatory cytokine [248]. Moreover, TNF-α stimulated MSC were demonstrated to sequester higher levels of chemokines such as CCL2 and CXCL8 [249] and enhance breast cancer metastasis [250]. Taking into account that breast cancer cells in culture are known to lose their ability to sequester endogenous pro-inflammatory cytokines [249], the detected endogenous TNF-α

levels might be even higher in MCF10A, however physiological concentrations of exogenous TNF-α were necessary for cell fusion rate elevation (100U/mL equals 5 ng/mL).

The TNF receptor signaling cascade starts with binding of trimeric TNF-α to mainly TNFR1 inducing a trimerization of this receptor that triggers association of TNFR1-associated death domain protein (TRADD). TRADD in turn can recruit additional adaptor proteins like TRAF2, FADD and RIP to forward activation signals though the apoptotic pathway or the NF-κB pathway [251, 252]. In addition, TNF-α is also able to activate the c-jun N-terminal kinase (JNK1/MAPK8) via TNFR1/2 and TRAF2 [253, 254].

Interestingly, a siRNA-mediated knockdown of TRADD in MSC and MCF10A abolished the TNF-α-mediated elevation in cell fusion substantiating the necessity of TNFR downstream signaling and excluding the possibility that trimerization of the receptors leading to altered structural conformation on the cell surface is sufficient. However, interference with downstream signaling via siRNA knockdown of p65 (RelA) or JNK1 (MAPK8) did not alter TNF-α stimulatory effect on MSC/MCF10A cell fusion indicating the involvement of the apoptotic pathway and / or additional NF-κB signaling with a dimer formation without p65 (RelA). Although the NF-κB pathway leads to anti-inflammatory signals in contrast to the caspase activation ending up in apoptosis, it is even feasible that whenever one of the three pathways is blocked, pro-fusogenic signals are mediated by the two others interfering with each other. These findings are in line with previous results allocating an involvement of apoptosis in MSC-breast cancer cell fusion [188] and proposing that MSC upon TNF-α stimulation (50ng/mL) or hypoxia secrete growth factors (VEGF, HGF, FGF2) by NF-κB, but not by JNK [255].

Although TNF-α elevated the amount of hybrid cells in MSC-MCF10A co-cultures, further pro-inflammatory cytokines may also contribute to this fusion event as previously demonstrated [206-211]. Nevertheless, immune regulatory functions of MSC can interfere with potential fusion signals [115, 256].

Besides TNF-α that has been identified as pro-fusogenic factor for MCF10A cells, further research is needed to elucidate the mechanisms that drive cell fusion between MSC and other breast cancer cells. In particular, the investigation of adhesion proteins together with lipids rafts and the role of the actin cytoskeleton represent promising targets to examine cell fusion [189, 190, 203, 204].

4. Outlook

To better estimate the role of MSC on tumorigenesis, the aim of this thesis was to illuminate molecular mechanisms that drive cell fusion and to characterize various hybrid cells generated by the fusion of MSC with breast and ovarian cancer cells.

The results from this thesis demonstrate the general occurrence of MSC-cancer cell fusion in vitro and in vivo. In consequence of highly malignant but also non-tumorigenic hybrid cell populations, more research is needed to screen a variety of further hybrid clones, also with MSC from more than 2 donors, in order to assess the role of fusion products in tumor development and progression. Considering the extremely aggressive MDA-hyb1 and -hyb2, mechanisms underlying cell fusion need to be further unraveled to get an idea for potential intervention sites. Thus, believing the cancer stem cell model that cancer arises from one aberrant cell and that tumor relapse results from dormant cancer stem cells [257], hybrid cells may potentially entail all properties of a cancer stem cell further strengthening the importance of prospective cancer cell fusion research.

5. References

1. Bray, F., Ferlay, J., Soerjomataram, I., Siegel, R.L., Torre, L.A., and Jemal, A., *Global cancer statistics 2018: GLOBOCAN estimates of incidence and mortality worldwide for 36 cancers in 185 countries.* CA Cancer J Clin, 2018.
2. Ferlay, J., Colombet, M., Soerjomataram, I., Dyba, T., Randi, G., Bettio, M., Gavin, A., Visser, O., and Bray, F., *Cancer incidence and mortality patterns in Europe: Estimates for 40 countries and 25 major cancers in 2018.* Eur J Cancer, 2018.
3. McPherson, K., Steel, C.M., and Dixon, J.M., *ABC of breast diseases. Breast cancer-epidemiology, risk factors, and genetics.* BMJ, 2000. 321(7261): p. 624-8.
4. Hulka, B.S. and Moorman, P.G., *Breast cancer: hormones and other risk factors.* Maturitas, 2008. 61(1-2): p. 203-13; discussion 213.
5. Miki, Y., Swensen, J., Shattuck-Eidens, D., Futreal, P.A., Harshman, K., Tavtigian, S., Liu, Q., Cochran, C., Bennett, L.M., Ding, W., and et al., *A strong candidate for the breast and ovarian cancer susceptibility gene BRCA1.* Science, 1994. 266(5182): p. 66-71.
6. Menes, T.S., Terry, M.B., Goldgar, D., Andrulis, I.L., Knight, J.A., John, E.M., Liao, Y., Southey, M., Miron, A., Chung, W., and Buys, S.S., *Second primary breast cancer in BRCA1 and BRCA2 mutation carriers: 10-year cumulative incidence in the Breast Cancer Family Registry.* Breast Cancer Res Treat, 2015. 151(3): p. 653-60.
7. Wooster, R., Bignell, G., Lancaster, J., Swift, S., Seal, S., Mangion, J., Collins, N., Gregory, S., Gumbs, C., and Micklem, G., *Identification of the breast cancer susceptibility gene BRCA2.* Nature, 1995. 378(6559): p. 789-92.
8. Apostolou, P. and Fostira, F., *Hereditary breast cancer: the era of new susceptibility genes.* Biomed Res Int, 2013. 2013: p. 747318.
9. Ghoncheh, M., Pournamdar, Z., and Salehiniya, H., *Incidence and Mortality and Epidemiology of Breast Cancer in the World.* Asian Pac J Cancer Prev, 2016. 17(S3): p. 43-6.
10. Zeng, H., Zheng, R., Zhang, S., Zou, X., and Chen, W., *Female breast cancer statistics of 2010 in China: estimates based on data from 145 population-based cancer registries.* J Thorac Dis, 2014. 6(5): p. 466-70.
11. Siegel, R.L., Miller, K.D., and Jemal, A., *Cancer Statistics, 2017.* CA Cancer J Clin, 2017. 67(1): p. 7-30.
12. Collaborative Group on Hormonal Factors in Breast, C., *Menarche, menopause, and breast cancer risk: individual participant meta-analysis, including 118 964 women*

with breast cancer from 117 epidemiological studies. Lancet Oncol, 2012. 13(11): p. 1141-51.

13. Breyer, J.Z., Wendland, E.M., Kops, N.L., Caleffi, M., and Hammes, L.S., *Assessment of potential risk factors for breast cancer in a population in Southern Brazil.* Breast Cancer Res Treat, 2018. 169(1): p. 125-131.
14. Abubakar, M., Sung, H., Bcr, D., Guida, J., Tang, T.S., Pfeiffer, R.M., and Yang, X.R., *Breast cancer risk factors, survival and recurrence, and tumor molecular subtype: analysis of 3012 women from an indigenous Asian population.* Breast Cancer Res, 2018. 20(1): p. 114.
15. Elebro, K., Butt, S., Dorkhan, M., Jernstrom, H., and Borgquist, S., *Age at first childbirth and oral contraceptive use are associated with risk of androgen receptor-negative breast cancer: the Malmo Diet and Cancer Cohort.* Cancer Causes Control, 2014. 25(8): p. 945-57.
16. Evans, D.G., Harkness, E.F., Howel, S., Woodward, E.R., Howell, A., and Lalloo, F., *Young age at first pregnancy does protect against early onset breast cancer in BRCA1 and BRCA2 mutation carriers.* Breast Cancer Res Treat, 2018. 167(3): p. 779-785.
17. Jernstrom, H., Lerman, C., Ghadirian, P., Lynch, H.T., Weber, B., Garber, J., Daly, M., Olopade, O.I., Foulkes, W.D., Warner, E., Brunet, J.S., and Narod, S.A., *Pregnancy and risk of early breast cancer in carriers of BRCA1 and BRCA2.* Lancet, 1999. 354(9193): p. 1846-50.
18. Bandera, E.V., Chandran, U., Hong, C.C., Troester, M.A., Bethea, T.N., Adams-Campbell, L.L., Haiman, C.A., Park, S.Y., Olshan, A.F., Ambrosone, C.B., Palmer, J.R., and Rosenberg, L., *Obesity, body fat distribution, and risk of breast cancer subtypes in African American women participating in the AMBER Consortium.* Breast Cancer Res Treat, 2015. 150(3): p. 655-66.
19. Connor, A.E., Baumgartner, R.N., Pinkston, C., and Baumgartner, K.B., *Obesity and risk of breast cancer mortality in Hispanic and Non-Hispanic white women: the New Mexico Women's Health Study.* J Womens Health (Larchmt), 2013. 22(4): p. 368-77.
20. Santen, R.J., Yue, W., and Wang, J.P., *Estrogen metabolites and breast cancer.* Steroids, 2015. 99(Pt A): p. 61-6.
21. Li, C.I., Daling, J.R., Haugen, K.L., Tang, M.T., Porter, P.L., and Malone, K.E., *Use of menopausal hormone therapy and risk of ductal and lobular breast cancer among women 55-74 years of age.* Breast Cancer Res Treat, 2014. 145(2): p. 481-9.

22. Goldhirsch, A., Winer, E.P., Coates, A.S., Gelber, R.D., Piccart-Gebhart, M., Thurlimann, B., Senn, H.J., and Panel, m., *Personalizing the treatment of women with early breast cancer: highlights of the St Gallen International Expert Consensus on the Primary Therapy of Early Breast Cancer 2013.* Ann Oncol, 2013. 24(9): p. 2206-23.
23. Fu, D., Zuo, Q., Huang, Q., Su, L., Ring, H.Z., and Ring, B.Z., *Molecular Classification of Lobular Carcinoma of the Breast.* Sci Rep, 2017. 7: p. 43265.
24. Li, C.I., Anderson, B.O., Daling, J.R., and Moe, R.E., *Trends in incidence rates of invasive lobular and ductal breast carcinoma.* JAMA, 2003. 289(11): p. 1421-4.
25. Zubeldia-Plazaola, A., Ametller, E., Mancino, M., Prats de Puig, M., Lopez-Plana, A., Guzman, F., Vinyals, L., Pastor-Arroyo, E.M., Almendro, V., Fuster, G., and Gascon, P., *Comparison of methods for the isolation of human breast epithelial and myoepithelial cells.* Front Cell Dev Biol, 2015. 3: p. 32.
26. Brenner, A.J., Stampfer, M.R., and Aldaz, C.M., *Increased p16 expression with first senescence arrest in human mammary epithelial cells and extended growth capacity with p16 inactivation.* Oncogene, 1998. 17(2): p. 199-205.
27. Yaswen, P. and Stampfer, M.R., *Molecular changes accompanying senescence and immortalization of cultured human mammary epithelial cells.* Int J Biochem Cell Biol, 2002. 34(11): p. 1382-94.
28. Garbe, J.C., Holst, C.R., Bassett, E., Tlsty, T., and Stampfer, M.R., *Inactivation of p53 function in cultured human mammary epithelial cells turns the telomere-length dependent senescence barrier from agonescence into crisis.* Cell Cycle, 2007. 6(15): p. 1927-36.
29. Stampfer, M.R., Garbe, J., Levine, G., Lichtsteiner, S., Vasserot, A.P., and Yaswen, P., *Expression of the telomerase catalytic subunit, hTERT, induces resistance to transforming growth factor beta growth inhibition in p16INK4A(-) human mammary epithelial cells.* Proc Natl Acad Sci U S A, 2001. 98(8): p. 4498-503.
30. Newbold, R.F., *The significance of telomerase activation and cellular immortalization in human cancer.* Mutagenesis, 2002. 17(6): p. 539-50.
31. Soule, H.D., Maloney, T.M., Wolman, S.R., Peterson, W.D., Jr., Brenz, R., McGrath, C.M., Russo, J., Pauley, R.J., Jones, R.F., and Brooks, S.C., *Isolation and characterization of a spontaneously immortalized human breast epithelial cell line, MCF-10.* Cancer Res, 1990. 50(18): p. 6075-86.
32. Subik, K., Lee, J.F., Baxter, L., Strzepek, T., Costello, D., Crowley, P., Xing, L., Hung, M.C., Bonfiglio, T., Hicks, D.G., and Tang, P., *The Expression Patterns of ER,*

PR, HER2, CK5/6, EGFR, Ki-67 and AR by Immunohistochemical Analysis in Breast Cancer Cell Lines. Breast Cancer (Auckl), 2010. 4: p. 35-41.

33. Santner, S.J., Dawson, P.J., Tait, L., Soule, H.D., Eliason, J., Mohamed, A.N., Wolman, S.R., Heppner, G.H., and Miller, F.R., *Malignant MCF10CA1 cell lines derived from premalignant human breast epithelial MCF10AT cells.* Breast Cancer Res Treat, 2001. 65(2): p. 101-10.
34. Soule, H.D., Vazguez, J., Long, A., Albert, S., and Brennan, M., *A human cell line from a pleural effusion derived from a breast carcinoma.* J Natl Cancer Inst, 1973. 51(5): p. 1409-16.
35. Brooks, S.C., Locke, E.R., and Soule, H.D., *Estrogen receptor in a human cell line (MCF-7) from breast carcinoma.* J Biol Chem, 1973. 248(17): p. 6251-3.
36. Rondon-Lagos, M., Verdun Di Cantogno, L., Marchio, C., Rangel, N., Payan-Gomez, C., Gugliotta, P., Botta, C., Bussolati, G., Ramirez-Clavijo, S.R., Pasini, B., and Sapino, A., *Differences and homologies of chromosomal alterations within and between breast cancer cell lines: a clustering analysis.* Mol Cytogenet, 2014. 7(1): p. 8.
37. Comsa, S., Cimpean, A.M., and Raica, M., *The Story of MCF-7 Breast Cancer Cell Line: 40 years of Experience in Research.* Anticancer Res, 2015. 35(6): p. 3147-54.
38. Gao, Y., Wang, Z., Hao, Q., Li, W., Xu, Y., Zhang, J., Zhang, W., Wang, S., Liu, S., Li, M., Xue, X., Zhang, W., Zhang, C., and Zhang, Y., *Loss of ERalpha induces amoeboid-like migration of breast cancer cells by downregulating vinculin.* Nat Commun, 2017. 8: p. 14483.
39. Iorns, E., Drews-Elger, K., Ward, T.M., Dean, S., Clarke, J., Berry, D., El Ashry, D., and Lippman, M., *A new mouse model for the study of human breast cancer metastasis.* PLoS One, 2012. 7(10): p. e47995.
40. Wang, K., Xie, S., Ren, Y., Xia, H., Zhang, X., and He, J., *Establishment of a bioluminescent MDA-MB-231 cell line for human triple-negative breast cancer research.* Oncol Rep, 2012. 27(6): p. 1981-9.
41. Cailleau, R., Young, R., Olive, M., and Reeves, W.J., Jr., *Breast tumor cell lines from pleural effusions.* J Natl Cancer Inst, 1974. 53(3): p. 661-74.
42. Satya-Prakash, K.L., Pathak, S., Hsu, T.C., Olive, M., and Cailleau, R., *Cytogenetic analysis on eight human breast tumor cell lines: high frequencies of 1q, 11q and HeLa-like marker chromosomes.* Cancer Genet Cytogenet, 1981. 3(1): p. 61-73.

43. Hass, R. and Bertram, C., *Characterization of human breast cancer epithelial cells (HBCEC) derived from long term cultured biopsies.* J Exp Clin Cancer Res, 2009. 28: p. 127.

44. RKI, *Krebs in Deutschland für 2013/2014.* Zentrum für Krebsregisterdaten und Gesellschaft der epidemiologischen Krebsregister in Deutschland E.V. 2017, 2017.

45. Reid, B.M., Permuth, J.B., and Sellers, T.A., *Epidemiology of ovarian cancer: a review.* Cancer Biol Med, 2017. 14(1): p. 9-32.

46. Vang, R., Shih Ie, M., and Kurman, R.J., *Ovarian low-grade and high-grade serous carcinoma: pathogenesis, clinicopathologic and molecular biologic features, and diagnostic problems.* Adv Anat Pathol, 2009. 16(5): p. 267-82.

47. Anglesio, M.S., Wiegand, K.C., Melnyk, N., Chow, C., Salamanca, C., Prentice, L.M., Senz, J., Yang, W., Spillman, M.A., Cochrane, D.R., Shumansky, K., Shah, S.P., Kalloger, S.E., and Huntsman, D.G., *Type-specific cell line models for type-specific ovarian cancer research.* PLoS One, 2013. 8(9): p. e72162.

48. Otte, A., Gohring, G., Steinemann, D., Schlegelberger, B., Groos, S., Langer, F., Kreipe, H.H., Schambach, A., Neumann, T., Hillemanns, P., Park-Simon, T.W., and Hass, R., *A tumor-derived population (SCCOHT-1) as cellular model for a small cell ovarian carcinoma of the hypercalcemic type.* Int J Oncol, 2012. 41(2): p. 765-75.

49. Eichhorn, J.H., Young, R.H., and Scully, R.E., *Primary ovarian small cell carcinoma of pulmonary type. A clinicopathologic, immunohistologic, and flow cytometric analysis of 11 cases.* Am J Surg Pathol, 1992. 16(10): p. 926-38.

50. Friedenstein, A.J., Petrakova, K.V., Kurolesova, A.I., and Frolova, G.P., *Heterotopic of bone marrow. Analysis of precursor cells for osteogenic and hematopoietic tissues.* Transplantation, 1968. 6(2): p. 230-47.

51. Friedenstein, A.J., Piatetzky, S., II, and Petrakova, K.V., *Osteogenesis in transplants of bone marrow cells.* J Embryol Exp Morphol, 1966. 16(3): p. 381-90.

52. Friedenstein, A.J., Chailakhjan, R.K., and Lalykina, K.S., *The development of fibroblast colonies in monolayer cultures of guinea-pig bone marrow and spleen cells.* Cell Tissue Kinet, 1970. 3(4): p. 393-403.

53. Hass, R., Kasper, C., Bohm, S., and Jacobs, R., *Different populations and sources of human mesenchymal stem cells (MSC): A comparison of adult and neonatal tissue-derived MSC.* Cell Commun Signal, 2011. 9: p. 12.

54. Friedenstein, A.J., Gorskaja, J.F., and Kulagina, N.N., *Fibroblast precursors in normal and irradiated mouse hematopoietic organs.* Exp Hematol, 1976. 4(5): p. 267-74.

55. Jarvinen, L., Badri, L., Wettlaufer, S., Ohtsuka, T., Standiford, T.J., Toews, G.B., Pinsky, D.J., Peters-Golden, M., and Lama, V.N., *Lung resident mesenchymal stem cells isolated from human lung allografts inhibit T cell proliferation via a soluble mediator.* J Immunol, 2008. 181(6): p. 4389-96.

56. Garikipati, V.N.S., Singh, S.P., Mohanram, Y., Gupta, A.K., Kapoor, D., and Nityanand, S., *Isolation and characterization of mesenchymal stem cells from human fetus heart.* PLoS One, 2018. 13(2): p. e0192244.

57. Banas, A., Teratani, T., Yamamoto, Y., Tokuhara, M., Takeshita, F., Quinn, G., Okochi, H., and Ochiya, T., *Adipose tissue-derived mesenchymal stem cells as a source of human hepatocytes.* Hepatology, 2007. 46(1): p. 219-28.

58. Li, S., Huang, K.J., Wu, J.C., Hu, M.S., Sanyal, M., Hu, M., Longaker, M.T., and Lorenz, H.P., *Peripheral blood-derived mesenchymal stem cells: candidate cells responsible for healing critical-sized calvarial bone defects.* Stem Cells Transl Med, 2015. 4(4): p. 359-68.

59. Pelekanos, R.A., Sardesai, V.S., Futrega, K., Lott, W.B., Kuhn, M., and Doran, M.R., *Isolation and Expansion of Mesenchymal Stem/Stromal Cells Derived from Human Placenta Tissue.* J Vis Exp, 2016(112).

60. Wang, H.S., Hung, S.C., Peng, S.T., Huang, C.C., Wei, H.M., Guo, Y.J., Fu, Y.S., Lai, M.C., and Chen, C.C., *Mesenchymal stem cells in the Wharton's jelly of the human umbilical cord.* Stem Cells, 2004. 22(7): p. 1330-7.

61. Lavrentieva, A., Hatlapatka, T., Winkler, R., Hass, R., and Kasper, C., *Strategies in umbilical cord-derived mesenchymal stem cells expansion: influence of oxygen, culture medium and cell separation.* BMC Proc, 2011. 5 Suppl 8: p. P88.

62. Lee, O.K., Kuo, T.K., Chen, W.M., Lee, K.D., Hsieh, S.L., and Chen, T.H., *Isolation of multipotent mesenchymal stem cells from umbilical cord blood.* Blood, 2004. 103(5): p. 1669-75.

63. Barlow, S., Brooke, G., Chatterjee, K., Price, G., Pelekanos, R., Rossetti, T., Doody, M., Venter, D., Pain, S., Gilshenan, K., and Atkinson, K., *Comparison of human placenta- and bone marrow-derived multipotent mesenchymal stem cells.* Stem Cells Dev, 2008. 17(6): p. 1095-107.

64. In 't Anker, P.S., Scherjon, S.A., Kleijburg-van der Keur, C., de Groot-Swings, G.M., Claas, F.H., Fibbe, W.E., and Kanhai, H.H., *Isolation of mesenchymal stem cells of fetal or maternal origin from human placenta.* Stem Cells, 2004. 22(7): p. 1338-45.

65. Kern, S., Eichler, H., Stoeve, J., Kluter, H., and Bieback, K., *Comparative analysis of mesenchymal stem cells from bone marrow, umbilical cord blood, or adipose tissue.* Stem Cells, 2006. 24(5): p. 1294-301.

66. Otte, A., Bucan, V., Reimers, K., and Hass, R., *Mesenchymal stem cells maintain long-term in vitro stemness during explant culture.* Tissue Eng Part C Methods, 2013. 19(12): p. 937-48.

67. Kulterer, B., Friedl, G., Jandrositz, A., Sanchez-Cabo, F., Prokesch, A., Paar, C., Scheideler, M., Windhager, R., Preisegger, K.H., and Trajanoski, Z., *Gene expression profiling of human mesenchymal stem cells derived from bone marrow during expansion and osteoblast differentiation.* BMC Genomics, 2007. 8: p. 70.

68. Yang, Y., Melzer, C., Bucan, V., von der Ohe, J., Otte, A., and Hass, R., *Conditioned umbilical cord tissue provides a natural three-dimensional storage compartment as in vitro stem cell niche for human mesenchymal stroma/stem cells.* Stem Cell Res Ther, 2016. 7: p. 28.

69. Conconi, M.T., Burra, P., Di Liddo, R., Calore, C., Turetta, M., Bellini, S., Bo, P., Nussdorfer, G.G., and Parnigotto, P.P., *CD105(+) cells from Wharton's jelly show in vitro and in vivo myogenic differentiative potential.* Int J Mol Med, 2006. 18(6): p. 1089-96.

70. Zhu, Y., Liu, T., Song, K., Fan, X., Ma, X., and Cui, Z., *Adipose-derived stem cell: a better stem cell than BMSC.* Cell Biochem Funct, 2008. 26(6): p. 664-75.

71. Baghaei, K., Hashemi, S.M., Tokhanbigli, S., Asadi Rad, A., Assadzadeh-Aghdaei, H., Sharifian, A., and Zali, M.R., *Isolation, differentiation, and characterization of mesenchymal stem cells from human bone marrow.* Gastroenterol Hepatol Bed Bench, 2017. 10(3): p. 208-213.

72. Kuhbier, J.W., Weyand, B., Radtke, C., Vogt, P.M., Kasper, C., and Reimers, K., *Isolation, characterization, differentiation, and application of adipose-derived stem cells.* Adv Biochem Eng Biotechnol, 2010. 123: p. 55-105.

73. Francis, M.P., Sachs, P.C., Elmore, L.W., and Holt, S.E., *Isolating adipose-derived mesenchymal stem cells from lipoaspirate blood and saline fraction.* Organogenesis, 2010. 6(1): p. 11-4.

74. La Rocca, G., Anzalone, R., Corrao, S., Magno, F., Loria, T., Lo Iacono, M., Di Stefano, A., Giannuzzi, P., Marasa, L., Cappello, F., Zummo, G., and Farina, F., *Isolation and characterization of Oct-4+/HLA-G+ mesenchymal stem cells from human umbilical cord matrix: differentiation potential and detection of new markers.* Histochem Cell Biol, 2009. 131(2): p. 267-82.

75. Marmotti, A., Peretti, G.M., Mattia, S., Mangiavini, L., de Girolamo, L., Vigano, M., Setti, S., Bonasia, D.E., Blonna, D., Bellato, E., Ferrero, G., and Castoldi, F., *Pulsed Electromagnetic Fields Improve Tenogenic Commitment of Umbilical Cord-Derived Mesenchymal Stem Cells: A Potential Strategy for Tendon Repair-An In Vitro Study.* Stem Cells Int, 2018. 2018: p. 9048237.

76. Moretti, P., Hatlapatka, T., Marten, D., Lavrentieva, A., Majore, I., Hass, R., and Kasper, C., *Mesenchymal stromal cells derived from human umbilical cord tissues: primitive cells with potential for clinical and tissue engineering applications.* Adv Biochem Eng Biotechnol, 2010. 123: p. 29-54.

77. Weiss, M.L., Medicetty, S., Bledsoe, A.R., Rachakatla, R.S., Choi, M., Merchav, S., Luo, Y., Rao, M.S., Velagaleti, G., and Troyer, D., *Human umbilical cord matrix stem cells: preliminary characterization and effect of transplantation in a rodent model of Parkinson's disease.* Stem Cells, 2006. 24(3): p. 781-92.

78. Li, J., Wong, W.H., Chan, S., Chim, J.C., Cheung, K.M., Lee, T.L., Au, W.Y., Ha, S.Y., Lie, A.K., Lau, Y.L., Liang, R.H., and Chan, G.C., *Factors affecting mesenchymal stromal cells yield from bone marrow aspiration.* Chin J Cancer Res, 2011. 23(1): p. 43-8.

79. Yang, H.J., Kim, K.J., Kim, M.K., Lee, S.J., Ryu, Y.H., Seo, B.F., Oh, D.Y., Ahn, S.T., Lee, H.Y., and Rhie, J.W., *The stem cell potential and multipotency of human adipose tissue-derived stem cells vary by cell donor and are different from those of other types of stem cells.* Cells Tissues Organs, 2014. 199(5-6): p. 373-83.

80. Yu, G., Wu, X., Dietrich, M.A., Polk, P., Scott, L.K., Ptitsyn, A.A., and Gimble, J.M., *Yield and characterization of subcutaneous human adipose-derived stem cells by flow cytometric and adipogenic mRNA analyzes.* Cytotherapy, 2010. 12(4): p. 538-46.

81. Dominici, M., Le Blanc, K., Mueller, I., Slaper-Cortenbach, I., Marini, F., Krause, D., Deans, R., Keating, A., Prockop, D., and Horwitz, E., *Minimal criteria for defining multipotent mesenchymal stromal cells. The International Society for Cellular Therapy position statement.* Cytotherapy, 2006. 8(4): p. 315-7.

82. Wagner, W., Wein, F., Seckinger, A., Frankhauser, M., Wirkner, U., Krause, U., Blake, J., Schwager, C., Eckstein, V., Ansorge, W., and Ho, A.D., *Comparative characteristics of mesenchymal stem cells from human bone marrow, adipose tissue, and umbilical cord blood.* Exp Hematol, 2005. 33(11): p. 1402-16.

83. Sarugaser, R., Ennis, J., Stanford, W.L., and Davies, J.E., *Isolation, propagation, and characterization of human umbilical cord perivascular cells (HUCPVCs).* Methods Mol Biol, 2009. 482: p. 269-79.

84. Kadam, S.S., Tiwari, S., and Bhonde, R.R., *Simultaneous isolation of vascular endothelial cells and mesenchymal stem cells from the human umbilical cord.* In Vitro Cell Dev Biol Anim, 2009. 45(1-2): p. 23-7.

85. Li, C.Y., Wu, X.Y., Tong, J.B., Yang, X.X., Zhao, J.L., Zheng, Q.F., Zhao, G.B., and Ma, Z.J., *Comparative analysis of human mesenchymal stem cells from bone marrow and adipose tissue under xeno-free conditions for cell therapy.* Stem Cell Res Ther, 2015. 6: p. 55.

86. Hou, T., Xu, J., Wu, X., Xie, Z., Luo, F., Zhang, Z., and Zeng, L., *Umbilical cord Wharton's Jelly: a new potential cell source of mesenchymal stromal cells for bone tissue engineering.* Tissue Eng Part A, 2009. 15(9): p. 2325-34.

87. Xu, W., Zhang, X., Qian, H., Zhu, W., Sun, X., Hu, J., Zhou, H., and Chen, Y., *Mesenchymal stem cells from adult human bone marrow differentiate into a cardiomyocyte phenotype in vitro.* Exp Biol Med (Maywood), 2004. 229(7): p. 623-31.

88. Ullah, I., Subbarao, R.B., and Rho, G.J., *Human mesenchymal stem cells - current trends and future prospective.* Biosci Rep, 2015. 35(2).

89. Campard, D., Lysy, P.A., Najimi, M., and Sokal, E.M., *Native umbilical cord matrix stem cells express hepatic markers and differentiate into hepatocyte-like cells.* Gastroenterology, 2008. 134(3): p. 833-48.

90. Datta, I., Mishra, S., Mohanty, L., Pulikkot, S., and Joshi, P.G., *Neuronal plasticity of human Wharton's jelly mesenchymal stromal cells to the dopaminergic cell type compared with human bone marrow mesenchymal stromal cells.* Cytotherapy, 2011. 13(8): p. 918-32.

91. Jiao, F., Wang, J., Dong, Z.L., Wu, M.J., Zhao, T.B., Li, D.D., and Wang, X., *Human mesenchymal stem cells derived from limb bud can differentiate into all three embryonic germ layers lineages.* Cell Reprogram, 2012. 14(4): p. 324-33.

92. Barzilay, R., Ben-Zur, T., Bulvik, S., Melamed, E., and Offen, D., *Lentiviral delivery of LMX1a enhances dopaminergic phenotype in differentiated human bone marrow mesenchymal stem cells.* Stem Cells Dev, 2009. 18(4): p. 591-601.

93. Chen, Q., Shou, P., Zheng, C., Jiang, M., Cao, G., Yang, Q., Cao, J., Xie, N., Velletri, T., Zhang, X., Xu, C., Zhang, L., Yang, H., Hou, J., Wang, Y., and Shi, Y., *Fate decision of mesenchymal stem cells: adipocytes or osteoblasts?* Cell Death Differ, 2016. 23(7): p. 1128-39.

94. Hass, R. and Otte, A., *Mesenchymal stem cells as all-round supporters in a normal and neoplastic microenvironment.* Cell Commun Signal, 2012. 10(1): p. 26.

95. Gao, F., Chiu, S.M., Motan, D.A., Zhang, Z., Chen, L., Ji, H.L., Tse, H.F., Fu, Q.L., and Lian, Q., *Mesenchymal stem cells and immunomodulation: current status and future prospects.* Cell Death Dis, 2016. 7: p. e2062.

96. Ruster, B., Gottig, S., Ludwig, R.J., Bistrian, R., Muller, S., Seifried, E., Gille, J., and Henschler, R., *Mesenchymal stem cells display coordinated rolling and adhesion behavior on endothelial cells.* Blood, 2006. 108(12): p. 3938-44.

97. Nitzsche, F., Muller, C., Lukomska, B., Jolkkonen, J., Deten, A., and Boltze, J., *Concise Review: MSC Adhesion Cascade-Insights into Homing and Transendothelial Migration.* Stem Cells, 2017. 35(6): p. 1446-1460.

98. Sordi, V., *Mesenchymal stem cell homing capacity.* Transplantation, 2009. 87(9 Suppl): p. S42-5.

99. Sordi, V., Malosio, M.L., Marchesi, F., Mercalli, A., Melzi, R., Giordano, T., Belmonte, N., Ferrari, G., Leone, B.E., Bertuzzi, F., Zerbini, G., Allavena, P., Bonifacio, E., and Piemonti, L., *Bone marrow mesenchymal stem cells express a restricted set of functionally active chemokine receptors capable of promoting migration to pancreatic islets.* Blood, 2005. 106(2): p. 419-27.

100. Hocking, A.M., *The Role of Chemokines in Mesenchymal Stem Cell Homing to Wounds.* Adv Wound Care (New Rochelle), 2015. 4(11): p. 623-630.

101. Kachgal, S. and Putnam, A.J., *Mesenchymal stem cells from adipose and bone marrow promote angiogenesis via distinct cytokine and protease expression mechanisms.* Angiogenesis, 2011. 14(1): p. 47-59.

102. Wang, N., Chen, C., Yang, D., Liao, Q., Luo, H., Wang, X., Zhou, F., Yang, X., Yang, J., Zeng, C., and Wang, W.E., *Mesenchymal stem cells-derived extracellular vesicles, via miR-210, improve infarcted cardiac function by promotion of angiogenesis.* Biochim Biophys Acta Mol Basis Dis, 2017. 1863(8): p. 2085-2092.

103. Hare, J.M., Traverse, J.H., Henry, T.D., Dib, N., Strumpf, R.K., Schulman, S.P., Gerstenblith, G., DeMaria, A.N., Denktas, A.E., Gammon, R.S., Hermiller, J.B., Jr., Reisman, M.A., Schaer, G.L., and Sherman, W., *A randomized, double-blind, placebo-controlled, dose-escalation study of intravenous adult human mesenchymal stem cells (prochymal) after acute myocardial infarction.* J Am Coll Cardiol, 2009. 54(24): p. 2277-86.

104. Miyahara, Y., Nagaya, N., Kataoka, M., Yanagawa, B., Tanaka, K., Hao, H., Ishino, K., Ishida, H., Shimizu, T., Kangawa, K., Sano, S., Okano, T., Kitamura, S., and Mori, H., *Monolayered mesenchymal stem cells repair scarred myocardium after myocardial infarction.* Nat Med, 2006. 12(4): p. 459-65.

105. Gregory, C.A., Gunn, W.G., Reyes, E., Smolarz, A.J., Munoz, J., Spees, J.L., and Prockop, D.J., *How Wnt signaling affects bone repair by mesenchymal stem cells from the bone marrow.* Ann N Y Acad Sci, 2005. 1049: p. 97-106.

106. de Windt, T.S., Vonk, L.A., Slaper-Cortenbach, I.C., van den Broek, M.P., Nizak, R., van Rijen, M.H., de Weger, R.A., Dhert, W.J., and Saris, D.B., *Allogeneic Mesenchymal Stem Cells Stimulate Cartilage Regeneration and Are Safe for Single-Stage Cartilage Repair in Humans upon Mixture with Recycled Autologous Chondrons.* Stem Cells, 2017. 35(1): p. 256-264.

107. Sasaki, M., Abe, R., Fujita, Y., Ando, S., Inokuma, D., and Shimizu, H., *Mesenchymal stem cells are recruited into wounded skin and contribute to wound repair by transdifferentiation into multiple skin cell type.* J Immunol, 2008. 180(4): p. 2581-7.

108. Galland, S., Vuille, J., Martin, P., Letovanec, I., Caignard, A., Fregni, G., and Stamenkovic, I., *Tumor-Derived Mesenchymal Stem Cells Use Distinct Mechanisms to Block the Activity of Natural Killer Cell Subsets.* Cell Rep, 2017. 20(12): p. 2891-2905.

109. Le Blanc, K., Rasmusson, I., Sundberg, B., Gotherstrom, C., Hassan, M., Uzunel, M., and Ringden, O., *Treatment of severe acute graft-versus-host disease with third party haploidentical mesenchymal stem cells.* Lancet, 2004. 363(9419): p. 1439-41.

110. Sotiropoulou, P.A., Perez, S.A., Gritzapis, A.D., Baxevanis, C.N., and Papamichail, M., *Interactions between human mesenchymal stem cells and natural killer cells.* Stem Cells, 2006. 24(1): p. 74-85.

111. Killer, M.C., Nold, P., Henkenius, K., Fritz, L., Riedlinger, T., Barckhausen, C., Frech, M., Hackstein, H., Neubauer, A., and Brendel, C., *Immunosuppressive capacity*

of mesenchymal stem cells correlates with metabolic activity and can be enhanced by valproic acid. Stem Cell Res Ther, 2017. 8(1): p. 100.

112. Di Nicola, M., Carlo-Stella, C., Magni, M., Milanesi, M., Longoni, P.D., Matteucci, P., Grisanti, S., and Gianni, A.M., *Human bone marrow stromal cells suppress T-lymphocyte proliferation induced by cellular or nonspecific mitogenic stimuli.* Blood, 2002. 99(10): p. 3838-43.
113. Kyurkchiev, D., Bochev, I., Ivanova-Todorova, E., Mourdjeva, M., Oreshkova, T., Belemezova, K., and Kyurkchiev, S., *Secretion of immunoregulatory cytokines by mesenchymal stem cells.* World J Stem Cells, 2014. 6(5): p. 552-70.
114. Lin, L. and Du, L., *The role of secreted factors in stem cells-mediated immune regulation.* Cell Immunol, 2018. 326: p. 24-32.
115. Ren, G., Zhang, L., Zhao, X., Xu, G., Zhang, Y., Roberts, A.I., Zhao, R.C., and Shi, Y., *Mesenchymal stem cell-mediated immunosuppression occurs via concerted action of chemokines and nitric oxide.* Cell Stem Cell, 2008. 2(2): p. 141-50.
116. Meisel, R., Zibert, A., Laryea, M., Gobel, U., Daubener, W., and Dilloo, D., *Human bone marrow stromal cells inhibit allogeneic T-cell responses by indoleamine 2,3-dioxygenase-mediated tryptophan degradation.* Blood, 2004. 103(12): p. 4619-21.
117. Sato, K., Ozaki, K., Oh, I., Meguro, A., Hatanaka, K., Nagai, T., Muroi, K., and Ozawa, K., *Nitric oxide plays a critical role in suppression of T-cell proliferation by mesenchymal stem cells.* Blood, 2007. 109(1): p. 228-34.
118. Zafranskaya, M., Nizheharodava, D., Yurkevich, M., Ivanchik, G., Demidchik, Y., Kozhukh, H., and Fedulov, A., *PGE2 contributes to in vitro MSC-mediated inhibition of non-specific and antigen-specific T cell proliferation in MS patients.* Scand J Immunol, 2013. 78(5): p. 455-62.
119. Yang, S.H., Park, M.J., Yoon, I.H., Kim, S.Y., Hong, S.H., Shin, J.Y., Nam, H.Y., Kim, Y.H., Kim, B., and Park, C.G., *Soluble mediators from mesenchymal stem cells suppress T cell proliferation by inducing IL-10.* Exp Mol Med, 2009. 41(5): p. 315-24.
120. Che, N., Li, X., Zhou, S., Liu, R., Shi, D., Lu, L., and Sun, L., *Umbilical cord mesenchymal stem cells suppress B-cell proliferation and differentiation.* Cell Immunol, 2012. 274(1-2): p. 46-53.
121. Asari, S., Itakura, S., Ferreri, K., Liu, C.P., Kuroda, Y., Kandeel, F., and Mullen, Y., *Mesenchymal stem cells suppress B-cell terminal differentiation.* Exp Hematol, 2009. 37(5): p. 604-15.

122. Rosado, M.M., Bernardo, M.E., Scarsella, M., Conforti, A., Giorda, E., Biagini, S., Cascioli, S., Rossi, F., Guzzo, I., Vivarelli, M., Dello Strologo, L., Emma, F., Locatelli, F., and Carsetti, R., *Inhibition of B-cell proliferation and antibody production by mesenchymal stromal cells is mediated by T cells.* Stem Cells Dev, 2015. 24(1): p. 93-103.

123. Bochev, I., Elmadjian, G., Kyurkchiev, D., Tzvetanov, L., Altankova, I., Tivchev, P., and Kyurkchiev, S., *Mesenchymal stem cells from human bone marrow or adipose tissue differently modulate mitogen-stimulated B-cell immunoglobulin production in vitro.* Cell Biol Int, 2008. 32(4): p. 384-93.

124. Ji, Y.R., Yang, Z.X., Han, Z.B., Meng, L., Liang, L., Feng, X.M., Yang, S.G., Chi, Y., Chen, D.D., Wang, Y.W., and Han, Z.C., *Mesenchymal stem cells support proliferation and terminal differentiation of B cells.* Cell Physiol Biochem, 2012. 30(6): p. 1526-37.

125. Rasmusson, I., Le Blanc, K., Sundberg, B., and Ringden, O., *Mesenchymal stem cells stimulate antibody secretion in human B cells.* Scand J Immunol, 2007. 65(4): p. 336-43.

126. Ren, G., Zhao, X., Wang, Y., Zhang, X., Chen, X., Xu, C., Yuan, Z.R., Roberts, A.I., Zhang, L., Zheng, B., Wen, T., Han, Y., Rabson, A.B., Tischfield, J.A., Shao, C., and Shi, Y., *CCR2-dependent recruitment of macrophages by tumor-educated mesenchymal stromal cells promotes tumor development and is mimicked by TNFalpha.* Cell Stem Cell, 2012. 11(6): p. 812-24.

127. Takeda, K., Webb, T.L., Ning, F., Shiraishi, Y., Regan, D.P., Chow, L., Smith, M.J., Ashino, S., Guth, A.M., Hopkins, S., Gelfand, E.W., and Dow, S., *Mesenchymal Stem Cells Recruit CCR2(+) Monocytes To Suppress Allergic Airway Inflammation.* J Immunol, 2018. 200(4): p. 1261-1269.

128. Vasandan, A.B., Jahnavi, S., Shashank, C., Prasad, P., Kumar, A., and Prasanna, S.J., *Human Mesenchymal stem cells program macrophage plasticity by altering their metabolic status via a PGE2-dependent mechanism.* Sci Rep, 2016. 6: p. 38308.

129. Deng, Y., Zhang, Y., Ye, L., Zhang, T., Cheng, J., Chen, G., Zhang, Q., and Yang, Y., *Umbilical Cord-derived Mesenchymal Stem Cells Instruct Monocytes Towards an IL10-producing Phenotype by Secreting IL6 and HGF.* Sci Rep, 2016. 6: p. 37566.

130. Spaggiari, G.M., Abdelrazik, H., Becchetti, F., and Moretta, L., *MSCs inhibit monocyte-derived DC maturation and function by selectively interfering with the*

generation of immature DCs: central role of MSC-derived prostaglandin E2. Blood, 2009. 113(26): p. 6576-83.

131. Spaggiari, G.M., Capobianco, A., Becchetti, S., Mingari, M.C., and Moretta, L., *Mesenchymal stem cell-natural killer cell interactions: evidence that activated NK cells are capable of killing MSCs, whereas MSCs can inhibit IL-2-induced NK-cell proliferation.* Blood, 2006. 107(4): p. 1484-90.

132. Spaggiari, G.M., Capobianco, A., Abdelrazik, H., Becchetti, F., Mingari, M.C., and Moretta, L., *Mesenchymal stem cells inhibit natural killer-cell proliferation, cytotoxicity, and cytokine production: role of indoleamine 2,3-dioxygenase and prostaglandin E2.* Blood, 2008. 111(3): p. 1327-33.

133. Sun, Q., Huang, Z., Han, F., Zhao, M., Cao, R., Zhao, D., Hong, L., Na, N., Li, H., Miao, B., Hu, J., Meng, F., Peng, Y., and Sun, Q., *Allogeneic mesenchymal stem cells as induction therapy are safe and feasible in renal allografts: pilot results of a multicenter randomized controlled trial.* J Transl Med, 2018. 16(1): p. 52.

134. Horwitz, E.M., Gordon, P.L., Koo, W.K., Marx, J.C., Neel, M.D., McNall, R.Y., Muul, L., and Hofmann, T., *Isolated allogeneic bone marrow-derived mesenchymal cells engraft and stimulate growth in children with osteogenesis imperfecta: Implications for cell therapy of bone.* Proc Natl Acad Sci U S A, 2002. 99(13): p. 8932-7.

135. Hare, J.M., Fishman, J.E., Gerstenblith, G., DiFede Velazquez, D.L., Zambrano, J.P., Suncion, V.Y., Tracy, M., Ghersin, E., Johnston, P.V., Brinker, J.A., Breton, E., Davis-Sproul, J., Schulman, I.H., Byrnes, J., Mendizabal, A.M., Lowery, M.H., Rouy, D., Altman, P., Wong Po Foo, C., Ruiz, P., Amador, A., Da Silva, J., McNiece, I.K., Heldman, A.W., George, R., and Lardo, A., *Comparison of allogeneic vs autologous bone marrow-derived mesenchymal stem cells delivered by transendocardial injection in patients with ischemic cardiomyopathy: the POSEIDON randomized trial.* JAMA, 2012. 308(22): p. 2369-79.

136. Nauta, A.J., Westerhuis, G., Kruisselbrink, A.B., Lurvink, E.G., Willemze, R., and Fibbe, W.E., *Donor-derived mesenchymal stem cells are immunogenic in an allogeneic host and stimulate donor graft rejection in a nonmyeloablative setting.* Blood, 2006. 108(6): p. 2114-20.

137. Eliopoulos, N., Stagg, J., Lejeune, L., Pommey, S., and Galipeau, J., *Allogeneic marrow stromal cells are immune rejected by MHC class I- and class II-mismatched recipient mice.* Blood, 2005. 106(13): p. 4057-65.

138. Zangi, L., Margalit, R., Reich-Zeliger, S., Bachar-Lustig, E., Beilhack, A., Negrin, R., and Reisner, Y., *Direct imaging of immune rejection and memory induction by allogeneic mesenchymal stromal cells.* Stem Cells, 2009. 27(11): p. 2865-74.

139. Squillaro, T., Peluso, G., and Galderisi, U., *Clinical Trials With Mesenchymal Stem Cells: An Update.* Cell Transplant, 2016. 25(5): p. 829-48.

140. Ferrara, J.L., Levine, J.E., Reddy, P., and Holler, E., *Graft-versus-host disease.* Lancet, 2009. 373(9674): p. 1550-61.

141. Le Blanc, K., Frassoni, F., Ball, L., Locatelli, F., Roelofs, H., Lewis, I., Lanino, E., Sundberg, B., Bernardo, M.E., Remberger, M., Dini, G., Egeler, R.M., Bacigalupo, A., Fibbe, W., Ringden, O., Developmental Committee of the European Group for, B., and Marrow, T., *Mesenchymal stem cells for treatment of steroid-resistant, severe, acute graft-versus-host disease: a phase II study.* Lancet, 2008. 371(9624): p. 1579-86.

142. Muller, I., Kordowich, S., Holzwarth, C., Isensee, G., Lang, P., Neunhoeffer, F., Dominici, M., Greil, J., and Handgretinger, R., *Application of multipotent mesenchymal stromal cells in pediatric patients following allogeneic stem cell transplantation.* Blood Cells Mol Dis, 2008. 40(1): p. 25-32.

143. Melzer, C., Yang, Y., and Hass, R., *Interaction of MSC with tumor cells.* Cell Commun Signal, 2016. 14(1): p. 20.

144. Halpern, J.L., Kilbarger, A., and Lynch, C.C., *Mesenchymal stem cells promote mammary cancer cell migration in vitro via the CXCR2 receptor.* Cancer Lett, 2011. 308(1): p. 91-9.

145. Karnoub, A.E., Dash, A.B., Vo, A.P., Sullivan, A., Brooks, M.W., Bell, G.W., Richardson, A.L., Polyak, K., Tubo, R., and Weinberg, R.A., *Mesenchymal stem cells within tumour stroma promote breast cancer metastasis.* Nature, 2007. 449(7162): p. 557-63.

146. Liu, S., Ginestier, C., Ou, S.J., Clouthier, S.G., Patel, S.H., Monville, F., Korkaya, H., Heath, A., Dutcher, J., Kleer, C.G., Jung, Y., Dontu, G., Taichman, R., and Wicha, M.S., *Breast cancer stem cells are regulated by mesenchymal stem cells through cytokine networks.* Cancer Res, 2011. 71(2): p. 614-24.

147. Rhodes, L.V., Antoon, J.W., Muir, S.E., Elliott, S., Beckman, B.S., and Burow, M.E., *Effects of human mesenchymal stem cells on ER-positive human breast carcinoma cells mediated through ER-SDF-1/CXCR4 crosstalk.* Mol Cancer, 2010. 9: p. 295.

148. Ling, X., Marini, F., Konopleva, M., Schober, W., Shi, Y., Burks, J., Clise-Dwyer, K., Wang, R.Y., Zhang, W., Yuan, X., Lu, H., Caldwell, L., and Andreeff, M., *Mesenchymal Stem Cells Overexpressing IFN-beta Inhibit Breast Cancer Growth and Metastases through Stat3 Signaling in a Syngeneic Tumor Model.* Cancer Microenviron, 2010. 3(1): p. 83-95.

149. Lee, Y., El Andaloussi, S., and Wood, M.J., *Exosomes and microvesicles: extracellular vesicles for genetic information transfer and gene therapy.* Hum Mol Genet, 2012. 21(R1): p. R125-34.

150. Melzer, C., von der Ohe, J., and Hass, R., *Concise Review: Crosstalk of Mesenchymal Stroma/Stem-Like Cells with Cancer Cells Provides Therapeutic Potential.* Stem Cells, 2018.

151. Lee, J.K., Park, S.R., Jung, B.K., Jeon, Y.K., Lee, Y.S., Kim, M.K., Kim, Y.G., Jang, J.Y., and Kim, C.W., *Exosomes derived from mesenchymal stem cells suppress angiogenesis by down-regulating VEGF expression in breast cancer cells.* PLoS One, 2013. 8(12): p. e84256.

152. Yang, Y., Bucan, V., Baehre, H., von der Ohe, J., Otte, A., and Hass, R., *Acquisition of new tumor cell properties by MSC-derived exosomes.* Int J Oncol, 2015. 47(1): p. 244-52.

153. Lin, R., Wang, S., and Zhao, R.C., *Exosomes from human adipose-derived mesenchymal stem cells promote migration through Wnt signaling pathway in a breast cancer cell model.* Mol Cell Biochem, 2013. 383(1-2): p. 13-20.

154. Vallabhaneni, K.C., Penfornis, P., Dhule, S., Guillonneau, F., Adams, K.V., Mo, Y.Y., Xu, R., Liu, Y., Watabe, K., Vemuri, M.C., and Pochampally, R., *Extracellular vesicles from bone marrow mesenchymal stem/stromal cells transport tumor regulatory microRNA, proteins, and metabolites.* Oncotarget, 2015. 6(7): p. 4953-67.

155. Cho, J.A., Park, H., Lim, E.H., and Lee, K.W., *Exosomes from breast cancer cells can convert adipose tissue-derived mesenchymal stem cells into myofibroblast-like cells.* Int J Oncol, 2012. 40(1): p. 130-8.

156. Caicedo, A., Fritz, V., Brondello, J.M., Ayala, M., Dennemont, I., Abdellaoui, N., de Fraipont, F., Moisan, A., Prouteau, C.A., Boukhaddaoui, H., Jorgensen, C., and Vignais, M.L., *MitoCeption as a new tool to assess the effects of mesenchymal stem/stromal cell mitochondria on cancer cell metabolism and function.* Sci Rep, 2015. 5: p. 9073.

157. Ramasamy, R., Lam, E.W., Soeiro, I., Tisato, V., Bonnet, D., and Dazzi, F., *Mesenchymal stem cells inhibit proliferation and apoptosis of tumor cells: impact on in vivo tumor growth.* Leukemia, 2007. 21(2): p. 304-10.

158. Mandel, K., Yang, Y., Schambach, A., Glage, S., Otte, A., and Hass, R., *Mesenchymal stem cells directly interact with breast cancer cells and promote tumor cell growth in vitro and in vivo.* Stem Cells Dev, 2013. 22(23): p. 3114-27.

159. Joly, E. and Hudrisier, D., *What is trogocytosis and what is its purpose?* Nat Immunol, 2003. 4(9): p. 815.

160. Rafii, A., Mirshahi, P., Poupot, M., Faussat, A.M., Simon, A., Ducros, E., Mery, E., Couderc, B., Lis, R., Capdet, J., Bergalet, J., Querleu, D., Dagonnet, F., Fournie, J.J., Marie, J.P., Pujade-Lauraine, E., Favre, G., Soria, J., and Mirshahi, M., *Oncologic trogocytosis of an original stromal cells induces chemoresistance of ovarian tumours.* PLoS One, 2008. 3(12): p. e3894.

161. Rappa, G., Mercapide, J., and Lorico, A., *Spontaneous formation of tumorigenic hybrids between breast cancer and multipotent stromal cells is a source of tumor heterogeneity.* Am J Pathol, 2012. 180(6): p. 2504-15.

162. Xue, J., Zhu, Y., Sun, Z., Ji, R., Zhang, X., Xu, W., Yuan, X., Zhang, B., Yan, Y., Yin, L., Xu, H., Zhang, L., Zhu, W., and Qian, H., *Tumorigenic hybrids between mesenchymal stem cells and gastric cancer cells enhanced cancer proliferation, migration and stemness.* BMC Cancer, 2015. 15: p. 793.

163. Yang, Y., Otte, A., and Hass, R., *Human mesenchymal stroma/stem cells exchange membrane proteins and alter functionality during interaction with different tumor cell lines.* Stem Cells Dev, 2015. 24(10): p. 1205-22.

164. Wei, H.J., Nickoloff, J.A., Chen, W.H., Liu, H.Y., Lo, W.C., Chang, Y.T., Yang, P.C., Wu, C.W., Williams, D.F., Gelovani, J.G., and Deng, W.P., *FOXF1 mediates mesenchymal stem cell fusion-induced reprogramming of lung cancer cells.* Oncotarget, 2014. 5(19): p. 9514-29.

165. Primakoff, P. and Myles, D.G., *Penetration, adhesion, and fusion in mammalian sperm-egg interaction.* Science, 2002. 296(5576): p. 2183-5.

166. Ishikawa, A., Omata, W., Ackerman, W.E.t., Takeshita, T., Vandre, D.D., and Robinson, J.M., *Cell fusion mediates dramatic alterations in the actin cytoskeleton, focal adhesions, and E-cadherin in trophoblastic cells.* Cytoskeleton (Hoboken), 2014. 71(4): p. 241-56.

167. Toufaily, C., Vargas, A., Lemire, M., Lafond, J., Rassart, E., and Barbeau, B., *MFSD2a, the Syncytin-2 receptor, is important for trophoblast fusion.* Placenta, 2013. 34(1): p. 85-8.

168. Khan, U.A., Hashimi, S.M., Bakr, M.M., Forwood, M.R., and Morrison, N.A., *Foreign body giant cells and osteoclasts are TRAP positive, have podosome-belts and both require OC-STAMP for cell fusion.* J Cell Biochem, 2013. 114(8): p. 1772-8.

169. Yagi, M., Miyamoto, T., Sawatani, Y., Iwamoto, K., Hosogane, N., Fujita, N., Morita, K., Ninomiya, K., Suzuki, T., Miyamoto, K., Oike, Y., Takeya, M., Toyama, Y., and Suda, T., *DC-STAMP is essential for cell-cell fusion in osteoclasts and foreign body giant cells.* J Exp Med, 2005. 202(3): p. 345-51.

170. Segal, D., Dhanyasi, N., Schejter, E.D., and Shilo, B.Z., *Adhesion and Fusion of Muscle Cells Are Promoted by Filopodia.* Dev Cell, 2016. 38(3): p. 291-304.

171. Carloni, V., Mazzocca, A., Mello, T., Galli, A., and Capaccioli, S., *Cell fusion promotes chemoresistance in metastatic colon carcinoma.* Oncogene, 2013. 32(21): p. 2649-60.

172. He, X., Li, B., Shao, Y., Zhao, N., Hsu, Y., Zhang, Z., and Zhu, L., *Cell fusion between gastric epithelial cells and mesenchymal stem cells results in epithelial-to-mesenchymal transition and malignant transformation.* BMC Cancer, 2015. 15: p. 24.

173. Ramakrishnan, M., Mathur, S.R., and Mukhopadhyay, A., *Fusion-derived epithelial cancer cells express hematopoietic markers and contribute to stem cell and migratory phenotype in ovarian carcinoma.* Cancer Res, 2013. 73(17): p. 5360-70.

174. Okada, Y., *Analysis of giant polynuclear cell formation caused by HVJ virus from Ehrlich's ascites tumor cells. I. Microscopic observation of giant polynuclear cell formation.* Exp Cell Res, 1962. 26: p. 98-107.

175. Okada, Y., *Analysis of giant polynuclear cell formation caused by HVJ virus from Ehrlich's ascites tumor cells. III. Relationship between cell condition and fusion reaction or cell degeneration reaction.* Exp Cell Res, 1962. 26: p. 119-28.

176. Okada, Y. and Tadokoro, J., *Analysis of giant polynuclear cell formation caused by HVJ virus from Ehrlich's ascites tumor cells. II. Quantitative analysis of giant polynuclear cell formation.* Exp Cell Res, 1962. 26: p. 108-18.

177. Barski, G., Sorieul, S., and Cornefert, F., *[Production of cells of a "hybrid" nature in culturs in vitro of 2 cellular strains in combination].* C R Hebd Seances Acad Sci, 1960. 251: p. 1825-7.

178. Ephrussi, B. and Weiss, M.C., *Interspecific hybridization of somatic cells.* Proc Natl Acad Sci U S A, 1965. 53(5): p. 1040-2.

179. Barski, G., Sorieul, S., and Cornefert, F., *"Hybrid" type cells in combined cultures of two different mammalian cell strains.* J Natl Cancer Inst, 1961. 26: p. 1269-91.

180. Barski, G. and Cornefert, F., *Characteristics of "hybrid"-type clonal cell lines obtained from mixed cultures in vitro.* J Natl Cancer Inst, 1962. 28: p. 801-21.

181. Ogle, B.M., Cascalho, M., and Platt, J.L., *Biological implications of cell fusion.* Nat Rev Mol Cell Biol, 2005. 6(7): p. 567-75.

182. Lu, X. and Kang, Y., *Efficient acquisition of dual metastasis organotropism to bone and lung through stable spontaneous fusion between MDA-MB-231 variants.* Proc Natl Acad Sci U S A, 2009. 106(23): p. 9385-90.

183. Lindstrom, A., Midtbo, K., Arnesson, L.G., Garvin, S., and Shabo, I., *Fusion between M2-macrophages and cancer cells results in a subpopulation of radioresistant cells with enhanced DNA-repair capacity.* Oncotarget, 2017. 8(31): p. 51370-51386.

184. Ding, J., Jin, W., Chen, C., Shao, Z., and Wu, J., *Tumor associated macrophage x cancer cell hybrids may acquire cancer stem cell properties in breast cancer.* PLoS One, 2012. 7(7): p. e41942.

185. Mortensen, K., Lichtenberg, J., Thomsen, P.D., and Larsson, L.I., *Spontaneous fusion between cancer cells and endothelial cells.* Cell Mol Life Sci, 2004. 61(16): p. 2125-31.

186. El Hallani, S., Colin, C., El Houfi, Y., Idbaih, A., Boisselier, B., Marie, Y., Ravassard, P., Labussiere, M., Mokhtari, K., Thomas, J.L., Delattre, J.Y., Eichmann, A., and Sanson, M., *Tumor and endothelial cell hybrids participate in glioblastoma vasculature.* Biomed Res Int, 2014. 2014: p. 827327.

187. Song, K., Song, Y., Zhao, X.P., Shen, H., Wang, M., Yan, T.L., Liu, K., and Shang, Z.J., *Oral cancer/endothelial cell fusion experiences nuclear fusion and acquisition of enhanced survival potential.* Exp Cell Res, 2014. 328(1): p. 156-63.

188. Noubissi, F.K., Harkness, T., Alexander, C.M., and Ogle, B.M., *Apoptosis-induced cancer cell fusion: a mechanism of breast cancer metastasis.* FASEB J, 2015. 29(9): p. 4036-45.

189. Lee, J.H., Hsieh, C.F., Liu, H.W., Chen, C.Y., Wu, S.C., Chen, T.W., Hsu, C.S., Liao, Y.H., Yang, C.Y., Shyu, J.F., Fischer, W.B., and Lin, C.H., *Lipid raft-associated stomatin enhances cell fusion.* FASEB J, 2017. 31(1): p. 47-59.

190. Shilagardi, K., Li, S., Luo, F., Marikar, F., Duan, R., Jin, P., Kim, J.H., Murnen, K., and Chen, E.H., *Actin-propelled invasive membrane protrusions promote fusogenic protein engagement during cell-cell fusion.* Science, 2013. 340(6130): p. 359-63.

191. Brett, C.L. and Merz, A.J., *Osmotic regulation of Rab-mediated organelle docking.* Curr Biol, 2008. 18(14): p. 1072-7.

192. Cang, C., Aranda, K., Seo, Y.J., Gasnier, B., and Ren, D., *TMEM175 Is an Organelle K(+) Channel Regulating Lysosomal Function.* Cell, 2015. 162(5): p. 1101-12.

193. Brett, C.L., Donowitz, M., and Rao, R., *Evolutionary origins of eukaryotic sodium/proton exchangers.* Am J Physiol Cell Physiol, 2005. 288(2): p. C223-39.

194. Karim, M.A. and Brett, C.L., *The Na(+)(K(+))/H(+) exchanger Nhx1 controls multivesicular body-vacuolar lysosome fusion.* Mol Biol Cell, 2018. 29(3): p. 317-325.

195. Mi, S., Lee, X., Li, X., Veldman, G.M., Finnerty, H., Racie, L., LaVallie, E., Tang, X.Y., Edouard, P., Howes, S., Keith, J.C., Jr., and McCoy, J.M., *Syncytin is a captive retroviral envelope protein involved in human placental morphogenesis.* Nature, 2000. 403(6771): p. 785-9.

196. Cheynet, V., Oriol, G., and Mallet, F., *Identification of the hASCT2-binding domain of the Env ERVWE1/syncytin-1 fusogenic glycoprotein.* Retrovirology, 2006. 3: p. 41.

197. Esnault, C., Priet, S., Ribet, D., Vernochet, C., Bruls, T., Lavialle, C., Weissenbach, J., and Heidmann, T., *A placenta-specific receptor for the fusogenic, endogenous retrovirus-derived, human syncytin-2.* Proc Natl Acad Sci U S A, 2008. 105(45): p. 17532-7.

198. Bjerregaard, B., Holck, S., Christensen, I.J., and Larsson, L.I., *Syncytin is involved in breast cancer-endothelial cell fusions.* Cell Mol Life Sci, 2006. 63(16): p. 1906-11.

199. Liang, C.Y., Wang, L.J., Chen, C.P., Chen, L.F., Chen, Y.H., and Chen, H., *GCM1 regulation of the expression of syncytin 2 and its cognate receptor MFSD2A in human placenta.* Biol Reprod, 2010. 83(3): p. 387-95.

200. Yang, M., Birnbaum, M.J., MacKay, C.A., Mason-Savas, A., Thompson, B., and Odgren, P.R., *Osteoclast stimulatory transmembrane protein (OC-STAMP), a novel protein induced by RANKL that promotes osteoclast differentiation.* J Cell Physiol, 2008. 215(2): p. 497-505.

201. Schultz, R. and Williams, C., *Developmental biology: sperm-egg fusion unscrambled.* Nature, 2005. 434(7030): p. 152-3.

202. Huovila, A.P., Almeida, E.A., and White, J.M., *ADAMs and cell fusion.* Curr Opin Cell Biol, 1996. 8(5): p. 692-9.

203. Li, N., Mak, A., Richards, D.P., Naber, C., Keller, B.O., Li, L., and Shaw, A.R., *Monocyte lipid rafts contain proteins implicated in vesicular trafficking and phagosome formation.* Proteomics, 2003. 3(4): p. 536-48.

204. Oikawa, T., Kuroda, Y., and Matsuo, K., *Regulation of osteoclasts by membrane-derived lipid mediators.* Cell Mol Life Sci, 2013. 70(18): p. 3341-53.

205. Ishii, M., Iwai, K., Koike, M., Ohshima, S., Kudo-Tanaka, E., Ishii, T., Mima, T., Katada, Y., Miyatake, K., Uchiyama, Y., and Saeki, Y., *RANKL-induced expression of tetraspanin CD9 in lipid raft membrane microdomain is essential for cell fusion during osteoclastogenesis.* J Bone Miner Res, 2006. 21(6): p. 965-76.

206. Horsley, V., Jansen, K.M., Mills, S.T., and Pavlath, G.K., *IL-4 acts as a myoblast recruitment factor during mammalian muscle growth.* Cell, 2003. 113(4): p. 483-94.

207. Enelow, R.I., Sullivan, G.W., Carper, H.T., and Mandell, G.L., *Induction of multinucleated giant cell formation from in vitro culture of human monocytes with interleukin-3 and interferon-gamma: comparison with other stimulating factors.* Am J Respir Cell Mol Biol, 1992. 6(1): p. 57-62.

208. Most, J., Neumayer, H.P., and Dierich, M.P., *Cytokine-induced generation of multinucleated giant cells in vitro requires interferon-gamma and expression of LFA-1.* Eur J Immunol, 1990. 20(8): p. 1661-7.

209. Kudo, O., Fujikawa, Y., Itonaga, I., Sabokbar, A., Torisu, T., and Athanasou, N.A., *Proinflammatory cytokine (TNFalpha/IL-1alpha) induction of human osteoclast formation.* J Pathol, 2002. 198(2): p. 220-7.

210. Kouris, N.A., Schaefer, J.A., Hatta, M., Freeman, B.T., Kamp, T.J., Kawaoka, Y., and Ogle, B.M., *Directed Fusion of Mesenchymal Stem Cells with Cardiomyocytes via VSV-G Facilitates Stem Cell Programming.* Stem Cells Int, 2012. 2012: p. 414038.

211. Leikina, E., Onaran, H.O., and Zimmerberg, J., *Acidic pH induces fusion of cells infected with baculovirus to form syncytia.* FEBS Lett, 1992. 304(2-3): p. 221-4.

212. Larsson, L.I., Bjerregaard, B., and Talts, J.F., *Cell fusions in mammals.* Histochem Cell Biol, 2008. 129(5): p. 551-61.

213. Mohr, M., Tosun, S., Arnold, W.H., Edenhofer, F., Zanker, K.S., and Dittmar, T., *Quantification of cell fusion events human breast cancer cells and breast epithelial cells using a Cre-LoxP-based double fluorescence reporter system.* Cell Mol Life Sci, 2015. 72(19): p. 3769-82.

214. Mondal Roy, S. and Sarkar, M., *Membrane fusion induced by small molecules and ions.* J Lipids, 2011. 2011: p. 528784.

215. Bartosh, T.J., Ullah, M., Zeitouni, S., Beaver, J., and Prockop, D.J., *Cancer cells enter dormancy after cannibalizing mesenchymal stem/stromal cells (MSCs).* Proc Natl Acad Sci U S A, 2016. 113(42): p. E6447-E6456.

216. Pedrazzoli, F., Chrysantzas, I., Dezzani, L., Rosti, V., Vincitorio, M., and Sitar, G., *Cell fusion in tumor progression: the isolation of cell fusion products by physical methods.* Cancer Cell Int, 2011. 11: p. 32.

217. Jacobsen, B.M., Harrell, J.C., Jedlicka, P., Borges, V.F., Varella-Garcia, M., and Horwitz, K.B., *Spontaneous fusion with, and transformation of mouse stroma by, malignant human breast cancer epithelium.* Cancer Res, 2006. 66(16): p. 8274-9.

218. Lizier, M., Anselmo, A., Mantero, S., Ficara, F., Paulis, M., Vezzoni, P., Lucchini, F., and Pacchiana, G., *Fusion between cancer cells and macrophages occurs in a murine model of spontaneous neu+ breast cancer without increasing its metastatic potential.* Oncotarget, 2016. 7(38): p. 60793-60806.

219. Freeman, B.T., Kouris, N.A., and Ogle, B.M., *Tracking fusion of human mesenchymal stem cells after transplantation to the heart.* Stem Cells Transl Med, 2015. 4(6): p. 685-94.

220. Searles, S.C., Santosa, E.K., and Bui, J.D., *Cell-cell fusion as a mechanism of DNA exchange in cancer.* Oncotarget, 2018. 9(5): p. 6156-6173.

221. Chitwood, C.A., Dietzsch, C., Jacobs, G., McArdle, T., Freeman, B.T., Banga, A., Noubissi, F.K., and Ogle, B.M., *Breast tumor cell hybrids form spontaneously in vivo and contribute to breast tumor metastases.* APL Bioengineering, 2018. 2(3).

222. Zhang, C., Zhai, W., Xie, Y., Chen, Q., Zhu, W., and Sun, X., *Mesenchymal stem cells derived from breast cancer tissue promote the proliferation and migration of the MCF-7 cell line in vitro.* Oncol Lett, 2013. 6(6): p. 1577-1582.

223. He, N., Kong, Y., Lei, X., Liu, Y., Wang, J., Xu, C., Wang, Y., Du, L., Ji, K., Wang, Q., Li, Z., and Liu, Q., *MSCs inhibit tumor progression and enhance radiosensitivity of breast cancer cells by down-regulating Stat3 signaling pathway.* Cell Death Dis, 2018. 9(10): p. 1026.

224. McLean, K., Gong, Y., Choi, Y., Deng, N., Yang, K., Bai, S., Cabrera, L., Keller, E., McCauley, L., Cho, K.R., and Buckanovich, R.J., *Human ovarian carcinoma-associated mesenchymal stem cells regulate cancer stem cells and tumorigenesis via altered BMP production.* J Clin Invest, 2011. 121(8): p. 3206-19.

225. Otte, A., Yang, Y., von der Ohe, J., Melzer, C., Hillemanns, P., Feuerhake, F., and Hass, R., *SCCOHT tumors acquire chemoresistance and protection by interacting*

mesenchymal stroma/stem cells within the tumor microenvironment. Int J Oncol, 2016. 49(6): p. 2453-2463.

226. Castells, M., Milhas, D., Gandy, C., Thibault, B., Rafii, A., Delord, J.P., and Couderc, B., *Microenvironment mesenchymal cells protect ovarian cancer cell lines from apoptosis by inhibiting XIAP inactivation.* Cell Death Dis, 2013. 4: p. e887.
227. Coffman, L.G., Choi, Y.J., McLean, K., Allen, B.L., di Magliano, M.P., and Buckanovich, R.J., *Human carcinoma-associated mesenchymal stem cells promote ovarian cancer chemotherapy resistance via a BMP4/HH signaling loop.* Oncotarget, 2016. 7(6): p. 6916-32.
228. Fortuna, M.B., Dewey, M.J., and Furmanski, P., *Cell fusion in tumor development and progression: occurrence of cell fusion in primary methylcholanthrene-induced tumorigenesis.* Int J Cancer, 1989. 44(4): p. 731-7.
229. Wakeling, W.F., Greetham, J., and Bennett, D.C., *Efficient spontaneous fusion between some co-cultured cells, especially murine melanoma cells.* Cell Biol Int, 1994. 18(3): p. 207-10.
230. Miller, F.R., McInerney, D., Rogers, C., and Miller, B.E., *Spontaneous fusion between metastatic mammary tumor subpopulations.* J Cell Biochem, 1988. 36(2): p. 129-36.
231. Hanahan, D. and Weinberg, R.A., *Hallmarks of cancer: the next generation.* Cell, 2011. 144(5): p. 646-74.
232. Dittmar, T. and Zanker, K.S., *Tissue Regeneration in the Chronically Inflamed Tumor Environment: Implications for Cell Fusion Driven Tumor Progression and Therapy Resistant Tumor Hybrid Cells.* Int J Mol Sci, 2015. 16(12): p. 30362-81.
233. Palermo, A., Doyonnas, R., Bhutani, N., Pomerantz, J., Alkan, O., and Blau, H.M., *Nuclear reprogramming in heterokaryons is rapid, extensive, and bidirectional.* FASEB J, 2009. 23(5): p. 1431-40.
234. Yamanaka, S. and Blau, H.M., *Nuclear reprogramming to a pluripotent state by three approaches.* Nature, 2010. 465(7299): p. 704-12.
235. Berndt, B., Zanker, K.S., and Dittmar, T., *Cell fusion is a potent inducer of aneuploidy and drug resistance in tumor cell/ normal cell hybrids.* Crit Rev Oncog, 2013. 18(1-2): p. 97-113.
236. Duelli, D. and Lazebnik, Y., *Cell fusion: a hidden enemy?* Cancer Cell, 2003. 3(5): p. 445-8.

237. Fujiwara, T., Bandi, M., Nitta, M., Ivanova, E.V., Bronson, R.T., and Pellman, D., *Cytokinesis failure generating tetraploids promotes tumorigenesis in p53-null cells.* Nature, 2005. 437(7061): p. 1043-7.

238. Sarrio, D., Rodriguez-Pinilla, S.M., Hardisson, D., Cano, A., Moreno-Bueno, G., and Palacios, J., *Epithelial-mesenchymal transition in breast cancer relates to the basal-like phenotype.* Cancer Res, 2008. 68(4): p. 989-97.

239. Blick, T., Widodo, E., Hugo, H., Waltham, M., Lenburg, M.E., Neve, R.M., and Thompson, E.W., *Epithelial mesenchymal transition traits in human breast cancer cell lines.* Clin Exp Metastasis, 2008. 25(6): p. 629-42.

240. Xu, M.H., Gao, X., Luo, D., Zhou, X.D., Xiong, W., and Liu, G.X., *EMT and acquisition of stem cell-like properties are involved in spontaneous formation of tumorigenic hybrids between lung cancer and bone marrow-derived mesenchymal stem cells.* PLoS One, 2014. 9(2): p. e87893.

241. Maffey, A., Storini, C., Diceglie, C., Martelli, C., Sironi, L., Calzarossa, C., Tonna, N., Lovchik, R., Delamarche, E., Ottobrini, L., and Bianco, F., *Mesenchymal stem cells from tumor microenvironment favour breast cancer stem cell proliferation, cancerogenic and metastatic potential, via ionotropic purinergic signalling.* Sci Rep, 2017. 7(1): p. 13162.

242. Nowicka, A., Marini, F.C., Solley, T.N., Elizondo, P.B., Zhang, Y., Sharp, H.J., Broaddus, R., Kolonin, M., Mok, S.C., Thompson, M.S., Woodward, W.A., Lu, K., Salimian, B., Nagrath, D., and Klopp, A.H., *Human omental-derived adipose stem cells increase ovarian cancer proliferation, migration, and chemoresistance.* PLoS One, 2013. 8(12): p. e81859.

243. Zhu, Y., Sun, Z., Han, Q., Liao, L., Wang, J., Bian, C., Li, J., Yan, X., Liu, Y., Shao, C., and Zhao, R.C., *Human mesenchymal stem cells inhibit cancer cell proliferation by secreting DKK-1.* Leukemia, 2009. 23(5): p. 925-33.

244. Pawelek, J.M. and Chakraborty, A.K., *Fusion of tumour cells with bone marrow-derived cells: a unifying explanation for metastasis.* Nat Rev Cancer, 2008. 8(5): p. 377-86.

245. Nagler, C., Hardt, C., Zanker, K.S., and Dittmar, T., *Co-cultivation of murine BMDCs with 67NR mouse mammary carcinoma cells give rise to highly drug resistant cells.* Cancer Cell Int, 2011. 11(1): p. 21.

246. Yan, B., Wang, J., and Liu, L., *Chemotherapy promotes tumour cell hybridization in vivo.* Tumour Biol, 2016. 37(4): p. 5025-30.

247. Buick, R.N., Pullano, R., and Trent, J.M., *Comparative properties of five human ovarian adenocarcinoma cell lines.* Cancer Res, 1985. 45(8): p. 3668-76.

248. van den Berk, L.C., Jansen, B.J., Siebers-Vermeulen, K.G., Roelofs, H., Figdor, C.G., Adema, G.J., and Torensma, R., *Mesenchymal stem cells respond to TNF but do not produce TNF.* J Leukoc Biol, 2010. 87(2): p. 283-9.

249. Katanov, C., Lerrer, S., Liubomirski, Y., Leider-Trejo, L., Meshel, T., Bar, J., Feniger-Barish, R., Kamer, I., Soria-Artzi, G., Kahani, H., Banerjee, D., and Ben-Baruch, A., *Regulation of the inflammatory profile of stromal cells in human breast cancer: prominent roles for TNF-alpha and the NF-kappaB pathway.* Stem Cell Res Ther, 2015. 6: p. 87.

250. Yu, P.F., Huang, Y., Han, Y.Y., Lin, L.Y., Sun, W.H., Rabson, A.B., Wang, Y., and Shi, Y.F., *TNFalpha-activated mesenchymal stromal cells promote breast cancer metastasis by recruiting CXCR2(+) neutrophils.* Oncogene, 2017. 36(4): p. 482-490.

251. Hsu, H., Xiong, J., and Goeddel, D.V., *The TNF receptor 1-associated protein TRADD signals cell death and NF-kappa B activation.* Cell, 1995. 81(4): p. 495-504.

252. Hsu, H., Shu, H.B., Pan, M.G., and Goeddel, D.V., *TRADD-TRAF2 and TRADD-FADD interactions define two distinct TNF receptor 1 signal transduction pathways.* Cell, 1996. 84(2): p. 299-308.

253. Reinhard, C., Shamoon, B., Shyamala, V., and Williams, L.T., *Tumor necrosis factor alpha-induced activation of c-jun N-terminal kinase is mediated by TRAF2.* EMBO J, 1997. 16(5): p. 1080-92.

254. Natoli, G., Costanzo, A., Ianni, A., Templeton, D.J., Woodgett, J.R., Balsano, C., and Levrero, M., *Activation of SAPK/JNK by TNF receptor 1 through a noncytotoxic TRAF2-dependent pathway.* Science, 1997. 275(5297): p. 200-3.

255. Crisostomo, P.R., Wang, Y., Markel, T.A., Wang, M., Lahm, T., and Meldrum, D.R., *Human mesenchymal stem cells stimulated by TNF-alpha, LPS, or hypoxia produce growth factors by an NF kappa B- but not JNK-dependent mechanism.* Am J Physiol Cell Physiol, 2008. 294(3): p. C675-82.

256. Casiraghi, F., Noris, M., and Remuzzi, G., *Immunomodulatory effects of mesenchymal stromal cells in solid organ transplantation.* Curr Opin Organ Transplant, 2010. 15(6): p. 731-7.

257. Melzer, C., von der Ohe, J., Lehnert, H., Ungefroren, H., and Hass, R., *Cancer stem cell niche models and contribution by mesenchymal stroma/stem cells.* Mol Cancer, 2017. 16(1): p. 28.

6. List of abbreviations

Abbreviation	Explanation
ADAM	A disintegrin and metalloprotein domain
ANOVA	Analysis of variance
ASCT1 or ASCT2	Alanine serine and cysteine selective transporter type 1 or type 2
AT-MSC	Adipose tissue MSC
ATP	Adenosine triphosphate
BM-MSC	Bone marrow MSC
bp	Base pair
BRAF	v-Raf murine sarcoma viral oncogene homolog B
BRCA1	Breast Cancer 1 / 2
CA-MSC	Carcinoma-associated mesenchymal stroma/stem cells
CCL	Chemokine (C-C motif) ligand
CCR	C-C chemokine receptor
CD11b	Integrin alpha M
CD14	Monocytic surface marker
CD19	B-lymphocyte antigen
CD29	Integrin beta 1
CD34	Hematopoietic stem cell surface marker
CD44	Receptor for hyaluronic acid
CD45	Protein tyrosine phosphatase receptor type C
CD73	Ecto-5´-nucleotidase
CD90	Thy 1
CD105	Endoglin
CD120a	TNF receptor 1
cDNA	Complementary DNA
CFU-F	Colony-forming unit fibroblasts
CHEK2	Checkpoint Kinase 2
CSC	cancer stem-like cells

CTNNB1	Catenin beta 1
CXCL	Chemokine (C-X-C motif) factor
CXCR	C-X-C chemokine receptor
DAPI	4´,6-diamidino-2-phenylindole
DC	Dendritic cells
DC-stamp	Dendritic cell-specific transmembrane protein
DNA	Desoxyribonucleic acid
dNTP	Desoxyribonucleosidtriphosphate
e.g.	For example
EGF	Epidermal growth factor
eGFP	Enhanced green fluorescent protein
EMT	Epithelial-mesenchymal-transition
epoB	Epothilone B
ERBB2	Erythroblastic oncogene B (Her2/neu)
FACS	Fluorescence-activated cell sorting
FADD	Fas-associated protein with death domain
FCS	Fetal calf serum
FGF	Fibroblast growth factor
FITC	Fluorescein isothiocyanate
GAPDH	Glyceraldehyde 3-phosphate dehydrogenase
GPI	Glycosylphosphatidylinositol
GOs	Gene ontologies
GvHD	Graft-versus-host disease
HBCEC	Human breast cancer-derived epithelial cells
HE	Hematoxylin/eosin
HER2	Human epithelial growth factor receptor 2
HERV-FRD	Human endogenous retrovirus group FRD member
HERV-W	Human endogenous retrovirus, type W
HGF	Hepatocyte growth factor
HLA-DR	Human leukocyte antigen
HMEC	Human mammary epithelial cells

HMGB1	High mobility group box 1
HR	Hormone receptor
hTERT	Human telomerase reverse transcriptase
HVJ	Hemagglutinating virus of Japan
Hyb	Hybrid
ICAM-1	Intercellular adhesion molecule 1
IDO	Indoleamine-2,3-dioxygenase
IFN-γ	Interferon gamma
IL	Interleukin
ISCT	International Society for Cellular Therapy
JNK1	c-Jun N-terminal kinase 1
kDa	Kilodalton
KRAS	Kirsten rat sarcoma virus gene
MAPK8	Mitogen-activated protein kinase 8
MCF	Michigan Cancer Foundation
MFSD-2A	Major facilitator superfamily domain containing 2A
MHC	Major histocompatibilty complex
MSC	Mesenchymal stroma/stem cells
MUC-1	Mucin-1
NK cells	Natural killer cells
NO	Nitric oxide
NOD-scid	Non-obese diabetic severe combined immunedeficiency
OC-stamp	Osteoclast-stimulatory transmembrane protein
PBS	Phosphate-buffered saline
PCR	Polymerase chain reaction
PDGF	Platelet-derived growth factor
PE	Phycoerythrin
PEG	Polyethylene glycol
PGE2	Prostaglandin E2
PIC3CA	Phosphatidylinositol-4,5-biphosphate 3-kinase catalytic subunit alpha
PR	Progesterone receptor

PRR	Pattern recognition receptor
PTEN	Phosphatase and tensin homolog
Rb	Retinoblastoma-protein
RelA (p65)	v-rel avian reticuloendotheliosis viral oncogene homolog A
RIP	Receptor-interacting serine/threonine protein kinase
RNA	Ribonucleic acid
mRNA	Messenger ribonucleic acid
RT-PCR	Reverse transcription polymerase chain reaction
SA-β-Gal	Senescence-associated β-galactosidase
SCCOHT-1	Small cell carcinoma of the ovary hypercalcemic type 1
SDF-1	Stromal cell-derived factor-1
SDS	Sodium dodecyl sulfate
siRNA	Small-interfering RNA
STR	Short tandem repeat
TBS	Tris-buffered saline
TGF-β	Transforming growth factor beta
TNF-α	Tumor necrosis factor alpha
TNFR1 or TNFR2	Tumor necrosis factor receptor 1 or 2
TP53	Tumor protein 53
TRADD	Tumor necrosis factor receptor type 1-associated death domain
TRAF2	Tumor necrosis factor receptor-associated factor 2
TRAP	Telomeric repeat amplification protocol
TRIC	Tetramethylrhodamine
UC-MSC	Umbilical-cord MSC
VCAM-1	Vascular cell adhesion protein 1
VEGF	Vascular endothelial growth factor
wt	Wildtype

7.2 Publication list

1. Melzer C, von der Ohe J, Hass R. MSC stimulate ovarian tumor growth during intercellular communication but reduce tumorigenicity after fusion with ovarian cancer cells. Cell Commun Signal. 2018 Oct 13;16(1):67. doi: 10.1186/s12964-018-0279-1.

2. Melzer C, von der Ohe J, Hass R. Cross-talk of mesenchymal stroma/stem-like cells with cancer cells provides therapeutic potential. Stem Cells. 2018 Jul;36(7):951-968. doi: 10.1002/stem.2829. Epub 2018 Apr 16. Review.

3. Melzer C, von der Ohe J, Hass R. In vitro fusion of normal and neoplastic breast epithelial cells with human mesenchymal stroma/stem cells partially involves tumor necrosis factor receptor signaling. Stem Cells. 2018 Jul;36(7):977-989. doi: 10.1002/stem.2819. Epub 2018 Mar 28.

4. Melzer C, von der Ohe J, Hass R. Enhanced metastatic capacity of breast cancer cells after interaction and hybrid formation with mesenchymal stroma/stem cells (MSC). Cell Commun Signal. 2018 Jan 5;16(1):2. doi: 10.1186/s12964-018-0215-4.

5. Melzer C, von der Ohe J, Hass R. Breast carcinoma: from initial tumor cell detachment to settlement at secondary sites. Biomed Res Int. 2017;2017:8534371. doi: 10.1155/2017/8534371. Epub 2017 Jul 12. Review.

6. Melzer C, von der Ohe J, Hass R, Ungefroren H. TGF-β-dependent growth arrest and cell migration in benign and malignant breast epithelial cells are antagonistically controlled by Rac1 and Rac1b. Int J Mol Sci. 2017 Jul 20;18(7). pii: E1574. doi: 10.3390/ijms18071574.

7. Melzer C, Hass R, von der Ohe J, Lehnert H, Ungefroren H. The role of TGF-β and its crosstalk with RAC1/RAC1b signaling in breast and pancreas carcinoma. Cell Commun Signal. 2017 May 12;15(1):19. doi: 10.1186/s12964-017-0175-0. Review.

8. Melzer C, von der Ohe J, Lehnert H, Ungefroren H, Hass R. Cancer stem cell niche models and contribution by mesenchymal stroma/stem cells. Mol Cancer. 2017 Feb 1;16(1):28. doi: 10.1186/s12943-017-0595-x. Review.

9. Otte A, Yang Y, von der Ohe J, Melzer C, Hillemanns P, Feuerhake F, Hass R. SCCOHT tumors acquire chemoresistance and protection by interacting mesenchymal stroma/stem cells within the tumor microenvironment. Int J Oncol. 2016 Dec;49(6):2453-2463. doi: 10.3892/ijo.2016.3735. Epub 2016 Oct 14.

10. Melzer C, Yang Y, Hass R. Interaction of MSC with tumor cells. Cell Commun Signal. 2016 Sep 8;14(1):20. doi: 10.1186/s12964-016-0143-0. Review.

11. Hoffmann A, Floerkemeier T, Melzer C, Hass R. Comparison of in vitro-cultivation of human mesenchymal stroma/stem cells derived from bone marrow and umbilical cord. J Tissue Eng Regen Med. 2017 Sep;11(9):2565-2581. doi: 10.1002/term.2153. Epub 2016 Apr 28. Review.

12. Yang Y, Melzer C, Bucan V, von der Ohe J, Otte A, Hass R. Conditioned umbilical cord tissue provides a natural 3-dimensional storage compartment as in vitro stem cell niche for human mesenchymal stroma/stem cells. Stem Cell Res Ther. 2016 Feb 11;7:28. doi: 10.1186/s13287-016-0289-0.

_____ _____

Ort, Datum Unterschrift

7.3 Conference contributions

1. Oral presentation: In vitro fusion of normal and neoplastic breast epithelial cells with human mesenchymal stroma/stem cells partially involves tumor necrosis factor receptor signaling. “Receptors, Mediators and Genes” – 22nd Meeting of the Signal Transduction Society (STS), (Weimar 2018).

2. Oral presentation: Cell fusion between mesenchymal stroma/stem-like cells (MSC) and breast cancer cells generates new breast cancer populations with high metastatic capacities. 38th annual conference of the German Society of Senology (Deutsche Gesellschaft für Senologie), (Stuttgart 2018).

3. Poster presentation: Altered breast cancer cell metabolism after interaction and hybrid formation with mesenchymal stroma/stem cells (MSC). “Receptors, Mediators and Genes” – 21st Meeting of the Signal Transduction Society (STS), (Weimar 2017).

4. Poster presentation: Direct and indirect interaction of MSC with tumor cells alter mutual functionalities. “Receptors, Mediators and Genes” – 20th Meeting of the Signal Transduction Society (STS), (Weimar 2016).

5. Poster presentation: Interaction of umbilical-cord derived mesenchymal stroma/stem cells with human breast epithelial cells. “Receptors, Mediators and Genes” – 19th Meeting of the Signal Transduction Society (STS), (Weimar 2015).

7.4 Erklärung

Hiermit erkläre ich, dass ich die Dissertation (Mechanisms of cellular interaction and role of mesenchymal stroma/stem cells during tumorigenesis) selbständig verfasst habe. Bei der experimentellen Durchführung wurden folgende Hilfen Dritter in Anspruch genommen:

- Prof. Detlef Neumann und Dr. Bastian Schirmer: Assistenz der qPCR Analysen
- Dr. Oliver Dittrich-Breiholz: Ausführung aller in dieser Dissertation aufgeführten Microarrays und Zusammenstellung dieser Rohdaten
- Dr. Matthias Ballmeier: Zellseparation über FACS (FACS core unit)
- Dr. Thomas Rothämel und PD Dr. Gudrun Göhring: STR Fragment Analyse
- Prof. Konstantin Miller: Karyotypisierung

Ich habe keine entgeltliche Hilfe von Vermittlungs- bzw. Beratungsdiensten (Promotionsberater oder anderer Personen) in Anspruch genommen. Niemand hat von mir unmittelbar oder mittelbar entgeltliche Leistungen für Arbeiten erhalten, die im Zusammenhang mit dem Inhalt der vorgelegten Dissertation stehen. Ich habe die Dissertation in der Arbeitsgruppe für Biochemie und Tumorbiologie in der Frauenklinik im Forschungszentrum angefertigt.

Die Dissertation wurde bisher nicht für eine Prüfung oder Promotion oder für einen ähnlichen Zweck zur Beurteilung eingereicht.

Ich versichere, dass ich die vorstehenden Angaben nach bestem Wissen vollständig und der Wahrheit entsprechend gemacht habe.

_____ _____

Ort, Datum Unterschrift